Capacity Enhancement, QoS and Rate Adaptation in IEEE 802.11s: A Performance Improvement Perspective

Sandip Chakraborty

Capacity Enhancement, QoS and Rate Adaptation in IEEE 802.11s: A Performance Improvement Perspective

Thesis submitted in partial fulfillment of the requirements for the degree of

Doctor of Philosophy

by

Sandip Chakraborty

Under the supervision of

Prof. Sukumar Nandi

Department of Computer Science and Engineering

INDIAN INSTITUTE OF TECHNOLOGY GUWAHATI

Guwahati 781039, India

May 11, 2014

"Om Vang Me Manasi Pratisthita"

"May my mind be fixed in my speech, May Atman manifest unto me, and reveal unto me the Highest Knowledge"

-Aitareya Upanishad

In Memory of

Dadu, Thakurda and Thamma

Dedicated to

Dida, Maam, Baba and Mampai

Whose blessings, constant inspiration and love made my path of success

Declaration

I certify that

a. The work contained in this thesis is original, and has been done by myself under the general supervision of my supervisor.

b. The work has not been submitted to any other institute for any degree or diploma.

c. Whenever I have used materials (data, theoretical analysis, results) from other sources, I have given due credit to them by citing them in the text of the thesis and giving their details in the references.

d. Whenever I have quoted written materials from other sources, I have put them under quotation marks and given due credit to the sources by citing them and giving required details in the references.

Place: IIT Guwahati
Date:

Sandip Chakraborty
Research Scholar
Department of Computer Science
and Engineering,
Indian Institute of Technology Guwahati,
Guwahati 781039, India

भारतीय प्रौद्योगिकी संस्थान गुवाहाटी
Indian Institute of Technology Guwahati

Dr. Sukumar Nandi
Professor, Computer Science & Engg.
& Deputy Director

Guwahati 781039, India
Phone: +91-361-2582011, 2690790
Fax: +91-361-2582014
E-mail: dd@iitg.ernet.in , sukumar@iitg.ernet.in

This is to certify that the thesis entitled "**Capacity Enhancement, QoS and Rate Adaptation in IEEE 802.11s: A Performance Improvement Perspective**" being submitted by **Sandip Chakraborty** to the Department of Computer Science and Engineering, Indian Institute of Technology Guwahati, is a record of bona-fide research work under my supervision, and is worthy of consideration for the award of the degree of Doctor of Philosophy of the institute.

Place: IIT Guwahati
Date:

Prof. Sukumar Nandi

Acknowledgements

"Don't look back when you are moving to success! But don't forget to look back after reaching success!"

This thesis is a culmination of a perfect working relationship with my supervisor, Prof. Sukumar Nandi, to whom I am eternally grateful. Prof. Nandi provided unreserved support during my M. Tech and PhD days, and generously paved the way for my development as a research scientist. Perhaps most importantly, I thank him for being my companion on our quest to discover what lies in the shadow of the statue. Literally speaking, he is my "friend, philosopher and guide" in these days. I enjoyed spending last four years with him both at work and otherwise. His attitude towards students and the countless hours of discussion on different issues have changed my personality, ability and nature in many ways.

I am also highly grateful to my Doctoral Committee members, Prof. Diganta Goswami, Prof. S. K. Bose and Dr. Sushanta Karmakar. Their comments and suggestions have truly deepened and widened my understanding of the problems I have worked on. I extend my gratitude to the thesis reviewers, Prof. C. Siva Ram Murthy from Indian Institute of Technology Madras, Dr. Lisandro Zambenedetti Granville from Federal University of Rio Grande do Sul (UFRGS), Brazil and Prof. Arobinda Gupta from Indian Institute of Technology Kharagpur. I express my sincere thanks to Prof. P. Bhaduri, the former Head, and Prof. S. B. Nair, the present Head of the Department of Computer Science and Engineering, for providing a nice research environment in the department, and support my research works in many ways.

I am thankful to TATA Consultancy Services, India for awarding me the research fellowship that gave me extremely good opportunities to broaden my research activities and interact with eminent researchers in the world, both from the industry as well from the academia. I am grateful to Dr. P. Balamuralidharan, principal research scientist, TCS Innovation Lab, Bangalore for providing valuable comments and suggestions on my research outputs, and giving a good exposure on the real world research challenges in the field of computer networking, through interactions at TCS Innovation Lab, Bangalore.

I thank Mr. Rahul Pandey, former Program Manager, and Mr. Sachin Parkhi, present Program Manager of TCS Research Scholar Program, for extending their helps and supports in technical and official activities. I am also beholden to National Internet Exchange of India (NIXI), for supporting my future research with NIXI Fellowship for the year 2013-2014, based on the research outcome during my PhD days.

I take this opportunity to express my sincere thanks to Prof. Samiran Chattopadhyay, Department of Information Technology, Jadavpur University, who was my supervisor in my B.Eng project, and was the first one who motivated and inspired me to go for higher studies, and to explore the research world. He has shown me the initial paths of success as a research scientist. I am also thankful to Dr. Debarshi Kumar Sanyal, Associate Professor, KIIT University Bhubaneswar, for mentoring my research works starting from my B.Eng days. Today also I can remind the first words from him that motivated me to choose computer networking as my broader field of research.

I would also like to express my hearty gratitude to Prof. Gautam Barua, the past Director of the institute, Prof. Gautam Biswas, the present Director of the institute, all the Deans and other managements of IIT Guwahati, whose collective efforts have made this institute a place for world-class studies and research. I am thankful to all the faculties and the staffs of the Department of Computer science and Engineering for extending their cooperation in terms of technical and official supports. I thank the research scholars, M. Tech and the B. Tech students of this institute, with whom I have closely worked. I am sorry for not to mention all of their names, however, I have learned a lot from them during our discussions times.

I am beholden to my friend Suchetana, without whose help, motivation and support, the work might not be possible with this duration of time. Whenever I faced any difficulty, either in work or otherwise, she was beside me to come out of that. Our countless discussions, and sharing of ideas and thoughts have helped us to debut most of the problems in research as well as in life, that surely accelerated both of our progresses. I also thank my childhood friend Sisir, for constantly motivating and supporting me during my PhD days. I am indebted to all my friends, only to name a few, Abhirup, Soumyadip, Abhijnan, Surajit, Priyanka, Subhendu-da, Niladri-da, Mahasweta, Prithu, Subhrangsu,

Abhijit, Debjani, Shounak and Subhrendu, with whom I have spent most of my times during my student life.

Last but not the least, I would like to express my gratitude to my parents and grandparents for their constant support and encouragement. Their motivation, assistance and guidance helped me to find my path for my future life. My sister deserves a special note of thanks for her enormous love and trust over me which helped me to overcome all the tough situations in life, and will always inspire me to move forward towards my destination.

Place: IIT Guwahati
Date: **Sandip Chakraborty**

Abstract

Current deployment of wireless community and municipal area networks provide ubiquitous connectivity to end users through wireless mesh backbone, that aims at replacing wired infrastructure through wireless multi-hop connectivity. IEEE 802.11s standard is published recently to support the mesh connectivity over well-deployed IEEE 802.11 architecture based on Wireless Fidelity (WiFi) access network. This thesis explores a number of research directions to optimize the mesh peering, channel access, scheduling and mesh path selection protocols for IEEE 802.11s mesh network. The standard provides three major protocols to support mesh functionality - *Mesh Peer Management Protocol* (MPM) to establish mesh connectivity and for topology management, *Mesh Coordinated Channel Access* (MCCA) for channel access and scheduling, and *Hybrid Wireless Mesh Protocol* (HWMP) to support mesh path establishment based on link layer characteristics. The objective of this thesis is to augment the existing protocols for better connectivity and efficient usage of the resources. In a mesh network, the efficiency of the backbone network can be improved through directional communication by exploring spatial reuse capability. However, uses of directional antennas impose several new research challenges that are explored in this thesis.

The first contribution of this thesis enhances the functionality of the mesh channel access and path selection protocols to support directional communication over an IEEE 802.11s mesh backbone. Though MCCA provides reservation based channel access, the standard does not implement any specific mechanism for multi-class traffic services to improve the *Quality of Service* (QoS) for the end-users. The next contribution in this direction is to provide QoS support and service differentiation for MCCA based channel access mechanism over the multi-interface communication paradigm. Modern wireless hardwares are capable of providing multiple data rate supports depending on wireless channel dynamics. As a consequence, the MPM protocol has been augmented to support multi-rate adaptation over IEEE 802.11s protocol elements. In the next contribution, a

two phase mesh path selection protocol has been proposed over HWMP, by exploring the limitations of the proactive and reactive path selection paradigms. Finally, the performances of the proposed set of protocols have been evaluated through the results obtained from a practical indoor mesh testbed. As a whole, this thesis improves the performance of the basic IEEE 802.11s mesh protocols in terms of network as well as end user throughput, end-to-end delay and fairness, with the addition of multi-rate and QoS supports as new features over the standard.

Contents

List of Figures

Nomenclature

AC	Access Categories
AIFS	Arbitration Inter-frame Spacing
AIFSN	Arbitration Inter-frame Space Number
ALM	Airtime Link Metric
BE	Best Effort
BEB	Binary Exponential Back-off
BG	Background
BSS	Basic Service Set
CA	Collision Avoidance
CDF	Cumulative Distribution Function
CSMA	Carrier Sense Multiple Access
CW	Contention Window
CWnd	TCP Congestion Window
DCF	Distributed Coordination Function
EDCA	Enhanced Distributed Channel Access
EDR	Effective Data Rate
ESR	Estimated service rate
ETM	Expected Transmission Cost
ETX	Expected Transmission Count
FTP	File Transfer Protocol
FQA	Fair QoS Agent
HWMP	Hybrid Wireless Mesh Protocol
LKM	Loadable Kernel Module
LP	Linear Programming
LSP	Local Search Problem
MAC	Medium Access Control

MAF	Mesh Access Fraction
MAFL	MAF Limit
MANET	Mobile Ad-Hoc Networks
MAP	Mesh Access Point
MARA	Metric Aware Rate Adaptation
MBSS	Mesh Basic Service Set
MBTT	Mesh Beacon Transmission Time
MCCA	Mesh Coordinated Channel Access
MCCAOP	MCCA Opportunities
MIMO	Multiple Input Multiple Output
MPM	Mesh Peer Management
OFDM	Orthogonal Frequency Division Multiplexing
PCF	Point Coordination Function
PPREQ	HWMP Proactive PREQ Message
PREP	HWMP Path Reply Message
PREQ	HWMP Path Request Message
QoS	Quality of Service
RTT	Round Trip Time
S-ALM	Schedule based Airtime Link Metric
SCV	Squared Coefficient of Variance
SNR	Signal to Noise Ratio
SOAR	Simple Opportunistic Adaptive Routing
STA	Mesh Station
TCP	Transmission Control Protocol
TDMA	Time Division Multiple Access
TFTP	Trivial File Transfer Protocol
UDP	User Datagram Protocol
VD	Video
VO	Voice
VoIP	Voice over IP
WiFi	Wireless Fidelity
WLAN	Wireless Loacl Area Network
WMN	Wireless Mesh Network

List of Symbols

STA_i	The i^{th} mesh STA
$\mathcal{I}$	A directional interface
$\mathcal{G}_{net}(\mathbb{V}_{net}, \mathbb{E}_{net})$	Network graph, with $\mathbb{V}_{net}$ vertices and $\mathbb{E}_{net}$ edges
$\mathcal{G}_{com}(\mathbb{V}_{com}, \mathbb{E}_{com})$	Communication graph, with $\mathbb{V}_{com}$ vertices and $\mathbb{E}_{com}$ edges
$\mathcal{G}_{inf}(\mathbb{V}_{inf}, \mathbb{E}_{inf})$	Interference graph, with $\mathbb{V}_{inf}$ vertices and $\mathbb{E}_{inf}$ edges
$\mathcal{G}_{ch}$	Channel sharing graph
$\mathcal{G}^i_{net}(\mathbb{V}^i_{net}, \mathbb{E}^i_{net})$	Network graph at interface $\mathcal{I}_i$, with $\mathbb{V}^i_{net}$ vertices and $\mathbb{E}^i_{net}$ edges
$\mathcal{G}^i_{com}(\mathbb{V}^i_{com}, \mathbb{E}^i_{com})$	Communication graph at interface $\mathcal{I}_i$, with $\mathbb{V}^i_{com}$ vertices and $\mathbb{E}^i_{com}$ edges
$\mathcal{G}^i_{inf}(\mathbb{V}^i_{inf}, \mathbb{E}^i_{inf})$	Interference graph at interface $\mathcal{I}_i$, with $\mathbb{V}^i_{inf}$ vertices and $\mathbb{E}^i_{inf}$ edges
$\mathcal{F}(\mathcal{I}_i, \mathcal{I}_j)$	Sub-flow from $\mathcal{I}_i$ to $\mathcal{I}_j$
$\mathbb{F}$	Set of flows
$\mathbb{S}(\mathcal{F})$	Set of sub-flows for the flow $\mathcal{F} \in \mathbb{F}$
$\lambda(.)$	Transmission rate for a flow, a sub-flow or a partial flow
$\mathbb{C}$	Set of maximal cliques from interference graph
$\mathbb{F}(\mathcal{I}_i)$	Set of flows passing through $\mathcal{I}_i$
$\mathbb{S}'(\mathcal{I}_i)$	Set of sub-flows for all the flows which are in 2-hop neighborhood of $\mathcal{I}_i$
$\wp(\mathcal{F})$	Priority of flow $\mathcal{F}$
$ORG(\mathcal{F})$	Originating interface for a flow $\mathcal{F}$
$DST(\mathcal{F})$	Destination interface for a flow $\mathcal{F}$
$PRV(\mathcal{I}_i, \mathcal{F})$	Previous hop interface for flow $\mathcal{F}$ with current interface $\mathcal{I}_i$
$NXT(\mathcal{I}_i, \mathcal{F})$	Next hop interface for flow $\mathcal{F}$ whith current interface $\mathcal{I}_i$
$\mathcal{N}$	Number of mesh STAs in a mesh network

$\mathfrak{C}$	Airtime Link Metric
$EDR_{\mathcal{F}_{new}}(\mathcal{I}_s)$	EDR for a new flow $\mathcal{F}_{new}$ at $\mathcal{I}_s$
$\mathbb{R}$	Set of real numbers
$\mathbb{R}^+$	Set of positive real numbers
$\boldsymbol{\lambda}$	Set of possible solutions over λ
$\boldsymbol{\lambda}^*$	Set of optimal solutions over $\boldsymbol{\lambda}$
$\mathcal{N}_{\mathcal{I}}$	Number of interfaces in a mesh network
$\mathcal{R}$	The rate region of a mesh architecture (set of supported data rates)
r_u	A data rate from $\mathcal{R}$
$\hbar$	number of different rates in $\mathcal{R}$
r_{min}	Minimum data rate from $\mathcal{R}$
r_{max}	Maximum data rate from $\mathcal{R}$
$N_1^i(r_u)$	Set of one hop neighbors of STA_i at data rate r_u
$\kappa(r_u)$	Number of one hop neighbors of a mesh STA at data rate r_u
Λ_i	Mean data arrival rate at STA_i
$\mu_i(r)$	Mean service rate of STA_i at data rate r
$\rho_i(r)$	Utilization factor of STA_i at data rate r
c_{Ai}^2	SCV of inter-arrival times at STA_i
c_{Bj}^2	SCV of service time at STA_i
Π_i	Mean number of packets at STA_i
$p_{ij}(r)$	Probability that a packet is forwarded from the queue of STA_i to the queue of STA_j at data rate r
$\Psi_i(r)$	Number of active interfering mesh STAs of STA_i at data rate r
$\Re(r)$	Rate region where data rate r can sustain
$\overline{X_i}(r_u)$	Service time of STA_i with data rate r_u in a DTIM interval
$C(r_u)$	Transmission range with data rate r_u
$I(r_u)$	Number of interfering neighbors when data rate r_u is used

Chapter 1

Introduction

Wireless Mesh Network (WMN) [1–7] is a self-organized and self-configured network of mesh routers that provide ubiquitous backbone connectivity to end users through multi-hop wireless communication between mesh clients and mesh gateways. The backbone network of a WMN is mainly comprised of mesh routers. Other than forwarding traffics from the associated clients, mesh routers are also responsible for relaying traffics from neighboring routers towards mesh gateways. One or more of the mesh routers act as mesh gateways, and are connected to the Internet. Most of the communications in a WMN are between mesh clients and mesh gateways. However, client-to-client communications are also possible using mesh routers as intermediate relays.

WMNs have widespread applications to provide last mile broadband wireless connectivity, such as community networks [8–12] and rural communications [13–17]. Several practical mesh networks and mesh testbeds are already set up for both the practical use and the research purposes, such as 'QuRiNet' at University of California Davis [18], 'Niigata University Mesh testbed' at Japan [19], 'Durban Wireless Community' [20], 'AirJaldi Community Mesh' at Dharamshala, India [21], 'Brismesh' at Brisbane, Australia [22], 'The Mesh' at Darwin, Australia [23], 'RHBMesh' at North Yorkshire, UK [24] etc. IEEE has standardized the mesh functionality over the well established IEEE 802.11 wireless local area network as an amendment to the Medium Access Control (MAC) sub-layer specifications, termed as IEEE 802.11s [25]. IEEE 802.11s extends the basic wireless functionality to support the topology formation, channel access and the multi-hop forwarding over the mesh network. Modern hardwares like 'Cisco WNBU Aironet 1500 Lightweight Mesh AP' [26] supports IEEE 802.11s MAC layer activities. With the new developments in WMN functionality and IEEE 802.11s standardization, several research challenges are be-

ing explored to design efficient wireless backbone technology that can effectively replace the wired backbone with a cost-effective and management-ease wireless solution.

The performance of a WMN depends on several factors. The initial factor is the optimal deployment of mesh routers and mesh gateways. Mesh routers should be deployed in a way such that connectivity among the neighboring routers can be assured. Further, the mesh gateways are required to be placed in an optimal position so that network load can be distributed equally, and from any router, gateways can be reached through the minimum cost path. Having the advantage of static connectivity, several algorithms exist to provide optimal deployment of mesh routers and mesh gateways [27–31]. These algorithms are efficient enough to deploy mesh routers and mesh gateways in optimal positions to effectively utilize the maximum capacity of the network. However, even with the optimal placement of the mesh routers and the mesh gateways, several other designing challenges remain unsolved till now, such as the capacity degradation problem at overloaded routers, the sub-optimal forwarding path establishment due to the network and the channel variation etc. The IEEE 802.11s standard for mesh networking technology has several drawbacks that limits the performance of both mesh routers and mesh clients. This thesis identifies some of the drawbacks of current design aspects of a WMN in the context of IEEE 802.11s standard, and provides efficient solutions for the performance improvement at different MAC layer activities, such as the capacity enhancement, QoS provisioning, rate adaptation and efficient multi-hop forwarding.

1.1 Motivation of the Research Work

Mesh routers build the core network architecture of a WMN. A mesh router can be equipped with multiple interfaces, and can operate in multiple channels. Every mesh router forms a static mesh connectivity with the neighboring routers. With such a connectivity, multiple paths exist between any pairs of mesh routers separated by multiple hops. Mobile ad-hoc networks (MANET) [32] provide similar type of multi-hop architecture, however have some key differences from mesh networks, that demand separate protocol designing challenges. First, the underline topology in a MANET changes with the time due to the mobility, and therefore the mesh path selection protocols are designed based on the reactive or on-demand approaches. On the other hand, WMN provides fixed mesh architecture where the proactive approaches are more preferable. The second difference is that in case of MANET, all nodes are of equal priority in terms of traffic forwarding characteristics. In a mesh network, mesh routers are heterogeneous in nature as they need

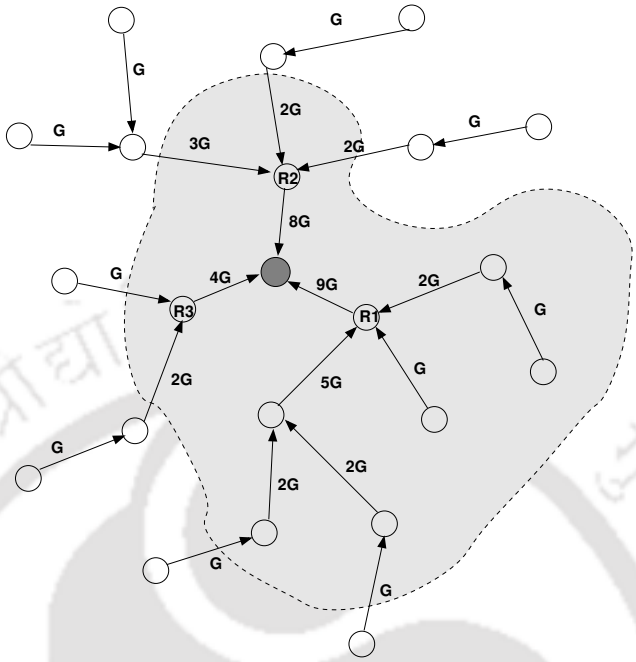

Figure 1.1: Forwarding Load and Capacity Calculation of a Mesh Network

to forward the relayed traffic along with the traffic from associated clients. Therefore, mesh routers need to be prioritized based on the traffic load they forward, such that a proper traffic distribution can be maintained. In a typical community mesh network, most of the traffics are towards or from mesh gateways. Therefore, mesh routers near the gateway are more loaded compared to the edge-routers, which are far from the gateway. With such differences, the well designed MANET protocols do not scale well in a mesh network, and a new set of protocols are required to be designed to support MAC layer mesh activities.

Capacity degradation due to heterogeneous load distribution among mesh routers is a fundamental problem of a mesh network built over the IEEE 802.11 technology [33, 34]. To illustrate the behavior of mesh routers, let us consider Fig. 1.1. The dark node is the mesh gateway, and all other nodes are mesh routers. For simplification in illustration, let us consider that there are G numbers of clients associated with every mesh router, and every client forwards unit amount of traffic towards the gateway. The arrow denotes the forwarding path from the mesh router towards the mesh gateway, and the values written beside the arrows denote the total traffic load to be forwarded by that mesh router, based on the above simplified assumption of uniform client distribution. Let us analyze the behavior of a mesh router $R1$. In a mesh network, two transmissions are called to be *interfered*, if they can not be performed simultaneously because the packets from one

transmission may collide with the other transmission, resulting in frequent packet losses. Interference generally happens if at least one of the two receivers fall within the common range of both the transmitters. In Fig. 1.1, $R1$ acts as one of the transmitters. The shaded region along $R1$ denotes the set of routers with which the transmission of $R1$ interferes. Let us call this region as the *'interference region'* for $R1$. The total traffic load to be forwarded by $R1$ is $9G$, whereas, the total traffic load for all the routers in the interference region of $R1$ is $34G$. Therefore, for a maximum capacity channel access, $R1$ should get $(9/34) \times 100\% = 26.47\%$ of the total bandwidth. However, as IEEE 802.11 provides equal time channel share to all contending nodes, $R1$ actually gets $(1/9) \times 100\% = 11.11\%$ of the channel share, as a total of 9 routers (excluding the gateway) are there in the interference region of the router $R1$. This bandwidth under-utilization results in severe performance degradation in a mesh network. As a consequence, the clients are suffered from the unfairness, when network load is high. The performance of mesh clients degrades as the hop distance between the associated router and the gateway increases, because of the insufficient bandwidth availability at the forwarding routers.

Every mesh router needs to contend with its neighboring routers to gain access to the shared media. The region of contention is defined by the *interference range*, the range upto which the transmission can interfere. In a wireless media, the transmitted signal gets faded as it propagates more from the transmitter. The *communication range* of a router is denoted by the distance upto which a transmission from that router can be decoded successfully. In general, the interference range is more than the communication range, that makes the contention issue oppressive for the mesh network. This increased contention reduces the effective capacity of a mesh network [34]. The mesh capacity can be improved by using high gain directional antennas to restrict the interference among the neighbors of a specific directions [35–38]. In directional mesh networks, mesh routers are equipped with multiple-beam multi-interface directional antennas to support more than one transmissions or more than one receptions simultaneously. Directional communications can improve the network performance by allowing multiple simultaneous communications in space (called the *spatial reuse*). However, the directional communication introduces the problem of interdependency among the link scheduling and the forwarding activities in a mesh network. The maximum transmission rates of individual directional links depend on the end-to-end path characteristics. On the contrary, the forwarding decision should result in a path that provides maximum end-to-end bandwidth with the minimum delay guarantee. Therefore, a joint link scheduling and mesh path selection protocol need to be designed to effectively schedule multiple directional links with the capacity constraint.

Quality of Service (QoS) is another important issue for community networks, both from the perspective of the service provider and end-users. Different types of network traffic requires different amount of network resources for sustaining. For example, the voice traffic requires strict delay and bandwidth guarantee, whereas the video traffic requires minimum jitter (variation in end-to-end delay) support. Therefore, for assuring QoS, reservation of the network resources are required to be allocated dynamically based on the specific service requirements. Two types of service provisioning architectures have been incorporated in the Internet design - the *integrated service architecture* [39], and the *differentiated service architecture* [40]. The integrated service architecture provides strict QoS requirements, however demands a centralized controller for the service provisioning. On the contrary, the differentiated service architecture provides soft service guarantee, and can work in a distributed fashion. IEEE 802.11 is more preferable to the differentiated service architecture compared to the integrated service architecture, because of its inherent inability of centralized control. The IEEE 802.11e amendment over the basic standard supports service differentiation using *Enhanced Distributed Channel Access* (EDCA) [41,42]. Unlike EDCA, the mesh channel access protocol in IEEE 802.11s, called the *Mesh Coordinated Channel Access* (MCCA), does not provide any service differentiation architecture[1]. Designing an efficient service differentiation technique over MCCA is challenging, because the priority based flow reservation technique follows a non-convex function, which is hard to solve in a distributed environment.

Topology control is another crucial aspect for the performance optimization in a multi-hop mesh architecture. IEEE 802.11s uses Mesh Peer Management (MPM) protocol to support the topology control in a mesh environment. Two neighbor mesh routers can not communicate directly until they establish a mesh peering using the MPM protocol. However, the standard MPM protocol supports fixed data rates only. On the other hand, most the physical layer technologies, like IEEE 802.11a/b/g/n support multiple physical data rates based on modulation techniques. Different data rates can sustain at different channel conditions, measured in terms of the 'Signal to Noise Ratio' (SNR). Low data rates can sustain for low SNR values, whereas high data rates require high SNR values for the correct decoding of the received signal. The current industry standard wireless access technologies support rate adaptation based on physical layer channel conditions [43]. On

[1]It can be noted that IEEE 802.11s supports EDCA as a mandatory MAC layer protocol and MCCA as an optional MAC layer protocol. However, MCCA provides better performance in a WMN compared to EDCA. EDCA is kept as compulsory protocol to support the backward compatibility, as discussed in the next chapter.

the contrary, IEEE 802.11s MPM uses a fixed data rate for peer establishment, therefore can not avail the advantages of the physical layer rate adaptation. This limits the performance of the IEEE 802.11s mesh technology to a fixed data rate support.

Topology control, channel access and mesh path selection are interdependent in multi-hop mesh networks. As discussed, topology control requires the physical data rate information to establish peering among the neighbors. Selection of an optimal physical layer data rate depends on the network interference and the channel quality of the forwarding path. Conversely, channel access requires the topology information and the interference characteristics of the forwarding path. At the same time, mesh path selection should find out an end-to-end path that provides maximum bandwidth based on the channel access information and minimum end-to-end delay depending upon the topological connectivity. This interdependency makes the performance optimization aspects of a mesh network more challenging. Further, the mesh path establishment in a mesh network faces several challenges. The proactive path selection mechanism finds out the optimum path before the actual forwarding requirements, and it may use the stale information for future decisions. As discussed earlier, traffic characteristics in a mesh network change arbitrarily with the variation of the number of mesh clients and their individual traffic demands. In addition, wireless channel dynamics, like the signal blocking, fading, and the shadowing may result in a stale path information in case of the proactive selection. Conversely, the reactive path selection introduces extra network overhead by flooding control packets every time a path is required to be established. IEEE 802.11s uses Hybrid Wireless Mesh Protocol (HWMP) for the mesh path selection and maintenance, that is based on a combination of both the proactive and the reactive approaches [44–46]. Therefore the shortcomings of both the proactive path selection and the reactive path selection are inherent in HWMP.

A number of proposals have been published in the literature for joint topology control, channel access and mesh path selection in a multi-hop wireless mesh network, like [47–66] and the references therein. These works model the problem of topology control, channel assignment and mesh path selection as a joint multivariate optimization problem, with either capacity maximization, or throughput maximization, or end-to-end delay minimization as the objective function. The fundamental demerits of these proposals can be summarized as follows,

- The solution of a multivariate optimization is known to be NP-hard [67]. Therefore, different heuristics are used to solve the problem from different perspectives. As a consequence, no uniform framework exists that gives a complete solution on the

basis of the mesh networking fundamentals.

- Most of the existing solutions assume either general contention based channel access, or time division multiple access (TDMA) channel reservation strategies. IEEE 802.11s mesh networking framework, being a new standard in the wireless domain, is not characterized by any of the above mentioned works. The earlier works are difficult to implement over the IEEE 802.11s framework, as it provides a complete new set of protocols for the topology management, channel access and mesh path selection. Compatibility becomes a serious issue when dealing with multivariate optimization based solutions for the performance optimization in an IEEE 802.11s mesh network.

Therefore IEEE 802.11s, the new standard for mesh networking over the well-established Wireless Local Area Network (WLAN) technologies, demands focused researches to optimize the performance of a WMN and to provide extra functionality over the basic protocols. The standard has the capability of providing last mile ubiquitous broadband access through a cost-effective wireless solution, however need to be enhanced with modern demands of QoS assurance and new features like multi-rate support, for effective usage of the available channel resources.

1.2 Contribution of the Thesis

The works proposed in this thesis augment the basic IEEE 802.11s protocols to optimize the performance and to support extra functionalities for the better utilization of the network resources. As discussed earlier, the mesh architecture suffers from the capacity degradation problem due to the increased interference among mesh routers. The capacity of a WMN can be increased by multi-interface support at the mesh routers, along with the high gain directional antennas. IEEE 802.11s channel access and mesh path selection protocols do not perform well with directional multi-interface support, because of the sub-optimal flow scheduling. Further, the MCCA protocol does not provide any advanced mechanism for the service differentiation based on the individual traffic classes for the QoS assurance. The advancement in the rate adaptation technologies is also not adopted in IEEE 802.11s architecture. At the same time, mesh path selection protocol also suffers from the inherent problems of the proactive and the reactive path selection mechanisms. This thesis targets these four issues of IEEE 802.11s standardization for providing better performance and improved capacity support.

1.2 Contribution of the Thesis

Flow scheduling in the directional multi-interface IEEE 802.11s WMN suffers from the problem of unbalanced traffic allocation, because of the increased interference among mesh routers. Let us consider an end-to-end flow between two mesh routers[2] STA_S and STA_D, that goes through intermediate routers $STA_{I_1}, STA_{I_2}, ...$ and so on. In a directional network, the end-to-end flow $STA_S \rightarrow STA_D$ can be subdivided into several sub-flows based on the intermediate path, such as $STA_S \rightarrow STA_{I_1}$, $STA_{I_1} \rightarrow STA_{I_2}$ and so on. The maximum end-to-end flow capacity for such a flow is the max-min capacity for all its sub-flows. However, in the IEEE 802.11s mesh network, intermediate mesh routers remain unaware of the maximum throughput that a flow can achieve, and inject packets more than the maximum capacity, which may cause throughput degradation for other flows. The upper layer end-to-end flow control fails to solve this problem, because an intermediate router may receive data from more than one flows, and may forward data to more than one next-hop routers. In this thesis, the problem of the balanced flow allocation is first modeled as a centralized convex optimization problem, considering the maximum end-to-end flow capacity and the network interference. Based on the convex nature of the solution set, the problem is decomposed into local sub-problems to calculate the solution at individual mesh routers, for their individual interfaces. The IEEE 802.11s MCCA based channel access mechanism is used to control the channel reservation, so that every interface can reserve maximum channel based on the solution of the flow-balancing problem. Further, the HWMP path selection metric has been augmented to cop up with directional multi-interface support to establish the optimal path based on the remaining bandwidth information obtained from the channel access protocol.

The above solution considers flow-balancing for the single-class homogeneous traffic only. The problem becomes more challenging when multiple classes of traffics are considered for the QoS based service differentiation. In this case, the minimum bandwidth demands for every classes of traffic need to be assured. Further the channel reservation should be based on the traffic class priority, i.e., a higher priority traffic flow should be able to reserve more amount of bandwidth compared to a lower priority traffic flow. This priority based bandwidth reservation strategy requires to support *proportional fairness* criteria among the contending flows. The centralized formulation for the proportional fairness criteria with the minimum traffic demand is known to be non-concave in nature [68]. Therefore, the optimization decomposition is difficult to design over a distributed network of mesh routers, considering the local information only. In this work, a sub-gradient optimization strategy is used to decompose the centralized

[2]According to IEEE 802.11s [25], mesh routers are termed as mesh stations (STA).

formulation, exploiting its log-convex property. The distributed decomposition enables local computation of the maximum capacity of every flows through every interface. IEEE 802.11s MCCA protocol is augmented to support channel reservation based on the maximum capacity information. HWMP is enhanced with extra capabilities to take decision for the admission control, whenever a new flow is introduced in the network with a minimum traffic demand and a service class priority.

The next work in this direction augments the IEEE 802.11s mesh networking with multi-rate support. The classical rate adaptation algorithms, such as [69] and the references therein, consider the physical rate selection based on the channel fluctuation due to fading, shadowing and other physical effects. However, rate adaptation is more challenging in a mesh network due to the *rate-hop-interference trade-off*. Lower data rates can sustain for longer transmission ranges, which may improve network performance by reducing number of intermediate relays towards the destination router. However, in a moderate to high load network, longer transmission range can increase interference, resulting in throughput degradation. This work theoretically models this trade-off using the queuing network analysis over the IEEE 802.11s mesh architecture. A set of amendments are proposed over the standard MPM, MCCA and HWMP for multi-rate support. The interference information is obtained from the MCCA protocol, and the hop information is extracted from HWMP, in terms of the path quality metric. Based on these information, the optimum data rate is selected that can sustain over the current channel condition and provides improved performance in terms of data delivery. The optimum data rate, once selected, is used for the peer establishment using the MPM protocol.

In the next work, the thesis concentrates on the performance improvement in the path selection using HWMP. HWMP is based on a cooperation of two different path selection strategies - the proactive selection and the reactive selection. As mentioned earlier, proactive selection are prone to stale information due to the channel and the network fluctuations in a mesh environment, and reactive selection floods the network with control packets. This work proposes an alternative path selection strategy, called the *'Selective Greedy Forwarding'*. In the proposed path selection strategy, the proactive HWMP is used to collect the initial information, where a set of potential forwarders are selected from the peer neighbors who can effectively forward the packets towards the destination. During the actual data transmission, the variability in the network and the channel conditions are explored to device a local greedy strategy to find out the best forwarder among the set of potential forwarders.

Finally the thesis reports the performance results of the IEEE 802.11s mesh protocols

from a practical indoor mesh testbed. The mesh testbed is built at the department of Computer Science and Engineering research labs, using IEEE 802.11n Multiple Input Multiple Output (MIMO) technology supported, dual interface Ra-Link [70] wireless chipset. The routers support open source Linux kernel, though the chipset driver is proprietary. Because of this limitation in the use of hardware drivers, some of the protocols, like the channel scheduling and mesh path selection are implemented as a loadable kernel module (LKM), that is executed when the specific functionality is required to be triggered. The performance of the mesh network with improved channel access and mesh path selection support is analyzed from the results obtained from the testbed, and compared with the standard MCCA and HWMP.

In summary, the major contributions of this thesis are as follows.

- The thesis proposes an improved mechanism for the capacity improvement in the IEEE 802.11s mesh networks, using multi-interface directional antenna support. IEEE 802.11s MCCA protocol is enhanced to assist the balanced flow allocation over the directional interfaces.
- IEEE 802.11s MCCA protocol is augmented for the QoS support during the channel reservation. The proposed modifications over the naive MCCA protocol enable service differentiation for the flows from different traffic classes, along with their minimum traffic demand. The compatibility of the proposed protocol with the standard EDCA based service differentiation is also analyzed in this context.
- The rate-hop-interference trade-off in a multi-rate mesh network is analyzed using a queuing network modeling over IEEE 802.11s protocol. The modeling provides the theoretical basis for the rate adaptation in a mesh network.
- An amendment is proposed over the standard IEEE 802.11s for multi-rate support with the physical layer rate adaptation techniques, based on the rate-hop-interference trade-off. MCCA and HWMP are augmented to collect necessary informations that are used to find out the optimal data rate in a particular network condition. The optimal data rate is used for the peer establishment during the operation of the MPM protocol.
- The performance of HWMP is enhanced for the improved path selection strategy for a multi-interface mesh network, where the proactive approach is used for the initial information gathering, and a greedy selection mechanism is used during the actual path establishment. This provides an improved next-hop information, compared to

the naive HWMP approach considering the fluctuation in the network load, channel condition and interference.

- Whenever necessary, the correctness of the proposed strategies are justified using mathematical proofs, theoretical arguments and modelings.
- All the proposed schemes are implemented in Qualnet-5.0.1 network simulator framework [71], and the performance of the proposed schemes are evaluated using simulation results. Further, the performance metrics are also compared with the similar state-of-art schemes proposed in the literature.
- The results from a practical indoor mesh testbed are used to analyze the performance improvement of a mesh network in terms of channel access and mesh path selection, and the results are compared with the naive MCCA and HWMP.

1.3 Organization of the Thesis

The rest of the thesis is organized as follows.

Chapter 2 provides a brief discussion about state-of-art works on WMN performance optimization, including the details of IEEE 802.11s protocol architecture and its improvements.

Chapter 3 proposes a new architecture for the performance optimization of an IEEE 802.11s mesh network using multi-interface multi-beam directional antennas. First, the interference information is characterized for directional communication, and then this information is used to model a centralized flow scheduling problem. A distributed variant of the centralized optimization is proposed based on the convexity of the centralized formulation. IEEE 802.11s channel access and mesh path selection protocols are tuned to support the distributed optimization for providing maximum throughput to all end-to-end flows. Finally, performance of the proposed scheme is evaluated using simulation results.

Chapter 4 amends the IEEE 802.11s MCCA for providing service differentiation, fairness and QoS based on traffic flow priorities. A centralized optimization is formulated for service differentiation, assuring maximum network throughput. The log-convex property of the centralized formulation is explored to provide a localized distributed solution using the sub-gradient optimization strategy. The performance of the proposed solution is evaluated using simulation results, and compared with other naive approaches.

Chapter 5 provides multi-rate adaptation support over IEEE 802.11s technology. In this chapter, the trade-off among data rate, number of hops towards destination and

the network interference has been studied using the diffusion approximation analysis over the IEEE 802.11s queuing network model. Based on the theoretical findings, the standard MPM, MCCA and HWMP are augmented for multi-rate support in a WMN. Simulation results are used to show the effectiveness of the proposed scheme over other state-of-the-art rate adaptation techniques for WMN and multi-hop mesh networks.

Chapter 6 discusses about the shortcomings of the IEEE 802.11s HWMP for path establishment using the proactive and the reactive approaches. An selective greedy mesh path selection protocol is proposed in this chapter, that works as an amendment of the standard HWMP. The properties of the proposed selective greedy mesh path selection protocol is analyzed using theoretical arguments. The effectiveness of the proposed protocol is evaluated using simulation results.

Chapter 7 analyzes the performance of the mesh network from the results obtained from a practical indoor mesh testbed. The results are compared with the naive mesh protocols, like MCCA and HWMP.

Finally, **Chapter 8** concludes the thesis with summarization of the works done, and suggests the directions for possible future works over the IEEE 802.11s mesh networking technology.

Chapter 2

Literature Survey and Background

The concept of WMN was proposed first in early twenties [72, 73], when the researchers explored the possibilities of extending the coverage of the wireless connectivity through multi-hop communications. Till then, WMN has gone through rapid developments, and finally IEEE standardizes mesh network as an amendment in IEEE 802.11 WLAN specifications [25], in September, 2011. In this chapter, the progresses in the field of WMN have been discussed with critical analysis, and several design issues are pointed out that are partially solved, or remained unsolved till now. For ease of presentation, the complete discussion has been classified into three groups - WMN designs over WLAN architectures, the IEEE 802.11s standardization and the works done over IEEE 802.11s standard.

2.1 WMN Designs over WLAN Architectures

This section discusses about the state-of-the-art works that consider the WMN design over general WLAN architectures, either based on the IEEE 802.11 standard, or the TDMA based networks. From the early stages of designing, one of the main concerns in WMN design is the capacity of a mesh network. Jun *et al.* [33] have first theoretically modeled the nominal capacity of a general purpose WMN. They have introduced the concept of the *'bottleneck collision domain'* in a mesh network, where they have shown that the mesh routers near the gateways suffer from the bottleneck capacity problem. Based on this observation, they have concluded that the asymptotic capacity of a WMN decreases with $O(\frac{1}{n})$, where n is the number of nodes in the network. In [74], the authors have shown that the capacity of a WMN depends on the deployment design. Further, they have shown that the uses of directional antenna improves the capacity significantly. Molle *et al.* [34] have analyzed the impact of traffic load distribution over the capacity of a WMN. They

have shown that the mesh capacity can be improved as much as 50%, using a proper load distribution through the gateway placements. Recently, Mansoori *et al.* [75] have shown that, in a multi-channel multi-interface WMN, the per-client throughput capacity varies based on the number of channels and the number of interfaces used. They have also provided the upper bound on number of gateways, beyond which per-client throughput can not be improved by increasing number of gateways.

Based on these capacity analysis techniques for a WMN, several works in the literature have revealed the performance issues based on the channel access, mesh path selection, scheduling and topology control protocols. Further, a class of works considers cross-layer technologies, and joint protocol design for the better performance assurance. A brief overview of these works have been discussed in next few subsections.

2.1.1 Channel Access and Scheduling Optimizations for WMN

Two different types of channel access and scheduling protocols are widely studied in the literature for WMN design - the TDMA based channel access and the contention based channel access. Both of these mechanisms have their own merits and demerits. The TDMA based channel access and scheduling protocols provide collision free channel access, and are efficient in terms of fairness. However, in a distributed mesh environment, hard TDMA is difficult to implement, because it requires perfect coordination and synchronization among mesh routers. On the contrary, the contention based channel access are distributed in nature, however does not guarantee collision free channel access. Further, it may result severe unfairness in a multi-hop environment.

TDMA based Channel Access and Link Scheduling

A number of works exists in the literature that discuss about link scheduling and channel access in TDMA based WMN. Most of the works in this domain models the scheduling and channel access problem as a graph theoretic problem of finding maximum number of conflict free nodes that can be scheduled simultaneously [76]. For this purpose, the network is modeled as a *communication graph*, where every node represents the mesh routers, and the links correspond to the ongoing communication. An *interference graph* is extracted from the communication graph, where the links of the communication graphs are represented as individual nodes, and there exists an edge between two nodes if the corresponding links interfere. The interference graph is used to find out an interference free scheduling in the network, and accordingly the TDMA time slots are allocated.

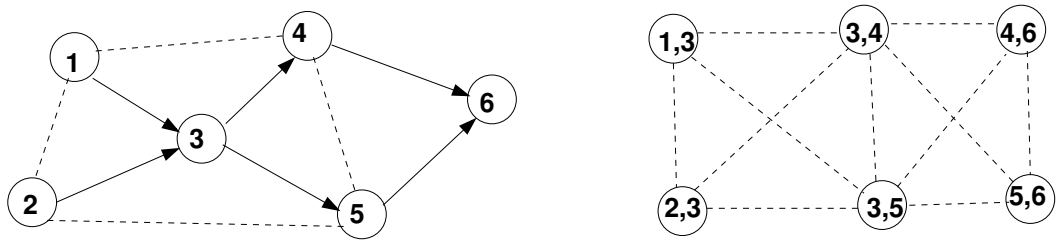

(a) Communication Graph **(b) Interference Graph**

Figure 2.1: Communication and Interference Graphs

As an example, let us consider Figure 2.1. The dotted edge denotes the physical link between two nodes and the arrow denotes an ongoing communication. An arrow in the communication graph is represented as a node in the interference graph. For example, the communication between the node 1 and the node 3 is represented as the node $\{1, 3\}$ in the interference graph. There exist and edge between the node $\{1, 3\}$ and the node $\{2, 3\}$ in the interference graph, because these two communications interfere with each other (both the node 1 and the node 2 can not transmit simultaneously to the node 3). With the help of this interference graph, the problem of finding an interference free scheduling is similar to find the maximum independent set from the interference graph. As an example, the node $\{1, 3\}$ and the node $\{5, 6\}$ from the interference graph forms a maximum independent sent, and hence they can transmit simultaneously. Therefore, these two communications can be scheduled in the same TDMA time slot.

The performance of the scheduling algorithms based on pure graph theoretic conjectures depends on how efficiently the interference graph is constructed from the communication graph. In [77], the authors propose a graph based solution for minimum delay scheduling in TDMA mesh networks. They have interpreted scheduling delay as the cost of transmission order of the links, and formulate an optimization that finds a transmission order with the min-max delay across a set of multiple paths. They have shown that the problem is NP-complete for arbitrary network graphs, and proposed a solution to find the transmission order with the min-max delay for a tree based network topology. Brar *et al.* [78] have proposed a graph based heuristics to find a near-optimal solution for spatial TDMA based mesh network, while considering the physical interference model. In [79], the authors have proposed a distributed link scheduling algorithm over the TDMA based WMN. Their algorithm runs in two phrases. In the first phrase, an iterative procedure is used to find locally feasible schedules by exchanging link scheduling information between

nodes. The iterative procedure uses a modified Bellman-Ford algorithm over the network conflict graph. The second phrase uses a wave based termination procedure to detect the termination of the local schedules. The algorithm results in a conflict free schedule within finite convergence time. TDMA based link scheduling can provide conflict free schedules, however have some disadvantages, as follows:

- The scalability is a serious issue for these scheduling algorithms. Every mesh router needs to have complete network information to design the communication graph and interference graph. Global communication graph is dynamic in nature, and changes when a new flow is introduced or an existing flow terminates. Most of the scheduling algorithms do not sustain for the dynamic communication and interference graphs. Similarly, the distributed scheduling algorithms, as proposed in [79] and others, may infer long convergence time when the network size is large.
- The second issue with these scheduling algorithms is the reliability. Though the algorithms theoretically guarantee conflict-free scheduling, however, in practice it may show problems for dynamic communication and interference graphs. A small variation from the conflict-free property may results in severe unfairness among the end-users because of the uncontrolled packet losses.

Contention based Channel Access and Link Scheduling

Most of the works in the literature propose to design protocol enhancements over the contention based channel access and link scheduling, as it resembles the well-established IEEE 802.11 Distributed Coordination Function (DCF) that uses a contention based channel access using binary exponential back-off (BEB) mechanism. Two different types of optimization procedures are designed for contention based channel access. First, the graph based optimization which is similar to the TDMA based access, as discussed earlier. The second type is to design a non-linear optimization based on the interference constraints, where the objective is to maximize the network performance. The objective function for such optimizations can have several variations, like maximizing the network throughput and fairness, or minimizing the end-to-end delay. In [80], the authors have used a dynamic programming mechanism for optimized link scheduling in a WMN. They have modeled the link scheduling problem as an integer programming problem. As integer programming is known to be NP-hard, they have proposed an approximate dynamic programming method to reduce the dimensionality in the integer programming, and provide a near-optimal solution. Yu *et al.* [81] have proposed a channel assignment and link scheduling mechanism

for multi-channel multi-radio WMN. They have modeled the scheduling problem as an optimization to maximize the network capacity with minimum bandwidth demand. Kumar *et al.* [82] have defined a 'Link Cost Metric' to order the scheduling of links for maximizing the overall capacity and throughput in a WMN. They have considered the joint problem of channel assignment and link scheduling over contention based protocols, that minimizes the network interference. Several other protocols have been designed in the literature, like [83–86] that uses non-linear optimization based methods for solving the channel assignment and scheduling in contention based WMN.

The fundamental problem of designing a non-linear optimization to model the channel access of a WMN is that, the distributed or randomized versions of the solutions require sufficient time to converge, therefore, not scalable for large networks. Further, most of these schemes assume equal communication and interference ranges for a mesh router, which is far from the practice. Recently, *'back-pressure scheduling'* [87] based channel access protocols have attracted much attention for the researchers. In this class of scheduling algorithms, whenever a mesh router detects congestion in the network, it back-propagate this information by falsely injecting some packets in the network, therefore, creating a temporal congestion effect that propagates towards the edge-routers. In [87], the authors have shown that back-pressure scheduling can significantly improve the performance of IEEE 802.11 based WMN. The advantage of this scheduling mechanism is that it is completely distributed in nature and does not make any assumption over the interference range of a mesh router. However, for the proper implementation of such access mechanisms, improved loss detection techniques are required, that can segregate normal packet errors from congestion related losses, as shown in [88].

2.1.2 Directional Antenna Support in Mesh Networks

Several works in the literatures have explored the directional antenna support over wireless multi-hop and mesh networks. Vaidya *et al.* [89] have proposed the first MAC protocol, called D-MAC, to employ directional antennas in IEEE 802.11 based wireless networks. The major drawback of this scheme is that it assumes the location of the destination node known to the transmitter node, and the destination node can estimate the angle of arrival to locate the transmitter. In [90], the authors have proposed a link scheduling algorithm for multi-radio multi-gateway wireless mesh networks, assuming that there are at-least two radio channels available, so that the communications at mesh clients do not interfere with the communications at mesh routers. However, the proposed scheme is centralized in nature and works for some fixed topologies. Dutta *et al.* [91] have

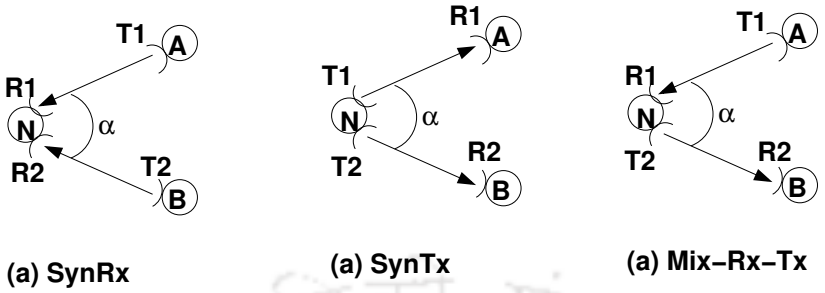

Figure 2.2: Communication Paradigms for Directional Antenna [95]

proposed an exponential size linear programming formulation for joint routing (or mesh path selection) and scheduling in multi-hop wireless networks with directional antennas. Although they have shown that the proposed algorithm performs better, the solution is based on TDMA scheduling and centralized in nature. In [92], the authors have designed a mixed integer linear programming solution to minimize the interference among different interfaces in multi-radio directional antenna based wireless mesh networks. In another work [93], the authors have provided a linear programming formulation for maximizing the network throughput, subject to the fairness constraint and the directional antenna based channel interference constraint. Based on the optimization formulation, they have proposed a heuristic for joint link scheduling and mesh path selection scheme, which aims at approximately attaining the optimal solution. Liu *et al.* [36] have analyzed the performance of wireless mesh network using a real test-bed. They have performed the experiment with three sectored antenna and static channel assignment. They have shown that three sectored antenna provides substantial performance improvement over two-antenna system and omni-directional antenna system. An angular MAC protocol for directional antenna based wireless mesh network is proposed in [37]. The angular MAC framework considers efficient neighbor discovery mechanism for throughput improvement in mesh network. In [94], the authors have provided a link scheduling algorithm for long-distance communication with a typical deployment scenario of a maritime mesh network. The proposed link scheduling algorithm provides better performance guarantee for long distance wireless communications.

In [95], the authors have proposed another efficient directional MAC protocol, called the 2P MAC, for long distance wireless mesh using single channel network. Based on the transmission natures of directional antennas, they have considered three scenarios, *SynRx*, *SynTx* and *Mix-Rx-Tx*, as shown in Figure 2.2. *SynRx* denotes that the receiver is same for both the transmitters, whereas *SynTx* denotes that the transmitter

is same for two different receivers. *Mix-Rx-Tx* denotes that a single node works as the transmitter for one communication, and the receiver for another communication, using two different directional antennas. The authors have shown that because of the physical proximity and the effect of side lobes, *Mix-Rx-Tx* is not feasible at a single node. In their protocol, mesh nodes periodically change their mode from *SynRx* to *SynTx* and vice-versa. They have designed a synchronization protocol to achieve this synchronous operation. However, current commercially available directional antennas are equipped with side lobe cancellation techniques [96]. Further due to physical layer capture effects, simultaneous transmission and receptions are possible using smart antennas [97]. So there is a requirement for further research exploiting the capacity of smart antennas supporting simultaneous transmissions and receptions through different interfaces.

2.1.3 Service Differentiation and Fairness Provisioning in Mesh Networks

The concept of service differentiation and fairness have been used interchangeably in the existing literatures. Several researchers have proposed the use of proportional fairness [98, 99] to provide service differentiation in a mesh network. In the case of proportional fairness, rate allocation for a flow is proportional to its traffic priority. On the other hand, max-min fairness [98] is used in the literature to support equity in the traffic demand among all flows. A flow assignment is said to be max-min fair if the rate of one flow cannot be increased without decreasing the rate of another flow, having equal or less data rate. QoS provisioning and fairness issues in IEEE 802.11 mesh network have been long studied in the literature. However for multi-class service flows, following two important requirements should be assured simultaneously,

- **Inter-Class Service Differentiation:** Traffic allocation for every flow should be proportional to its service class priority. This requirement can be modeled using proportional fairness criteria. Further, minimum service level demand for every service class should also be assured.

- **Intra-Class Fairness:** Traffic allocation for every flow with similar service priority should have equal traffic allocation. This can be modeled as max-min fairness.

Proportional fairness for DCF and EDCA based channel access has been well-studied in the literature. In [100], the authors have discussed the inter-dependency of the end-to-end flow control and the link layer channel access for random access wireless multi-hop

networks. They have proposed a joint optimization that finds out the end-to-end traffic flows based on link access probabilities for the CSMA based wireless multi-hop network. In [101], the authors have introduced log-convex utility to find out transmission rates in a multi-hop network using a distributed mechanism. They have proposed a cooperative proportional scheduling where base stations in the network share information among themselves to reach out at the consensus. This type of cooperation is costly for mesh networks and information sharing is limited only up-to few hops among local routers. Yoo *et al.* [102] have analyzed the requirement for proportional fairness in mesh networks, and provide a centralized flow-coordination mechanism at mesh gateways to ensure the proportional fairness. However, centralized coordination at mesh gateways limits the scalability of the scheme. In [103], the authors have shown that proportional fairness can enhance QoS in an IEEE 802.11e network. However it can degrade network capacity by over-biasing the performance towards high priority flows, resulting in an indefinite starvation of low priority flows [104].

On the other hand, several research works exist in the literature that explore the max-min fairness in the context of multi-hop and mesh networks. The authors in [105] have proposed a max-min fair allocation strategy where the gateway node calculates the traffic demand to ensure fair access. This scheme is inherently centralized and not scalable. Zhang *et al.* [106] have proposed a max-min fair allocation strategy over DCF, using a per-destination queuing mechanism. However, they have only considered the rate adjustment, and have ignored the effect of the channel access. In [107], the authors have characterized the log-convexity of the rate region in a DCF based mesh network. They have proposed a max-min fair rate allocation strategy based on the log-convex characteristics of the DCF rate region.

There are few works exist in the literature that target to improve QoS, and assure fairness for multi-class service networks. Park *et al.* [108] have proposed a model for fair QoS agent (FQA) to simultaneously provide per-class QoS enhancement and per-station fairness. Their approach is based on a dual service differentiator that maintains priority scheduling based on a dual queuing approach. The FQA mechanism ensures the fairness and the end-to-end QoS at the network layer. On the contrary, according to the current mesh networking standard, forwarding information is maintained at the MAC layer and on per-hop basis. Dual queuing approach is difficult to implement at the MAC layer as queue management may interfere with the channel access protocols.

Two different approaches have been explored in the literature to model the trade-off between the proportional fairness and the max-min fairness. The first one is mixed-bias

fairness [104] and the second one is $(\alpha, \wp)$ proportional fairness [109]. In [110], Singh *et al.* have proposed a resource biasing strategy to improve the network throughput in a wireless multi-hop network. They have shown that providing more resources to the longer connections leads to poor network utilization. Their proposed scheme provides a controlled bias to longer connections by limiting the maximum resource utilization for them, that improves the throughput for shorter connections significantly. However, this scheme affects the longer connections to achieve required QoS. Furthermore, for multi-class connections, high priority traffics with longer connections may get affected. On the contrary, Mo *et al* [109] have proposed the concept of $(\alpha, \wp)$ proportional fairness to model the end-to-end congestion control for multi-class traffic. $(\alpha, \wp)$ proportional fairness is a trade-off between the proportional fairness and the max-min fairness. Let $\wp = \{\wp_1, ..., \wp_k\}$ be the flow priority, and $\alpha \geq 1$ be a constant. $\lambda = \{\lambda_1, ..., \lambda_k\}$ is the rate vector for the flows. A rate vector λ^* is $(\alpha, \wp)$ proportional fair if it is feasible and for any other feasible vector λ,

$$\sum_i \frac{\wp_i(\lambda_i - \lambda_i^*)}{\lambda_i^{*\alpha}} \leq 0 \tag{2.1}$$

When $\alpha = 1$, the rate allocation becomes proportional fair, and it converges to the max-min fairness when α is large. Mo *et al.* [109] have shown that with the limiting bias over the α and the $\wp$ values, a controlled balance can be achieved between the proportional fairness and the max-min fairness. However, to the best of our knowledge no paper exists in the literature that uses $(\alpha, \wp)$ proportional fairness in the context of WMN design.

2.1.4 Rate Adaptation and Topology Control in Mesh Network

The classical rate adaptation algorithms are designed based on the sustainability of the data rates for a specific path loss component. Figure 2.3 shows the throughput for different data rates with respect to the path loss component. The figure indicates that different data rates can sustain for different path loss values. The high data rates sustain for low path loss values, whereas the low data rates can sustain for high path loss values. Most of the rate adaptation protocols proposed in the literature over the IEEE 802.11 technology are based on this concept. *SampleRate* [111] is a rate adaptation protocol that is based on this concept, and extensively implemented in commercial hardwares. SampleRate tries to maximize the network throughput by transmitting frames at a data rate which is calculated based on a parameter, called the *'Average Frame Transmission Time'* (AFTT). AFTT includes the time required to recover from the packet losses. SampleRate uses a periodic sampling mechanism to find out the optimal data rate from the gathered information.

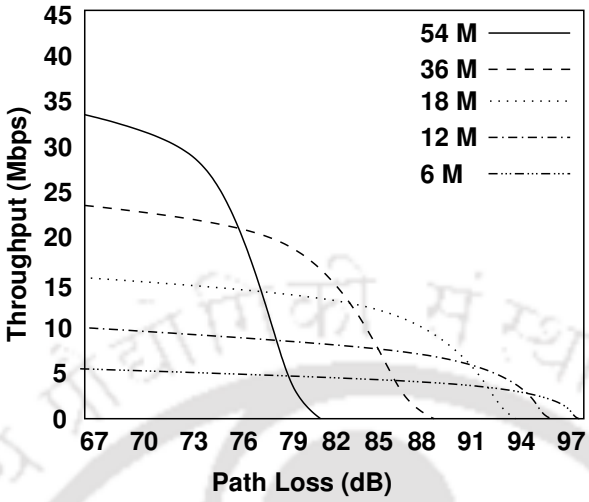

Figure 2.3: Performance of Fixed Data Rates

To track channel condition changes and find an optimal data rate, control frames are periodically sent at data rates other than the currently estimated optimal data rate. This periodic control broadcast is used to gather information, and update the AFTT values for other data rates. In the sampling mechanism the data rates that results in three consecutive packet losses are discarded for 10 seconds. Further the sampling mechanism selects the data rates that provides loss free frame transmission time lower than the AFTT value. The optimal data rate is chosen from the sampled data rates, that provides the minimum AFTT value. AFTT value is periodically updated based on the average frame transmission time of the sampled data rates. In [112], the authors have shown that SampleRate can provide a near optimal throughput in a single user network. However, SampleRate performs poorly for multi user multi-hops networks [113].

Other classical rate adaptation algorithms, like *Auto-Rate Fallback*, *Receiver-Based AutoRate* [114], *Cooperative Relay-Based AutoRate* [115], and their variants, are also designed upon the packet loss estimation due to the channel error. Improved packet loss detection techniques have been proposed [116] to differentiate between the congestion loss and the loss due to channel errors. Several other rate adaption protocols have been proposed [113, 117–119] to find out the sustainable data rates based on SNR (or the path loss component) between the sender and the receiver. All of these algorithms primarily focus on the rate adaptation for an infrastructure BSS where the wireless clients communicate through an AP. Therefore, these algorithms do not consider the effect of communication range fluctuations due to changes in the data rates (called the *'rate versus*

Table 2.1: Data Rate vs Range in 802.11g

Data Rate (Mbps)	6	9	12	18	24	36	48	54
Modulation Technology	BPSK	BPSK-3	QPSK	QPSK-1	16-QAM	16-QAM	64-QAM	64-QAM
Communication Range (feet)	300	250	210	180	140	100	95	90

range dilemma' [120]) that impacts the performance of the multi-hop and mesh networks. The path loss value increases with the increase in the distance between the transmitter and the receiver. Therefore, low data rates can sustain for long communication ranges, whereas the high data rates are sustained for short communication ranges. The current industry standard data rates versus communication ranges for IEEE 802.11g physical layer are shown in Table 2.1 [121]. The table clearly indicates that communication range decreases as the data range increases. This phenomena is termed as *'rate versus range dilemma'* in the existing literature, that plays a major role in designing the rate adaptation protocols for multi-hop networks.

Several schemes have been proposed in the literature to design rate-adaptive routing or path selection protocols for multi-hop wireless networks. Sheu *et al.* [122] have proposed a path metric for routing in multi-rate multi-hop networks, that considers the affects of rate selection over number of hops. However, the underlying rate selection mechanism does not select the optimal rate based on the number of hops. They have proposed a routing metric that selects the best path depending on the underlying topology and the selected data rate. Another multi-rate aware routing protocol has been proposed in [123], that selects the forwarding path that provides high data rate support. However it can degrade the end-to-end throughput due to the increase in the number of hops. Further, the nodes with high data rates may suffer due to bottleneck problem. Li *et al.* [124] have proposed a rate adaptive MAC protocol for wireless ad-hoc networks, that uses the cooperation between the sender and the receiver. In [125], the authors have proposed another routing metric, called the *'Bottleneck Link Capacity'*, that considers the capacity of every link based on the underlying data rate. Recently Kim *et al.* [126] have proposed a mechanism that considers both the routing and the rate selection for a multi-rate multi-hop wireless network. They define a new routing metric, called *'Expected Transmission Cost'* (ETM), that can be used to determine the best end-to-end path using a greedy strategy. At the same time, ETM can find the best transmission rate for every link using a dynamic programming mechanism.

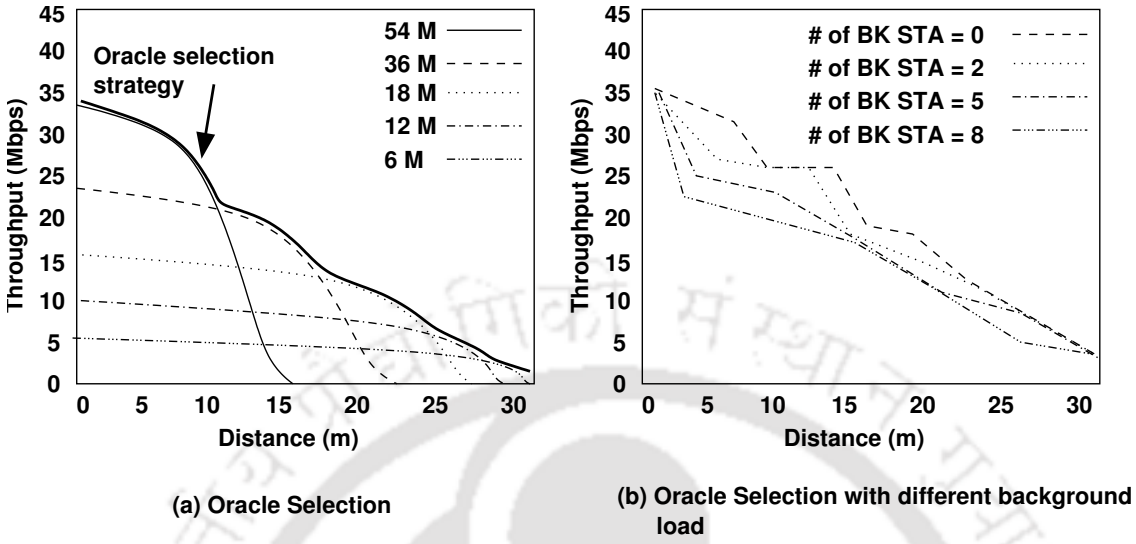

Figure 2.4: Effect of Background Traffic [129]

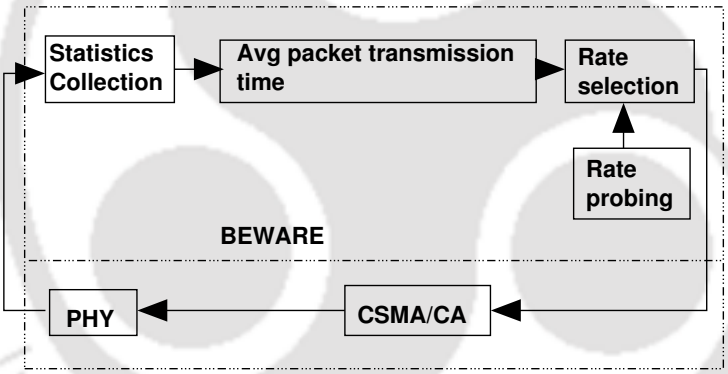

Figure 2.5: Structure of BEWARE Design [129]

A class of rate adaptation algorithms considers the MAC layer scheduling based on multiple data rate support at the physical layer. In [127], the authors have proposed an opportunistic media access protocol for multi-rate ad-hoc networks. The proposed *Opportunistic Auto-Rate* protocol sends multiple back-to-back data packets, whenever the channel quality is good. Luo *et al.*. [128] have proposed a joint scheduling, routing, and power optimization method for multi-rate mesh networks. They have designed a joint optimization to maximize the minimum throughput among all the flows, considering the power control, rate adaptation, routing, and the scheduling. The problem is modeled as a mixed integer linear program, and they have provided an approximation algorithm that can result in a near-optimal solution.

A set of cross layer approaches has been proposed in the literature for rate adaptation in wireless networks. Wang *et al.*. [129] have proposed a rate adaptation algorithm, where they consider the network traffic load along with SNR. They have shown the impact of the background traffic over the data rate selection, and proposed a novel algorithm, called *BEWARE*, for optimum data rate selection based on the background traffic load. Considering Figure 2.4, the selection strategy that results in optimal data rate at different distances is termed as the *oracle selection strategy* in the BEWARE protocol. The authors have shown that with different background traffic load, the oracle selection strategy changes, as shown in Figure 2.4(b). Based on this observation the authors have designed a strategy where the expected packet transmission time is estimated with each available data rate, with consideration of mixed effects from wireless channel condition and collisions. The design of BEWARE is shown in Figure 2.5. After every packet transmission, the statistics collection module gathers the information about the channel busy time, failure probability, and packet transmission time. From this information, the expected packet transmission time is calculated. BEWARE uses periodic rate probing to collect the information for the data rates other than the currently chosen one. The rate selection module constantly compares the packet transmission time to select the data rate that provides the shortest transmission time. Though BEWARE outperforms existing rate adaptation protocols by considering background traffic load, it is does not considers the effect on the number of hops due to changes in the communication ranges. BEWARE operates independently from the topology management and mesh path selection protocols, and therefore does not incorporate the inter-dependency in rate selection, topology management and mesh path selection for a multi-hop and mesh environment.

Similar other cross layer protocols for the rate adaptation has been proposed in the literature. In [130], the authors have proposed to measure *'Channel Busy Time'* to provide extra information to the rate adaptation algorithm. Another cross layer rate adaptation technique has been proposed in [131], where the authors have used physical layer bit error rate at the receiver, for making rate adaptation decision. In [132], the authors have proposed to tune carrier sensing threshold based on the selected data rate to increase the spatial reuse. Though the scheme provides better spatial support, it may increase interference in a dense mesh network. In [133], the authors have proposed another rate adaptation algorithm based on channel contention estimates. All the rate adaptation schemes discussed so far are based on infrastructure wireless and multi-hop networks. However, in the case of mesh network, the rate adaption mechanism is more challenging because of following reasons,

1. Low data rates increase the transmission ranges. For multi-hop networks, long transmission range decreases the number of hops between a source, destination pair. It is well known for the multi-hop networks, that the throughput decreases as the number of hops increases [134]. Therefore, it may be possible that one-hop communication using a low data rate improves the network throughput compared to the two-hop communication using a high data rate. The existing protocols, like BEWARE, does not consider this phenomenon.

2. For a network with moderate to high traffic load, long transmission range increases the possibility of interference among ongoing communications, resulting in throughput degradation.

The above arguments indicate that there is a trade-off among the data rate, the number-of-hops and the interference for multi-rate mesh networks. The existing rate adaptation algorithms do not consider the rate-hops-interference trade-off in the context of mesh networks. Passos *et al.* have proposed a *Metric Aware Rate Adaptation* (MARA) technique [135] that considers joint routing and rate adaptation based on a metric. The metric component of MARA depends upon the expected end-to-end delay. The metric computation approach in MARA is based on a process of conversion of the link success probabilities. This conversion happens in two steps. First, the average SNR of the links is estimated using the information provided by periodic probe packets. Second, the average SNR is used to estimate the link success probabilities at every rate, which is later used to compute the metric value for each rate. While computing the metric value, MARA considers end-to-end semantics for every data rate, which indirectly considers the data rate versus number of hops trade-off. Further, the link success probabilities indirectly measures the interference characteristic at every link. This way, MARA indirectly incorporates rate-hops-interference trade-off. MARA selects the data rate that provides minimum metric value, and that metric value is used to find out the forwarding path.

Though MARA considers the rate-hops-interference trade-off indirectly based on the metric value, the control overhead for MARA is significantly high for 802.11s protocol, as the routing metric does not consider the effect of peer selection, and therefore results in frequent re-peering. The probing overhead of MARA is also significantly high. In a survey paper [4], the authors have first pointed out the possibility of the rate-hops-interference trade-off for multi-rate 802.11s mesh network. However, the paper does not give any concrete model to analyze the trade-off. To the best of our knowledge, no prior work exists to find out the optimal data rate for 802.11s supported mesh routers, considering

the effect of this trade-off over the peer selection, channel access, and the routing decisions.

2.1.5 Design of Path Selection Protocols for Mesh Network

The existing routing, forwarding or path selection protocols for mesh networks can be broadly classified into three groups - proactive [136–140], reactive [141–143] or hybrid [144–148]. The proactive path selection protocols decide the forwarding path before the actual data communication takes place. Therefore the performance of the proactive protocols are affected by the wireless channel dynamics, such as fading, shadowing, multi-path propagation and path loss components. The path diversity in wireless mesh networks does not guarantee that the current best path would remain best for the entire duration of the communication. In [149] and [150], the authors have shown that the proactive path selection performs poorly under variable path loss components. On the other hand, reactive protocols find out the forwarding path in an on-demand basis. Though reactive protocols are more adaptive to the network channel variability, it floods the network with control packets every-time a new flow is introduced in the network. As discussed in [151], the reactive protocols do not perform well for static wireless mesh backbone, and the path selection overhead becomes higher than the communication efficiency.

To cop up with these, hybrid path selection protocols [144–148, 152] have been studied in the literature. The hybrid path selection protocols, being a combination of the proactive and reactive approaches, select the path upto some pivot points using the reactive approach, and the paths from the pivot points to the final destination is discovered using a proactive approach. In [146], the authors have proposed a hybrid path selection scheme for mesh networks, called *'Hybrid On-demand Distance Vector Routing'* (HOVER). HOVER is designed on the top of an on-demand distance vector routing protocol. The protocol uses a link estimation strategy, through HELLO packets, to find out the optimal route towards the mesh gateways. With the link quality estimation, the route request (RREQ) and route reply (RREP) packets are used to find out the best path to the final destination. HOVER minimizes the routing packets broadcast by storing the already found routes in the proactive path selection tables. Though hybrid protocols perform better than proactive and reactive protocols in a mesh backbone network [153], the deficiency of the proactive and reactive protocols still exist upto some extent. The hybrid protocol mainly considers the mobility related issues in the proactive protocol design, and therefore uses reactive protocols upto the point where mobility is high. However, apart from the mobility, network dynamics like the channel and the interference conditions also affect the stability and the flexibility of the proactive path selection, which are not considered in the hybrid

path selection protocol design.

Most of the works in the literature, that discuss about the routing, forwarding or path selection optimization in multi-interface multi-channel mesh networks, like [53, 154–161] and the references therein, are about the joint optimization of MAC layer scheduling, channel access and routing. Though these schemes devise efficient protocols for joint optimization, their main objective is to design the routing metric, considering the channel access and the scheduling information. Nevertheless, almost all of these protocols use either one of the traditional approaches of path selection - proactive, reactive or hybrid.

Another class of routing protocols is recently designed and investigated for mesh networks, called the *'opportunistic routing'* [162–165], that explores the broadcast properties of wireless networks to reduce control overhead in forwarding path selection through the use of network coding. The opportunistic routing mechanism works in two phases. In the first phase, a set of forwarders are selected from the neighbors, that can work as the next-hop relay. In the second stage, the wireless broadcast property is used to send the packet to all of these candidates in a set of forwarders, and the forwarders coordinate among themselves, using network coding and other approaches, to select the node that should broadcast the packet further. In [162], the authors have designed an opportunistic forwarding scheme over mesh protocols, called the *'Simple Opportunistic Adaptive Routing'* (SOAR). The SOAR protocol works in two phases. In the first phase a set of forwarding nodes is selected based on the shortest paths. Every packet is broadcast to the forwarding nodes. The node among the set of forwarding nodes that receives the packet first, rebroadcast the packet. This way, the packet is routed to the destination node. The protocol assumes that all the nodes in the set of forwarding nodes are in one hop distance, and therefore on overhearing the rebroadcast of the packet, they stops forwarding to avoid duplicate packet transmission. The major problem of this routing architecture is the assumption of complete connectivity among the forwarding nodes. Further the protocol does not consider the effect of local information over the global path selection, and there is a high possibility that the node which rebroadcast the packet first, may not use the optimal path.

The biggest challenge in the opportunistic routing is to design a proper coordination among the forwarders, so that duplicate broadcast can be avoided. In a mesh topology, it is not always true that all the forwarders can overhear each other directly (they may not be in the direct communication range). In [166], the authors have proposed a routing metric considering the interference for multi-interface networks. The routing metric considers both the intra-flow and the inter-flow interference and selects a high-throughput path.

Another interference aware routing metric, using bottleneck capacity, is proposed in [167] for making routing decisions. However, all the routing mechanisms as well as the routing metrics have inherent problems of the proactive and the reactive routing protocols - possibility of the stale information in the proactive protocols, and excessive control packet flooding in the reactive protocols.

2.2 IEEE 802.11s Standardization

IEEE has standardized mesh networking in September, 2011 as an amendment to the well established IEEE 802.11 WLAN standard, and subsequently published the revised IEEE 802.11 standard in 2012, popularly known as IEEE 802.11-2012 [25]. According to the IEEE 802.11s terminologies, a QoS associated wireless node that implements the IEEE 802.11s mesh functionality is termed as the mesh station (STA). A basic service set (BSS) with a self-contained network of mesh STAs is called the mesh BSS (MBSS). In a MBSS, one or more mesh STAs, known as mesh gates, work as the gateway to the outside Internet. A mesh STA act as an wireless access point (AP) to the clients, as well as perform relay activities to forward traffic to or from mesh gates, or other mesh STAs.

According to the IEEE 802.11s MAC layer standard, direct communication between two mesh STAs in a MBSS is allowed only if they are mesh peers. After joining in a mesh network, two neighbor mesh STAs use the MPM protocol to establish connections with each other. The standard supports EDCA as the mandatory and MCCA as the optional channel access protocols in a MBSS. EDCA uses the contention based channel access mechanism. On the contrary, MCCA uses a channel reservation mechanism to provide better QoS support among mesh STAs. During the MCCA reservation procedure, every mesh STA reserves the channel bandwidth depending on the interference information obtained from peer neighbors. HWMP is used to find out the best path from a mesh STA to the mesh gate using a combination of the proactive and the reactive approaches.

2.2.1 Enhanced Distributed Channel Access

IEEE 802.11s standard defines EDCA as the mandatory MAC layer channel access protocol. The existing IEEE 802.11 DCF is extended in EDCA to incorporate a number of mechanisms to provide differentiated QoS service by giving different access priorities to different access categories (AC). EDCA adopts the exponential back off scheme of IEEE 802.11 DCF. The initial values for back off counters are randomly selected from the interval $[0, CW - 1]$, where CW is a function of the physical layer specific $CW_{min}\,[AC]$

and $CW_{max}\,[AC]$ attributes. At the first transmission attempt, CW is set equal to the minimum CW, $CW_{min}\,[AC]$. After every unsuccessful transmission, CW is doubled up, upto a maximum value $CW_{max}\,[AC] = 2^m \times CW_{min}\,[AC]$, where the value of m limits the maximum number of attempts after every unsuccessful transmission. For a successful transmission, the CW value is reset to the $CW_{min}\,[AC]$.

In EDCA, a station contending for channel access has to wait for the duration of *'Arbitration Inter-frame Spacing'* (AIFS) before it attempts to access the channel. Each AC is assigned a different $AIFS\,[AC]$ value to differentiate QoS. $AIFS\,[AC]$ is determined by $AIFS\,[AC] = SIFS + AIFSN\,[AC] \times Tslot$. $AIFSN$ is a system parameter for each AC. $SIFS$ is the short inter-frame space time, and $Tslot$ is the time duration of a slot.

IEEE 802.11 EDCA defines four ACs for four classes of services - voice (VO), video (VD), background (BG) and best effort (BE). VO traffics have the highest priority, whereas BE traffics are of lowest priority. The standard defines CW and $AIFSN$ values for the four ACs are as follows:

AC	$CW_{min}\,[AC]$	$CW_{max}\,[AC]$	**AIFSN**
VO	7	15	2
VD	15	31	2
BG	31	1023	3
BE	31	1023	7

2.2.2 Mesh Coordinated Channel Access

MCCA is a reservation based channel access method that aims to optimize the efficiency of the frame transfer inside a MBSS. MCCA is an optional access method that allows mesh STAs to access the wireless media at selected times with lower contention. MCCA is a reservation based channel access protocol where the mesh STAs reserve future channel through MCCA Opportunities (MCCAOP). The MCCA setup is done through mesh beaconing. The mesh STA that transmits a MCCA setup request frame to initiate a reservation becomes the MCCAOP owner of the MCCAOP reservation. The receivers of the MCCA setup request frames are the MCCAOP responders. The MCCAOP owner and the MCCAOP responder advertise the MCCAOP reservation to their neighbors through MCCAOP advertisement messages. The neighbors, after receiving MCCAOP advertisement, defer their transmissions for the MCCAOP period. This reduces the contention between MCCA-supported mesh STAs. However, contention is still possible with non-MCCA nodes. During the MCCAOP, the MCCAOP owner obtains the transmission opportunity through the EDCA based channel access, by contending with

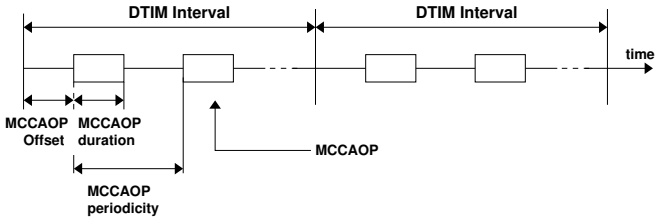

Figure 2.6: MCCAOP Reservation with Periodicity 2

non-MCCA nodes. In order to use MCCA, mesh STAs keep synchronized with their neighboring mesh STAs. The mesh STAs use a DTIM interval for the beaconing and reservation purpose.

The reservation of a MCCAOP is initiated by MCCAOP owner. The MCCAOP owner build a map of the neighborhood MCCAOP periods in the DTIM interval, after hearing advertisement from all its neighbors. Then it determines MCCAOP reservations. The MCCAOP reservation parameters are as follows,

- *duration* of the MCCAOP in slots,
- *offset* of the MCCAOP in slots with respect to the beginning of the DTIM interval,
- *periodicity* to specify how many MCCAOP are to be allocated within the DTIM interval.

The duration, offset and periodicity of MCCAOP in a DTIM interval is shown in Figure 2.6.

Based on the MCCAOP reservation request, the MCCAOP responder either accept or reject the MCCAOP, and send this information through MCCAOP reply message. Once the request is granted, both MCCAOP owner, and MCCAOP responder broadcast this information through MCCAOP advertisement messages. The advertisement message contains the *MCCAOP TX-RX period*, *MCCAOP broadcast period* and the *MCCAOP interference period* report. Based on this information, the neighboring mesh STAs defer their transmission period. The MCCAOP advertisement message also contains *Mesh Access Fraction* (MAF), the ratio between the sum of the TX-RX period, broadcast period and the interference period, to the DTIM interval. The amount of channel capacity reserved for MCCA transmission is upper bounded by the *MAF limit*. It should be noted that, every mesh STAs keep up-to-date list of its neighbors, using the MPM protocol. Periodic beaconing after *'Mesh Beacon Transmission Time'* (MBTT) is used to synchronize between neighboring mesh STAs.

2.2.3 Mesh Path Selection Protocol in IEEE 802.11s

IEEE 802.11s uses HWMP as a mesh path selection protocol. HWMP is a hybrid protocol that aims at merging the advantages of both the proactive and the reactive path selection mechanisms. The protocol can be configured to operate in two modes - the on-demand reactive mode and the tree-based proactive mode. The combination of reactive and proactive modes of path selection enables efficient forwarding in a wide variety of mesh networks. HWMP uses a common set of protocol elements, generation and processing rules inspired by the 'Ad Hoc On-Demand Distance Vector' (AODV) routing protocol [168]. HWMP supports two mode of operation based on network configuration. These modes support different level of functionality as follows:

- **On-demand Reactive Mode:** The functionality of this mode is always available irrespective of whether a mesh gate is configured as a root mesh STA, such that all traffics are forwarded towards/from the root mesh STA (in general, mesh gates). This model allows the mesh STAs to communicate via a peer-to-peer paths.
- **Proactive Tree Building Mode:** This mode amends the functionality of on-demand reactive mode, where a mesh STA (in general, mesh gates) is configured as a root mesh STA. The proactive mechanism create the paths from all the mesh STAs to the root mesh STA, forming a tree-like architecture.

In a mesh networks, both of these modes are used concurrently, and the proactive mode is an extension of the on-demand mode. The standard [25] defines *Airtime Link Metric* (ALM) as the path selection metric for each link. ALM ($\mathfrak{C}$) is defined as follows,

$$\mathfrak{C} = \left[O_{ca} + O_p + \frac{B_t}{r} \right] \frac{1}{1 - e_f} \tag{2.2}$$

Where O_{ca} and O_p are the constants, named as the channel access overhead and the protocol overhead, respectively. B_t is the test frame size. The input parameters r and e_f are the bit rate in Mbps and the frame error rate for the test frame size B_t. The standard defined values for O_{ca}, O_p and B_t are as follows,

Parameter	802.11a	802.11b
O_{ca}	$75\mu s$	$355\mu s$
O_p	$110\mu s$	$364\mu s$
B_t	8224	8224

HWMP uses sequence numbers to avoid the creation of path loops and to distinguish stale and fresh path information. For the shake of completeness, a brief outline of both the reactive mode and the proactive mode based path selection mechanism is described here.

2.2.4 On-Demand Reactive Mode

In on demand reactive mode, the path selection mechanism works as follows,

- The source mesh STA broadcasts a *'Path Request'* (PREQ) message with the destination address and the metric value initialized to zero.
- Upon reception of the PREQ message, a mesh STA drops it if it already received another PREQ message from the same path originator, with the same sequence number, and the old PREQ message offered better path metric value. Otherwise it processes the received PREQ message, and creates or updates the mesh path information to the path originator.
  - If the mesh STA is not the path target, it increases the metric value received with the PREQ message, by the metric value towards the previous hop mesh STA, and broadcasts the updated PREQ message.
  - If the mesh STA is the destination mesh STA, it replies with a *'Path Reply'* (PREP) message towards the best path selected using the PREQ message.
- If a mesh STA receives several PREP messages with the same identifier, but sent through different paths, it saves the information about the path with the best metric value.

2.2.5 Tree Based Proactive Mode

In this mode, a mesh gate is configured as the root, and HWMP sets up a tree to this root. The path selection mechanism works as follows,

- Root mesh gate periodically broadcasts *'Proactive PREQ'* (PPREQ) messages with the destination address set to all ones.
- A mesh STA, on hearing a PPREQ, creates or updates its mesh path information to the mesh gate, updates the metric and hop count of the PPREQ message, and then broadcasts the updated PPREQ message.

- PPREQ message header contains a special bit to denote whether a *'Gratuitous PREP'* message is required to be sent by the mesh STA, to set up a bidirectional path to the mesh gate. If this bit is set, the mesh STA sends a gratuitous PREP message.

2.2.6 Peer Management and Topology Control

The MPM protocol is used to establish, maintain and close mesh peering between mesh STAs. Mesh Peering Open frames are used to establish the mesh peering between two neighbor mesh STAs. The protocol succeeds in establishing a mesh peering when both mesh STAs have sent (or received) a 'Mesh Peering Open' frame and a corresponding 'Mesh Peering Confirm' frame. The mesh peering is valid for a timeout interval called the *MeshHoldingTimeout*. After the expiry of the *MeshHoldingTimeout*, the mesh peering needs to be re-established. A mesh STA can also tear down a peering forcefully by sending a Mesh Peering Close frame. The mesh STAs periodically transmits mesh beacons in order to assist mesh discovery and synchronization among peer mesh STAs.

2.3 Developments over IEEE 802.11s Standardization

Very few works exist on the development of IEEE 802.11s mesh network, as the standard is relatively new. In a survey paper [4], Wang *et al.* have discussed the IEEE 802.11 framework and its design challenges. Garroppo *et al.* [169] have analyzed the performance of IEEE 802.11s from the implementation point of view. Their analysis from a 802.11s mesh testbed reveals that HWMP along with the PMP and MCCA performs better compared to the contention based EDCA protocol. In [170], the authors have proposed a channel assignment strategy for performance optimization of 802.11s mesh network. They have shown that efficient channel assignment strategy can improve the capacity of 802.11s mesh networks. Fu *et al.* [171] have discussed the potential of IEEE 802.11s for intra-mesh congestion control. They have shown that intra-mesh congestion control can avoid packet losses significantly, and therefore improves the overall performance of the mesh backbone.

The channel access protocol for IEEE 802.11s mesh network has been studied by a group of works. In [172], the authors have analyzed the traffic concentration problem at the mesh STAs. They have designed an adaptive hybrid MAC protocol to handle this traffic concentration problem. The proposed protocol is a combination of DCF and Point Coordination Function (PCF) of IEEE 802.11 networks. They have shown that the proposed MAC protocol can accommodate 60% more users compared to the standard

802.11s channel access. Krasilov *et al.* [173] have analyzed the performance of MCCA based channel access in the presence of EDCA supported mesh STAs. They have shown that in a combined mesh network with both EDCA and MCCA support, non-MCCA mesh STAs can cause interference at the MCCA supported mesh STAs. They have proposed a solution to mitigate this problem by allowing MCCA supported mesh STAs to collect information about non-MCCA mesh STAs, before they start channel reservation. Their analysis has revealed that this extra information processing can significantly improve the performance of MCCA supported mesh STAs.

Improvements over HWMP based on directional communication are studied in some of the existing literature. Rafique *et al.* [174] have proposed a simple modification over HWMP to incorporate different smart antenna transmission schemes. The scheme enables mesh node to select spatial multiplexing and beam-forming adaptively according to the channel condition. They have differentiated between omni-directional and directional communication and HWMP is tuned based on the communication mode. However, the work does not consider the scheduling policy at MAC layer for efficient beam-forming. In [175], the authors show that ALM does not provide efficient path for MCCA based channel access. They propose a modification in ALM in HWMP so that the protocol performs better in MCCA based channel access. The modification in HWMP based on sectored antenna is proposed in [35]. They propose a new amendment to reduce the routing overhead related to use of multiple interfaces. However the scheme is based on positioning information of mesh nodes, and thus difficult to implement in practical scenario.

In [176], the author has discussed about the requirements of implementing the mesh path selection at the MAC layer, with a brief insight of the HWMP. Pinherio *et al.* [177] have proposed a distributed hash table (DHT) based cluster-routing protocol over the HWMP. Though the protocol reduces peer searching complexity, it shows scalability problem due to the DHT maintenance. Yang *et al.* [178] have proposed HWMP+, an improvement over basic HWMP, considering the traffic load along with the channel conditions, to determine the mesh path. Though the scheme can improve the network performance, it does not consider the impact of multiple interfaces over the mesh path selection decision. In [46], the authors have reported thorough experimental and simulation studies to analyze the performance of the HWMP. It has been observed from their analysis that small deviation in the ALM from its actual value can result in significant performance degradation in the mesh path selection protocol. This shows the inefficiency of the proactive path selection mechanism in HWMP where the routing (or forwarding) table is precomputed beforehand, and the path selection decisions are made afterwards.

In a recent work [179], the authors have shown that ALM may result in a ping pong effect during mesh path selection. They have characterized the nature of path fluctuations over mesh network, and concluded that the problem with ALM is its inconstancy with the underlying rate adaptation protocols. They have evaluated the ping pong effect caused by ALM through rigorous experiments over a number of rate adaptation algorithms, and found that transmission rate adaptation is the principal cause behind the effect. The authors have shown that the effect is an inherent behavior, and that an accurate characterization of it can help improve network performance. Accordingly, they have presented a pingpong-aware mechanism that, by detecting when a link undergoes such an effect, adapts the mesh path selection protocol for better network performance. In another work [180], the authors have studied QoS aware path selection based on the HWMP proactive and reactive elements. Their scheme is a joint scheduling and path selection mechanism, where HWMP selects a path maintaining end-to-end QoS requirements, and MCCA is tuned to meet that requirement. However, the approach does not consider inter-protocol interactions among channel access and path selection, which is required to ensure performance benefit in a high throughput mesh network.

2.4 Summary

The discussions till now have revealed that, though several research works have pioneered the development in the field of WMN, a set of designing issues are partially solved, or remained unsolved till now. Most of the works in the literature mainly concentrate on mesh protocols based on the naive IEEE 802.11 contention based channel access. With the advent of recent IEEE 802.11s standardization, the basic protocols need to be enhanced according to the standard support. Accordingly, this thesis proposes a set of amendments over the standard protocols, like MCCA, HWMP and MPM, for effective use of the IEEE 802.11s technology. To begin with, the next chapter designs a joint scheduling and mesh path selection mechanism over standard MCCA and HWMP protocols for efficient directional communications in a mesh network.

Chapter 3

Directional Multi-interface Mesh Networks: Scheduling and Mesh Path Selection

As discussed in previous chapters, IEEE 802.11s supports multi-hop connectivity between wireless cliens and mesh gates using intermediate mesh STAs as relay nodes. WMN with omni-directional interfaces has the problem of the low spatial reuse because of the contention among neighboring mesh STAs. Directional interface can solve this problem by transmitting signal in the direction of communication. Uses of multiple directional interfaces at mesh STAs can increase the network capacity significantly through improved spacial reuse [35]. This chapter considers a multi-interface WMN where mesh STAs are equipped with multiple interfaces and directional antenna support. However, use of multiple directional interfaces introduces the problem of interface scheduling for minimizing interference among different interfaces, when operating in a single channel. Because of the limitations on number of channels in the IEEE 802.11 physical layer standard[1], interference can not be eliminated completely, even with multiple channels. Further static channel assignments limits the scalability of the network, and dynamic channel assignment problem is known to be NP-hard. Therefore, a proper interface scheduling mechanism in a directional multi-interface WMN is required to be designed to optimize the channel utility, while maximizing concurrent packet transmissions. To support directional multi-interfaces at mesh STAs, three issues are required to be

[1]The most rigorous commercially used physical layer standard is IEEE 802.11 b/g, that supports only 3 non-overlapping channels.

addressed, as follows.

- Proper scheduling of directional interfaces is required to be designed that minimizes the interference between directional beams and maximizes concurrent packet transmissions.
- Fairness should be assured among contending flows. In the context of the flow fairness in a WMN with homogeneous traffic classes, max-min fairness among the flows need to be assured, where the minimum data rate that a flow can achieve needs to be maximized.
- The mesh path selection decision in a WMN depends on the interface scheduling. Therefore, the optimal mesh paths between two mesh STAs, as well as between a mesh STA and the mesh gate, are required to be find out based on the properties extracted from the scheduling mechanism.

This chapter provides an efficient probabilistic scheduling on the top of the MCCA channel access for efficient scheduling, that minimizes interference among contending beams. The probabilistic scheduling tune the parameter '*MAF limit*' for MCCA channel access, that represents the maximum number of MCCAOPs that can be reserved within a single DTIM interval. The MAF limit is tuned based on the requirement for channel access. If requirement is more, the channel is accessed in an aggressive way, by reserving more number of MCCAOPs. On the contrary, if requirement is less, the channel is reserved in a restrictive way. However the requirements for all the contending beams are taken into consideration to provide a fair access to all the interfaces involved in communication. This requirement calculation is modeled as a convex optimization problem. The global convex optimization problem is subdivided into local optimization based on the convexity property - 'the local optima is the global optima'. Every mesh STA requires only its local information to solve the local optimization - thus the requirement calculation is fully distributive in nature. Based on the information extracted during the scheduling mechanism, a MAC layer mesh path selection protocol is proposed on the top of the HWMP protocol, that targets to find the optimal path for a newly admitted flow.

The rest of the chapter is organized as follows. Section 3.1 provides the motivation behind the requirement of a proper scheduling for directional multi-interface WMN, using an example. The network model and the assumptions are briefly described in section 3.2. Section 3.3 provide the characterization of the interference model in a directional multi-interface WMN. The proposed probabilistic scheduling on the top of the MCCA channel

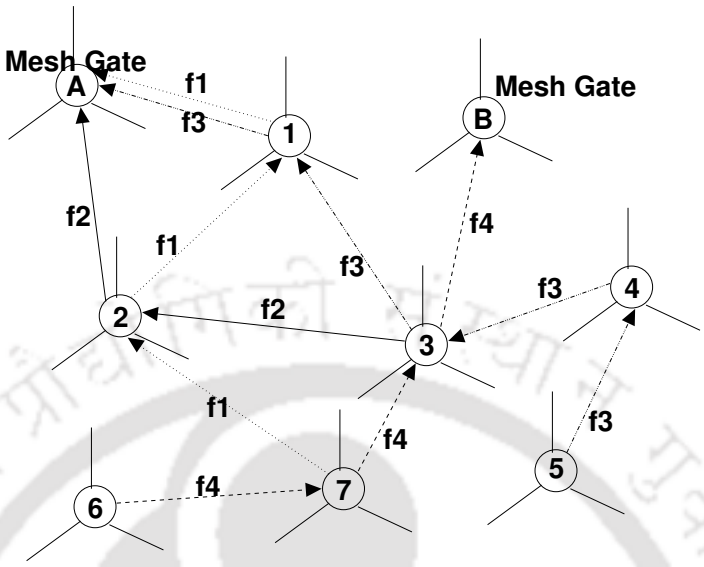

Figure 3.1: Multiple Flow Scenario

access is described in Section 3.4. Section 3.5 discusses the modifications in the HWMP protocol designed for providing an effective mesh path selection protocol based on the interface scheduling. The performance of the proposed scheme is analyzed using simulation results, which is reported in section 3.6. Finally, section 3.7 concludes the chapter.

3.1 Motivation for Scheduling

The requirement for a proper scheduling in a directional WMN is analyzed in this subsection with an example network scenario. Fig. 3.1 shows an example network with 2 mesh gates (STA_A and STA_B) and 7 mesh STAs (STA_1-STA_7). Every mesh STA is equipped with two three-sectored antennas connected with two different interfaces. So simultaneous transmission and reception are possible wither by channel separation or by spatial reuse. There are 4 traffic flows from the mesh STAs to the mesh gates. Considering flow $f3$, the sub-flow $f3(STA_5 \rightarrow STA_4)$ does not interfere with any other flows, and thus STA_5 can transmit packets for flow $f3$ with normalized transmission rate 1. The next-hop sub-flow $f3(STA_4 \rightarrow STA_3)$ contends with the sub-flow $f4(STA_3 \rightarrow STA_B)$, and so STA_4 can transmit the packets for the flow $f3$ with normalized transmission rate equals to 0.5. The sub-flow $f3(STA_3 \rightarrow STA_1)$ contends with two other sub-flows, and therefore can achieve the maximum normalized transmission rate of 0.33. Finally, the sub-flow $f3(STA_1 \rightarrow STA_A)$ can achieve normalized transmission rate of 0.5. So, it

can be observed that the flow $f3$ can transmit data packets at an overall normalized transmission rate of 0.33 (minimum transmission rate among all the sub-flows). However, because of the sub-flow $f3(STA_4 \rightarrow STA_3)$, the data packets can be overloaded at STA_3. Thus a proper scheduling should restrict the transmission rate of this sub-flow to 0.33. It can also be observed that, because of the sub-flow $f3(STA_4 \rightarrow STA_3)$ and the sub-flow $f1(STA_7 \rightarrow STA_2)$, flow $f4$ achieves overall transmission rate of 0.5, whereas it can achieve transmission rates upto 0.66, if it can be scheduled properly. This shows the requirement of a proper scheduling mechanism that should restrict the transmission rates of all the sub-flows to the maximum achievable transmission rate for the corresponding end-to-end flow. This reduces the packet overflows at the intermediate mesh STAs, as well as maximizes the network capacity and the spacial reuse.

3.2 Network Model and Assumptions

In this chapter, switched beam smart antennas [181] are considered for communication. These types of directional antennas are cost-effective, and are widely used in modern commercially available wireless routers. Further, static channel assignment algorithms give considerably better results for switched beam smart antenna, as the possible beam directions are known a priori. For switched beam smart antenna, an interface can be either in the transmit or in the receive mode at any instance of time. Simultaneous transmissions and receptions are not possible. However, every mesh STA is equipped with multiple such interfaces, and thus simultaneous transmissions and receptions are possible at a single mesh STA, provided they use different channels or there exists sufficient spatial diversity between the sender and the receiver beams. This chapter assumes that an off-line static channel assignment algorithm, such as [182] exists to statically assign channels based on the interference characteristics. It can be noted that some of the works in literature, such as [183] and the references therein, propose dynamic channel assignment strategies for effective network utilization. However, dynamic channel assignment makes a circular dependency among the channel assignment, interface selection, MAC layer channel access and the mesh path selection schemes. Further it is known to be NP-hard [184]. Therefore assigning channel dynamically imposes significant overhead on the network design [185].

Although use of multiple channels improves network performance significantly, it can not avoid interference completely. Current physical layer standards, such as IEEE 802.11b/g/n have only three non-overlapping channels. Though IEEE 802.11a has more number of non-overlapping channels, different countries apply their own regulations to

the allowable channels. For this reason, actual number of channels that can be used for commodity mesh networks is restricted. Number of interfering interfaces is likely to be substantially more than the number of available channels for a multi-interface mesh network. Therefore, interference still exists in a multi-radio multi-channel mesh network, that needs to be addressed during the channel access and scheduling mechanisms.

It is assumed that every mesh STA uses MCCA as the MAC layer channel access protocol, and HWMP as the mesh path selection protocol. To allow simultaneous operations using different interfaces, every interface maintains separate MAC layer scheduling parameters. With the limitations of the number of channels, it can be safely assumed that the interfaces attached with a single mesh STA uses separate non-overlapping channels to avoid self-interference due to simultaneous transmissions and receptions. However in the proposed scheduling mechanism, the problem is modeled from the view of the individual interfaces, rater than on per-STA basis. This type of modeling is justifiable when every interface independently participate in the scheduling mechanism, with its own set of scheduling and MAC parameters. Further, interface based modeling for directional multi-interface WMNs can be easily tuned based on the network setup and the interference characteristics. Therefore, without the loss in generality, the rest of this chapter uses the term 'interface' instead of the term 'mesh STA', to denote a particular interface of a particular mesh STA. Every interface in a WMN can be uniquely identified by its MAC address. This chapter assumes that every flow in the network are of equal priority.

3.3 Interference Model and Characterization

This work considers *'Protocol Interference Model'* [186,187] to capture interference among the contending interfaces. Let R_c be the communication range of an interface. According to the protocol interference model, two interfaces interfere with each other if their physical distance is less than $\rho \times R_c$, where the value of ρ depends on the physical carrier sensing and the packet reception model. The supports of null steering [188] and capture effects [189] in modern wireless hardwares limit the interference such that in general, $\rho \leq 2$ [190]. Protocol interference model is an approximation of the physical interference model. However, it is distributed in nature, and can be used locally at every interface with the local neighborhood information [187]. In [191], the authors have shown that with proper parameter settings (such as the transmit power and the capture threshold), the protocol interference model can perform as good as the physical interference model. Further if $\rho \leq 2$, the protocol interference model can be used correctly to capture the interference

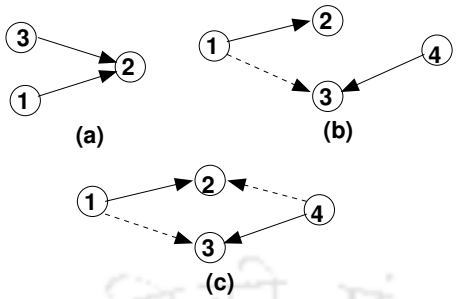

Figure 3.2: (a) Same Receiver (b) Different Receiver, One-sided Interference (c) Different Receiver, Both-sided Interference

information with the two-hop broadcasting and the network overhearing.

A WMN can be represented as a directed graph $\mathcal{G}_{net}(\mathbb{V}_{net}, \mathbb{E}_{net})$, where $\mathbb{V}_{net}$ is the set of directional interfaces, and $\mathbb{E}_{net}$ is the set of communication links between them. In case of directional antenna based communications, an edge $e(\mathcal{I}_i, \mathcal{I}_j) \in \mathbb{E}_{net}$ is used to connect two nodes, where $\{\mathcal{I}_i, \mathcal{I}_j\} \in \mathbb{V}_{net}$, if the transmitter beam of $\mathcal{I}_i$ and the receiver beam of $\mathcal{I}_j$ are calibrated towards each other. In this case, $\mathcal{I}_i$ can directly communicate with $\mathcal{I}_j$.

Definition 3.1. *A **Communication Graph** $\mathcal{G}_{com}(\mathbb{V}_{com}, \mathbb{E}_{com}) \subseteq \mathcal{G}_{net}(\mathbb{V}_{net}, \mathbb{E}_{net})$, where $\mathbb{V}_{com} = \mathbb{V}_{net}$ and $e(\mathcal{I}_i, \mathcal{I}_j) \in \mathbb{E}_{com}$ if $\mathcal{I}_i$ is communicating with $\mathcal{I}_j$, denoted as $\mathcal{I}_i \rightarrow \mathcal{I}_j$.*

Definition 3.2. *Given a network graph $\mathcal{G}_{net}(\mathbb{V}_{net}, \mathbb{E}_{net})$ and the corresponding communication graph $\mathcal{G}_{com}(\mathbb{V}_{com}, \mathbb{E}_{com})$, the **Interference Graph** $\mathcal{G}_{inf}(\mathbb{V}_{inf}, \mathbb{E}_{inf})$ for the network can be constructed as follows. Let $\mathbb{V}_{inf} = \mathbb{V}_{com}$. There exist a directional edge from $\mathcal{I}_j \in \mathbb{V}_{inf}$ to $\mathcal{I}_k \in \mathbb{V}_{inf}$ if the transmissions of $\mathcal{I}_j$ interfere with the transmission of $\mathcal{I}_k$.*

It can be noted that interference is not symmetrical [192], i.e. I_j interfering with I_k does not indicate that I_k is also interfering with I_j. Further, the receiver for I_j and I_k may be same or different. In Figure 3.2(a), interface 1 and interface 3 transmit to the same interface 2. Therefore interface 1 and interface 3 interfere with each other. There would be directed edges from 1 to 3 as well as 3 to 1 in the interference graph. In Figure 3.2(b), interface 1 and interface 4 transmit to different receivers, however, the transmissions of interface 1 affect transmissions of interface 4 only. So, there would be directed edge only from 1 to 4 in the corresponding interference graph. There would be no edge from 4 to 1. Similarly in Figure 3.2(c), though interface 1 and interface 4 transmit to different receivers, their transmissions interfere with each other. Accordingly there would be directed edges from both 1 to 4 and 4 to 1 in the interference graph. This interface based interference graph is different from the link interference graph [193] used in the existing literatures, as

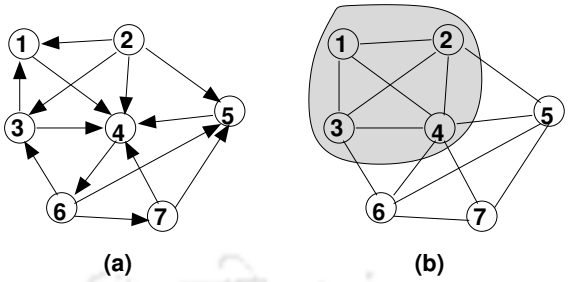

Figure 3.3: (a) Interference Graph (b) Channel Sharing Graph and Maximal Cliques

discussed in Chapter 2, where the edges in a communication graph represent the vertices in the interference graph and there exists an edge if two links interfere with each other. Interface based interference graphs are efficient for directional communications in a multi-interface directional mesh network because of the following reasons.

- For multi-interface network, interference is interface specific rather than node specific. An interface can either be in transmit or receive mode. Only the interfaces that are in transmit mode, contribute to the network interference.
- Interface based interference is easy to capture in the MCCA based mesh network. Let every mesh STA broadcast the transmissions and the interference informations of its two-hop neighbors through the MCCAOP advertisement messages. As a result every mesh STA has three hop communication information for every interfaces, from where the local interference graph up to three hops can be constructed using the protocol interference model, through a method similar to [187]. Later it would be shown that three hop interference graph is sufficient to design an effective channel access mechanism.
- Interface based interference model can easily capture the asymmetric nature of the interference from the directed interference graph.

Network interference is an important parameter that characterizes the maximum network capacity as well as the maximum throughput guarantee for the traffic flows. Let $\mathcal{G}_{inf}$ be the interference graph. The corresponding undirected graph of $\mathcal{G}_{inf}$ is constructed by removing the directionality of the edges. Then the corresponding graph is called *Channel Sharing Graph*, $\mathcal{G}_{ch}$. The reason behind removing the directionality of edges can be explained using an example. Let interface I_j interferes with interface I_k, however, interface I_k does not interfere with I_j. This indicates that when I_k transmits, I_j should

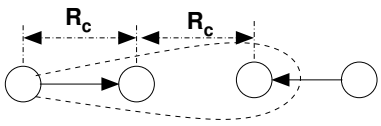

Figure 3.4: Worst case interference scenario

remain silent. Otherwise it would affect the transmissions of I_k. Similarly, when I_j transmits, I_k should remain silent as it would affect its own transmissions. Let both the interfaces are of equal priority. Then the total channel share should be divided equally between the two interfaces to have a minimum interference channel access.

Figure 3.3(a) shows an interference graph, and Figure 3.3(b) shows the corresponding channel sharing graph by removing the directionality of the edges. The maximal cliques in a channel sharing graph are used to characterize the maximum throughput that an edge in a communication graph can achieve. A maximal clique in a channel sharing graph indicates that all the interfaces in that clique interfere with each other, and therefore the total channel share should be divided among all those interfaces. An important proposition from the channel sharing graph can be derived, stated as follows.

Proposition 3.1. *Let C be a maximal clique in $\mathcal{G}_{ch}$. Then,*

$$\sum_{I_j \in C} \left(\sum_{\forall \mathcal{F}_{I_j}} \lambda(\mathcal{F}_{I_j}) \right) \leq \eta \tag{3.1}$$

where $\mathcal{F}_{I_j}$ is a traffic flow through the interface I_j, and $\lambda(\mathcal{F}_{I_j})$ is the data rate for that flow. η is the maximum network capacity. Equation (3.1) is also called the *'clique constraint'*, and η is called the *'clique capacity'*. As an example, the total channel share for the interfaces 1, 2, 3 and 4 from Figure 3.3(b) should be less than the clique capacity.

The MCCA reservation procedure uses MCCAOP advertisement messages that broadcast two-hop interference information (both at the sender and at the receiver) to the neighborhood. Therefore, every mesh STA can find out the three hop interference graph using MCCAOP advertisement messages and the protocol interference model. Following theorem bounds the clique constraint in three hop neighborhood.

Theorem 3.1. *Let C be a maximal clique in $\mathcal{G}_{ch}$. Then any two interfaces $I_j \in C$ and $I_k \in C$ can be at maximum three-hop away.*

Proof. It has been assumed that based on the protocol interference model, interference range is $\rho \times R_c$, where $\rho \leq 2$. Then for the interface based interference graph, the worst

case interference scenario is shown in Figure 3.4. Accordingly, the receiver of the interface I_k can be at most in two hop distance from I_j. This indicates that I_j and I_k are at most in three hop distance. □

Following corollary can be derived directly from Theorem 3.1.

Corollary 3.1. *Let $I_j \in \mathbb{V}_{com}$. Then I_j can compute all the maximal cliques to which it belongs with three-hop neighbor information.*

Proof. Let C be a maximal clique and $I_j \in C$. Then $\forall I_k \in C; I_k \neq I_j$, I_j and I_k are at most three hop distance away (according to Theorem 3.1). This indicates that I_j can compute C with three hop neighbor information. □

Therefore, broadcasting two hop neighbor information with MCCAOP advertisement message helps the mesh STAs to characterize the interference constraints independently at every interface. This can capture the asymmetric behavior of the interference as well as can model the real-time interference scenario, where the interference range is more than the communication range. As discussed earlier, modern technologies, such as the adaptive power control [194], null steering [188] and the capture effect [189] are used to limit the interference range within twice the communication range. In this context, the proposed model can effectively characterize the interference in a multi-interface mesh network.

Once the interference information is characterized, it can be used to find out the required traffic demand at every interface. For this, a centralized optimization problem is formulated to find out the optimum traffic demand, as discussed in the following section.

3.4 Flow Scheduling for Directional Multi-interface WMN

The proposed scheme finds the maximum achievable transmission rate for all flows based on the interference information. A linear programming (LP) formulation is proposed to find out the maximum theoretical achievable transmission rate for all flows, that minimizes the interference among neighboring communications.

3.4.1 Centralized Formulation for Flow Scheduling

To find out the maximum achievable transmission rates for all the in the network, a centralized linear convex optimization problem is formulated, when the communication graph $\mathcal{G}_{com}(\mathbb{V}_{com}, \mathbb{E}_{com})$ and the channel sharing graph, corresponding to the interference graph $\mathcal{G}_{inf}(\mathbb{V}_{inf}, \mathbb{E}_{inf})$, are known. Let the sub-flow for a flow $\mathcal{F}$ from $\mathcal{I}_i \rightarrow \mathcal{I}_j$, denoted

as $\mathcal{F}_{(\mathcal{I}_i,\mathcal{I}_j)}$, be the part of the flow where $\mathcal{I}_i$ and $\mathcal{I}_j$ are in one-hop distance. For example, if flow $\mathcal{F}$ follows the path $\{\mathcal{I}_s \rightarrow \mathcal{I}_p \rightarrow \mathcal{I}_q \rightarrow \mathcal{I}_r \rightarrow \mathcal{I}_d\}$, then it can be divided into four sub-flows as $\{(\mathcal{I}_s \rightarrow \mathcal{I}_p), (\mathcal{I}_p \rightarrow \mathcal{I}_q), (\mathcal{I}_q \rightarrow \mathcal{I}_r)$ and $(\mathcal{I}_r \rightarrow \mathcal{I}_d)\}$. The constraint for this problem is that, for all the set of interfering sub-flows, the summation of their normalized transmission rates should be less than the normalized link capacity. As the set of sub-flows, that interfere with each other, essentially forms a maximal clique in the channel sharing graph, the constraint can be expressed as the maximal clique constraint, which is expressed as follows. For all sets of maximal cliques of an channel sharing graph $\mathcal{G}_{ch}$, the normalized transmission rates should be less than the network capacity. The constants and variables used to formulate the centralized problem are as follows,

- $\mathbb{F}$ is the set of flows,
- $\mathbb{S}(\mathcal{F})$ is the set of sub-flows for the flow $\mathcal{F} \in \mathbb{F}$,
- $\lambda(.)$ is the transmission rate for a flow or a sub-flow,
- $\mathbb{C}$ is the set of maximal cliques from the channel sharing graph $\mathcal{G}_{ch}$,
- $C_i \in \mathbb{C}$ is the i^{th} maximal clique.

The optimization problem is formulated as follows,

Problem 3.1.

$$\max \sum_{\forall \mathcal{F} \in \mathbb{F}} \lambda(\mathcal{F}) \tag{3.2a}$$

$$\lambda(\mathcal{F}) = \min\{\lambda(\mathcal{F}_{(\mathcal{I}_i,\mathcal{I}_j)}) | \forall \mathcal{F}_{(\mathcal{I}_i,\mathcal{I}_j)} \in \mathbb{S}(\mathcal{F})\} \quad ; \forall \mathcal{F} \in \mathbb{F} \tag{3.2b}$$

$$\sum_{\forall \mathcal{I}_k \in C_i} \left(\sum_{\forall \mathcal{F}_{\mathcal{I}_k}} \lambda(\mathcal{F}_{\mathcal{I}_k}) \right) \leq \eta \quad ; \forall C_i \in \mathbb{C} \tag{3.2c}$$

$$\lambda(\mathcal{F}_{(\mathcal{I}_k,\mathcal{I}_l)}) > 0 \quad ; \forall \mathcal{F}_{(\mathcal{I}_k,\mathcal{I}_l)} \in \mathbb{S}(\mathcal{F}) \wedge \forall \mathcal{F} \in \mathbb{F} \tag{3.2d}$$

The objective function denotes that the normalized transmission rates for all flows have to be maximized. The first set of constraints denote that the normalized transmission rate for a flow is the minimum achievable transmission rate among all its sub-flows. It will be discussed later that, maximizing the minimum transmission rates among all the sub-flows ensures the max-min fairness among the flows. The second set of constraints are the clique constraints and the third set of constraints are for the non-zero satisfiability. The LP given in Problem 3.1 can be solved in a centralized way when the complete communication

graph and the interference graph are known. The transmission rates for different sub-flows are obtained by solving the LP, which maximizes the total normalized transmission rate.

Lemma 3.1. *Let* $\boldsymbol{\lambda} = [\lambda(\mathcal{F}_1), \lambda(\mathcal{F}_2), ..., \lambda(\mathcal{F}_n)]^T$. *Then the centralized optimization given in Problem 3.1 is a convex optimization of* $\boldsymbol{\lambda}$.

Proof. Let $U_c(\boldsymbol{\lambda})$ denotes the objective function given in equation (3.2a), i.e. $U_c(\boldsymbol{\lambda}) = \sum_{\forall \mathcal{F}} \lambda(\mathcal{F})$. Let

$$V_c^i(\boldsymbol{\lambda}) = \sum_{\forall \mathcal{I}_k \in C_i} \left(\sum_{\forall \mathcal{F} \in \mathbb{F}}^{\mathcal{F}_{(\mathcal{I}_k,\mathcal{I}_l)} \in \mathbb{S}(\mathcal{F})} \lambda(\mathcal{F}_{(\mathcal{I}_k,\mathcal{I}_l)}) \right)$$

Then the Lagrangian of the centralized scheduling is written as,

$$\begin{aligned} \zeta(\boldsymbol{\lambda}, p_1, p_2, ..., p_i, q_1, q_2 ..., q_{\mathcal{F}_{(\mathcal{I}_i,\mathcal{I}_j)}}) \; &= U_c(\boldsymbol{\lambda}) + \sum_i p_i (V_c^i(\boldsymbol{\lambda}) - 1) - \\ &\sum_{\mathcal{F}_{(\mathcal{I}_k,\mathcal{I}_l)}} q_{\mathcal{F}_{(\mathcal{I}_k,\mathcal{I}_l)}} . \lambda(\mathcal{F}_{(\mathcal{I}_k,\mathcal{I}_l)}) \end{aligned} \tag{3.3}$$

Where p_1, p_2, ..., p_i, q_1, q_2, ..., $q_{\mathcal{F}_{(\mathcal{I}_i,\mathcal{I}_j)}}$ are positive Lagrange multipliers. Now partially differentiating equation (3.3) with respect to $\lambda(\mathcal{F}_{(\mathcal{I}_k,\mathcal{I}_l)})$,

$$\frac{\delta}{\delta \boldsymbol{\lambda}} \zeta = 1 + \left(\sum_{i \in \|\lambda(\mathcal{F}_{(\mathcal{I}_k,\mathcal{I}_l)})\|} p_i \right) - q_{\mathcal{F}_{(\mathcal{I}_k,\mathcal{I}_l)}} \tag{3.4}$$

and

$$\frac{\delta^2}{\delta \boldsymbol{\lambda}^2} \zeta = 1 > 0 \tag{3.5}$$

From equation (3.5), the optimization problem is a convex optimization with finite number of elements. The solution set is also a discrete finite convex set with zero as the lower bound and η as the upper bound. □

As discussed earlier, an interface can have only its local three-hop information based on the MCCA protocol. So a distributed solution is required to be designed to find out the maximum achievable transmission rates of all flows, based on the partially available per-interface information. This is presented in the next subsection.

3.4.2 Distributed Flow Scheduling

In wireless network, each node has partial information about its neighborhood. It can be safely assumed that every interface has its three-hop network graph as well as three-hop

communication graph (from two-hop broadcast of MCCAOP Advertisement messages, as discussed earlier). From these information, an interface can find out the local interference graph as well as the channel sharing graph for its three-hop neighborhood. The local maximal cliques (the cliques formed using the three-hop channel sharing graph) can be computed from the local channel sharing graph. The following theorem and corollary give the basis for the distributed computation of scheduling decisions,

Theorem 3.2. *The local maximal cliques are also globally maximal.*

Proof. Let $\mathcal{C}_\ell(\mathcal{I}_s)$ be a local maximal clique computed at an interface $\mathcal{I}_s$ and $\mathcal{C}_g$ be a global maximal clique where $\mathcal{I}_s \in \mathcal{C}_g$. Also let $\mathcal{I}_u$ be another interface from the channel sharing graph, and assume,

$$\mathcal{C}_g = \mathcal{C}_\ell(\mathcal{I}_s) \cup \{\mathcal{I}_u\} \tag{3.6}$$

Now, $\mathcal{I}_s \in \mathcal{C}_g$ and $\mathcal{I}_u \in \mathcal{C}_g$ implies one of the following three cases in the corresponding interference graph,

- $\mathcal{I}_s \rightarrow \mathcal{I}_u$, i.e. $\mathcal{I}_s$ interferes with $\mathcal{I}_u$,
- $\mathcal{I}_s \leftarrow \mathcal{I}_u$, i.e. $\mathcal{I}_u$ interferes with $\mathcal{I}_s$,
- $\mathcal{I}_s \leftrightarrow \mathcal{I}_u$, i.e. $\mathcal{I}_s$ and $\mathcal{I}_u$ both interfere with each other

In either of the three cases, $\mathcal{I}_s$ and $\mathcal{I}_u$ are within two hop neighborhood according to the protocol interference model. As the proposed model assumes that every interface has two hop communication graph as well as two hop interference graph, the assumption given in equation (3.6) can not hold true. Therefore, $\mathcal{C}_{ell}(\mathcal{I}_s) = \mathcal{C}_g$. □

Following corollary can be derived directly from Theorem 3.2.

Corollary 3.2. *The union of all local maximal cliques is the complete set of global maximal cliques.*

With the local information obtained from local maximal cliques, every interface solves a local search problem (LSP). The notion of *"partial flow"*, required for the LSP formulation, is defined as follows.

Definition 3.3. *The **partial flow** for a flow $\mathcal{F}$ from $\mathcal{I}_i$ to $\mathcal{I}_j$ ($\mathcal{F}_{(\mathcal{I}_i,\mathcal{I}_j)}$) is defined as the union of all sub-flows of the flow $\mathcal{F}$ from $\mathcal{I}_i$ to $\mathcal{I}_j$.*

It can be noted that, according to the definition of the sub-flow and the partial-flow, all sub-flows are partial-flows, but the reverse is not true. The following local variables are used for the formulation of the LSP for distributed scheduling,

- $\mathbb{F}(\mathcal{I}_i)$ is the set of flows passing through $\mathcal{I}_i$,
- $\mathbb{S}'(\mathcal{I}_i)$ is the set of sub-flows for all the flows which are in two-hop neighborhood[2] of $\mathcal{I}_i$,
- $\lambda(\mathcal{F}_{(\mathcal{I}_i,\mathcal{I}_j)})$ is the transmission rate for the partial-flow $\mathcal{F}_{(\mathcal{I}_i,\mathcal{I}_j)}$,
- $ORG(\mathcal{F})$ be the originating interface for a flow $\mathcal{F}$,
- $DST(\mathcal{F})$ be the destination interface for flow $\mathcal{F}$,
- $PRV(\mathcal{I}_i,\mathcal{F})$ is the previous hop interface for flow $\mathcal{F}$ where the current interface is $\mathcal{I}_i$,
- $\mathbb{C}(\mathcal{I}_i)$ is the set of local maximal cliques at $\mathcal{I}_i$

The LSP at $\mathcal{I}_s$ is formulated as follows;

Problem 3.2.

$$\max \sum_{\mathcal{F}\in\mathbb{F}(\mathcal{I}_s)} \lambda(\mathcal{F}) \tag{3.7a}$$

$$\lambda(\mathcal{F}) = \min\left\{\lambda(\mathcal{F}_{(ORG(\mathcal{F}),PRV(\mathcal{I}_s,\mathcal{F}))}), \lambda(\mathcal{F}_{(PRV(s,\mathcal{F}),s)}), \lambda(\mathcal{F}_{(\mathcal{I}_s,DST(\mathcal{F}))})\right\} \quad ;\forall\mathcal{F}\in\mathbb{F}(\mathcal{I}_s) \tag{3.7b}$$

$$\sum_{\forall\mathcal{I}_k\in C_i}\left(\sum_{\forall\mathcal{F}_{(\mathcal{I}_k,\mathcal{I}_l)}\in\mathbb{S}'(\mathcal{I}_s)} \lambda(\mathcal{F}_{(\mathcal{I}_k,\mathcal{I}_l)})\right) \leq \eta \quad ;\forall C_i\in\mathbb{C}(\mathcal{I}_s) \tag{3.7c}$$

$$\lambda(\mathcal{F}_{(PRV(\mathcal{I}_s,\mathcal{F}),\mathcal{I}_s)}) > 0 \quad ;\forall\mathcal{F}\in\mathbb{F}(\mathcal{I}_s) \tag{3.7d}$$

Every interface tries to maximize the transmission rates of all flows passing through it. The first set of constraints say that the transmission rate for a flow is the minimum transmission rate of three partial-flows - from the source to the previous-hop interface, from the previous-hop interface to the interface in consideration, and from the interface in consideration to the destination interface. The second set of constraints are the local maximal clique constraints. The third set of constraints are for the non-zero satisfiability.

Theorem 3.3. *The solution of the centralized problem given in Problem 3.1 remains within the solutions of the LSP given in Problem 3.2.*

[2]Though every interface has three-hop flow informations, only two hop flow informations are used to bound the local maximal cliques to avoid possible overlapping of clique constraints during computation.

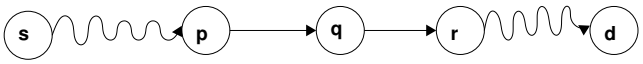

Figure 3.5: Example Flow from $\mathcal{I}_s$ to $\mathcal{I}_d$

Proof. By Lemma 3.1, there is an optimum for the optimization problem given in Problem 3.1, and it must satisfy the Karush-Kuhn-Tucker (KKT) optimality condition, i.e.

$$\frac{\delta}{\delta \boldsymbol{\lambda}} U_c \boldsymbol{\lambda} + \sum_i \nu_i . \frac{\delta}{\delta \boldsymbol{\lambda}} V_c^i \boldsymbol{\lambda} - \sum_{\mathcal{F}_{(\mathcal{I}_k,\mathcal{I}_l)}} \upsilon_{\mathcal{F}_{(\mathcal{I}_k,\mathcal{I}_l)}} . \frac{\delta}{\delta \boldsymbol{\lambda}} \lambda(\mathcal{F}_{(\mathcal{I}_k,\mathcal{I}_l)}) = 0 \tag{3.8}$$

where $\{\nu_i | C_i \in \mathbb{C}\}$ and $\{\upsilon_{\mathcal{F}_{(\mathcal{I}_k,\mathcal{I}_l)}} | \mathcal{F}_{(\mathcal{I}_k,\mathcal{I}_l)} \in \mathbb{S}(\mathcal{F})\}$ are the positive KKT multipliers.

Consider the LSP at an interface s. Then,

(i) $\mathbb{S}'(\mathcal{I}_s) \subset \mathbb{S}(\mathcal{F})$;

(ii) $\mathbb{F}_{(\mathcal{I}_i)} \subset \mathbb{F}$;

(iii) $\mathbb{C}(\mathcal{I}_s) \subset \mathbb{C}$ and

(iv) $\bigcup_{\forall \mathcal{I}_s} \mathbb{C}(\mathcal{I}_s) = \mathbb{C}$ (from Corollary (3.2)).

Thus Problem 3.2 is a convex subset of Problem 3.1. Then the optimality condition for Problem 3.2 satisfies if the optimality condition for Problem 3.1 (i.e. equation (3.8)) gets satisfied.

Conversely, because of the convexity property of Problem 3.1 and Problem 3.2, the local optimum tends to the global optimum. The solution of Problem 3.1 remains within the local solutions of Problem 3.2. □

The working of the proposed LSP is explained using a diagram given in Fig. 3.5. To solve the LSP correctly at an interface q, following three partial flow components need to be known,

(i) $\lambda(\mathcal{F}_{(\mathcal{I}_s,\mathcal{I}_p)})$;

(ii) $\lambda(\mathcal{F}_{(\mathcal{I}_p,\mathcal{I}_q)})$;

(iii) $\lambda(\mathcal{F}_{(\mathcal{I}_q,\mathcal{I}_d)})$.

$\lambda(\mathcal{F}_{(\mathcal{I}_p,\mathcal{I}_q)})$ is known to $\mathcal{I}_q$, as it is the receiving rate of flow $\mathcal{F}$ at $\mathcal{I}_q$. It can be noted that the receiving rate provides more accurate result compared to the sending rate, while calculating the overall transmission rate of a flow, as the channel loss can be captured

through the receiving rate. Let, the receiving rate for flow $\mathcal{F}$ at $\mathcal{I}_q$ is initialized at $\xi(\mathcal{F}, \mathcal{I}_q)$. The value of $\xi(\mathcal{F}, \mathcal{I}_q)$ is determined at every interface based on the priority of the flow. Let the priority of flow $\mathcal{F}$ is $\wp_{\mathcal{F}}$. Then $\xi(\mathcal{F}, \mathcal{I}_q)$ is calculated as follows:

$$\xi(\mathcal{F}, \mathcal{I}_q) = \eta \times \frac{\wp_{\mathcal{F}}}{\sum_{\mathcal{F}' \in \mathbb{C}(\mathcal{I}_q)} \wp_{\mathcal{F}'}} \tag{3.9}$$

The three components are initialized as,

(i) $\lambda(\mathcal{F}_{(\mathcal{I}_s, \mathcal{I}_p)}) = \eta$

(ii) $\lambda(\mathcal{F}_{(\mathcal{I}_p, \mathcal{I}_q)}) = \xi(\mathcal{F}, \mathcal{I}_q)$

(iii) $\lambda(\mathcal{F}_{(\mathcal{I}_q, \mathcal{I}_d)}) = \eta$

It can be observed, that $\lambda(\mathcal{F}_{(\mathcal{I}_s, \mathcal{I}_p)})$ can be obtained from the solution of the LSP at $\mathcal{I}_p$, and $\lambda(\mathcal{F}_{(\mathcal{I}_q, \mathcal{I}_d)})$ can be obtained from the solution of the LSP at $\mathcal{I}_r$. To reduce the network overhead, these solutions are piggybacked with the DATA and the ACK packets of the flow $\mathcal{F}$. Thus at i^{th} iteration, $\mathcal{I}_q$ uses the solution obtained at the $(i-1)^{th}$ iteration at $\mathcal{I}_p$ and $\mathcal{I}_r$. The global solution is obtained in an iterative way. The working of the LSP is formally given in Algorithm 3.1. $SOL_k(\mathcal{F}, \mathcal{I}_s)$ denotes the solution obtained at k^{th} iteration at $\mathcal{I}_s$. $NXT(\mathcal{I}_s, \mathcal{F})$ denotes the next hop interface for flow $\mathcal{F}$, where the interface in consideration is $\mathcal{I}_s$. $SOL(\mathcal{F}, \mathcal{I}_s)$ is the final solution for the flow $\mathcal{F}$ at $\mathcal{I}_s$. This is also the global solution according to the formulation.

It can be noted that each interface broadcasts the solution tuple $< \mathcal{F}, \lambda(\mathcal{F}) >$ through mesh beacons to its two-hop neighborhood so that every other interfaces get synchronized with the information of all the flows in their two-hop neighborhood. According to IEEE 802.11s standard [25], mesh beacons are broadcast in every TBTT. In these beacons, an extra information element is added that contains the value of $< \mathcal{F}, \lambda(\mathcal{F}) >$. Thus, the beaconing incurs only a small amount of extra overhead.

3.4.3 Equilibrium Analysis

Every interface follows Algorithm 3.1 in an iterative way. Based on the information received in $(i-1)^{th}$ iteration, the local solution is computed, and this solution is propagated through the DATA and the ACK packets. The equilibrium of Algorithm 3.1 is justified through Lemma 3.2 and Theorem 3.4. Before proceeding to these lemma and theorem, the term "***Network Bottleneck***" is defined as follows.

Algorithm 3.1 Working of Local Search Problem 3.2 at $\mathcal{I}_s$ for flow $\mathcal{F}$

1. **Initialize:**
   (i) $\lambda(\mathcal{F}_{(ORG(\mathcal{F}),PRV(\mathcal{I}_s,\mathcal{F}))}) = \eta$
   (ii) $\lambda(\mathcal{F}_{(PRV(\mathcal{I}_s,\mathcal{F}),\mathcal{I}_s)}) = \xi(\mathcal{F},\mathcal{I}_s)$
   (iii) $\lambda(\mathcal{F}_{(\mathcal{I}_s,DST(\mathcal{F}))}) = \eta$
2. **At** i^{th} **Iteration**
   (i) $\lambda(\mathcal{F}_{(ORG(\mathcal{F}),PRV(\mathcal{I}_s,\mathcal{F}))}) = SOL_{i-1}(\mathcal{F}, PRV(\mathcal{I}_s,\mathcal{F}))$
   (ii) $\lambda(\mathcal{F}_{(\mathcal{I}_s,DST(\mathcal{F}))}) = SOL_{i-1}(\mathcal{F}, NXT(\mathcal{I}_s,\mathcal{F}))$
   Solve Problem 3.2 to get the values of $\lambda(\mathcal{F}_{(PRV(\mathcal{I}_s,\mathcal{F}),\mathcal{I}_s)}$ and $\lambda(\mathcal{F})$. Piggyback the solution with the DATA and the ACK packets.
3. **if** $SOL_{k-1}(\mathcal{F},\mathcal{I}_s) \approx SOL_k(\mathcal{F},\mathcal{I}_s)$ **then**
4. $\quad SOL(\mathcal{F},\mathcal{I}_s) = SOL_k(\mathcal{F},\mathcal{I}_s)$
5. **else**
6. $\quad$ **GOTO** 2
7. **end if**

Definition 3.4. ***Network Bottleneck*** *is defined as the links which are fully utilized, i.e. the total transmission rates of all sub-flows through the network bottleneck is* η.

Lemma 3.2. *The solution of Problem 3.1 occurs at network bottlenecks.*

Proof. Without any loss in generality, let us assume that flow $\mathcal{F}$ can be divided into n sub-flows $\mathcal{F}_{(\mathcal{I}_1,\mathcal{I}_2)}, \mathcal{F}_{(\mathcal{I}_2,\mathcal{I}_3)}, ..., \mathcal{F}_{(\mathcal{I}_{n-1},\mathcal{I}_n)}$. The transmission rate of the sub-flow $\mathcal{F}_{(\mathcal{I}_i,\mathcal{I}_j)}$ is $\lambda(\mathcal{F}_{(\mathcal{I}_i,\mathcal{I}_j)})$. Then the transmission rate of the flow $\mathcal{F}$ is calculated as,

$$\lambda(\mathcal{F}) = \min(\lambda(\mathcal{F}_{(\mathcal{I}_1,\mathcal{I}_2)}), ..., \lambda(\mathcal{F}_{(\mathcal{I}_{n-1},\mathcal{I}_n)}))$$

Let the minimum value occurs at the sub-flow $\mathcal{F}_{(\mathcal{I}_k,\mathcal{I}_l)}$. Further assume that, the link $(\mathcal{I}_k,\mathcal{I}_l)$ is not a network bottleneck, and the total transmission rates of all sub-flows through is $\Gamma_{(\mathcal{I}_k,\mathcal{I}_l)} < \eta$.

As $\lambda(\mathcal{F}_{(\mathcal{I}_k,\mathcal{I}_l)}) \leq \lambda(\mathcal{F}_{(\mathcal{I}_i,\mathcal{I}_j)}) \quad \forall \mathcal{F}_{(\mathcal{I}_i,\mathcal{I}_j)} \neq \mathcal{F}_{(\mathcal{I}_k,\mathcal{I}_l)}$, the overall transmission rate of flow

$\mathcal{F}$ can be given according to the objective function given in equation (3.2a),

$$\lambda(\mathcal{F}) = \min\Big\{(\lambda(\mathcal{F}_{(\mathcal{I}_k,\mathcal{I}_l)}) + \eta - \Gamma_{(\mathcal{I}_k,\mathcal{I}_l)}), \lambda(\mathcal{F}_{(\mathcal{I}_i,\mathcal{I}_j)}) \\ |\forall\lambda(\mathcal{F}_{(\mathcal{I}_i,\mathcal{I}_j)}) \neq \lambda(\mathcal{F}_{(\mathcal{I}_k,\mathcal{I}_l)})\Big\}$$

This contradicts our assumption that $\lambda(\mathcal{F}_{(\mathcal{I}_k,\mathcal{I}_l)})$ is the minimum, while link $(\mathcal{I}_k, \mathcal{I}_l)$ is not a network bottleneck. □

Theorem 3.4. *Every interface, while executing Algorithm 3.1, will eventually reach to the equilibrium state. This equilibrium is globally asymptotically stable.*

Proof. From Lemma 3.2, the solutions of Problem 3.1 occurs at network bottlenecks. For a network graph $\mathcal{G}_{net}(\mathbb{V}_{net}, \mathbb{E}_{net})$ with $|\mathbb{E}_{net}|$ edges, there can be at most $O(|\mathbb{E}_{net}|)$ bottlenecks (in a chain like topology, there are exactly $|\mathbb{E}_{net}|$ number of bottlenecks). The interfaces with network bottlenecks can calculate the solution directly by solving the LSP given in Problem 3.2. From Algorithm 3.1, these solutions are propagated to the network through the DATA and the ACK packets, within finite rounds of data communication. Thus within finite rounds of iterations, all the interfaces can solve Problem 3.1 using the LSP given in Problem 3.2, and the system reaches in equilibrium state.

Let us consider $U_c(\boldsymbol{\lambda})$, given in equation (3.2a) as the Lyapunov Function of the system. It can be shown directly that $U_c(\boldsymbol{\lambda})$ is 1-Lipschitz, as

$$U_c(\lambda(\mathcal{F}_1)) - U_c(\lambda(\mathcal{F}_2)) = \lambda(\mathcal{F}_1) - \lambda(\mathcal{F}_2) = \| \boldsymbol{\lambda} \|_1$$

Differentiating $U_c(\boldsymbol{\lambda})$ along trajectories,

$$\dot{U}_c = \nabla U_c.\dot{\boldsymbol{\lambda}} = \dot{\boldsymbol{\lambda}} \geq 0$$

where $\dot{\boldsymbol{\lambda}}$ is the time-derivative of $\boldsymbol{\lambda}$.

Then $\boldsymbol{\lambda} = \boldsymbol{\lambda}^*$ is a solution of Problem 3.1 only when it is a solution of Problem 3.2. Moreover $\dot{U}_c = 0$, only when $\dot{\boldsymbol{\lambda}} = 0$, and $\boldsymbol{\lambda} = \boldsymbol{\lambda}^*$ is a solution of Problem 3.1. Invoking Theorem 3.2 in [195], the equilibrium is globally asymptotically stable. □

3.4.4 Convergence Analysis

Algorithm 3.1 provides distributed mechanism to solve the LSP. The convergence of the algorithm is based on sub-gradient analysis. The definition of a sub-gradient for a function is as follows.

Definition 3.5. *Let* ***dom*** g *defines the domain of the function* $g : \mathbb{R}^n \to \mathbb{R}$. *A vector* $\overline{g} \in \mathbb{R}^n$ *is a sub-gradient of function* g *at* $x \in$ ***dom*** g, *if for all* $z \in$ ***dom*** g,

$$g(z) \geq g(x) + \overline{g}^T(z - x) \tag{3.10}$$

Theorem 3.5. *The sub-gradients of the LSP given in Problem 3.2 are also convex sub-gradients of Problem 3.1.*

Proof. From Theorem 3.3, Problem 3.2 is a convex subset of Problem 3.1. Hence it is straightforward that the sub-gradient of the LSP given in Problem 3.2 are convex sub-gradients of Problem 3.1 for interface s. □

With Theorem 3.5, the convergence of Algorithm 3.1 can be analyzed using sub-gradient analysis [196]. Assume every interface acts as an agent for the sub-gradient updation. Following conditions are true throughout the network;

1. **Connectivity:** Every interface is connected with other interfaces.
2. **Bounded inter-communication interval:** Every interface forwards its own solution through the DATA and the ACK packets.
3. **Simultaneous information exchange:** Every interface forwards the solutions simultaneously.
4. **Symmetric weight:** Every interface behaves similarly, and gives equal priority to its own solution.

Then according to Proposition 3 of [196], the convergence can be achieved in $O(\mathcal{N}_\mathcal{I})$ iterations where $\mathcal{N}_\mathcal{I}$ is number of interfaces in the network. However, most of the traffic for an WMN are to and from mesh gates. So the links connected to the interfaces at the mesh gates act as the network bottleneck. In a community WMN, traffic is forwarded from end user to the mesh gate and vice-versa following a directed acyclic graph, without producing any forwarding loop. So the interfaces attached with the mesh gate can independently solve the LSP. Once these interfaces solves the LSP, the solution are propagated through piggybacking, and in an average all other interfaces can solve the LSP in $O(d)$ rounds where d is the maximum hop distance of an interface from the mesh gate. However, for a fast convergence, the mesh path selection protocol should uniformly distribute the flows through the network.

3.4.5 Fairness Analysis

Problem 3.1 shows an important property of scheduling that it is balanced under max-min fairness. The balancing criteria for max-min fairness can be addressed as follows [98].

Definition 3.6. *Max-min fairness is balanced if and only if for some $L \geq 1$, the network reduces to a set of L independent links in the sense that there exists a partition $I_1, ..., I_L$ of the set of classes and some positive constants $\kappa_1, ..., \kappa_L$ such that,*

$$\mathbb{K} = \left\{ \varphi : \sum_{i \in I_1} \varphi_i \leq \kappa_1, ..., \sum_{i \in I_L} \varphi_i \leq \kappa_L \right\}$$

where φ is the allocation vector of transmission rates to different flows.

Problem 3.1 maximizes the minimum achievable transmission rate for all the sub-flows of a flow. Thus it satisfies max-min fairness criteria during flow scheduling.

Theorem 3.6. *Problem 3.1 is balanced under max-min fairness.*

Proof. The proof can be derived in a straightforward way from Lemma 3.2. As the solution occurs at network bottleneck, so the transmission rates of all the flows is bounded by the capacity of the network bottlenecks. This satisfies the balanced criteria under max-min fairness. □

3.4.6 Tuning MCCA for Scheduling based on Requirement

As discussed earlier, adaptive MAF limit can solve the problem of service-differentiation in MCCA. This work proposes an adaptive MAF limit where the MAF limit is tuned at the beginning of DTIM interval, based on traffic demand. For better performance, per interface MAF limit is maintained where different MAF values are used for every interface. Consider an interface I_j. Let $\lambda(I_j)$ denote the data rate for the flows through interface I_j. $\mathbb{C}(I_j)$ denotes the set of cliques in which interface I_j belongs, according to the protocol interference model. Then the MAF limit for interface I_j, $MAFL_{I_j}$, is set as follows.

$$MAFL_{I_j} = \min_{\forall C \in \mathbb{C}(I_j)} \left\{ \frac{\lambda(I_j)}{\sum_{I_k \in C} \lambda(I_k)} \right\} \tag{3.11}$$

The adaptive MAF limit solves the problem of service differentiation among contending interfaces. Every interface can reserve channel in a DTIM interval according to the traffic demand based on the scheduling. Therefore an interface can reserve sufficient

number of MCCAOPs within a DTIM interval that meets its traffic demand based on the scheduling information.

3.5 Mesh Path Selection based on Interface Scheduling

As discussed earlier in Chapter 2, IEEE 802.11s uses HWMP for mesh path selection. As a hybrid protocol, HWMP aims at merging advantages of both the proactive and the reactive path selection mechanisms. It can be configured to operate either in on-demand reactive mode or in tree-based proactive mode. The standard defines ALM as the path selection metric for each link. ALM ($\mathfrak{C}$) is defined as follows,

$$\mathfrak{C} = \left[O_{ca} + O_p + \frac{B_t}{r}\right] \frac{1}{1 - e_f} \tag{3.12}$$

Where O_{ca} and O_p are constants named as channel access overhead and protocol overhead respectively. B_t is the test frame size. The input parameters r and e_f are bit rate in Mbps and the frame error rate for the test frame size B_t.

3.5.1 Limitations of HWMP

Scheduling and path selection are interdependent in a directional antenna based mesh network. The elements of a mesh path selection protocol should configure the end-to-end path so that it provides maximum efficiency, while at the same time minimizes the contention among communicating beams. The scheduling algorithm should use this information to schedule the beam-forming to further improve network performance. IEEE 802.11s integrates HWMP for efficient mesh path selection based on MAC layer information. However, HWMP is designed for omni-directional MAC, and does not consider existing scheduling information while allocating path for a new flow.

HWMP uses ALM as the path selection metric. However, the link cost for this metric is calculated using a test frame. Lets consider the scenario given in Fig. 3.6. For the ease of presentation a single interface is considered at every mesh STA. Similar situation can arise with multiple interface scenario based on the interference graph. The dotted lines denote the connection links between the mesh STAs. There is an ongoing flow between $\mathcal{I}_2$ and $\mathcal{I}_3$. Because there is a single ongoing flow, based on the scheduling policy given in section 3.4, the link between $\mathcal{I}_2$ and $\mathcal{I}_3$ will be fully utilized. In this scenario, a new flow between $\mathcal{I}_5$ and $\mathcal{I}_8$ needs to be scheduled. The sub-flows $\mathcal{I}_2 \rightarrow \mathcal{I}_3$ and $\mathcal{I}_6 \rightarrow \mathcal{I}_7$ interfere with each other. When $\mathcal{I}_7$ sends a test frame to calculate airtime cost between $\mathcal{I}_6$ and $\mathcal{I}_7$, the cost will be very high because the two links are contending, and at that time, link

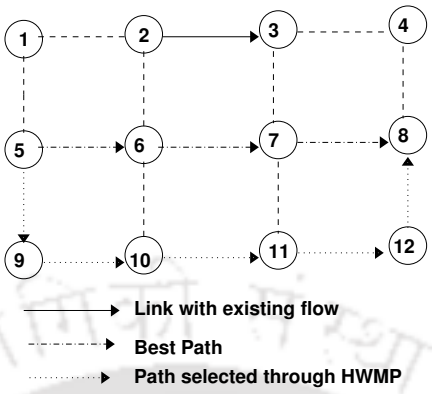

Figure 3.6: Two Flow Scenario

$\mathcal{I}_2 \rightarrow \mathcal{I}_3$ utilizes the complete capacity based on the proposed scheduling. Thus HWMP may select an alternate path $\mathcal{I}_5 \rightarrow \mathcal{I}_9 \rightarrow \mathcal{I}_{10} \rightarrow \mathcal{I}_{11} \rightarrow \mathcal{I}_{12} \rightarrow \mathcal{I}_8$. However, if the capacity is equally divided between the contending flows, then the path $\mathcal{I}_5 \rightarrow \mathcal{I}_6 \rightarrow \mathcal{I}_7 \rightarrow \mathcal{I}_8$ may give minimum airtime cost. This is not possible using test frame based per-hop airtime link cost calculation. The next subsection provides an amendment over HWMP based on the scheduling mechanism given in section 3.4 for efficient path selection in a direction mesh network.

3.5.2 HWMP Path Metric: Scheduling Based ALM

The ALM, when calculated using a test frame, may provide stale information because the actual transmission rate based on the scheduling policy is not known. However, when a new flow is admitted in a stable network, its actual transmission rate can be predicted based on current scheduling constraints. Let a newly generated flow has to be scheduled at link $\mathcal{I}_s \rightarrow \mathcal{I}_t$. First, the current condition of the link need to be predicted. The link is called to be *"maximally loaded"* if the remaining bandwidth in that link is less than the required bandwidth for an arbitrary minimum priority flow. Note that the proposed scheduling mechanism initially allocate the transmission rates based on their priority requirements, as given in equation (3.9). Formally *"maximally loaded"* link can be defined as follows:

Definition 3.7. *A link $\mathcal{I}_s \rightarrow \mathcal{I}_t$ is called to be **maximally loaded**, if the following condition holds,*

$$\eta - \sum_{\mathcal{F} \in \mathbb{C}(\mathcal{I}_s)} \lambda(\mathcal{F}) \leq \xi(\mathcal{F}_{minp}, \mathcal{I}_s) \tag{3.13}$$

where $\mathcal{F}_{minp}$ is an arbitrary flow with the minimum priority, and $\xi(\mathcal{F}_{minp}, \mathcal{I}_s)$ is calculated

according to equation (3.9).

Based on this definition, following theorem can be derived.

Theorem 3.7. *If a link $\mathcal{I}_s \rightarrow \mathcal{I}_t$ is maximally loaded, then based on the proposed scheduling policy, a newly admitted sub-flow $\mathcal{F}_{new}(\mathcal{I}_s, \mathcal{I}_t)$ can achieve at most $\xi(\mathcal{F}_{new}, \mathcal{I}_s)$ amount of transmission rate.*

Proof. Let there are n number of sub-flows through the link $\mathcal{I}_s \rightarrow \mathcal{I}_t$, denoted as $\mathcal{F}_1(\mathcal{I}_s, \mathcal{I}_t)$, $\mathcal{F}_2(\mathcal{I}_s, \mathcal{I}_t)$, ..., $\mathcal{F}_n(\mathcal{I}_s, \mathcal{I}_t)$ corresponding to the flows $\mathcal{F}_1, \mathcal{F}_2, ..., \mathcal{F}_n$. Further assume that based on flow priority, the proposed scheduling mechanism allocates $\xi(\mathcal{F}_{new}, \mathcal{I}_s)$ amount of transmission rate initially for newly admitted flow $\mathcal{F}_{new}$. Note that,

$$\xi(\mathcal{F}_{new}, \mathcal{I}_s) \geq \xi(\mathcal{F}_{minp}, \mathcal{I}_s)$$

Let equation (3.13) is satisfied. This implies,

$$\eta - \sum_{\mathcal{F} \in \mathbb{C}(\mathcal{I}_s)} \lambda(\mathcal{F}) \leq \xi(\mathcal{F}_{new}, \mathcal{I}_s)$$

So, if $\xi(\mathcal{F}_{new}, \mathcal{I}_s)$ amount of transmission rate needs to be allocated to sub-flow $\mathcal{F}_{new}(\mathcal{I}_s, \mathcal{I}_t)$, then the transmission rate of other flows have to be reduced. Consider any arbitrary flow $\mathcal{F}_i$. Based on Problem 3.1, $\mathcal{F}_i$ is already in the minimum of the maximum achievable transmission rates of all its sub-flows. If the transmission rate for sub-flow $\mathcal{F}_i(\mathcal{I}_s, \mathcal{I}_t)$ is reduced to allocate $\xi(\mathcal{F}_{new}, \mathcal{I}_s)$, then $\lambda(\mathcal{F}_i)$ would be the reduced transmission rate for sub-flow $\mathcal{F}_i(\mathcal{I}_s, \mathcal{I}_t)$. This is true for all the flows. Thus the maximum achievable transmission rate for sub-flow $\mathcal{F}_{new}(\mathcal{I}_s, \mathcal{I}_t)$ is the initially allocated rate based on flow priority, which is $\xi(\mathcal{F}_{new}, \mathcal{I}_s)$. □

When a new flow $\mathcal{F}_{new}$ is going to be scheduled in a link $\mathcal{I}_s \rightarrow \mathcal{I}_t$, there can be two possibilities,

1. The link is maximally loaded. Then the flow can get at most $\xi(\mathcal{F}_{new}, \mathcal{I}_s)$ amount of bandwidth through that link.
2. Otherwise, the flow can get at most $\eta - \sum_{\mathcal{F} \in \mathbb{C}(\mathcal{I}_s)} \lambda(\mathcal{F})$ amount of bandwidth through that link.

In the proposed modifications over HWMP, the PREQ message contains a field called *"effective data rate" (EDR)* which is used as the data rate value (r) for airtime link cost

calculation, as given in equation (3.12). Based on this observation, EDR at every $\mathcal{I}_s$ for a newly admitted flow $\mathcal{F}_{new}$ ($EDR_{\mathcal{F}_{new}}(\mathcal{I}_s)$) is calculated as follows:

$$EDR_{\mathcal{F}_{new}}(\mathcal{I}_s) = \max\left\{\left(\eta - \sum_{\mathcal{F}\in\mathbb{C}(\mathcal{I}_s)} \lambda(\mathcal{F})\right), \xi(\mathcal{F}_{new}, \mathcal{I}_s)\right\} \tag{3.14}$$

The HWMP protocol is augmented as follows. The source interface initializes EDR to ∞ and airtime link cost to zero, and broadcasts PREQ through all its interfaces. When an interfaces receives the PREQ message, it calculates EDR as follows:

$$EDR_{\mathcal{F}_{new}} = \min(\overline{EDR_{\mathcal{F}_{new}}}, EDR_{\mathcal{F}_{new}}(\mathcal{I}_s)) \tag{3.15}$$

Where $\overline{EDR_{\mathcal{F}_{new}}}$ is the EDR value received through the PREQ packet. Then the *Schedule based ALM* (S-ALM) is calculated as follows:

$$\mathfrak{C}_S = \left[O_{ca} + O_p + \frac{B_t}{EDR_{\mathcal{F}_{new}}}\right]\frac{1}{1-e_f} \tag{3.16}$$

If the interface is not the final destination, then it broadcasts the updated PREQ through all its interfaces. The updated PREQ contains the updated EDR and updated metric value. The rest of the HWMP protocol works similar to the standard.

3.6 Performance Analysis through Simulation

The proposed scheme is simulated using Qualnet-5.0.1 [71] network simulator. The performance is measured for both TCP traffic and UDP traffic. Jain Fairness Index [197] is used to measure fairness between flows. The simulation setup and network model used for simulation is described in following subsection.

3.6.1 Simulation Setup

The simulation scenario is shown in Fig. 3.7. A mesh STA is placed in every square of an 6×8 grids. 4 mesh STAs work as the mesh gate, and rest other mesh STAs work as the mesh STA. The mesh gates are placed using an off-line heuristic similar to the approach described in [198]. The dotted lines show the connectivity between the mesh STAs. Mesh STAs are distributed uniformly in the arena. Every mesh STA is equipped with two three-sectored multi-beam antenna with 120° beam-width, one for transmission, and another for reception. The SINR Threshold is considered to be $4dB$ with transmit power as $2.0mW$. The main lobe gain is $7dB$ with side lobe gain as $-20dB$. Channel

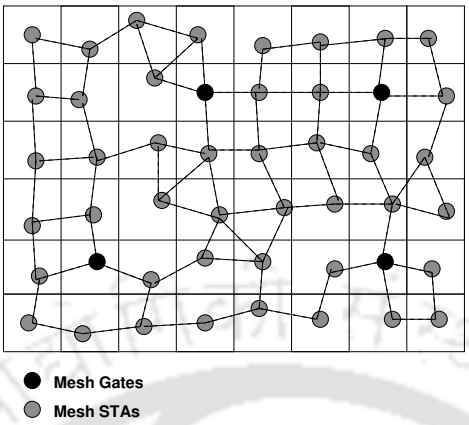

Figure 3.7: Simulation Scenario

bit error rate is modeled according to equation (17) and equation (18) from [199]. IEEE 802.11b with 11 Mbps channel bandwidth is used as physical layer specification that can provide about 5.9 Mbps using TCP and 7.1 Mbps using UDP. There are 4 mesh gates each equipped with three interfaces. So there are maximum 12 simultaneous communication possible at all the mesh gates. This implies that if there are less than 12 flows, each flow in the network can achieve maximum throughput, provided all the flows use different (mesh gate, Interface) pair for communication.

CBR is used as application layer traffic for UDP flows. CBR packet size is taken as 8 bytes. Traffic is generated based on Weibull Distribution with mean 32 μs. As shown in [200], wireless traffic characteristics can be captured correctly using Weibull distribution. The duration of each flow is selected according to Log-Normal random variables [200], with mean 20s and standard deviation 2. For TCP simulation, persistent FTP connections are taken as the application layer traffic. A TCP variant, called TCP NJ-Plus [201] is used, that is more suitable for WMN. TCP NJ-Plus is capable of distinguishing non-congestion losses from the packet reordering in WMNs, and thus reduce unnecessary drops in TCP congestion window.

Traffic sources are selected randomly among the mesh STAs. Sinks are also selected randomly among the 4 mesh gates. Every simulation is executed 10 different times with random (source,destination) pair and random seed values for the traffic generation. The average is taken as the final result. The proposed scheduling scheme is simulated with both ALM and S-ALM as the link metric for the HWMP protocol. The results are compared with the standard MCCA channel access.

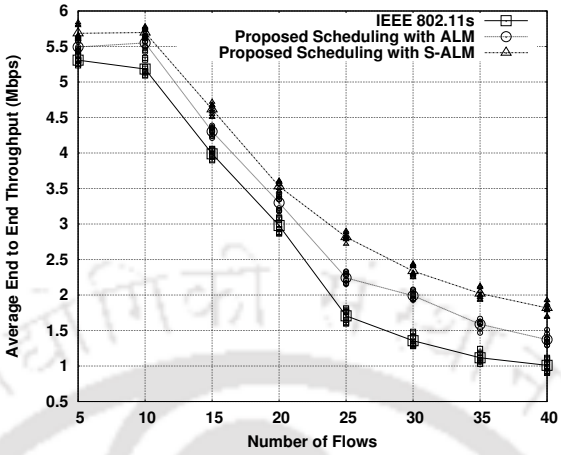

Figure 3.8: TCP Average Throughput

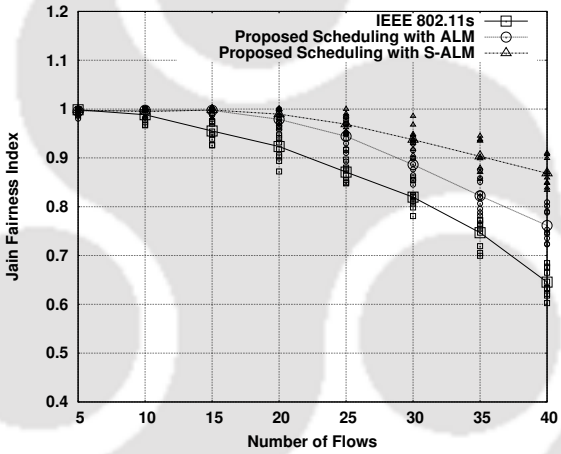

Figure 3.9: TCP Average Fairness Index

3.6.2 Analysis of the TCP Performance

TCP performance in the proposed scheme is analyzed through the end-to-end throughput and the average fairness index. Fig. 3.8 shows the average end-to-end throughput for the TCP traffics with respect to the number of flows. Fig. 3.9 shows the average fairness index for the TCP traffic. Both the figures indicate that the performance of the proposed scheduling mechanism is better compared to the standard MCCA based channel access. Furthermore, the performance improves significantly if the S-ALM is used as the metric for HWMP, along with the proposed scheduling mechanism. As there are 12 different interfaces for communication through mesh gates, the network gets saturated with approximately 12 number of TCP flows. It has been observed from the analysis

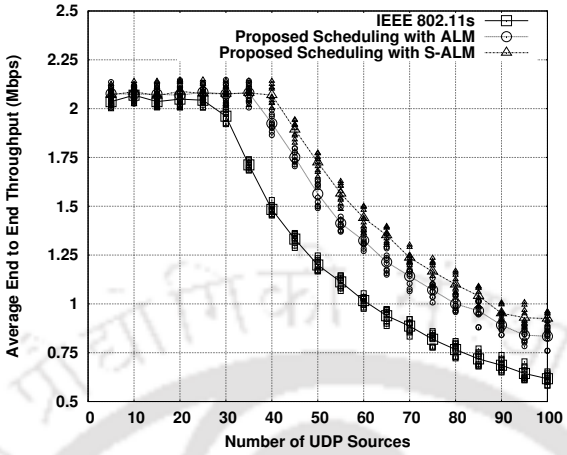

Figure 3.10: Average UDP Throughput

of the simulation trace that TCP congestion is more in case of the MCCA, and buffer overflow occurs at the intermediate mesh STAs because of the severe unfairness among the sub-flows of a TCP flow. For example, the simulation trace shows that the Jain Fairness Index for the sub-flows of a single TCP flows drops as much as 0.2 for MCCA. The beam prioritization method used in the proposed scheduling mechanism solves this problem by providing max-min fairness among the sub-flows of different flows based on their required transmission rate. This max-min fairness among different flows provides the equal-time fairness among the sub-flows of a single flow, and thus reduce the buffer overflow at intermediate mesh STAs. The HWMP protocol along with S-ALM further improves the performance by distributing the flows in the network, and thus reduces the congestion at the network bottlenecks. The reduction in the congestion improves the TCP performance significantly. As seen from Fig. 3.9, TCP fairness increases for the proposed scheduling along with S-ALM, compared to other schemes, as number of flows are increased in the network.

3.6.3 Analysis of the UDP Performance

The average UDP throughput versus the number of UDP sources is shown in Fig. 3.10. UDP sinks are selected randomly among the mesh gates. From the scenario set-up, the average data rate for the CBR transmissions is approximately 2 Mbps. Fig. 3.10 shows that the UDP throughput improves significantly in the proposed scheduling scheme, compared to the MCCA based channel access. The HWMP protocol along with S-ALM further improves the average UDP throughput.

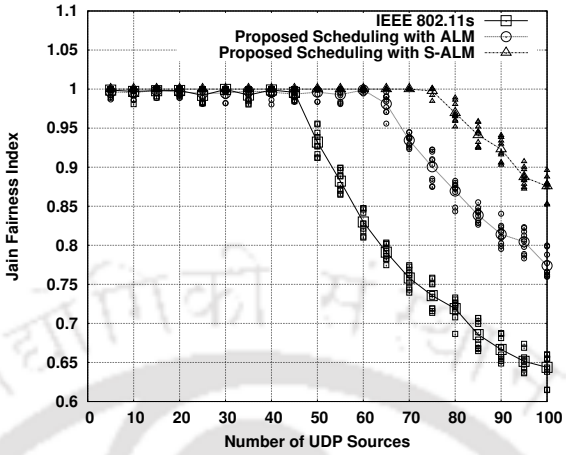

Figure 3.11: Average UDP Fairness

Fig. 3.11 shows the average fairness index versus the number of UDP sources. It can be seen from the figure that, after the network gets saturated (which is with 45 number of flows, the fairness index for UDP flows in case of the MCCA drops drastically. From the simulation analysis, it has been observed that the packet delivery rates for the UDP traffic flows depend on the amount of contention near the UDP sources. So the flows which face less contention near the UDP sources forward more number of packets, resulting in packet overflow near the mesh gates. This affects the flows with the high contention near the UDP source. However, contention is same near the mesh gates for both type of flows. This makes severe unfairness in case of the MCCA based access mechanism. In the proposed scheduling mechanism, the packet delivery rate of a flow depends on the overall contention of the network. As contention is more near the mesh gates, each and every flow forwards packet in a balance delivery rate which is equal to the transmission rate of the sub-flows near the mesh gates. This reduces the unfairness among different UDP flows, as seen from Fig. 3.11. The unfairness is further reduced by using S-ALM as the link metric for mesh path selection, along with the proposed scheduling.

The end-to-end delay for the UDP traffic versus the number of UDP sources is shown in Fig. 3.12. It can be seen from the figure that the average end-to-end delay for the proposed scheme is similar to the delay with MCCA based channel access. Thus the proposed beam-prioritization method does not incurs any extra packet delivery delay. However, the HWMP protocol along with S-ALM reduces the packet delay by admitting new flows based on the scheduling mechanism, and by distributing the flows evenly in the network.

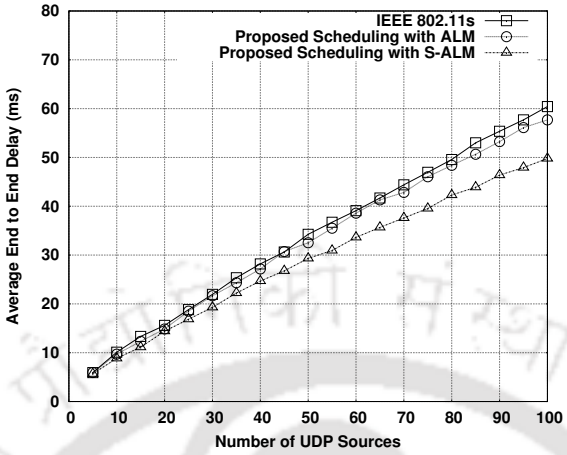

Figure 3.12: UDP Average Delay

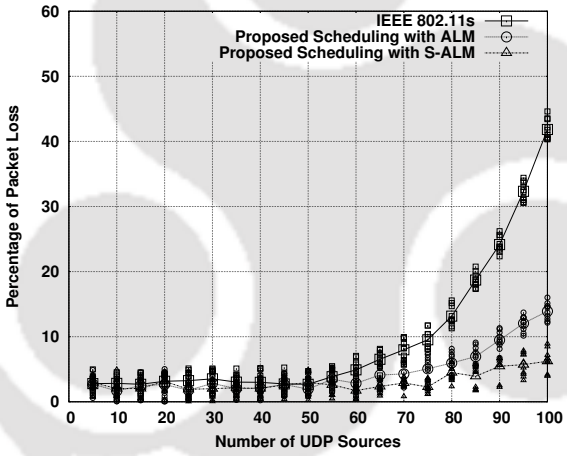

Figure 3.13: UDP % Packet Loss

Fig. 3.13 shows the percentage packet loss for the UDP traffic versus the number of traffic sources. As the network becomes saturated, the packet loss for the UDP traffic increases exponentially. From the analysis of the simulation trace, it has been observed that the packet losses are due to the network congestion and the buffer overflow at the intermediate mesh STAs. In the proposed scheduling mechanism, the total packet arrival rate at the network bottlenecks can not exceed the the link capacity, as formulated in Problem 3.1. So the buffer overflow is reduced significantly in the proposed scheme. The HWMP protocol along with S-ALM further reduces the buffer overflow by selecting the best path for the newly admitted flows.

3.7 Summary

In this chapter a scheme is proposed to improve the performance of MCCA based WMNs where each mesh STA is equipped with multiple switched beam directional antenna with multi-beam antenna array. A decentralized optimization scheme is formulated and a distributed local search mechanism is proposed to find out the theoretical maximum achievable transmission rate for each communication flow in the network. Based on this information, the MAF limit of MCCA is tuned to minimize the difference between the actual transmission rate and the theoretical maximum transmission rate. The performance of the proposed scheduling mechanism is improved further by tuning the ALM for the HWMP path selection mechanism, based on the scheduling information. Simulation result shows that the proposed scheme performs better compared to the standard IEEE 802.11s MCCA based channel access mechanism.

This chapter assumes all the traffic flows in the network are of similar priority. However, to support better QoS to the end users, real time flows are prioritized based on the service level agreement with the end users. In this scenario, the flow scheduling problem needs to support proportional fairness, where the data rates of the flows should be proportional to their service class priority. The utility function for multi-class traffics is non-convex, and therefore, the distributed convex decomposition method, as proposed is this chapter, becomes inapplicable. The next chapter provides the scheduling, mesh path selection and service differentiation method for multi-class traffics in a directional multi-interface WMN.

Chapter 4

Multi-Class Traffic in Directional Mesh Networks: Scheduling, Path Selection and Service Differentiation

The joint scheduling and mesh path selection mechanism proposed in the previous chapter has assumed a single-class traffic, where the traffic priority of every flow is similar, and the channel allocation depends only on the traffic load, not on the individual traffic priority and the service level agreement. However, QoS is an important requirement for modern days network to provide guaranteed service to the end users. To support better QoS assurance, network traffic has been traditionally classified into four service classes - voice, video, background and best effort [202]. While inter-class service differentiation is necessary to assure proportional resource distribution among different classes of services, based on their class priority, intra-class fairness is also need to be assured so that traffics from similar service classes get equal opportunity to utilize network resources.

As discussed in Chapter 2, $(\alpha, \wp)$ proportional fairness provides a good trade-off between the proportional fairness and the max-min fairness for supporting inter-class service differentiation and intra-class fairness simultaneously. This chapter proposes a service differentiation strategy over the MCCA channel access protocol. The optimum bandwidth allocation problem based on the service differentiation is modeled as a centralized optimization based on $(\alpha, \wp)$ proportional fairness criteria. The log-convexity of the centralized optimization is explored to design a localized distributed solution using

the sub-gradient approximation method. The convergence and equilibrium criteria of the distributed mechanism is analyzed theoretically. Finally the HWMP protocol is augmented to support admission control for the proper working of the service differentiation strategy. The effectiveness of the proposed scheme is analyzed using simulation results.

The rest of the chapter is organized as follows. The motivation behind designing a new QoS adaptation protocol over IEEE 802.11s MCCA is described in Section 4.1. The centralized problem formulation for the inter-class service differentiation and the intra-class fairness is discussed in Section 4.2. Section 4.3 provides the distributed decomposition method for the proposed centralized optimization by designing a per-STA solution using sub-gradient optimization method. The call admission control mechanism over the HWMP protocol is discussed in Section 4.4. The performance of the proposed scheme is analyzed using simulation results, as reported in Section 4.5. Finally Section 4.6 concludes the chapter.

4.1 Motivation

As discussed in Chapter 2, IEEE 802.11e EDCA supports service differentiation by maintaining separate CW and AIFSN for different service classes. However, IEEE 802.11s does not provide any service differentiation mechanism on the top of MCCA protocol. EDCA like service differentiation can not be directly incorporated in MCCA, because the design philosophy for EDCA is different from the design philosophy of MCCA. EDCA is a probabilistic contention-based channel access protocol, whereas MCCA is a reservation-based channel access protocol. Further, EDCA is known to perform poorly in terms of fairness for multi-hop networks, though it provides better QoS support for service differentiation [202].

MCCA has an inbuilt limitation that prevents it to provide service level QoS guarantee. The maximum number of MCCAOPs that can be reserved within a DTIM interval is bounded by *MAF limit*. The standard proposes to use a fixed MAF limit. In [203], the authors have shown that fixed MAF limit at every mesh STA provides equal air-time usage to the contending mesh STAs. Therefor, every mesh STA can have equal channel access opportunity in a DTIM interval. This approach provides equal time fairness among the mesh STAs and is not suitable for a multi-class service network. mesh STAs with higher priority traffic may require more channel access compared to mesh STAs having low priority traffic. EDCA provides service differentiation by maintaining separate CW and AIFSN values for different service classes. Similar approach of maintaining separate

MAF limits is not possible in MCCA as it may lead to network inconsistency if a single mesh STA serves for both high priority and low priority traffics. The reason behind this is as follows: MAF limit determines how many MCCAOPs a mesh STA can reserve within a DTIM interval, whereas CW or AIFSN denotes how many slots a node have to wait before accessing the channel. If a single mesh STA uses different MAF limits for different service classes within a single DTIM interval, then maintaining contention free reservation would become impossible. Therefore every mesh STA should maintain a single MAF limit for the complete DTIM interval that can be tuned adaptively at the beginning of DTIM interval. The adaptive MAF limit should be based on the current channel requirement for the mesh STA that assures QoS for all flows passing through it.

4.2 Centralized Problem Formulation for Service-Differentiation and Fairness

Similar to Chapter 3, it is considered that every mesh STA uses switched beam smart antenna system [181] for directional communication. It is assumed that every mesh STA uses MCCA as the MAC layer channel access protocol, and HWMP as the mesh path selection protocol. To allow simultaneous operations using different interfaces, every interface maintains separate MAC layer scheduling parameters. The protocol interference model, as described in Chapter 3, section 3.3 is also considered for this chapter. However, it has been assumed that every flow has different priority. The concept of the network graph ($\mathcal{G}_{net}$), communication graph ($\mathcal{G}_{com}$), interference graph ($\mathcal{G}_{inf}$) and the channel sharing graph ($\mathcal{G}_{ch}$) are also used in this chapter without any change in the definitions.

Let $\mathbb{F}$ denote the set of flows in the network. As discussed in previous chapter, a flow $\mathcal{F} \in \mathbb{F}$ can be divided in several MAC layer sub-flows. Let $\mathbb{F}(\mathcal{F})$ denote the set of sub-flows for flow $\mathcal{F}$. It can be noted that each sub-flow represents an edge in the communication graph. Let $\lambda(\mathcal{I}_j, \mathcal{I}_k)$ denote the rate for the sub-flow $(\mathcal{I}_j, \mathcal{I}_k)$. Every flow $\mathcal{F} \in \mathbb{F}$ is associated with an utility function $U_{\mathcal{F}} : \mathbb{R}^+ \rightarrow \mathbb{R}$. Thus flow $\mathcal{F}$ attains an utility $U_{\mathcal{F}}(\lambda(\mathcal{F}))$ when it sends data at rate $\lambda(\mathcal{F})$, satisfying $\lambda(\mathcal{F}) \geq \overline{\lambda(\mathcal{F})}$. Here $\overline{\lambda(\mathcal{F})}$ is the minimum rate bound to satisfy service level QoS agreement. $\wp(\mathcal{F})$ is the priority for flow $\mathcal{F}$. For $(\alpha, \wp)$ proportional fairness, the utility function is defined as follows, using a similar method proposed in [109];

$$U_{\mathcal{F}}(\lambda(\mathcal{F})) = \begin{cases} \wp(\mathcal{F})(1-\alpha)^{-1}\lambda(\mathcal{F})^{1-\alpha}, & \text{if } \alpha \neq 1; \\ \wp(\mathcal{F})\log(\lambda(\mathcal{F})), & \text{if } \alpha = 1. \end{cases} \tag{4.1}$$

The correctness of the utility function can be proved using following lemma.

Lemma 4.1. *Let $\boldsymbol{\lambda}^*$ be the optimal solution of the problem;*

$$\max \qquad \sum_{\mathcal{F}\in\mathbb{F}} U_{\mathcal{F}}(\lambda(\mathcal{F}))$$

where $U_{\mathcal{F}}(\lambda(\mathcal{F}))$ is given in equation (4.1). Then $\boldsymbol{\lambda}^*$ is $(\alpha, \wp)$ proportional fair.

Proof. The lemma can be proved directly by extending the proof for Lemma 2 given in [109]. □

Let $\Gamma(\alpha)$ be an indicator variable such that,

$$\Gamma(\alpha) = \begin{cases} 1, \text{if } \alpha = 1; \\ 0, \text{if } \alpha \neq 1. \end{cases} \tag{4.2}$$

Then the utility function can be represented as;

$$U_{\mathcal{F}}(\lambda(\mathcal{F})) = \Gamma(\alpha)\wp(\mathcal{F})\log(\lambda(\mathcal{F})) + (1-\Gamma(\alpha))\wp(\mathcal{F})(1-\alpha)^{-1}\lambda(\mathcal{F})^{1-\alpha} \tag{4.3}$$

Let $\boldsymbol{\lambda} = \{\lambda(\mathcal{F})|\forall f \in \mathbb{F}\}$ be the rate vector. Then $\boldsymbol{\lambda}$ is a convex set. The following theorem characterizes the utility function.

Theorem 4.1. *$U_{\mathcal{F}}(\lambda(\mathcal{F}))$ is a continuously differentiable strictly concave utility function.*

Proof. From equation (4.3),

$$\frac{\delta}{\delta\lambda(\mathcal{F})}U_{\mathcal{F}}(\lambda(\mathcal{F})) = \Gamma(\alpha)\wp(\mathcal{F})\lambda(\mathcal{F})^{-1} + (1-\Gamma(\alpha))\wp(\mathcal{F})\lambda(\mathcal{F})^{-\alpha}$$

Similarly,

$$\frac{\delta^2}{\delta\lambda(\mathcal{F})^2} = -\Gamma(\alpha)\wp(\mathcal{F})\lambda(\mathcal{F})^{-2} - (1-\Gamma(\alpha))\wp(\mathcal{F})\alpha\lambda(\mathcal{F})^{-\alpha-1}$$

As $\lambda(\mathcal{F}) > 0$;

$$\frac{\delta^2}{\delta\lambda(\mathcal{F})^2} < 0$$

Therefore the function $U_{\mathcal{F}}(\lambda(\mathcal{F}))$ is continuously differentiable and monotonic increasing. Therefore, it is concave. □

Let $\mathbb{C}$ denotes the set of maximal cliques in the channel sharing graph G_{ch}. The rate optimization problem for $(\alpha, \wp)$ proportional fairness can be formalized as follows;

Problem 4.1.

$$\max \quad \sum_{\mathcal{F}\in\mathbb{F}} U_{\mathcal{F}}(\lambda(\mathcal{F})) \tag{4.4a}$$

$$s.t. \quad \lambda(\mathcal{F}) = \min\left\{\lambda(\mathcal{F}(\mathcal{I}_j,\mathcal{I}_k))|\mathcal{F}(\mathcal{I}_j,\mathcal{I}_k)\in\mathbb{S}(\mathcal{F})\right\}; \quad \forall\mathcal{F}\in\mathbb{F} \tag{4.4b}$$

$$\sum_{\mathcal{I}_j\in C}\left(\sum_{\forall\mathcal{F}_{\mathcal{I}_j}}\lambda(\mathcal{F}_{\mathcal{I}_j})\right)\leq\eta; \quad \forall C\in\mathbb{C} \tag{4.4c}$$

$$\lambda(\mathcal{F})\geq\overline{\lambda(\mathcal{F})}; \quad \forall f\in\mathbb{F} \tag{4.4d}$$

The objective is to maximize the utility for all flows ensuring a set of constraints. The first constraint ensures that the data rate for a flow is the minimum among all the rates for its sub-flows. The second constraint ensures the interference minimization in terms of clique constraint. The third constraint ensures the feasibility of solution for minimum service level QoS guarantee. The value α is tuned by the service provider to make a balance between proportional fairness and max-min fairness. The effect of α is analyzed later in this chapter using simulation results.

Lemma 4.2. *Problem 4.1 is a convex optimization over* $\boldsymbol{\lambda}$.

Proof. Theorem 4.1 shows that the utility function is continuously differentiable concave function defined over a convex set $\boldsymbol{\lambda}$. All the three constraints are also linear with $\boldsymbol{\lambda}$. So the optimization is convex over $\boldsymbol{\lambda}$. □

In the next section, a distributed method is designed to solve this centralized optimization formulation based sub-gradient projection method.

4.3 Distributed Convex Decomposition and Per-Interface Solution

The distributed per-interface solution has three steps;

(i) The centralized problem is decomposed for per-interface such that the distributed problem becomes a convex subset of the centralized problem (called distributed convex decomposition).

(ii) The sub-gradient of the centralized problem is calculated using penalty based approach.

(iii) The distributed convex decomposition is used to solve the sub-gradients iteratively to find the global optimum solution (called sub-gradient projection).

4.3.1 Distributed Convex Decomposition

Problem 4.1 is centralized in nature, and requires complete network information to solve. The convexity of the problem along with the observation from interference characterization, given in Corollary 3.1 of Chapter 3, help to decompose the problem in per-interface basis. Let $\mathcal{I}_z$ be the intended interface. $\mathbb{F}_z$ is the set of flows through $\mathcal{I}_z$. $\mathbb{C}_z$ is the set of maximal cliques to which $\mathcal{I}_z$ belongs. $\mathbb{C}_z$ can be computed locally, as shown in Corollary 3.1 in Chapter 3. Then the centralized Problem 4.1 can be decomposed at the interface $\mathcal{I}_z$ as follows.

Problem 4.2.

$$\max \quad \sum_{\mathcal{F}\in\mathbb{F}_z} U_{\mathcal{F}}(\lambda(\mathcal{F})) \tag{4.5a}$$

$$s.t. \quad \lambda(\mathcal{F}) = \min\left\{\lambda(\mathcal{F}_{(\mathcal{I}_j,\mathcal{I}_k)})|\mathcal{F}_{(\mathcal{I}_j,\mathcal{I}_k)} \in \mathbb{S}(\mathcal{F})\right\}; \qquad \forall \mathcal{F} \in \mathbb{F}_z \tag{4.5b}$$

$$\sum_{I_x\in C}\left(\sum_{\forall \mathcal{F}_{I_x}} \lambda_{\mathcal{F}_{I_x}}\right) \leq \eta; \qquad \forall C \in \mathbb{C}_z \tag{4.5c}$$

$$\lambda(\mathcal{F}) \geq \overline{\lambda(\mathcal{F})}; \qquad \forall \mathcal{F} \in \mathbb{F}_z \tag{4.5d}$$

Following theorem characterized the distributed decomposition.

Theorem 4.2. *Problem 4.2 is a convex subset of Problem 4.1.*

Proof. It can be noted that;

$$\mathbb{F}_z \subset \mathbb{F}; \qquad \bigcup_z \mathbb{F}_z = \mathbb{F} \tag{4.6}$$

$$\mathbb{C}_z \subset \mathbb{C}; \qquad \bigcup_z \mathbb{C}_z = \mathbb{C} \tag{4.7}$$

Consequently Problem 4.2 is a subset of Problem 4.1. Any bounded subset of a convex set is also convex. So Problem 4.2 is also convex. □

4.3.2 Sub-gradient Calculation

The solution of Problem 4.1 is based on distributed sub-gradient method [204, 205] over Problem 4.2. Let;

$$G_{\mathcal{F}}(\lambda(\mathcal{F})) = \lambda(\mathcal{F}) - \min\left\{\lambda(\mathcal{F}_{(\mathcal{I}_j,\mathcal{I}_k)})|\mathcal{F}_{(\mathcal{I}_j,\mathcal{I}_k)} \in \mathbb{S}(\mathcal{F})\right\} \tag{4.8}$$

$$H_C(\lambda(\mathcal{F})) = \sum_{I_x \in C}\left(\sum_{\forall \mathcal{F}_{I_x}} \lambda_{\mathcal{F}_{I_x}}\right) - \eta \tag{4.9}$$

$$R_{\mathcal{F}}(\lambda(\mathcal{F})) = \overline{\lambda(\mathcal{F})} - \lambda(\mathcal{F}) \tag{4.10}$$

Therefore, equation (4.4b) becomes $G_{\mathcal{F}}(\lambda(\mathcal{F})) = 0$. However, equality constants are difficult to model for distributed sub-gradient method. The boundary points exist at infinity for equity constraints, and the solution may be trapped within those points. As the objective function maximizes rate for every flow, a relaxation can be given over equation (4.4b), by making it $G_{\mathcal{F}}(\lambda(\mathcal{F})) \leq 0$. Although this does not effect the final solution, it helps to avoid infinite boundary points. $\boldsymbol{\lambda}$ is the rate vector. Therefore the centralized optimization given in Problem 4.1 can be represented as;

Problem 4.3.

$$\max \quad \sum_{\mathcal{F}\in\mathbb{F}_z} U_{\mathcal{F}}(\boldsymbol{\lambda}) \tag{4.11a}$$

$$s.t. \quad G_{\mathcal{F}}(\boldsymbol{\lambda}) \leq 0; \qquad \forall f \in \mathbb{F} \tag{4.11b}$$

$$H_C(\boldsymbol{\lambda}) \leq 0; \qquad \forall C \in \mathbb{C} \tag{4.11c}$$

$$R_{\mathcal{F}}(\boldsymbol{\lambda}) \leq 0; \qquad \forall f \in \mathbb{F} \tag{4.11d}$$

This chapter uses penalty based approach for distributed sub-gradient optimization [204, 206]. A penalty function should impose a positive penalty at infeasible points and no penalty at feasible points. A suitable penalty function β for the constraints in Problem 4.3 can be defined as;

$$\beta(\boldsymbol{\lambda}) = \sum_{\mathcal{F}\in\mathbb{F}} \phi(G_{\mathcal{F}}(\boldsymbol{\lambda})) + \sum_{C\in\mathbb{C}} \psi(H_C(\boldsymbol{\lambda})) + \sum_{\mathcal{F}\in\mathbb{F}} \kappa(R_{\mathcal{F}}(\boldsymbol{\lambda})) \tag{4.12}$$

where ϕ, ψ and κ are continuous functions satisfying following constraints;

$$\phi(s) = 0 \quad \text{if} \quad s \leq 0 \quad \text{and} \quad \phi(s) > 0 \quad \text{if} \quad s > 0 \tag{4.13}$$

$$\psi(s) = 0 \quad \text{if} \quad s \leq 0 \quad \text{and} \quad \psi(s) > 0 \quad \text{if} \quad s > 0 \tag{4.14}$$

$$\kappa(s) = 0 \quad \text{if} \quad s \leq 0 \quad \text{and} \quad \kappa(s) > 0 \quad \text{if} \quad s > 0 \tag{4.15}$$

The functions ϕ, ψ and κ can be written as the form;

$$\phi(s) = (\max\{0, s\})^m \tag{4.16}$$

$$\psi(s) = (\max\{0, s\})^m \tag{4.17}$$

$$\kappa(s) = (\max\{0, s\})^m \tag{4.18}$$

where m is a positive integer. This chapter assumes $m \geq 2$ that provides a smooth penalty function [204, 206]. The gradient projection method is directly applicable in this case.

The auxiliary function for Problem 4.3 can be defined as;

$$\sum_{\mathcal{F} \in \mathbb{F}} U_{\mathcal{F}}(\boldsymbol{\lambda}) - \omega\beta(\boldsymbol{\lambda}) \tag{4.19}$$

Here ω is the penalty scaling factor. The penalty based approach solves following problem;

$$\theta(\boldsymbol{\lambda}, \omega) = \max_{\boldsymbol{\lambda}} \left\{ \sum_{\mathcal{F} \in \mathbb{F}} U_{\mathcal{F}}(\boldsymbol{\lambda}) - \omega\beta(\boldsymbol{\lambda}) \right\} \tag{4.20}$$

Here $\theta(\boldsymbol{\lambda}, \omega)$ is an unconstrained optimization problem. If $m \geq 2$, optimal solutions of $\theta(\boldsymbol{\lambda}, \omega)$ do not give exact solution of Problem 4.3. However from Theorem 9.2.2 of [204], by making ω sufficiently large, $\theta(\boldsymbol{\lambda}, \omega)$ can be made to represent Problem 4.3.

4.3.3 Sub-gradient Projection

The sub-gradient method solves the unconstrained optimization given in equation (4.20). To solve equation (4.20), every interface needs to know the solution vector $\boldsymbol{\lambda}$. This value is calculated iteratively using sub-gradient projection. Let $\boldsymbol{\lambda}^{(n)}$ be the solution received at n^{th} iteration. The sub-gradient projection method updates $\boldsymbol{\lambda}$ as follows;

$$\boldsymbol{\lambda}^{(n+1)} = \left[\boldsymbol{\lambda}^{(n)} + \gamma \xi_z^{(n)} \right] \tag{4.21}$$

Here γ is a constant step size. $\xi_z^{(n)}$ is the sub-gradient of the local objective (distributed decomposition) which is calculated as follows.

Let $\beta_z(\lambda)$ be the penalty function calculated from the distributed decomposition using similar way as described earlier. The local unconstrained optimization for the distributed decomposition, given in Problem 4.2, can be represented as;

$$\theta_z(\boldsymbol{\lambda}, \omega) = \max_{\boldsymbol{\lambda}} \left\{ \sum_{\mathcal{F} \in \mathbb{F}_z} U_{\mathcal{F}}(\boldsymbol{\lambda}) - \omega \beta_z(\boldsymbol{\lambda}) \right\} \tag{4.22}$$

Therefore,

$$\xi_z = \frac{\delta}{\delta \boldsymbol{\lambda}} \theta_z(\boldsymbol{\lambda}, \omega) \tag{4.23}$$

Equation (4.23) can be solved numerically at $\mathcal{I}_z$, for every flow passing through it. The sub-gradient update procedure works as follows;

1. At every interface, $\boldsymbol{\lambda}$ is initiated to zero.
2. Let $\mathcal{F} \in \mathbb{F}_z$. The sub-gradient for flow $\mathcal{F}$ is updated using equation (4.21).
3. The solution for flow $\mathcal{F}$ is piggybacked with the DATA packets for that flow. All the interfaces update $\boldsymbol{\lambda}$, on receiving the DATA packet.
4. Every interface also broadcasts its own $\boldsymbol{\lambda}$ within three hops. This is required to maintain interference constraints.

In next subsection, the convergence and the equilibrium of the proposed method is analyzed theoretically.

4.3.4 Convergence and Equilibrium Analysis

In distributed sub-gradient methods, several communicating entities (called the *agent*) coordinate to find globally optimal solution from their local information. The convergence and the equilibrium of a distributed sub-gradient method depends on four criteria [196];

1. **Connectivity:** All the agents should be connected with each other.
2. **Bounded Inter-communication Interval:** Agents should inform their local solutions to the neighborhood periodically.
3. **Simultaneous Information Exchange:** Agents should exchange their local solutions simultaneously.

4. **Symmetric Weight:** Agents should behave similarly, and give equal priority to their local solutions.

In the proposed mechanism, the interfaces act as the agents. These four conditions are satisfied in the proposed mechanism. Every interface is connected with other interfaces (through multi-hop communication). The interfaces forward their local solutions through the DATA packets. They also exchange the solutions in three-hop neighborhood through periodic broadcasting. Further the values of α and ω are uniform throughout the network (set by the service provider) which provides equal scaling to the solutions from all interfaces. Then according to Proposition 3 of [196], following theorem can be derived directly for the convergence of the proposed scheme.

Theorem 4.3. *The proposed scheme converges in $O(\mathbb{N}_{\mathcal{I}})$ rounds where $\mathbb{N}_{\mathcal{I}}$ is the number of interfaces in the network.*

The equilibrium for the proposed scheme is derived through following lemmas and theorems.

Lemma 4.3. *The sub-gradient defined in equation (4.23) is Lipschitz continuous.*

Proof. From Theorem 4.1, $U_{\mathcal{F}}(\boldsymbol{\lambda})$ is continuously differentiable. $\beta_z(\boldsymbol{\lambda})$ is linear to $\boldsymbol{\lambda}$. Therefore;

$$\frac{\delta}{\delta\lambda(\mathcal{F})}\beta(\boldsymbol{\lambda}) = \text{constant}$$

So, $\frac{\delta}{\delta\boldsymbol{\lambda}}\theta_z$ is continuously differentiable. Hence, ξ_z, defined in equation (4.23) is Lipschitz continuous. □

Theorem 4.4. *The solution of Problem 4.2 is globally asymptotically stable.*

Proof. Lemma 4.3 states that the sub-gradient is Lipschitz continuous. From Theorem 4.2, Problem 4.2 is convex. As $U_{\mathcal{F}}(\boldsymbol{\lambda})$ is strictly concave (from Theorem 4.1) and $\beta(\boldsymbol{\lambda})$ is linear, $\theta(\boldsymbol{\lambda}, \omega)$ is strictly concave (subtraction of a linear function from a concave function results in a concave function). So there exists $\boldsymbol{\lambda}^* \in \mathbb{R}^+$, for which the sequence given in equation (4.21) converges to the globally asymptotically stable state [204]. □

Once the required data rate for every flow is known, MCCA is tuned to get required data rate based on service demand. The MCCA tuning mechanism is given in the next subsection.

4.3.5 Tuning MCCA for Service-Differentiation

A similar method is used as proposed in Chapter 3 for tuning MAF limits based on traffic demand. Consider an interface $\mathcal{I}_j$. Let $\lambda(\mathcal{F}_{\mathcal{I}_j})$ denote the total data rate for the flows through interface $\mathcal{I}_j$. $\mathbb{C}(\mathcal{I}_j)$ denotes the set of cliques in which interface $\mathcal{I}_j$ belongs, according to protocol model. Then the MAF limit for interface $\mathcal{I}_j$, $MAFL_{\mathcal{I}_j}$, is set as follows.

$$MAFL_{\mathcal{I}_j} = \min_{\forall C \in \mathbb{C}(\mathcal{I}_j)} \left\{ \frac{\lambda(\mathcal{F}_{\mathcal{I}_j})}{\sum_{\mathcal{I}_k \in C} \lambda(\mathcal{F}_{\mathcal{I}_k})} \right\} \tag{4.24}$$

The adaptive MAF limit solves the problem of service differentiation among contending mesh STAs. Every mesh STA can reserve channel in a DTIM interval proportional to its service demand. The service demand is calculated based on minimum service level QoS assurance. Therefore a mesh STA can reserve sufficient number of MCCAOPs within a DTIM interval that meets the requirement for the flow based on its priority. Further the conditions for $(\alpha, \wp)$ proportional fairness ensures QoS maintaining minimum service demand as well as equity among the flows with similar service priority.

Once the total required channel share within a DTIM interval is determined using equation (4.24), per-class reservation at a single interface can be assured using standard MCCAOP reservation procedure. Let interface $\mathcal{I}_j$ has two flows within it - one high priority flow and another low priority flow. Then during MCCAOP reservation procedure for every flow, the MCCAOP duration and periodicity would be set according to the priority for that flow. This can be computed locally at every interface based on standard priority queuing mechanism.

4.4 Call Admission Control using HWMP

In the proposed scheme the network utilization is maximized while ensuring minimum service requirement and fairness among the flows. However, tuning MAF limit alone can not provide complete service-differentiation. When a new flow arrives, the flow should be admitted to the network if its required service demand can be satisfied, without affecting minimum service demands for other flows. For this purpose, the reactive HWMP protocol is augmented to check whether the service demand for the new flow can be satisfied, without degrading QoS requirements for other flows.

IEEE 802.11s uses HWMP for MAC layer path selection. As a hybrid protocol,

Algorithm 4.1 An interface Receives PREQ with ESR, $\wp(\mathcal{F}_{new})$, $\overline{\lambda(\mathcal{F}_{new})}$

1: $\lambda(\mathcal{F}_{new}) \leftarrow ESR$
2: $\overline{\boldsymbol{\lambda}} \leftarrow [\boldsymbol{\lambda}, \lambda(\mathcal{F}_{new})]$
3: Update sub-gradient given in equation (4.23) using $\overline{\boldsymbol{\lambda}}$, and find the maximum achievable rate ($\lambda^*(\mathcal{F}_{new})$) using equation (4.21).
4: **if** solution is feasible **then**
5: $ESR^* \leftarrow \lambda^*(\mathcal{F}_{new})$
6: Broadcast PREQ with ESR^*, $\wp(\mathcal{F}_{new})$, $\overline{\lambda(\mathcal{F}_{new})}$.
7: **else**
8: Drop the PREQ message.
9: **end if**

HWMP aims at merging advantages of both proactive and reactive routing mechanisms. It can be configured to operate in two modes - on-demand reactive mode and tree-based proactive mode. For mesh path selection, the IEEE 802.11s standard [25] defines *ALM* as the path selection metric for each link. For the ease of presentation, the definition of ALM ($\mathfrak{C}$) is reproduced in this chapter, given as follows,

$$\mathfrak{C} = \left[O_{ca} + O_p + \frac{B_t}{r}\right] \frac{1}{1 - e_f} \tag{4.25}$$

Where O_{ca} and O_p are constants named as the channel access overhead and the protocol overhead, respectively. B_t is the test frame size. The input parameters r and e_f are bit rate in Mbps and the frame error rate for the test frame size B_t respectively. Based on the reactive mode of HWMP, a call admission control mechanism is proposed. The HWMP protocol with support for call admission control, is termed as *CAC-HWMP*. The detailed working procedure of CAC-HWMP is given in following sub-section.

4.4.1 Working Procedure of CAC-HWMP

In the proposed modification of HWMP, apart from ALM, three parameters have been incorporated in PREQ message - the service class priority of the new flow to be admitted ($\wp(\mathcal{F}_{new})$), the minimum traffic demand for service level QoS agreement ($\overline{\lambda(\mathcal{F}_{new})}$) and *Estimated Service Rate* (ESR) that determines maximum data rate the flow can achieve. Let $\mathcal{F}_{new}$ be the new flow that is admitted in the network. The actions performed by an interface on receiving such a PREQ message is shown in Algorithm 4.1.

According to Algorithm 4.1, every interface executes the local sub-gradient update method to find out whether the local solution is feasible with the minimum service demand

for the new flow to be admitted. If the minimum service demand is satisfied, then ESR is updated with the locally found optimal solution for the newly admitted flow. The PREQ message is further broadcast with the updated ESR value. If the solution is not feasible, it indicates that the path can not provide minimum service demand for that flow. Then the PREQ message is dropped. As a result, the destination interface receives PREQ messages only through the paths that can assure minimum service demand. It then selects the best PREQ based on airtime metric value, and forwards the PREP message through that path.

If the flow can not be admitted in the network satisfying its traffic demand, then the source interface does not receive PREP messages within a timeout interval. In this case, the flow is dropped. The time-out interval can be set based on the end-to-end delay requirement for that flow. The timeout value should be less than the end-to-end delay requirement.

The convergence of Algorithm 4.1 is based on the following theorem.

Theorem 4.5. *Let the network be in stable state, indicating* $\boldsymbol{\lambda}$ *at every interface is the optimal solution. Let a new flow* $\mathcal{F}_{new}$ *is admitted such that* $\overline{\boldsymbol{\lambda}} = [\boldsymbol{\lambda}, \lambda(\mathcal{F}_{new})]$. $\lambda(\mathcal{F}_{new})$ *is initialized to zero. If* $\overline{\boldsymbol{\lambda}}$ *is feasible, then* $\overline{\boldsymbol{\lambda}}$ *can be calculated directly from equation (4.21).*

Proof. The proof for this theorem comes from Lipschitz continuity of the sub-gradient given in equation (4.23). As the sub-gradient is Lipschitz continuous, there exists $\tau \geq 0$, such that for two flows $\mathcal{F}_1$ and f_2 where $\mathcal{F}_1 \neq f_2$,

$$\frac{|\theta(\lambda(\mathcal{F}_1), \omega) - \theta(\lambda(\mathcal{F}_2), \omega)|}{|\lambda(\mathcal{F}_1) - \lambda(\mathcal{F}_2)|} \leq \tau$$

Consider an arbitrary flow $\mathcal{F}_a$ which is in stable condition. Let the rate for flow $\mathcal{F}_a$ is $\lambda^{(stable)}(\mathcal{F}_a)$ before the new flow is introduced, and $\lambda^{(upd)}(\mathcal{F}_a)$ after the admission of the new flow. Then according to Lipschitz continuity criteria before the admission of $\mathcal{F}_{new}$;

$$\frac{|\theta(\lambda^{(stable)}(\mathcal{F}_a), \omega)|}{|\lambda^{(stable)}(\mathcal{F}_a)|} \leq \tau \tag{4.26}$$

Similarly after the admission of the new flow;

$$\frac{|\theta(\lambda^{(upd)}(\mathcal{F}_a), \omega) - \theta(\lambda(\mathcal{F}_{new}), \omega)|}{|\lambda^{(upd)}(\mathcal{F}_a) - \lambda(\mathcal{F}_{new})|} \leq \tau \tag{4.27}$$

As θ is strictly concave, from equation (4.26) and equation (4.27), it can be concluded that;

$$\theta(\lambda^{(upd)}(\mathcal{F}_a), \omega) \leq \theta(\lambda^{(stable)}(\mathcal{F}), \omega)$$

Therefore, whenever a new flow is introduced, the solutions for existing flows are non-oscillating, and decrease uniformly. If feasible solution exists, the sub-gradient directly converges to the updated solution [196], giving the optimal solution for the newly admitted flow. □

Therefore, in a stable network, HWMP can be used to find out whether minimum service demand for a newly admitted flow can be assured or not. If the demand can be assured, the flow is admitted in the network. Once the flow is admitted, the network again converges to the stable state rapidly according to Theorem 4.5, by updating traffic demand for every affected flow.

Consequently, whenever an existing flow leaves the network, the solutions for existing flows are non-oscillating and increases uniformly (can be proved using similar argument as of Theorem 4.5. Then all the affected flows increase their rates based on sub-gradient update using equation (4.21). In a stable network, the sub-gradient update depends only on the flow priorities, not on their actual traffic rate. Further, flow join and leave operations are atomic in nature. Every interface assumes the presence of a flow whenever it receives either a DATA packet for that flow, or broadcast information from its neighbor. If it does not receives this information within a timeout interval, it assumes that the flow is terminated, and updates rate vector $\boldsymbol{\lambda}$ accordingly. Therefore the sub-gradient update at each interface for flow join and for flow leave are mutually independent, and are executed atomically. This assures first convergence when a new flow is admitted in the network, or an existing flow leaves the network.

4.4.2 Applicability of the Proposed Scheme for Four Class Service System

IEEE 802.11 defines four classes of services - voice (VO), video (VD), background (BK) and best effort (BE). The proposed scheme can be extended to support these four classes of service. The specific service requirements fo these four classes are as follows;

- **Voice (VO):** Highest priority traffic, requires minimum bandwidth guarantee, minimum delay and negligible packet loss.
- **Video (VD):** Next highest priority, delay should be as small as possible, jitter should be negligible, can tolerate limited packet loss.
- **Background (BK):** Priority is less than video traffic, however loss rate should be as less as possible.

- **Best-Effort (BE):** No specific QoS requirement.

Following criteria should be satisfied to support these four class services over the proposed scheme;

$$\wp_{VO} > \wp_{VD} > \wp_{BK} > \wp_{BE} \tag{4.28}$$

Equation (4.28) denotes that the priority of VO traffic is maximum, and the traffic priority decreases in the order of VD to BK and BE traffic. Further following minimum traffic guarantee should be ensured.

$$\begin{aligned} &\overline{\lambda_{BE}} \geq 0 \\ &\overline{\lambda_{VO}} > \overline{\lambda_{VD}} \geq \overline{\lambda_{BK}} > \overline{\lambda_{BE}} \end{aligned} \tag{4.29}$$

The specific service parameters can be set by the service provider. It can be noted that the end-to-end delay guarantee can be ensured by the timeout interval of HWMP PREP reception during flow admission. The above considerations are sufficient to support QoS provisioning for four class service system. The proposed scheme allocates channel share to the traffic from every class proportionally to their class priority, maintaining minimum bandwidth demand. The minimum bandwidth demand also ensures delay and jitter guarantee. Further, the α value ensures that no traffic class can overuse channel share that may affect BE services. The effectiveness of $(\alpha, \wp)$ proportional fairness over max-min fairness and proportional fairness is analyzed in the next section using simulation results.

4.5 Simulation Results

The proposed scheme is implemented using Qualnet 5.0.1 [71] network simulator framework. The performance of the proposed scheme is analyzed for service-differentiation and fairness, and compared with IEEE 802.11s standard. Further the effectiveness of the proposed scheme for $(\alpha, \wp)$ fairness is compared with max-min fairness and proportional fairness. Standard IEEE 802.11 four class service is considered for performance measurement in various scenarios.

4.5.1 Simulation Set-up

In the simulation scenario, 40 mesh STAs have been deployed in the simulation arena uniformly using mean connectivity 4. This indicates that every mesh STA has on an

average 4 mesh STAs in its communication range. Out of these mesh STAs, 3 mesh STAs have been selected as mesh gate. The mesh gates are selected using degree based Greedy Dominating Tree Set Partitioning (degree based GDTSP) algorithm proposed in [207]. Degree based GDTSP algorithm optimizes connectivity among the mesh gates and other mesh STAs in the network. Every mesh STA is equipped with 3 interfaces. Every interface is connected with switched beam smart antenna with main lobe gain as $15dB$ and side lobe gain as $-20dB$. IEEE 802.11g $54Mbps$ physical layer technology is used for communication. Capture effect is enabled at physical layer with capture threshold of $4dB$ with transmit power $16dBm$. These physical layer settings are according to CISCO 1500 series MAPs [208].

MCCA is used as the MAC layer standard. DTIM interval is kept at $600\mu s$. The beacon transmission time is set as $200\mu s$. HWMP is used for mesh path selection. HWMP route timeout is kept as $3sec$, and number of PREQ attempts is set to 2. That means a mesh STA can try to find out the the path for a flow at most 2 times. If no PREP message arrives for 2 consecutive times, the flow is dropped.

Four classes of traffic are considered for simulation purpose. The traffic are generated using Qualnet traffic generator framework. The traffic priority, minimum bandwidth demand and average flow duration for each service class is given in Table 4.1. It can be noted that the properties shown in Table 4.1 may vary in real system. For example, the average flow durations are taken smaller compared to their actual durations, to avoid lengthy simulation process. However, for the comparative analysis purpose, the variance in the data matters, not their actual values. For example, the average duration of a VO flow should be less compared to a VD flow. In real system, the results can be scaled up or scaled down based on the actual parameters used. Here we are only interested in a comparative performance analysis. The parameters shown in Table 4.1 are sufficient for this purpose.

The flow durations are chosen using log-normal distribution with mean values given in Table 4.1. This captures real time traffic distribution characteristics in a community network. Every experiment is executed for 10 different times with 10 different seed values. The average values are taken to plot the graphs. However, the confidence intervals are also shown in every graph.

4.5.2 Effect of Inter-Class Flow Differentiation and Intra-Class Fairness

For this class of experiments, two types of flows are taken - high priority VO flows, and low priority BE flows. The traffic generation rate for VO flows is exponentially distributed with

Table 4.1: Traffic properties for different service classes

Traffic Class	**Priority**	**Minimum Demand (kbps)**	**Mean Flow Duration (min)**
VO	7	64	1
VD	5	48	5
BK	3	20	5
BE	1	0	20

mean $100Kbps$ and variance $10Kbps$. Similarly the traffic generation rate for BE flows is Poisson distributed with mean $1Mbps$ and variance $0.1Mbps$. Service differentiation gets affected just after the network saturation (total traffic demand overshoots network capacity). Therefore number of flows are selected based on saturation point. Jain fairness index [197] is used to check fairness among the flows from similar traffic classes. Jain fairness index is defined as follows;

$$F(\lambda) = \frac{(\sum \lambda(\mathcal{F}))^2}{n(\sum \lambda(\mathcal{F})^2)} \tag{4.30}$$

where $\lambda(\mathcal{F})$ is the throughput for flow f, and n is the total number of such flows. For these set of experiments, α value is taken as 20 that provides a trade-off between proportional fairness and max-min fairness.

Figure 4.1 shows the throughput of VO flows with respect to increasing number of BE flows. For this experiment, network saturation occurs with 40 numbers of BE flows. 30 VO flows are distributed uniformly in the network. BE flows are also distributed uniformly so that complete network would get saturated. Without uniform distribution of flows, performance comparison is difficult as some portion of the network gets saturated whereas some portion may still remain in unsaturation. Average throughput for VO flows is considered to plot the graph. It can be observed from the graph that before saturation, both the proposed scheme and standard IEEE 802.11s performs similarly. However after saturation, the performance for VO flows drops exponentially in case of IEEE 802.11s network. On the other hand, the throughput for the VO flows in the proposed scheme is always maintained to its minimum demand, $64Kbps$. In case of IEEE 802.11s, the BE flows reserve maximum MCCAOPs in the DTIM interval, which affects the performance of VO flows. In the proposed scheme maximum MCCAOP reservation for BE flows is limited by number of high priority VO flows present in the network.

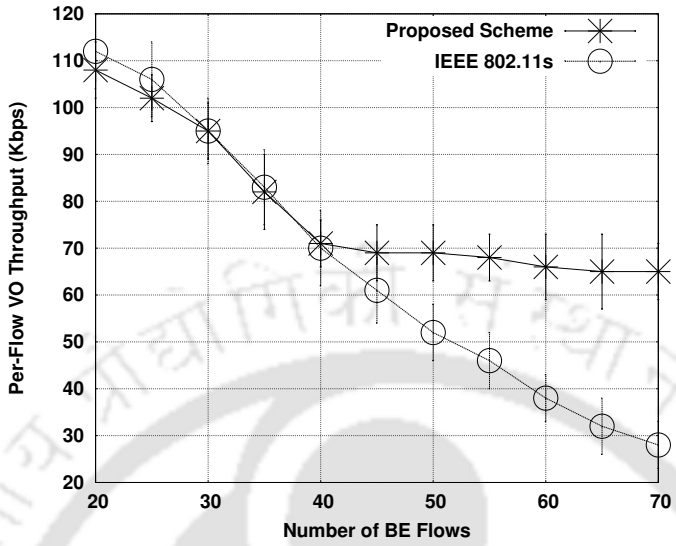

Figure 4.1: Throughput: VO Flows in Presence of BE Flows

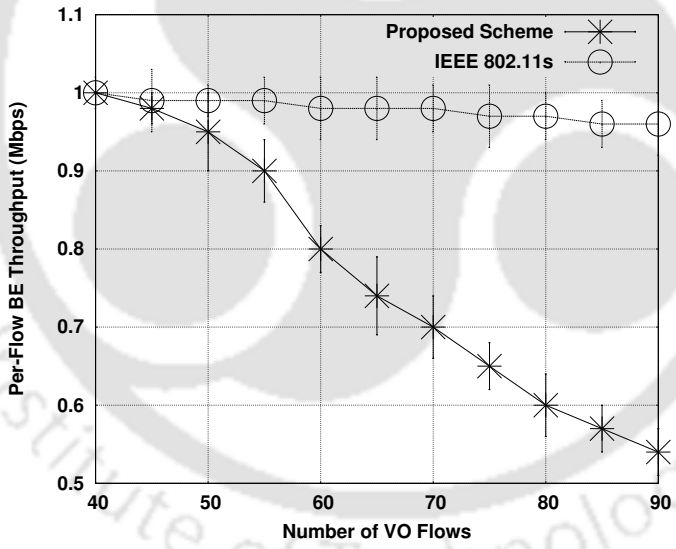

Figure 4.2: Throughput: BE Flows in Presence of Voice Flows

Figure 4.2 shows the throughput for BE flows with respect to increasing number of VO flows. For this experiment, 20 numbers of BE flows are considered. Like previous, the BE and VO flows are distributed uniformly in the network. For this scenario, network saturation occurs with 50 numbers of VO flows. It can be noted that there is no minimum traffic demand for BE services. Therefore, as the number of VO flows increase in the network, the throughput for the BE flows drops in the proposed scheme to

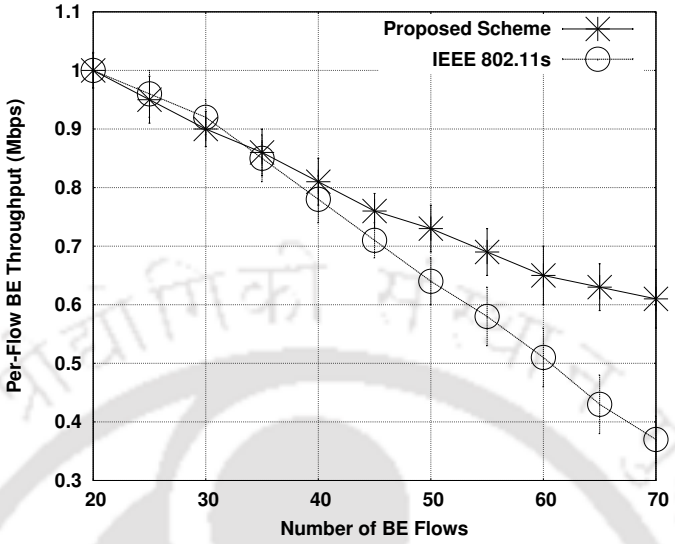

Figure 4.3: Throughput: BE Flows in Presence of BE Flows

accommodate the high priority VO flows. Standard IEEE 802.11s does not make service class differentiation. Therefore, increasing number of VO flows in the network does not affect the performance of BE flows. As the data rate for BE flows is significantly higher than the VO flows, BE flows reserve most of the MCCAOPs in the DTIM interval for IEEE 802.11s, affecting performance of VO flows.

Figure 4.3 shows the performance of BE flows with increasing number of BE flows in the network. For this experiment the network contains only BE flows. Network saturation occurs with 35 numbers of BE flows. In this case, the throughput for BE flows drops for both the cases - the proposed scheme and standard IEEE 802.11s. However, average per-flow throughput for the proposed scheme is higher compared to IEEE 802.11s. The reason behind this is intra-class fairness provisioning used in the proposed scheme. In IEEE 802.11s standard, some flows get starved when traffic demand is very high. Fairness assurance in the proposed scheme solves the problem of starvation, resulting increase in per-flow throughput.

Intra-class fairness for the above three experiments have been shown in Figure 4.4-Figure 4.6. Figure 4.4 shows fairness among VO flows with respect to increasing number of BE flows. Figure 4.5 plots the fairness index for BE flows with increasing number of VO flows. Similarly Figure 4.6 shows fairness among BE flows when number of BE flows are increased in the network. In all the three cases, the proposed scheme provides more intra-class fairness compared to standard IEEE 802.11s.

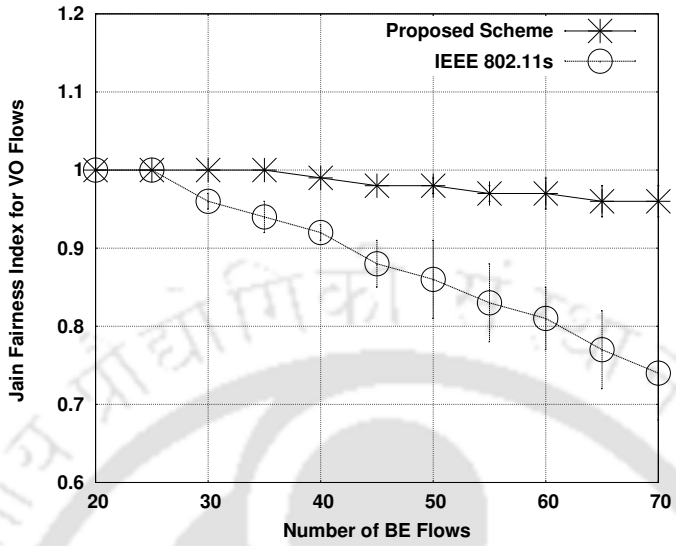

Figure 4.4: Fairness Index: VO Flows in Presence of BE Flows

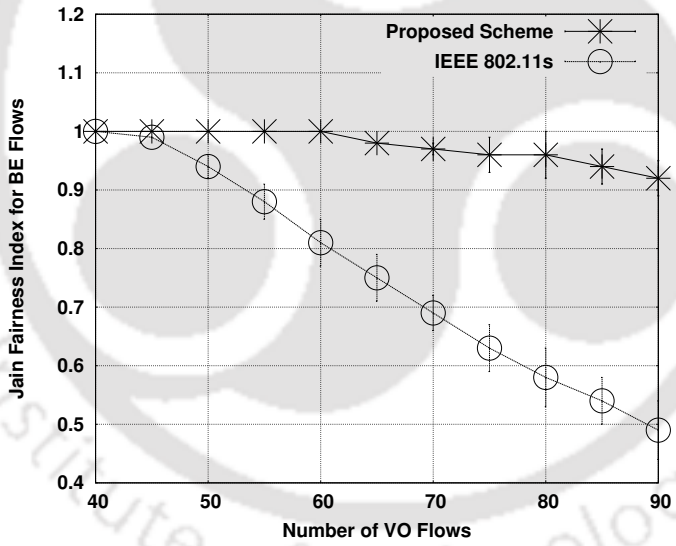

Figure 4.5: Fairness Index: BE Flows in Presence of Voice Flows

4.5.3 Trade-off Between Proportional Fairness and Max-Min Fairness

A set of experiments have been performed to analyze the trade-off between proportion fairness and max-min fairness. For these experiments, 20 BE flows with $1Mbps$ mean data rate is distributed uniformly in the network. The fairness index is measured by varying number of VO flows. Max-min fairness is measured by Jain fairness index, whereas proportional fairness is measured using proportional fairness index. Proportional fairness

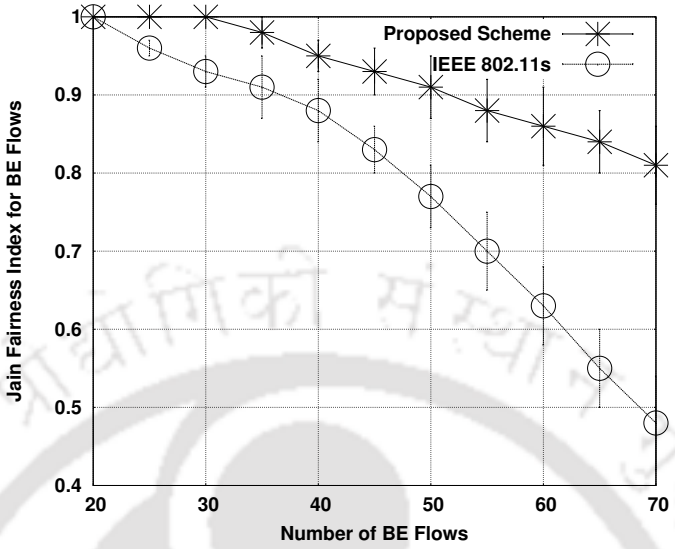

Figure 4.6: Fairness Index: BE Flows in Presence of BE Flows

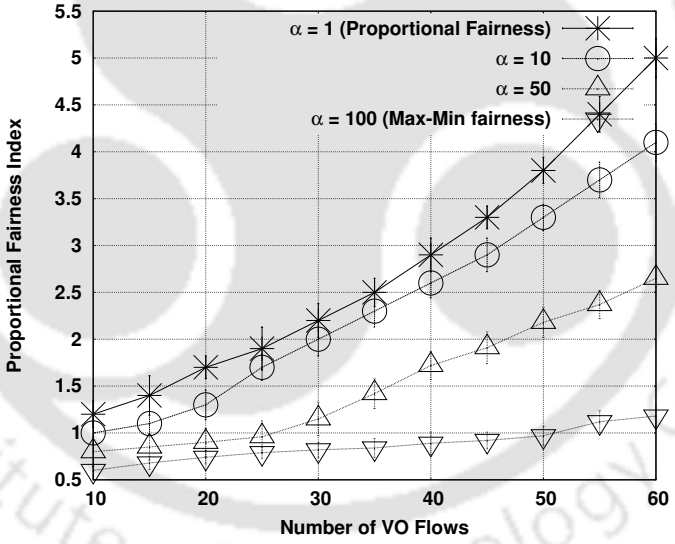

Figure 4.7: Proportional Fairness Index

index ($F_p(\lambda)$) can be measured as;

$$F_p(\lambda) = \sum_{\forall \mathcal{F}} \wp(\mathcal{F}) \log \lambda(\mathcal{F}) \tag{4.31}$$

where $\wp(\mathcal{F})$ is the priority of flow $\mathcal{F}$.

Figure 4.7 shows the proportional fairness index for different α values. As discussed earlier, $\alpha = 1$ is similar to proportional fairness, and large α value denotes max-min

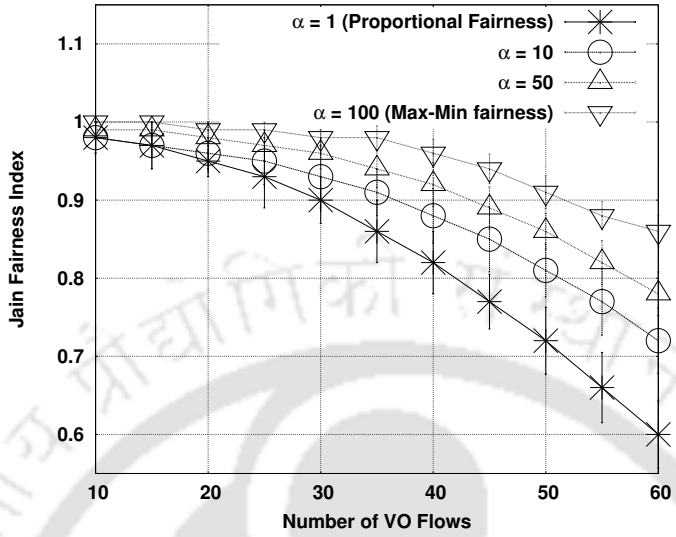

Figure 4.8: Jain Fairness Index

fairness. It can be seen from the figure that proportional fairness index is maximum when $\alpha = 1$. As α value increases, proportional fairness index decreases. Another observation can be made that proportional fairness index value increases as number of VO flows increase in the network. This indicates that more proportionality in channel share is required when high priority flows dominate the network.

Figure 4.8 shows the Jain fairness index for different α values. Jain fairness index reflects the equity in channel share. Therefore it is used to measure max-min fairness criteria in the network. It can be observed from Figure 4.8 that Jain fairness index value is minimum for $\alpha = 1$. The reason behind this is that proportionality in the network violates max-min fairness criteria by starving low priority flows. Further Jain fairness index decreases as number of high priority flow dominates the network.

Figure 4.9 compares network utilization with different α values and compares it with MCCA. Network utilization for multi-class service flows can be defined as percentage of data traffic transferred successfully compared to the actual demand based on service priority. It can be seen that network utilization is better in the proposed scheme compared to other three mechanisms - proportional fairness, max-min fairness and IEEE 802.11s. Theoretically, proportional fairness should give maximum utilization. However in proportional fairness, BE flows are starved when VO flows dominate the network, resulting in lower utilization. For max-min fairness, network utilization is lower than that of proportional fairness, because even the high priority traffic may not get sufficient

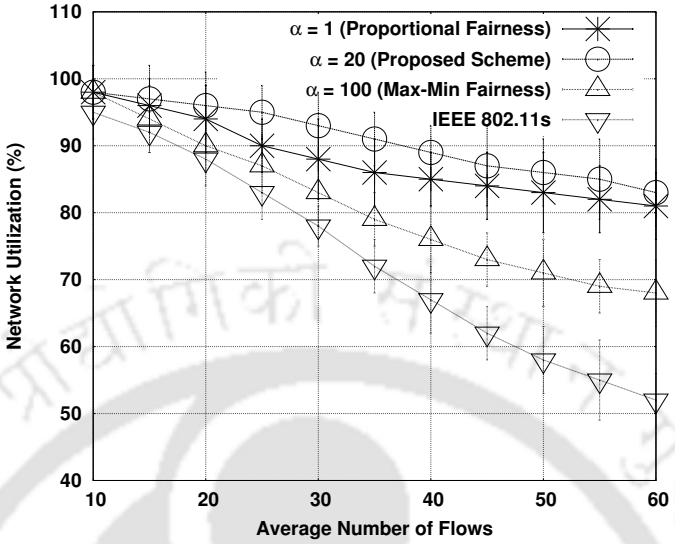

Figure 4.9: Network Utilization

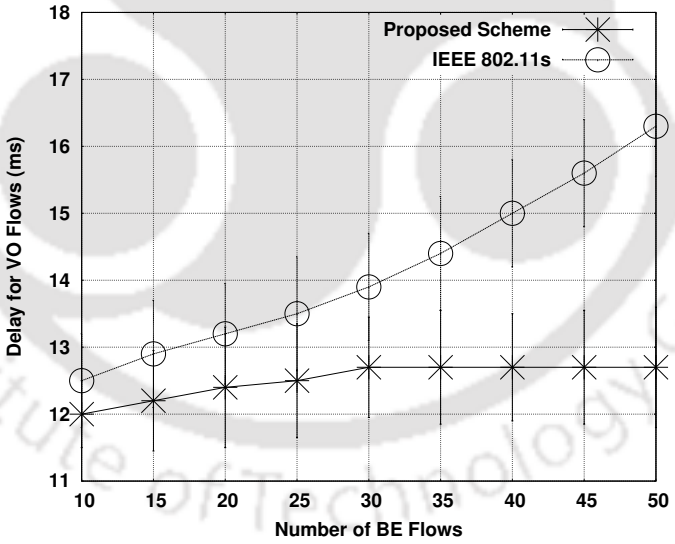

Figure 4.10: Delay for VO flows

channel share based on their service class demand. The proposed scheme is a trade-off between these two and improves network utilization by providing sufficient channel share to the high priority traffic and avoiding starvation for the low priority traffic.

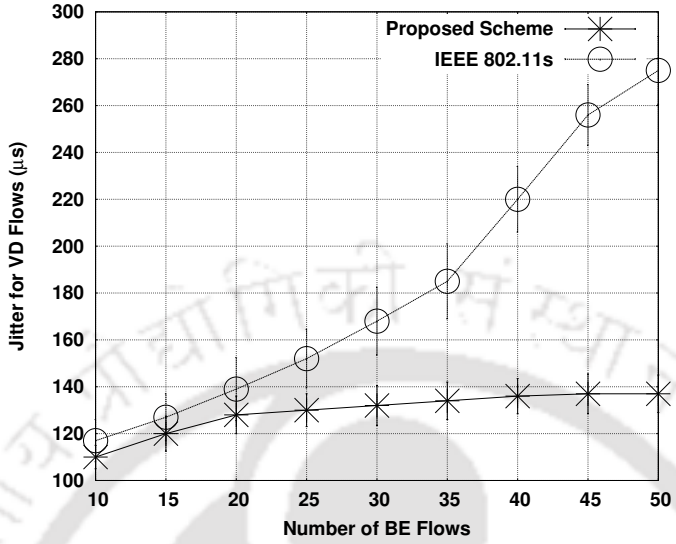

Figure 4.11: Jitter for VD flows

4.5.4 General Performance Parameters

Figure 4.10 shows the average end-to-end delay observed for the VO traffic with respect to varying number of BE flows. For this experiment, 20 VO flows and 10 VD flows are uniformly distributed in the network. For this experiment the VD traffic acts as the background traffic in the network. The VD traffic is incorporated to check the performance of VO flows in presence of traffics from different service classes. The graph is plotted by varying number of BE flows. It can be seen from the figure that average end-to-end delay for VO flows increases for IEEE 802.11s network, as number of BE flows increases. On the contrary, end-to-end delay for VO flows remains almost constant in the proposed scheme. This is because the proposed scheme always guarantees minimum data rate for the high priority traffic, and gives maximum priority to the VO packets.

Figure 4.11 shows average jitter for VD traffic. For this experiment, 20 VD flows and 10 VO flows are distributed uniformly in the network. The VO flows act as the background traffic, and limit the maximum rate for the VD traffic (priority of VO traffic is more than VD traffic). The average jitter for VD traffic is checked by varying number of BE flows. The figure shows that average jitter is very small for the proposed scheme, whereas it increases exponentially in case of IEEE 802.11s. The priority assignment and assurance of minimum data rate keep the jitter constant in the proposed scheme.

One severe problem for multi-hop mesh network is that end-to-end throughput decreases drastically as number of hops increases. The reason for this is that the long

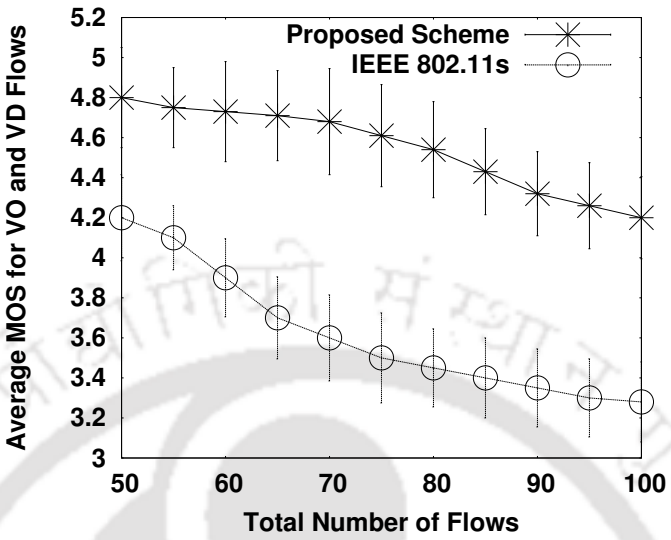

Figure 4.12: Hop vs Throughput

distance flows get starved by the short distance flows. The proposed scheme also solves this problem by limiting the maximum channel share that a flow can use, irrespective of number of hops it traverses. Figure 4.12 shows average throughput with respect to number of hops. In IEEE 802.11s, average throughput degrades exponentially as number of hops increases. On the contrary, the average throughput degradation with the increase in number of hops is significantly less. In the proposed scheme, channel share is limited based on traffic demand and flow priority. So the shorter flows can not overuse the channel, leading to efficient channel usage for all flows in the network.

4.6 Summary

This chapter proposes a service differentiation strategy in IEEE 802.11s MCCA based mesh network while ensuring fairness. Two issues have been addressed in this chapter for multi-class service network - inter-class service differentiation and intra-class fairness. The concept of $(\alpha, \wp)$ proportional fairness is used to balance the trade-off between proportional fairness and max-min fairness that solves these two issues. The service demand with fairness requirement is modeled as a non-linear convex optimization problem, considering the effect of interference. A distributed mechanism is designed based on sub-gradient method to solve the optimization locally at every mesh STA. The convergence and equilibrium of the method is analyzed theoretically. To provide better service level

agreement, the HWMP protocol is augmented to support the call admission control mechanism. The effectiveness of the proposed scheme is analyzed using simulation results.

Till now, this thesis has considered single-rate mesh networks where every mesh STAs operates in a single data rate. However, modern wireless routers supports multi-rate features where one of the data rates from the list of supported data rates is chosen dynamically based on channel condition. Multi-rate support can handle the wireless channel dynamics by adopting the most sustainable data rate that can operate optimally in the present channel condition. IEEE 802.11s MPM, MCCA and HWMP protocols do not provide any standard mechanism for rate adaptation in mesh networks. Multi-rate support in mesh networks introduces additional problem of rate-hops-interference trade-off. The next chapter analyzes this trade-off theoretically and provides an augmentation over the standard protocols to support multi-rate adaptation in IEEE 802.11s mesh networks.

Chapter 5

Multi-Rate Support in Mesh Networks: The Rate-Hops-Interference Trade-off

Now a days, most of the commercially available wireless routers are equipped with multi-rate support to adopt the physical data rates based on the channel condition fluctuations. However, IEEE 802.11s does not provide any mechanism for rate adaptation in mesh networks. The recent studies in multi-rate support have shown that the low data rates are much effective when the channel error rate is high. Because of the physical layer modulation and signal decoding issues, low data rates are sustainable for long transmission ranges. Therefore, for the multi-hop mesh networks, low data rates may scale down the number of hops towards the destination, resulting less end-to-end delay. However, for a highly loaded network, long transmission ranges may increase the network interference. This chapter theoretically analyzes the rate-hop-interference trade-off in IEEE 802.11s multi-rate mesh network and uses the theoretical analysis to propose a rate adaptation mechanism over the standard protocols. In summary, the major contributions of this chapter are as follows.

- IEEE 802.11s mesh architecture has been represented as a queuing network to theoretically model the rate-hop-interference trade-off. This theoretical analysis helps in understanding the effect of different data rate selections over the performance of the mesh network.

- The functionality of IEEE 802.11s MPM, MCCA and HWMP are enhanced to

support rate adaptation based on the optimal data rate selection. The proposed rate adaptation protocol, ***H**op-**I**nterference **T**rade-off based **R**ate **A**daptation for **M**esh (HITRAM)*, explores the rate-hop-interference trade-off, and provides a rate-adaptation technique over the standard protocols.

- The protocol is implemented in Qualnet-5.0.1 network simulator and the effectiveness of the proposed rate adaptation scheme is established through simulation results. The performance of the *HITRAM* protocol is compared with other state-of-the-art works.

The rest of the chapter is organized as follows. Section 5.1 gives the motivation of designing an efficient rate adaptation mechanism over the IEEE 802.11s technology. In section 5.2, the queuing network analysis is used to theoretically model the rate-hop-interference trade-off for multi-rate IEEE 802.11s mesh network. Based on this theoretical analysis, the rate adaptation in IEEE 802.11s mesh network, *HITRAM*, has been proposed in section 5.3. The scheme is implemented in Qualnet simulator, and the performance of *HITRAM* is analyzed and compared with other schemes, as reported in section 5.4. Finally section 5.5 concludes the chapter.

5.1 Motivation

IEEE 802.11s MAC layer technology can operate above any of the physical layer technologies supported by the IEEE 802.11b/g/n standards. Current standard for 802.11b/g/n physical layer technologies support multiple data rates for the communication between two wireless nodes. As discussed in Chapter 2, 802.11g supports eight data rates using Orthogonal Frequency Division Multiplexing (OFDM) for data transmission, shown in Table 5.1[1]. Due to different channel encoding and modulation techniques for different data rate support, the transmission ranges are different for the different data rates [120]. The industry standard transmission ranges for different 802.11g data rates are shown in Table 5.1, as reported by the CISCO white chapter.

Table 5.1 shows that the transmission range decreases as the data rate increases. Most of the rate adaption algorithms proposed in the literature, such as [113, 117–119], and the references therein, mainly focus on the mechanism to find a sustainable data rate based on the channel fluctuations, measured in terms of Signal to Noise Ratio (SNR).

[1]The table is reproduced from Chapter 2 for illustration purpose.

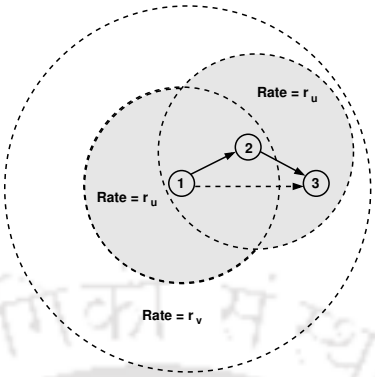

Figure 5.1: Three mesh STAs scenario with different data rates

Table 5.1: Data Rate vs Range in 802.11g

Data Rate (Mbps)	6	9	12	18	24	36	48	54
Modulation Technology	BPSK	BPSK-3	QPSK	QPSK-1	16-QAM	16-QAM	64-QAM	64-QAM
Communication Range (feet)	300	250	210	180	140	100	95	90

However, in the case of mesh network, the rate adaption mechanism is more challenging because of following reasons,

1. Low data rates increase the transmission ranges. For multi-hop networks, long transmission range decreases the number of hops between a source, destination pair. Considering Fig. 5.1, with data rate r_u, mesh STA 1 and mesh STA 3 are connected by two-hops, using mesh STA 2 as an intermediate relay. However, mesh STA 3 can be reached directly in one hop, if data rate r_v ($r_v < r_u$) is used. It is well known for the multi-hop networks, that the throughput decreases as the number of hops increases [134]. Therefore, it may be possible that one-hop communication using data rate r_v improves the network throughput compared to the two-hop communication using a high data rate r_u.

2. For a network with moderate to high traffic load, long transmission range increases the possibility of interference among ongoing communications, resulting in throughput degradation.

The above arguments indicate that there is a trade-off among the data rate, the number-of-hops and the interference for multi-rate mesh network. This trade-off is

theoretically modeled in the next section. Based on the trade-off, the IEEE 802.11s protocols are augmented for the support of rate adaptation technology, as discussed is subsequent sections.

5.2 Queuing Analysis of IEEE 802.11s for a Specific Rate Region

This section models the performance of IEEE 802.11s by applying diffusion approximation method [209] over time-varying queuing network. The objective of this analysis is to capture the behavior of different data rates at two extreme scenarios: the maximum interference scenario (when all mesh STAs interfere with each other) and the minimum interference scenario (the communication is in a chain, only the mesh STAs in the communication path interfere), keeping the Euclidean distance between the source and destination fixed. Thus changes in the data rate also effects number of hops between a fixed source-destination pair and the interference level.

It can be noted that this chapter considers single-interface mesh networks for the ease of presentation. The proposed scheme can be easily extended for multi-interface network by adopting the protocol interference model, as proposed in Chapter 3, and using per-interface rate adaptation decision, rather than per-STA decisions as discussed in this chapter.

5.2.1 Network Model

Let us assume that the rate region is defined as $\mathcal{R} = \{r_u | u \in (1, ..., \hbar)\}$, i.e. there are $\hbar$ different data rates available, with $r_{min} = r_1$ be the minimum data rate and $r_{max} = r_\hbar$ be the maximum data rate. Further, $r_u > r_v$; $r_u, r_v \in \mathcal{R}$ if $u > v$. To make the analysis simple and understandable, the arena is considered to be divided into non-overlapping hexagonal zones. The hexagonal zone is considered as an approximation of communication coverage to avoid the complexities introduced in the analysis due to the edge effects. Every hexagonal zone has a mesh STA. It has been considered that two mesh STAs, STA_i and STA_j, are capable of communicate at r_{max} if their zones share a common point. The set of one-hop neighbors for the STA_i, with data rate r, is denoted as $N_1^i(r)$. The number of one-hop neighbors for every mesh STAs is equal because of the hexagonal zone assumption. Suppose, $\kappa_r = |N_1^i(r)|$ is the number of one-hop neighbors at data rate r. The *rate subset property* of the neighbor set is satisfied with respect to the data rate, which can be defined as follows. Consider two different data rates r_u and r_v such that $r_u > r_v$. Then

$N_1^i(r_u) \subseteq N_1^i(r_v)$ and $\kappa_{r_u} < \kappa_{r_v}$. Without the loss in generality, this chapter assumes single channel wireless mesh network. The proposed analysis can be extended for multiple channel network by grouping the mesh routers that are using similar channel (co-channel interference) or the overlapping channels (adjacent channel interference).

The mesh network can be represented as a queuing network where the data forwarding of every mesh STA in a DTIM interval can be modeled as a G/G/1 queue, as follows;

- Packets arrive at every STA_i according to a Poisson process with the mean arrival rate as Λ_i (packet arrival in a multi-hop wireless network can be effectively modeled as a Poisson process, because of its random but self-similar nature [210]). The packet arrival includes both the clients' packets and the relayed packets from the neighboring mesh STAs.
- Due to the MCCAOP channel reservation procedure, the packets from STA_i are forwarded with effective service rate $\mu_i(r)$, which is based on the channel reservation in the current DTIM interval, with the selected data rate r.

It can be noted that the service rate $\mu_i(r)$ may differ in different DTIM interval, and without the loss in generality, the analysis of the effect of multi-rate is confined within one DTIM interval. Similar procedure is repeated for consecutive DTIM intervals.

5.2.2 Derivation of the Parameters for Queuing Network

Two different events of packet arrival can occur in a mesh STA. First, the packet may arrive from the clients, and second the packet may be a relayed packet. Let us assume that Λ_e denotes the packet arrival rate from the clients to every mesh STA. The *visit ratio* of a mesh STA, is defined as the average number of time a packet is forwarded by the mesh STA. The visit ratio of STA_i, denoted as e_i, is given by,

$$e_i = p_{0i} + \sum_{r' \in \mathcal{R}} \sum_{STA_j \in N_1^i(r')} p_{ji}(r').e_j \tag{5.1}$$

where p_{0i} denotes the probability that a packet enters the queuing network from the clients of STA_i, and $p_{ji}(r')$ denotes the probability of forwarding a packet to STA_i from $STA_j \in N_1^i(r')$.

The arrival rate Λ_i is the *effective arrival rate* at STA_i that has two components - *i)* arrival from the clients, and *ii)* relayed packet arrival from the neighbors. Therefore, Λ_i can be expressed as,

$$\Lambda_i = \Lambda_e.e_i \tag{5.2}$$

The *utilization factor* for STA_i with data rate r, denoted as $\rho_i(r)$, is given by;

$$\rho_i(r) = \frac{\Lambda_i}{\mu_i(r)} \tag{5.3}$$

Suppose, c_{Ai}^2 denotes the *Squared Coefficient of Variance* (SCV) of the inter-arrival times at STA_i. Using the diffusion approximation method, c_{Ai}^2 can be expressed as,

$$c_{Ai}^2 = 1 + \sum_{r' \in \mathcal{R}} \left(\sum_{STA_j \in N_1^i(r')} (c_{Bj}^2 - 1) p_{ji}^2 . e_j . e_i^{-1} \right) \tag{5.4}$$

where c_{Bj}^2 is the SCV of the service time at STA_j.

According to diffusion approximation of G/G/1 queuing network, the mean number of packets at STA_i, denoted as Π_i, can be expressed as follows;

$$\Pi_i = \frac{\rho_i}{1 - \overline{\rho_i}} \tag{5.5}$$

where,

$$\overline{\rho_i} = \exp\left(-\frac{2(1-\rho_i)}{c_{Ai}^2 . \rho_i + c_{Bi}^2} \right)$$

The parameters of the G/G/1 queuing network for the multi-rate mesh networks are calculated based on a set of lemmas, as stated follows.

Lemma 5.1. *The probability that a packet is forwarded from the queue of STA_i to the queue of STA_j at data rate r, denoted by $p_{ij}(r)$, is given by*

$$p_{ij}(r) = \begin{cases} 2(1 - \frac{1}{\kappa_r}) \prod_{u=1}^{\hbar} (1 - \Gamma(u, r)); & STA_j \in N_1^i(r) \\ 0; & Otherwise \end{cases} \tag{5.6}$$

where,

$$\Gamma(u, r) = \frac{\hbar - (u-1)}{\hbar(\kappa_{r_{u-1}} - \kappa_{r_u})}$$

Proof. Suppose, S and R are the sender and receiver mesh STAs respectively. For a successful transmission, S and R have to first reserve channel in the DTIM interval, according to the MCCA reservation procedure. S can successfully send a MCCAOP reservation request, if no other station in the transmission range of S reserves channel that overlaps with the reservation of S. At the same time R can forward back a MCCAOP

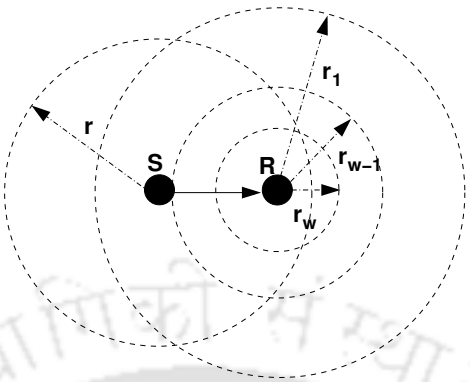

Figure 5.2: Transmission from mesh STA S to mesh STA R

reply if no other mesh STAs transmits simultaneously, that interfere at R. Suppose, $P[.]$ denotes the probability of an event occurred. Then,

$$P[\text{Packet is forwarded successfully at rate } r] = P[\text{No overlapping channel reservation at } S] \times P[\text{No other mesh STAs interfere with } R] \tag{5.7}$$

Overlapping channel reservation may occur either due to a transmission, or a reception, in the transmission range of S. Therefore,

$$P[\text{No overlapping channel reservation at } S] = 2(1 - \frac{1}{\kappa_r}) \tag{5.8}$$

To find out that no other mesh STAs transmits that cause interference at R, let us consider Fig. 5.2. The dotted regions show the area where a particular data rate can sustain. Suppose, $\Re(r)$ denotes the region where data rate r can sustain. As discussed earlier, transmission range increases as the data rate decreases. Therefore $\Re(r_\hbar) \subset \Re(r_{\hbar-1}) \subset ... \subset \Re(r_1)$. Starting from the minimum data rate r_1 (with maximum transmission range), interference occurs at R, if the mesh STAs at $\Re(r_1) - \Re(r_2)$ transmit at the data rate r_1. Similarly, interference can occur at R, if the mesh STAs at $\Re(r_3) - \Re(r_2)$ transmit at the data rates r_1 and r_2. Proceedings this way, interference can occur at R, if the mesh STAs at $\Re(r_\hbar)$ transmits at one of the data rates $r_1, r_2, ..., r_\hbar$.

Let us consider the mesh STAs at $\Re(r_{u-1}) - \Re(r_u)$ where $r_u, r_{u-1} \in \mathcal{R}$. There is no interference at R, if none of the mesh STAs in $\Re(r_{u-1}) - \Re(r_u)$ transmits at the data rates $r_u, r_{u+1}, ..., r_\hbar$. This indicates that there are $\hbar - (u-1)$ possible data rates in which the mesh STAs in $\Re(r_{u-1}) - \Re(r_u)$ cannot transmit to avoid interference at R. Suppose, $\mathcal{E}_1$ denotes the event that one of the nodes in $\Re(r_{u-1}) - \Re(r_u)$ transmits. Then $P[\mathcal{E}_1]$ is given

as,

$$P[\mathcal{E}_1] = \frac{1}{\kappa_{r_{u-1}} - \kappa_{r_u}}$$

Suppose, the event $\mathcal{E}_2$ denotes that one of the data rates in $\{r_u, r_{u+1}, ..., r_\hbar\}$ is chosen. $P[\mathcal{E}_2]$ is derived as,

$$P[\mathcal{E}_2] = \frac{\hbar - (u-1)}{\hbar}$$

As the events $\mathcal{E}_1$ and $\mathcal{E}_2$ are mutually exclusive,

$$P[\mathcal{E}_1.\mathcal{E}_2] = P[\mathcal{E}_1] \times P[\mathcal{E}_2] = \frac{\hbar - (u-1)}{\hbar(\kappa_{r_{u-1}} - \kappa_{r_u})}$$

Suppose, $\overline{\mathcal{E}_u}$ denotes the event that no mesh STAs in $\Re(r_{u-1}) - \Re(r_u)$ transmit at data rate $r_u, r_{u+1}, ..., r_\hbar$. Then,

$$P[\overline{\mathcal{E}_u}] = 1 - P[\mathcal{E}_1.\mathcal{E}_2] = 1 - \frac{\hbar - (u-1)}{\hbar(\kappa_{r_{u-1}} - \kappa_{r_u})} = 1 - \Gamma(u, r)$$

Suppose, $\overline{\mathcal{E}}$ denotes the event that no other mesh STAs interfere with R. Then,

$$P[\overline{\mathcal{E}}] = \prod_{u=1}^{\hbar} P[\overline{\mathcal{E}_u}] = \prod_{u=1}^{\hbar} (1 - \Gamma(u, r)) \tag{5.9}$$

Using equation (5.7), equation (5.8) and equation (5.9), the value of $p_{ij}(r)$ can be derived. □

Lemma 5.2. *Suppose, there are on average φ number of clients under every mesh STA. The visit ratio of STA_i, denoted as e_i, can be expressed as,*

$$e_i = \frac{1}{\varphi\left(1 - \sum_{r' \in \mathcal{R}} \left(\prod_{u=1}^{\hbar} (1 - \Gamma(u, r'))\right)\right)} \tag{5.10}$$

Proof. The packets arrive at each mesh STA according to an independent and identically distributed Poisson process. Therefore, the probability that a new packet arrives at STA_i from one of its clients equals $1/\varphi$. Therefore, $p_{0i} = 1/\varphi$. Substituting p_{0i} and p_{ji} in equation (5.1),

$$e_i = \frac{1}{\varphi} + \sum_{r' \in \mathcal{R}} \left(\sum_{STA_j \in N_1^i(r')} \frac{1}{\kappa_{r'}} \prod_{u=1}^{\hbar} (1 - \Gamma(u, r')).e_j \right)$$

In a stable and steady state queuing network, the visit ratio for all the mesh STAs become symmetrical [209]. Therefore, $e_i = e_j$. Substituting the value of e_j,

$$e_i = \frac{1}{\varphi} + e_i \sum_{r' \in \mathcal{R}} \left(\prod_{u=1}^{\hbar} (1 - \Gamma(u, r')) \right)$$

Rearranging the values, e_i can be expressed in terms of equation (5.10).

□

Lemma 5.3. *The effective arrival rate at STA_i, denoted as Λ_i, can be expressed as,*

$$\Lambda_i = \frac{\Lambda_e}{\varphi \sum_{r' \in \mathcal{R}} \left(\prod_{u=1}^{\hbar} (1 - \Gamma(u, r')) \right)}$$

Proof. The proof can be directly derived using lemma 5.2 and equation (5.2). □

Suppose, O denotes the mesh STA where the packet enters the mesh network, called the originator mesh STA, and G is the mesh gate, from where the packet leaves the mesh network. The packet is forwarded from O to G using a set of mesh STAs as intermediate relays. The next-hop relay is selected based on the data rate. Let us assume that if an intermediate relay I selects data rate r, then it forwards the packet to the next hop relay at the maximum Euclidean distance from I, where data rate r sustains. This subsection presents a backward formulation, where the data rate is first assumed, and then its effect is analyzed over the number of hops and the interference. Though the data rate is selected based on the number of hops and the interference conditions during actual protocol design, the backward formulation is helpful for analyzing the effect of different data rate selections on the network performance. For a particular scenario, the optimal data rate can be chosen that provides best network performance according to the theoretical analysis. The effect of the selected data rate over the number of hops and the interference can be expressed using following lemmas and theorems.

Lemma 5.4. *A mesh STA is said to be active if it has a packet to transmit. Suppose, Ψ_i denotes number of active interfering mesh STAs for STA_i. Then,*

$$E[\Psi_i] = \sum_{r' \in \mathcal{R}} \kappa_{r'} . \rho_i(r') \tag{5.11}$$

$$E[\Psi_i^2] = \sum_{r' \in \mathcal{R}} \kappa_{r'} \rho_i(r')(1 + (\kappa_{r'} - 1)\rho_i(r')) + 2 \sum_{u<v} \kappa_u \kappa_v \rho_i(r_u) \rho_i(r_v) \tag{5.12}$$

Proof. Suppose, $\Psi_i(r)$ denotes the number of active interfering mesh STAs of STA_i, when

it transmits at data rate r. Then,

$$\Psi_i = \sum_{r' \in \mathcal{R}} \Psi_i(r')$$

$$\Psi_i^2 = \left(\sum_{r' \in \mathcal{R}} \Psi_i(r') \right)^2 = \sum_{r' \in \mathcal{R}} \Psi_i^2(r') + 2 \sum_{u<v} \Psi_i(r_u)\Psi_i(r_v)$$

It can be noted that the random variables $\Psi_i(r_u)$ and $\Psi_i(r_v)$ are independent. Taking expectation at both sides,

$$E[\Psi_i] = \sum_{r' \in \mathcal{R}} E[\Psi_i(r')] \tag{5.13}$$

$$E[\Psi_i^2] = \sum_{r' \in \mathcal{R}} E[\Psi_i^2(r')] + 2 \sum_{u<v} E[\Psi_i(r_u)]E[\Psi_i(r_v)] \tag{5.14}$$

STA_i can have a packet to transmit at data rate r, if its utilization $\rho_i(r) > 1$, that is the arrival rate is more than the service rate. Therefore $\Psi_i(r)$ is a binomial distribution with parameters $(\kappa_r, \rho_i(r))$. This follows,

$$E[\Psi_i(r)] = \kappa_r.\rho_i(r);\ E[\Psi_i^2(r)] = \kappa_r \rho_i(r)(1 + (\kappa_i - 1)\rho_i(r))$$

Replacing the value of $E[\Psi_i(r)]$ in equation (5.13) and equation (5.14), equation (5.11) and equation (5.12) directly follow. □

Lemma 5.4 characterizes the interference scenario expressed as the expected numbers of active interfering mesh STAs. The next theorem characterizes the service times of the mesh routers based on the interference information.

Theorem 5.1. *Suppose, L is the packet size and $X_i(r)$ is the service time of STA_i, when it transmits at data rate r. Then,*

$$E[X_i(r)] = \frac{\frac{L}{r}}{1 - \frac{L}{r}\Lambda_i \kappa_r \sum\limits_{r' \in \mathcal{R} \setminus \{r\}} \kappa_{r'} E[X_i(r')]} \tag{5.15}$$

$$E[X_i^2(r)] = \frac{L^2}{r^2}\big(E[\Psi_i^2] + 2E[\Psi_i] + 1\big) \tag{5.16}$$

Proof. The average service time of STA_i has two components - the time when the neighbors of STA_i reserve channel in the DTIM interval and the time when STA_i reserves channel in the DTIM interval with data rate r. Therefore,

$$X_i(r) = \frac{L}{r}\Psi_i + \frac{L}{r};$$

$$X_i^2(r) = \frac{L^2}{r^2}\Psi_i^2 + 2\frac{L^2}{r^2}\Psi_i + \frac{L^2}{r^2}$$

Taking expectation at both sides, and using equation (5.11) yield,

$$E[X_i(r)] = \frac{L}{r}\sum_{r'\in\mathcal{R}}\kappa_{r'}\rho_i(r') + \frac{L}{r}$$

Now, $\rho_i(r) = \Lambda_i E[X_i(r)]$. Therefore,

$$\begin{aligned} E[X_i(r)] &= \frac{L}{r}\sum_{r'\in\mathcal{R}}\kappa_{r'}\Lambda_i E[X_i(r')] + \frac{L}{r} \\ &= \frac{L}{r}\Lambda_i\kappa_r E[X_i(r)]\sum_{r'\in\mathcal{R}\setminus\{r\}}\kappa_{r'}E[X_i(r')] + \frac{L}{r} \end{aligned}$$

Rearranging the values, equation (5.15) yields. Similarly equation (5.16) can be derived by taking expectation at both sides of the equation of $X_i^2(r)$ and using equation (5.12). □

The SCV of service time of STA_i can be calculated using equation (5.15) and equation (5.16), as follows,

$$c_{Bi}^2 = \frac{E[X_i^2(r)] - E[X_i(r)]^2}{E[X_i(r)]^2} \tag{5.17}$$

Using the value of c_{Bi}^2, the value of c_{Ai}^2 and Π_i can be calculated through equation (5.4) and equation (5.5). Once the service rates of the individual mesh STAs are determined based on the interference information, the next task is to determine the average number of hops between the end-pairs. Following theorem characterizes the average number of hops required to transmit a packet, based on the selected data rates at intermediate mesh STAs.

Theorem 5.2. *Suppose, $\overline{D}_{OG}$ be the Euclidean distance between the packet originator O and the mesh gate G. The average number of hops between O and G, denoted as $\overline{S}_{OG}$, is given by,*

$$\overline{S}_{OG} = \frac{1}{\hbar}\sum_{r'\in\mathcal{R}}\frac{\overline{D}_{OG}}{C(r')} \tag{5.18}$$

where $C(r')$ denotes transmission range with data rate r'.

Proof. If the packet is forwarded using data rate r, then average number of hops between O and G is given by $\overline{D}_{OG}/C(r)$. Every intermediate mesh STA can select a data rate from $\mathcal{R}$, and there are $\hbar$ numbers of supported data rates. Therefore, averaging over number of supported data rates, equation (5.18) yields. □

Finally, the end-to-end delay is calculated based on the selected data rate, the number of hops between the end pairs (as characterize in Theorem 5.2), and the interference scenario (expressed through the service time, as presented in Theorem 5.1).

Theorem 5.3. *In the steady state mesh network with multi-rate support, the average end-to-end delay from mesh STA O to mesh gate G, denoted as $\overline{\delta}_{OG}$, is given as,*

$$\overline{\delta}_{OG} = \frac{\varphi \Pi}{\hbar \Lambda_e} \sum_{r' \in \mathcal{R}} \frac{\overline{D}_{OG}}{C(r')} \left(\prod_{u=1}^{\hbar} (1 - \Gamma(u, r')) \right) \tag{5.19}$$

where Π denotes average number of packets in a mesh STA at steady state. According to diffusion approximation of queuing network, at steady state, $\Pi = \Pi_i$.

Proof. Suppose, δ_i denotes the average packet delay at STA_i. According to Little's law, $\delta_i = \Pi_i / \Lambda_i$. Therefore, the average end-to-end delay can be represented as, $\overline{\delta}_{OG} = \overline{S}_{OG} \times \delta_i$. Replacing these values using Lemma 5.3 and Theorem 5.2, equation (5.19) yields. □

The steady state maximum achievable throughput of the mesh routers can also be characterized, as expressed in the following theorem.

Theorem 5.4. *In the steady state mesh network with multi-rate support, the maximum achievable throughput for STA_i, denoted as Z_i, is given as,*

$$Z_i = \frac{\varphi r B}{L(1 + \kappa_r A)} \tag{5.20}$$

where,

$$A = \sum_{r' \in \mathcal{R} \setminus \{r\}} \kappa_{r'} E[X_i(r')];$$

$$B = \sum_{r' \in \mathcal{R}} \left(\prod_{u=1}^{\hbar} (1 - \Gamma(u, r')) \right)$$

Proof. The *maximum achievable throughput* of STA_i is the maximum value of packet arrival rate at clients (Λ_e), for which average end-to-end delay remains finite. According to diffusion approximation of G/G/1 queue, in order to have finite delay, following inequality must be satisfied [209].

$$\Lambda_i E[X_i(r)] < 1$$

Based on equation (5.15), replacing the value of $E[X_i(r)]$,

$$\Lambda_i \frac{\frac{L}{r}}{1 - \frac{L}{r} \Lambda_i \kappa_r A} < 1 \qquad \Rightarrow \frac{\frac{L}{r}}{\frac{1}{\Lambda_i} - \frac{L}{r} \kappa_r A} < 1$$

$$\Rightarrow \frac{1}{\Lambda_i} > \frac{L}{r}(1 + \kappa_r A) \qquad \Rightarrow \Lambda_i < \frac{r}{L(1 + \kappa_r A)}$$

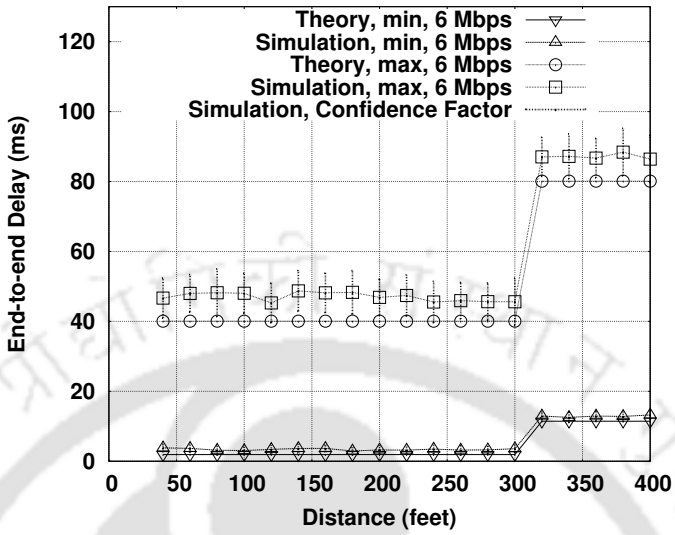

Figure 5.3: Theory versus Simulation (6 Mbps)

Replacing the value of Λ_i using Lemma 5.3 and rearranging,

$$\Lambda_e < \frac{\varphi r B}{L(1+\kappa_r A)}$$

This leads to equation (5.20). □

For a data rate r, equation (5.19) shows the effect of the selected data rate on the end-to-end delay based on the number of hops and the interference information, according to the transmission ranges of the selected data rates. Similarly equation (5.20) shows the effect of the selected data rate on maximum achievable throughput. The rate-hop-interference trade-off has been shown in the next subsection using numerical results obtained from the theoretical analysis.

5.2.3 Validation and Analysis of the Model

This subsection validates the theoretical model derived for end-to-end delay in a multi-rate mesh network by comparing the theoretical result with the simulation result. Then the results obtained from the theoretical model are analyzed to show the trade-off among rate, hop and interference for multi-rate mesh networks.

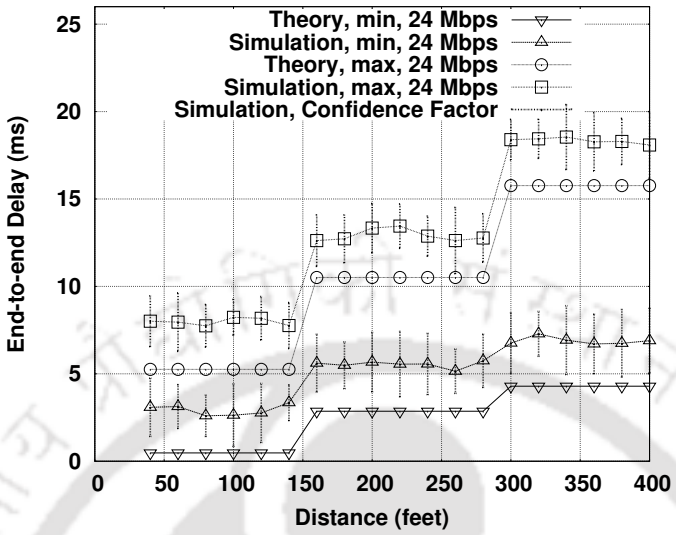

Figure 5.4: Theory versus Simulation (24 Mbps)

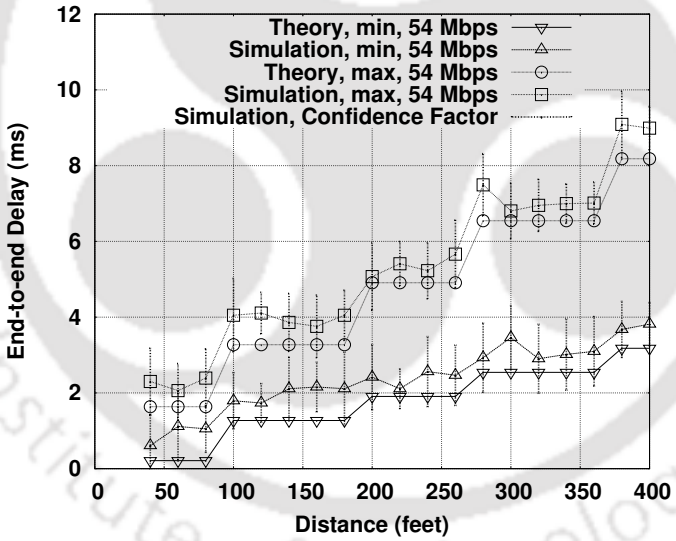

Figure 5.5: Theory versus Simulation (54 Mbps)

Model Validation

To validate the proposed theoretical model, the results obtained from the theoretical analysis are compared with the simulation results from Qualnet 5.0.1 [71] network simulator framework. Qualnet-5.0.1 has in-built support for IEEE 802.11s mesh networking. 802.11g rate region is used for simulation purpose that supports eight different data rates as shown in Table 5.1. Two different network setups have been considered - first a network with

the maximum interference, and second a network with the minimum interference. For maximum interference network, 144 mesh STAs are placed in an approximate hexagonal structure (similar to the scenario considered in the theoretical analysis), where all the mesh STAs have data to transmit, and they content for reserving channels in the DTIM interval. The mesh gate is considered at one corner of the arena. The position of the originator mesh STA is shifted gradually through the diagonal of the arena to increase the Euclidean distance between the originator mesh STA and the mesh gate. The communication distance for different data rates are considered according to the CISCO white paper [121]. On the other hand, for minimum interference network, the communication is only between the packet originator and the mesh gate, and the interference is limited only among the mesh STAs in the data forwarding path. The data generation rate at the clients have been taken as 512 Kbps, and on average 10 clients are associated with every mesh STA. The DTIM interval is taken as 200 ms. Every simulation scenario is executed for 10 times with different seed values, and average is taken to plot the graphs. The confidence factor, determines as the variance of the results obtained in different simulation trials with different seed values, have been shown in the figures using a vertical line. Fig. 5.3 to Fig. 5.5 show the comparison between the theoretical results and the simulation results for three different data rates - the minimum data rate (6 Mbps), the maximum data rate (54 Mbps) and an intermediate data rate (24 Mbps). In the figures 'max' denotes the maximum interference scenario, and 'min' denotes the minimum interference scenario. It can be seen from the figures that the results obtained from the theoretical model are similar with the simulation results for all the three data rates. It can be noted that the throughput value is not compared with the simulation results, as the theoretical analysis reveals the maximum achievable throughput based on the bound on end-to-end delay. However, it has been observed from simulation traces that the actual network throughput for different data rates follows a similar pattern as obtained from the theoretical bound. Nevertheless, the simulation values are less than their theoretical counterpart, as a result of compulsory physical and MAC layer signaling overhead.

Model Analysis

Similar scenarios, as described earlier, have been used to analyze the results obtained from the theoretical model. Fig. 5.6 shows the end-to-end delay for different 802.11g data rates in the minimum interference scenario of IEEE 802.11s mesh networking technology. Similarly, Fig. 5.7 shows the end-to-end delay for different data rates in the maximum interference scenario. In the minimum interference scenario, 54 Mbps and 48 Mbps perform

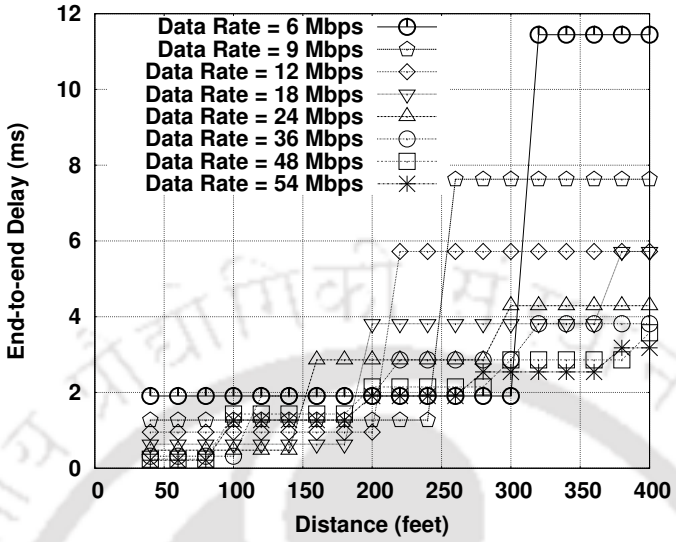

Figure 5.6: Delay at minimum interference

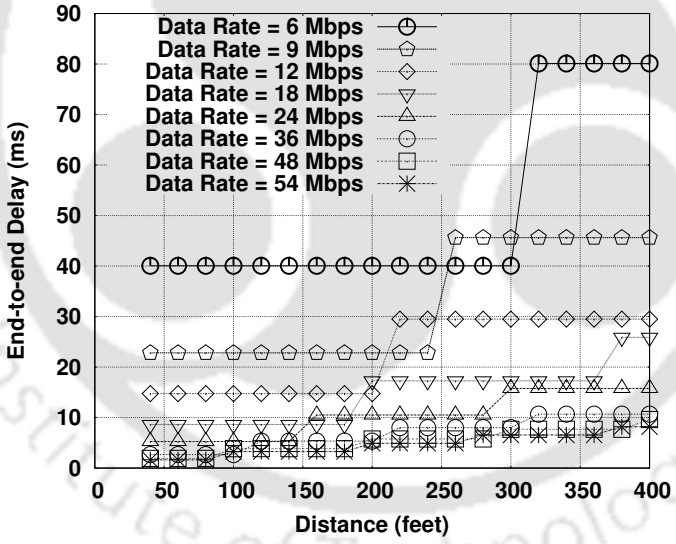

Figure 5.7: Delay at maximum interference

better than other data rates when the distance between the originator mesh STA and the mesh gate is less than 100 feet. At 100 feet distance, 36 Mbps provides less end-to-end delay. The trend changes again after 100 feet distance. This time 24 Mbps achieves better result than other data rates. Proceeding this way, it can be observed that 6 Mbps performs better than all other high data rates when the distance is 300 feet. This variation of end-to-end delay is the result of the different number of hops between the end pair for different

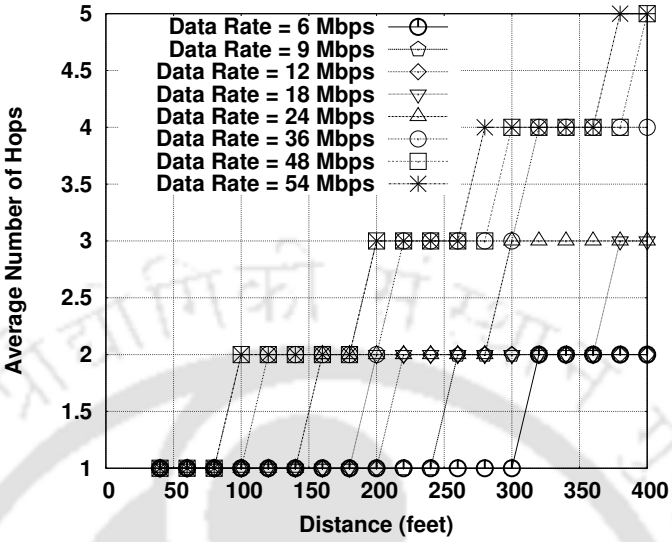

Figure 5.8: Data rate vs number of hops

data rates. Fig. 5.8 shows the average number of hops between the originator mesh STA and the mesh gate for different data rates. When the distance is less that 100 feet, the mesh gate can be reached from the originator mesh STA using single hop only. Therefore 54 Mbps performs better than all other rates. However, at 100 feet distance, 54 Mbps and 48 Mbps require two hops to transmit the packet, whereas the packet can be forwarded using single hop if 36 Mbps data rate is used. As per-hop processing delay increases with the increase in number of hops, 36 Mbps achieves less end-to-end delay than other rates in this case. Similarly at 300 feet distance, 6 Mbps requires only single hop to transmit the packets, whereas 54 Mbps requires four hops. At this stage 6 Mbps performs better because the originator mesh STA can directly communicate with the mesh gate, whereas 9 Mbps and 12 Mbps require two hops and rest other high rates require even more number of hops.

The minimum interference scenario clearly shows the effect of the selected data rate on network performance based on number of hops required to transmit the packets. However, the interference is limited only among the previous hop and the next hop forwarder mesh STAs for this scenario. Fig. 5.7 shows the effect of interference over the performance for different data rates, using the maximum interference scenario. In this scenario, all the mesh STAs in the 12×12 grid topology have data to transmit. It can be seen from the figure that at maximum interference scenario, 54 Mbps functions better than all other low rates, irrespective of the hop distance. Fig. 5.9 shows average number of active neighbors

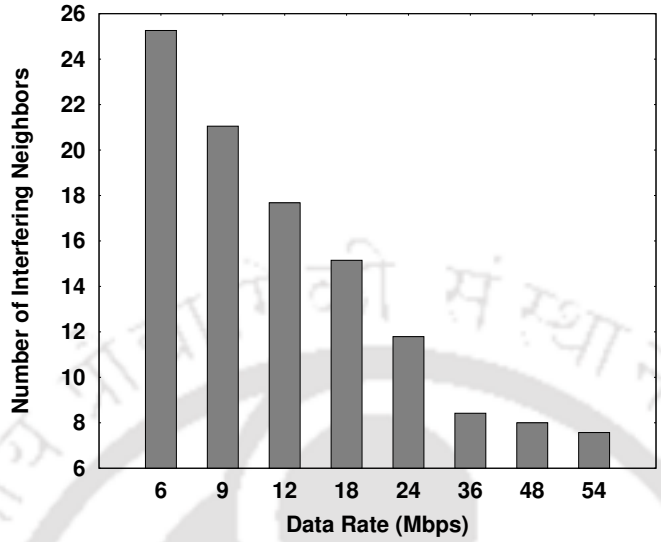

Figure 5.9: Data rate vs interfering neighbors

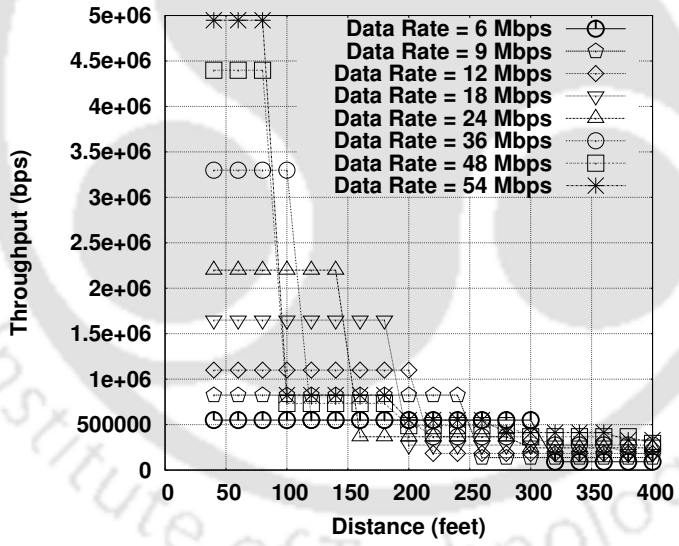

Figure 5.10: Throughput at minimum interference

at different data rates that interfere with the transmission of a mesh STA. The figure shows that the average number of interfering mesh STAs increases exponentially as the data rate decreases. High interference reduces the chance of obtaining MCCAOPs in the DTIM interval during the channel reservation procedure. Therefore, average channel reservation delay increases significantly, that suppresses the advantages obtained by reducing number of hops using low data rates.

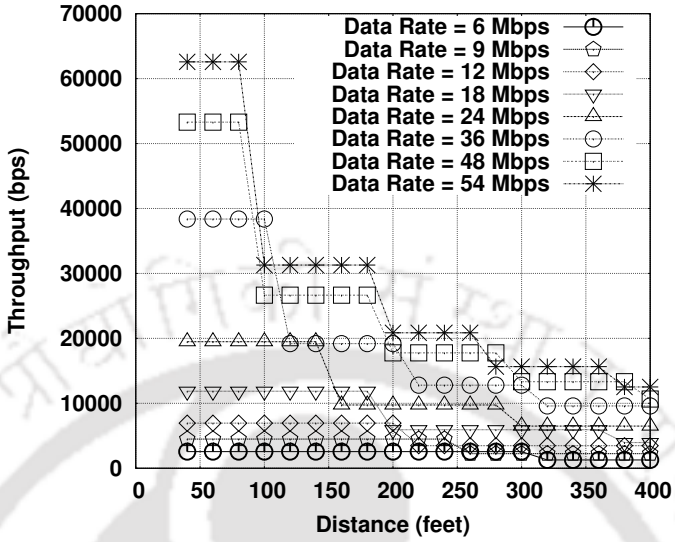

Figure 5.11: Throughput at maximum interference

Fig. 5.10 shows average throughput for the minimum interference scenario. In the minimum interference scenario, the rate-hop-interference trade-off significantly impacts maximum achievable throughput at the mesh STAs. Similar to the earlier cases, the data rate that provides maximum throughput changes with the change in the distance between the originator mesh STA and the mesh gate. Nevertheless, 54 Mbps data rate always provides maximum throughput in case of maximum interference scenario, as shown in Fig. 5.11.

In the real life community and commodity wireless mesh networks, the number of interfering neighbors changes with time, based on the number of associated clients and their individual traffic demands. Low data rates may be selected when number of active mesh STAs in the neighborhood is less, to reduce the number of hops between end-to-end communication pairs. On the contrary, high data rates should be selected when interference level is more. This rate-hop-interference trade-off is explored in this chapter to enhance the basic IEEE 802.11s mesh protocols to support multi-rate functionality, as discussed in the next section.

5.3 HITRAM: Protocol Design and Implementation

According to IEEE 802.11s standard, the mesh STAs adopt the supported data rates of a MBSS through a parameter called *BSSBasicRateSet*. However, the MPM protocol

specified in the standard does not provide any mechanism for choosing optimum peer mesh STAs based on the network interference and the selected data rate. To support rate adaptation in IEEE 802.11s, a coordination is required among the MPM, MCCA and HWMP protocols to adaptively select the peer mesh STAs and the next hop mesh STA based on the optimal data rate. The detailed design and implementation aspects of *HITRAM* with respect to the standard IEEE 802.11s protocols are discussed in the following subsections.

5.3.1 Mesh Beaconing

IEEE 802.11s uses mesh beaconing to collect neighbor information periodically. Every mesh STA broadcast mesh beacons after a timeout interval. However, the standard does not specify which data rate to use for the beacon broadcast in case of multi-rate support. In *HITRAM*, periodic mesh beaconing is done at the minimum supported data rate from *BSSBasicRateSet*. This enables all the mesh STAs to get informed about the complete neighborhood, irrespective of their data rate. However, the maximum sustainable data rate for every neighbor should be estimated to support for the rate adaptation. On receiving a beacon message from the neighbor mesh STA, every mesh STA builds a neighbor map (NMAP) that contains the tuple $< MAC, SDR_{max} >$ information, where MAC is the MAC address, works as the unique identifier for the mesh STA in the MBSS and SDR_{max} is the maximum sustainable data rate for that mesh STA. The maximum sustainable data rate is calculated using the well known Shannon Capacity formula as follows;

$$SDR_{max} = f(B \log(1 + SNR)) \tag{5.21}$$

Where B is the channel bandwidth, and $f : x \rightarrow r$ is a function that maps x to the nearest supported data rate, less than or equals to $r \in$ *BSSBasicRateSet*. SNR is calculated from the received beacons signal strength.

Implementation Issues

Though most of the wireless hardware returns *Received Signal Strength Indication* (RSSI) as the signal strength measurement, it is actually the SNR value. For example, the well known MadWifi driver calculates RSSI in terms of SNR, as specified in MadWiFi documentation [211]. The reason for reporting RSSI in terms of SNR is that the hardware specifies the measured value in dBm which is the difference between the signal level and the noise level for each packet. Therefore the driver calculates the absolute signal level by adding RSSI with the noise level.

However, the measured SNR values fluctuate with time due to the signal blocking, shadowing and multi-path propagation. The SNR predication mechanism proposed by the RAM protocol [113] has been adopted to deal with the irregular SNR measurements from the hardware. In this scheme, a moving average of SNR values has been used, based on the mean and the deviation, as follows;

$$S_{mean} = (1 - \epsilon)S_{mean} + \epsilon S_{curr}, \tag{5.22}$$

$$S_{dev} = (1 - \eta)S_{dev} + \eta(|S_{curr} - S_{mean}|) \tag{5.23}$$

$$S_{est} = S_{mean} - \vartheta S_{dev} \tag{5.24}$$

where $S_{mean}, S_{curr}, S_{dev}$, and S_{est} denote the mean value, the current value, the deviation and the estimated value of the SNR respectively, and $\epsilon, \eta, \vartheta$ are the design parameters. The values of ϵ, η, and ϑ are set up based on the real time measurement traces.

The estimated SNR value is used to find out the maximum sustainable data rate for every neighbor mesh STA by the help of the equation (5.21). Once the neighbor information are populated, the MPM protocol can start functioning. Further it can be mentioned that, wireless links may sometime deviate from bi-directional behavior, because of propagation and path loss effects. In the proposed scheme, the mesh beaconing procedure gives an initial estimation of the probable mesh STAs, with which single-hop communication may sustain with a data rate from *BSSBasicRateSet*. However, the actual data rate is selected based on the three way handshaking procedure during peer establishment. Therefore, the deviation in bi-directional behavior does not affect data communication within DTIM intervals.

5.3.2 Initial Peer Selection and Mesh Functioning

Initially the MPM protocol establishes peer only with the neighbors that support communication with maximum data rate from *BSSBasicRateSet*. The MCCA and the HWMP protocols operate according to the maximum data rate peering. Then every mesh STA periodically probes the network to find out whether performance can be improved by switching to a low data rate. On the contrary, if a mesh STA finds out performance degradation with low data rate due to increased interference, it switches back to the high rate. It can be noted that switching from one rate to another requires re-establishment of mesh peering. Therefore, the data rates are switched only during the normal peering procedure. According to MPM protocol, mesh peering are renewed

after *MeshHoldingTimeout*. The default value of *MeshHoldingTimeout* is set to 40 ms. Therefore, for every expiry of *MeshHoldingTimeout* value, the mesh STAs check for possibility of improving performance by switching to another data rate. The MCCA and HWMP protocols are augmented for this purpose, as discussed in following subsection.

5.3.3 Estimation of Rate-Hops-Interference Trade-off

For estimating the rate-hop-interference trade-off based on a selected data rate, the interference parameter is estimated from the information obtained during the channel access and scheduling based on MCCA. HWMP uses airtime value instead of hop count for finding out the best path between the end-to-end communication pairs. Therefore, this chapter uses the airtime value as an alternative to the hop count. The path quality information is obtained from the HWMP path-metric probing. The detailed procedures for the interference estimation and the path quality measurement are given next.

Interference Estimation

During MCCAOP channel reservation, every mesh STA broadcast MCCAOP advertisement messages that contain the channel reservation information. STA_i interfere with STA_j if the channel reservation of STA_i overlaps with the channel reservation of STA_j. Suppose, STA_i transmits at data rate r_u in the current DTIM interval. The service time of STA_i with data rate r_u in a DTIM interval, denoted as $\overline{X_i}(r_u)$, is the average time the mesh STA has to wait to get a MCCAOP, starting from the beginning of the DTIM interval. Following theorem characterizes the expected service time of STA_i, if data rate r_v is used instead of data rate r_u.

Theorem 5.5. *Suppose, $C(r_u)$ denotes the transmission range with data rate r_u. Then following inequality holds,*

$$\overline{X_i}(r_v) \leq \overline{X_i}(r_u)\frac{C^2(r_v)}{C^2(r_u)} \tag{5.25}$$

Proof. Suppose, $I(r_u)$ denotes number of interfering neighbors when data rate r_u is used. Then, due to the symmetry and the fairness properties of the MCCA reservation procedure,

$$\overline{X_i}(r_v) = \overline{X_i}(r_u)\frac{I(r_v)}{I(r_u)} \tag{5.26}$$

As discussed earlier, r_{max} sustains for minimum transmission range. Suppose, STA_i transmits at data rate r_u. Assuming r_{max} as the basis for minimum distance neighbor selection, the maximum number of mesh STAs that can remain within the communication

range with data rate r_u can be calculated using the *'ball packing'* result as provided in [212]. The *'ball packing'* result shows that, the maximum number of balls of radius θ that can be "packed" into a ball of radius $q\theta$, $q > 0$ is bounded by Lq^2, where $L = \pi\sqrt{3}/6$. In the present scenario, $q = \frac{C(r_u)}{C(r_{max})}$, where $C(r_u)$ denotes the transmission range at data rate r_u. Therefore,

$$I(r_u) \leq L\frac{C^2(r_u)}{C^2(r_{max})}; \qquad I(r_v) \leq L\frac{C^2(r_v)}{C^2(r_{max})}$$

Henceforth,

$$\frac{I(r_v)}{I(r_u)} \leq \frac{C^2(r_v)}{C^2(r_u)}$$

Replacing the values at equation (5.26), the result yields. □

Theorem 5.5 provides the expected service time for other data rates based on the current interference information with the selected data rate. This information is used to select the data rate for the next peering after *MeshHoldingTimeout* expires.

Path Quality Measurement

HWMP uses *airtime link metric* to check the path quality with the selected data rate. The protocol probes a test packet of size B_t with data rate r, and finds out the frame error rate e_f for the test frame. The metric value, denoted as $\mathfrak{C}$, is calculated using following equation,

$$\mathfrak{C}(r) = \left[O_p + \frac{B_t}{r}\right]\frac{1}{1-e_f}$$

where O_p is a constant that depends on the physical layer modulation technique. The airtime value reflects amount of the time required to transmit the test frame to the next hop.

HWMP provides complete path information from the originator mesh STA to the mesh gate. Therefore, every intermediate mesh STA remains aware of the next hops towards the mesh gate. Considering Fig. 5.1, suppose the mesh STAs transmit with data rate r_u in the current DTIM interval. Every mesh STA is aware of the supported data rates for all its neighbors from the *NMAP* table. Therefore, mesh STA 1 knows the supported data rate to reach mesh STA 3 directly, without relaying through mesh STA 2. In the proposed augmentation in the HWMP protocol, mesh STA 1 also periodically probes to mesh STA 3 for the path metric value using data rate r_v, and stores that value in the link metric table. This way, every mesh STA periodically probe for the metric value through low data rates, by avoiding one-hop or two-hop relays. The HWMP link metric probing

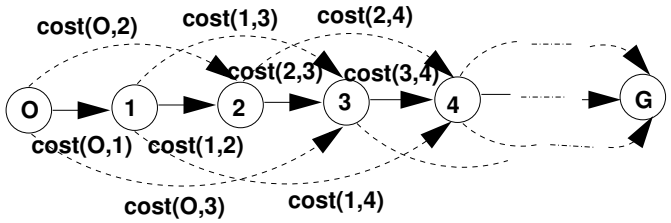

Figure 5.12: Multi-rate path selection

with low rates gives an estimation of the possibility of hop count reduction. *HITRAM* bounds the percentage of extra messages used for link metric probing at different data rates to the 5% of the total control messages, to limit the extra signaling overhead.

5.3.4 Selection of Optimal Data Rate

Suppose there exists a maximum data rate path from the originator mesh STA O to the mesh gate G, through the intermediate relays $1, 2, ...$, as shown in Fig. 5.12. If the data rate is decreased, the number of hops can be reduced, which is shown using dotted links in the figure. $cost(i, j)$ is the cost of every link, defined as follows;

$$cost(i,j) = \mathfrak{C}(\hat{r}(i,j)) + \overline{X_i}(\hat{r}(i,j)) \tag{5.27}$$

where $\hat{r}(i, j)$ is the optimal data rate for the link (i, j), which is the solution of the following unconstrained optimization problem.

$$\hat{r}(i,j) = \underset{\substack{r \le SDR_{max}(i,j),\\ r \in BSSBasicRateSet}}{\arg\max} \left(\frac{r}{\mathfrak{C}(r) + \overline{X_i}(r)} \right) \tag{5.28}$$

where $SDR_{max}(i, j)$ is the maximum sustainable data rate from STA_i to STA_j. The unconstrained optimization finds out the maximum sustainable data rate that reduces the service time $(\overline{X_i}(r))$ as well as the packet forwarding time $(\mathfrak{C}(r))$. Therefore, the problem of finding the optimal data rate for every mesh STA is reduced to the problem of finding minimum cost path in the graph shown in Fig. 5.12, and assigning the data rate to every mesh STA that minimizes the cost.

Implementation of Rate Down-gradation

The minimum cost path finding, using equation (5.27) and equation (5.28), is difficult in implementation perspective as every mesh STA requires global network knowledge. Therefore an approximation of this scheme is used in *HITRAM*, where every mesh STA

requires the knowledge of only its two-hop information using current data rate. Let us consider an instance of the network with three mesh STAs, where STA_i forwards packet to STA_j using data rate r_u, and STA_j forwards to STA_k using data rate r_v. However, STA_i can transmit to STA_k directly, with $SDR_{max}(i,k) = r_{\mathrm{w}}$. Based on equation (5.25), following unconstrained optimization is executed at STA_i,

$$\hat{r}_{\mathrm{w}} = \underset{\substack{r' \leq r_{\mathrm{w}}, \\ r' \in BSSBasicRateSet}}{\arg\max} \left(\frac{r}{\mathfrak{C}(r) + \overline{X_i}(r_u)\frac{C^2(r)}{C^2(r_u)}} \right) \tag{5.29}$$

STA_i can solve equation (5.29) within constant time (because of finite number of elements in *BSSBasicRateSet*), and get $\hat{r}_{\mathrm{w}}$. $\mathfrak{C}(r)$ can be obtained through the HWMP link metric probing mechanism, as described earlier. $\hat{r}_{\mathrm{w}}$ is selected as the data rate for the next peering after *MeshHoldingTimeout*, if following condition is satisfied,

$$\overline{X_i}(r_u)\frac{C^2(\hat{r}_{\mathrm{w}})}{C^2(r_u)} + \mathfrak{C}(\hat{r}_{\mathrm{w}}) < \overline{X_i}(r_u) + \overline{X_j}(r_v) + \mathfrak{C}(r_u) + \mathfrak{C}(r_v) \tag{5.30}$$

STA_i can check the condition for downgrading data rate only with the two-hop information. This way, every mesh STA in the network checks for possibility of using low data rate for reducing number of hops. If the rate is downgraded, the MPM protocol establishes peers based on the selected data rate.

Implementation of Rate Up-gradation

In *HITRAM* mechanism, mesh STAs upgrade their data rates to the high rates available in *BSSBasicRateSet*, if a performance degradation is observed with the current data rate. Suppose in the previous three mesh STAs scenario, STA_i downgrades its data rate from r_u to $\hat{r}_{\mathrm{w}} < r_u$ to improve end-to-end performance by reducing number of hops. Before downgrading to data rate $\hat{r}_{\mathrm{w}}$, STA_i stores the value $(\overline{X_i})(r_u) + \overline{X_j}(r_v) + \mathfrak{C}(r_u) + \mathfrak{C}(r_v))$ to a local variable called *pCost*. STA_i reverts back to data rate r_u from data rate $\hat{r}_{\mathrm{w}}$, if following condition is satisfied,

$$pCost < \overline{X_i}(\hat{r}_{\mathrm{w}}) + \mathfrak{C}(\hat{r}_{\mathrm{w}}) \tag{5.31}$$

At this stage, $\overline{X_i}(\hat{r}_{\mathrm{w}})$ can be calculated directly from the information obtained during the MCCA channel access. As discussed earlier, high data rates provide optimum performance in a highly-loaded network with high degree of interference. Further, as the network is static, performance degradation with low data rates indicate that the degree of interference has been increased in the network. Therefore upgrading data rate increases the possibility of reducing interference in the network, resulting performance gain.

5.4 Simulation Results

The HITRAM protocol is implemented in Qualnet 5.0.1 [71] discrete event simulator framework. For comparison purpose, three more state-of-the-art rate adaptation protocols have been implemented in Qualnet, as follows;

(a) *SampleRate* [111]: This rate adaptation protocol maximizes the throughput by estimating per-frame transmission time for each data rate, and selecting the rate with lower per-frame transmission time. SampleRate is implemented in Qualnet framework by strictly following the MadWiFi implementation.

(b) *BEWARE* [129]: This protocol dynamically adjust the rate selection decision with respect to the different background traffic levels, as well as wireless link condition fluctuations. However, the BEWARE scheme estimates packet transmission time based on the CSMA/CA MAC. In the current implementation of the protocol for IEEE 802.11s MAC, the estimation of packet transmission time is modified based on [213]. However, the *Rate Selection Engine* works as per the basic BEWARE protocol.

(c) *MARA* [135]: This protocol uses a routing metric to evaluate expected end-to-end delay based on *Expected Transmission Count* (ETX) routing metric, as follows;

$$MARA_{ij} = \min_{u} \left(\frac{ETX_{ij}^{u}.ps}{r_u} \right) \tag{5.32}$$

where ETX_{ij}^{u} represents the ETX between STA_i and STA_j with data rate r_u, and ps is the size of the probe packet. MARA sends ETX probes at every available rates and adopts the rate that provides minimum metric value.

5.4.1 Simulation Setup

The proposed scheme is implemented as an extension to IEEE 802.11s protocols, that operates above the data rates supported by 802.11g, as shown in Table 5.1. The other rate adaptation schemes, SampleRate, BEWARE and MARA have been implemented as Loadable Kernel Modules (LKM) for Qualnet kernel. The IEEE 802.11s protocols call the LKM module for a specific rate adaptation technique as and when data rate is required for functioning. To consider realistic wireless channel condition, *Ricean fading model* is considered with K-factor fixed at 6. This reflects average fading scenario in a general indoor environment. The simulation scenario consists of 144 mesh STAs placed in an approximate grid of 12×12, based on the transmission range for the maximum data rate

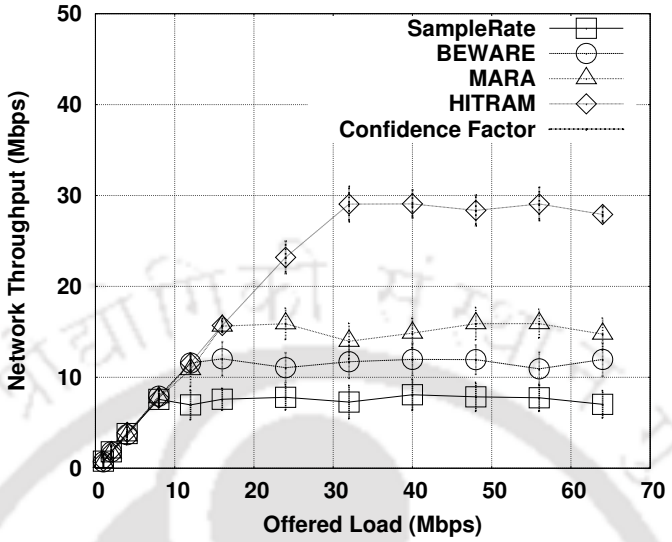

Figure 5.13: Impact of traffic load over UDP

(54 Mbps). Two mesh STAs at two corner act as the mesh gate. Both the mesh gates are connected to a corresponding node (CN) through wired interface. The mesh gate selection is based on HWMP RANN mechanism. All the mesh STAs and clients are supported with IEEE 802.11s MAC functionality with multi-rate support. Number of flows has been varied during simulation based on load and interference scenarios. Each scenario is 10 minutes long, and repeated 10 times to ensure tight confidential intervals.

5.4.2 Performance for UDP Traffic

In this set of simulation experiments, the impact of network load and number of clients are examined on the rate adaptation schemes. For the first experiment, 32 clients have been randomly distributed in the network. For each of the 10 trials of the experiment, the clients are distributed using different random seed values, and both the average result and the confidence factor are shown in the graphs. The UDP data generation rate of each of the clients is varied from 32 Kbps to 2 Mbps, with fixed packet size of 1500 bytes. In turn, the overall load on the network varies from 1 Mbps to 64 Mbps. The maximum theoretical bandwidth of the network is 54 Mbps with 802.11g technology. However, the mandatory MAC and physical layer overheads limit the maximum network throughput to lower values. Fig. 5.13 plots the total network throughput as a function of offered load. It can be observed that the network throughput saturates at 8 Mbps for SampleRate, at 12 Mbps for BEWARE, and at 15 Mbps for MARA. SampleRate does not consider the effect

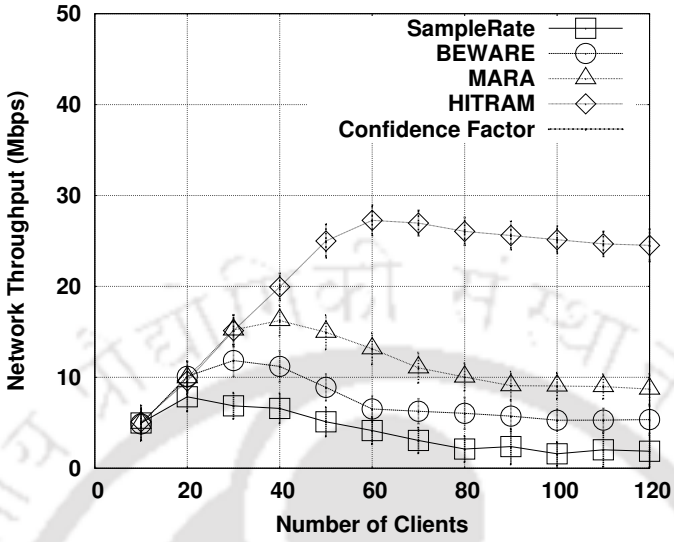

Figure 5.14: Impact of number of clients over UDP

of data rate selection over the number of hops and interference, and only concentrate on the packet loss. Therefore it continuously use low data rates as an effect of congestion-related losses. BEWARE can identify congestion effects, however inefficient for hop-reduction based on the selected data rate. On the other hand, the metric value used in MARA can partially identify the rate-hop-interference trade-off. The performance of MARA is affected because of frequent re-peering due to changes in data rates, as it does not consider the interdependence of the peer selection, channel access, and routing protocols in IEEE 802.11s. The proposed *HITRAM* protocol considers the rate-hop-interference trade-off for multi-rate mesh networks, and adopt the best data rate based on the current network information obtained through the channel access and the routing protocols. It can be observed from the figure that *HITRAM* saturates at 29 Mbps, a considerably higher throughput compared to SampleRate, BEWARE and MARA.

In the second set of simulation experiments through UDP traffic, the interference effect is observed over different rate adaptation schemes. The scenario configurations are similar to the earlier, except that the number of clients have been varied from 10 to 120, with every client generates traffic at a rate of 512 Kbps. Fig. 5.14 plots the graph with the network throughput as a function of number of clients. Higher number of clients reflects more interference in the network. To explain the behavior of different data rates, the cumulative distribution function (CDF) of the fraction of packets received with different transmission rates have been plotted for two different scenarios, a low interference

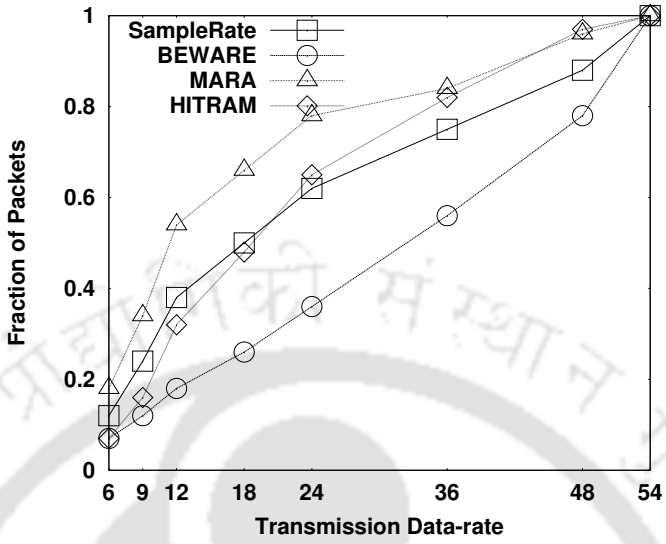

Figure 5.15: Distribution of rates in low interference

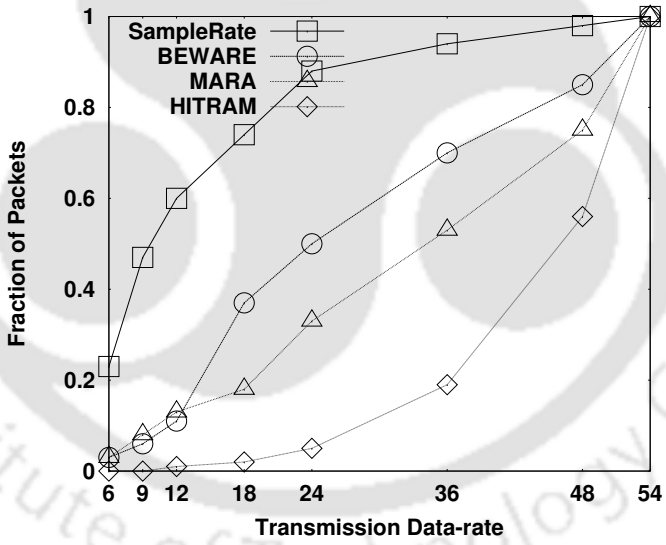

Figure 5.16: Distribution of rates in high interference

scenario (with 10 clients), as shown in Fig. 5.15, and a high interference scenario (with 120 clients), as shown in Fig. 5.16. SampleRate is always affected by the congestion effects, and it switches to low data rates frequently even in the low interference scenario. At high Interference scenario, SampleRate aggressively uses low rates most of the time, and the performance is affected severely. BEWARE and MARA shows a conservative behavior for both the low interference and high interference scenarios, by using $18, 24, 36$, and 48

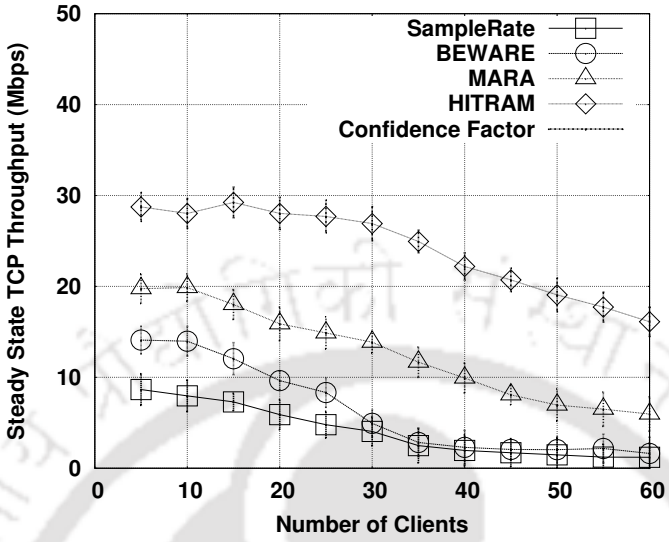

Figure 5.17: TCP steady state throughput

Mbps data rates most of the time. However, BEWARE uses 36 and 48 Mbps rates more at low interference scenario, and 18 and 24 Mbps rates more at high interference scenario. BEWARE considers background traffic as the reason for congestion, and therefore uses low rates, which is preferable for the infrastructure wireless networks. However, it affects the performance of mesh networks. MARA shows more preferable rate adaptation for mesh networks, by selecting the high rates at the high interference scenario and the low rates at the low interference scenario. However its conservative nature prevents it to excessively use 54 Mbps rate during the high interference scenario. The proposed *HITRAM* protocol adopts the best rates at the low interference, mostly $12, 18, 24$, and 36 Mbps. Further it extensively uses 48 and 54 Mbps during the high interference, resulting better performance gain compared to other techniques, as shown in Fig. 5.14.

5.4.3 Performance for TCP Traffic

In these sets of experiments, the TCP performance is evaluated for different rate adaptation techniques. As earlier, the clients are randomly distributed in the network with different seed values for 10 different trials of the simulation. Every client transfer an 1 GB file to the CN using broadly used TCP new Reno protocol. The performance of TCP is measured in terms of steady state TCP throughput and average end-to-end packet delay. Fig. 5.17 shows average steady state TCP throughput as a function of number of TCP clients. The frequent rate fluctuations at SampleRate and BEWARE

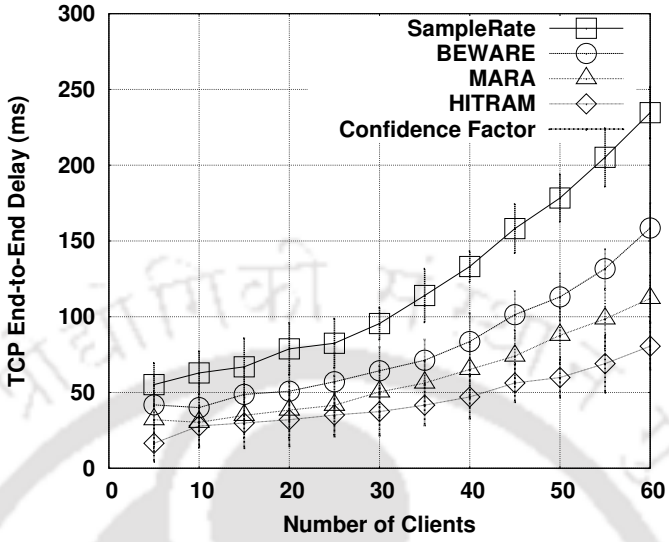

Figure 5.18: TCP end-to-end delay

techniques affects TCP performance at high interference, by dropping TCP congestion window (CWnd) value. TCP maintains retransmit timer values based on estimated round trip time (RTT). The RTT changes as data rate changes, and therefore TCP falsely triggers retransmit timeouts, which results congestion avoiding actions by dropping CWnd values and sender's data rate. MARA performs better than SampleRate and BEWARE protocols, however the throughput is affected due to frequent peer changes. The *HITRAM* protocol balances between rate selection and peer establishment, and outperforms other protocols at higher interference. The gradual performance degradation of *HITRAM* with increased number of clients is only because of the bandwidth sharing between the TCP flows, and the bottleneck behavior near the mesh gateways. It has been observed from the simulation traces, that number of retransmit timeouts and CWnd drops are considerably less for *HITRAM*, compared to other rate adaptation techniques. Fig. 5.18 shows average end-to-end TCP packet delay for different rate adaptation techniques. The average end-to-end TCP delay for *HITRAM* is considerably less than other rate adaptation techniques,

5.4.4 Compatibility with Other Rate Adaptations

In this set of simulation experiments, the gains obtained in the throughput is evaluated with the incremental deployment of *HITRAM* in a environment of SampleRate support. The scenario configurations are similar as described in Subsection 5.4.2. Fig. 5.19 plots the throughput with respect to the fraction of mesh STAs upgraded from SampleRate

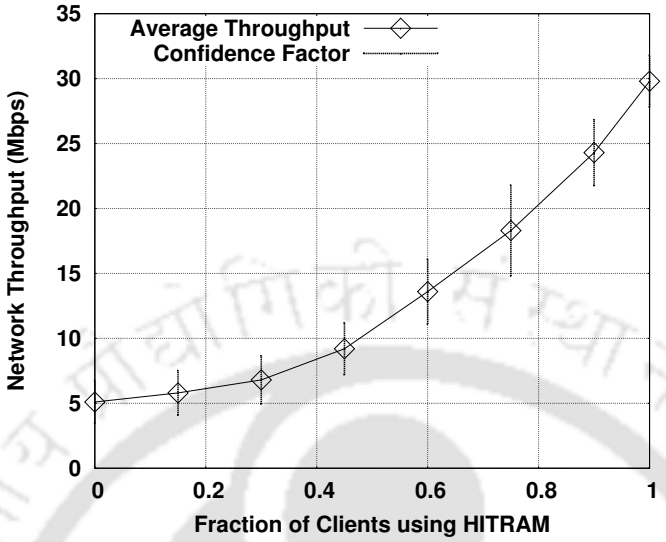

Figure 5.19: Throughput in a mixed network

to *HITRAM*. 30 number of clients are deployed randomly, as earlier, with each client generates traffic at a rate of 2 Mbps, resulting network saturation. It can be observed that the overall network throughput improves as the mesh STAs are upgraded from SampleRate to *HITRAM*. This indicates that the incremental deployment of the *HITRAM* supported mesh STAs provides network performance gains. The *HITRAM* supported mesh STAs adjust data rates based on interference and hop-counts towards destination, resulting best possible performance gain.

5.4.5 Impact of Different Channel Conditions

In this set of simulation experiments, similar setup is used as described in Subsection 5.4.2, except that the Ricean fading parameter K is varied. As the value of K increases, the line-of-sight signal component becomes stronger, and overall channel SNR increases. Fig. 5.20 and Fig. 5.21 plots overall network throughput as a function of number of UDP clients, with two different K values, $K = 0$ and $K = 12$ respectively. It can be observed from the figures, that *HITRAM* outperforms all other rate adaptations for both at low SNR link scenario (with $K = 0$) and at high SNR link scenario (with $K = 12$). However, the overall throughput for the low SNR scenario is less because the low data rates are used more to sustain the communications between the end-to-end pairs, according to equation (5.21).

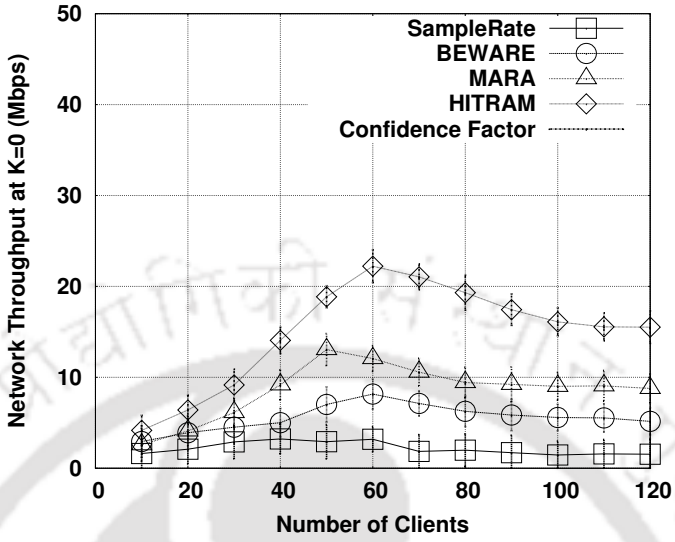

Figure 5.20: UDP throughput for $K = 0$

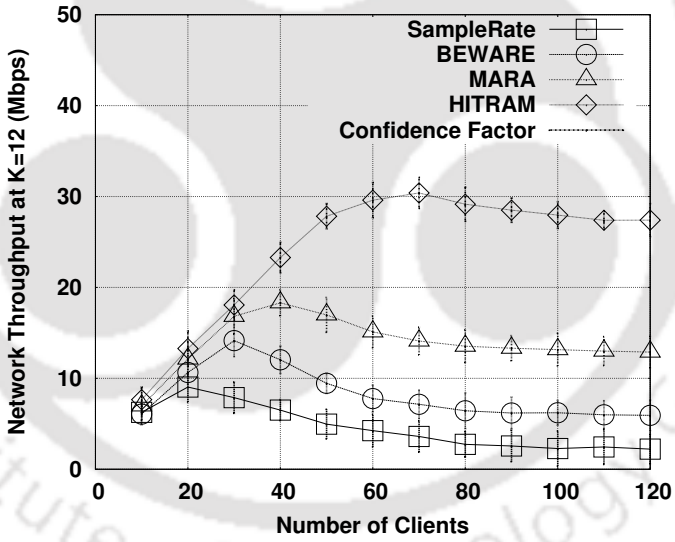

Figure 5.21: UDP throughput for $K = 12$

5.5 Summary

This chapter proposes a rate-adaptation mechanism for IEEE 802.11s standard. The rate-hop-interference trade-off for multi-rate mesh network is analyzed theoretically. The standard IEEE 802.11s protocols have been enhanced to support rate adaptation based on the rate-hop-interference trade-off. The performance as well as the interoperability of the proposed scheme have been evaluated through simulation results. The performance

comparison with existing rate adaptation techniques shows that the proposed *HITRAM* protocol performs better than other schemes for different network scenarios. The proposed *HITRAM* protocol addresses the rate-hop-interference trade-off for multi-rate mesh networks, and provides better MAC layer performance at various network conditions. It can be noted that rate-adaptation in a mesh network handles the effect of channel variability over the channel access protocol by selecting the optimal data rate that provides best performance. In a multi-hop mesh network, the variability in the channel and the network conditions also affect the mesh path selection protocols. The next chapter proposes an improved mesh path selection protocol to deal with the variable channel and network conditions in a mesh network.

Chapter 6

Selective Greedy Path Selection: Exploring the Path Diversity in Backbone Mesh Networks

As discussed earlier, the interdependency among the transmission scheduling and mesh path selection in a multi-interface mesh network has indulged the researchers to incorporate the mesh path selection protocols at the MAC layer. The traditional path selection protocols use either proactive or reactive based approaches. The proactive protocols do not adapt to the wireless link fluctuations and path loss constraints, as they precalculate a fixed mesh path based on the decision time network conditions and channel quality measurements. On the contrary, the reactive path selection protocols can adjust to the channel conditions through on-demand path finding, but clog the network with control packet flooding. This chapter proposes a new mesh path selection paradigm for multi-interface mesh networks, called the *'Selective Greedy'* (SelG) mesh path selection protocol, that can adapt with the changing path diversity in a mesh network. The protocol works over the standard IEEE 802.11s HWMP protocol. The proposed protocol operates in two stages. In the first stage, the proactive approach is used to find out a set of *'potential next-hop candidates'* (PNC) that can work as the competent next hop relay. This selection is based on the HWMP airtime link metric. In the second stage during the actual data communication, a greedy selection strategy is used to find out the local best among the set of PNCs. The greedy selection is based on two parameters - the network interference and the impact of the local variability in the channel condition over the metric value, that is used for the computation of the forwarder set. The characteristics of IEEE 802.11s mesh network is

explored to devise the network interference constraint locally at every mesh STA, using the well-established protocol interference model [186]. The proposed protocol does not flood control packets to adapt with the channel variability, like reactive protocols. However, it considers the impact of the channel variability over the proactive path calculation, by reflecting the statistical dispersion in the current link metric value over the path metric value, and considering the effect of the interference over the path selection strategy. The effectiveness of the proposed scheme is analyzed and compared with other traditional path selection protocols for multi-hop and mesh networks, using simulation results.

The rest of the chapter is organized as follows. The motivation behind designing a new mesh path selection protocol is discussed in Section 6.1. Section 6.2 discusses the network model and assumptions used for designing the proposed mesh path selection protocol. The design and implementation details of the proposed protocol is discussed in section 6.3. The performance of the proposed scheme is analyzed using simulation results, as reported in section 6.4. This section also compares the performance of the proposed protocol with other state-of-the-art protocols proposed in the literature. Finally, section 6.5 concludes the chapter.

6.1 Motivation

The existing path selection protocols for mesh networks can be broadly classified into three groups - proactive [136], reactive [141] or hybrid [147]. The proactive path selection protocols decide the mesh path before the actual data communication takes place. Therefore the performance of the proactive protocols are affected by the wireless channel dynamics, such as fading, shadowing, multi-path propagation and path loss components. The path diversity in wireless mesh networks does not guarantee that the current best path would remain best for the entire duration of the communication. In [149] and [150], the authors have shown that the proactive path selection performs poorly under variable path loss components. On the other hand, reactive protocols find out the mesh path in an on-demand basis. Though reactive protocols are more adaptative to the network channel variability, it floods the network with control packets every-time a new flow is introduced in the network. As discussed in [151], the reactive protocols do not perform well for static wireless mesh backbone, and the control overhead becomes higher than the communication efficiency. The hybrid path selection protocols, being a combination of the proactive and reactive approaches, select the path upto some pivot points using the reactive approach, and the paths from the pivot points to the final destination is discovered using a proactive

approach. Though hybrid protocols perform better than proactive and reactive protocols in a mesh backbone network [153], the deficiency of the proactive and reactive protocols still exist upto some extent.

As discussed earlier, IEEE 802.11s supports HWMP to captivate the MAC layer mesh path selection functionality through multi-hop communications. HWMP operates in two modes - proactive tree based path selection, and reactive on-demand mesh path selection. HWMP uses airtime link value as the path selection metric. However, HWMP along with the airtime link metric do not perform well for multi-interface multi-channel mesh networks, because of the following two reasons.

- The number of pair-wise interfaces in a neighborhood is likely to be more than the number of non-overlapping channels available. Only 3 non-overlapping channels are available for the most commercially used IEEE 802.11b/g physical layer. Though IEEE 802.11a and IEEE 802.11n have more number of non-overlapping channels, different countries apply their own regulations to the allowable channels. Therefore, interference cannot be avoided completely even with multiple channels. Finding optimal interface depends on the interference condition at the channel in which the interface is operating.
- The demerits of the proactive and the reactive path selection protocols, as discussed earlier, are also applicable for the HWMP protocol.

To cop up with the problems associated with the proactive and the reactive path selection protocols, this chapter proposes a new mesh path selection protocol, called the 'Selective Greedy', that can adapt to the channel variability, however, does not use on-demand control packets flooding. The proposed SelG protocol works in two phases. In the first phase, a set of PNCs are selected using a proactive approach, those can work as the next-hop relay. In the second stage, the variability in the network and channel conditions are explored to device a local greedy strategy to find out the best forwarder among the set of PNCs. The design details of the proposed SelG protocol is discussed in subsequent sections.

6.2 Network Model

In the proposed system architecture, every mesh STA is equipped with multiple interfaces operated in different channels, based on existing channel assignment protocols [170]. Though most of the works in literature talk about interdependency of channel assignment

and mesh path selection, these two operations are segregated in this chapter to make the protocol simple and easily implementable. As mesh STAs are fixed and pre-deployed, centralized channel assignment can be implemented at mesh STAs without the violation of scalability. This chapter assumes the centralized channel assignment scheme proposed in [170] which is independent of mesh path selection. Communication is possible between a pair of mesh STAs if they have at least one interface each tuned in the same channel. It may not be necessary that every mesh STA has same number of interfaces. However, every such pair of interfaces have different path selection elements due to channel interference and dynamic network conditions. The objective is to find out the best pair of interfaces for the optimum mesh path selection protocol performance.

As discussed earlier, due to unavailability of the sufficient number of channels, interference is still possible among the mesh STAs. The protocol model for interference [186] is assumed in this chapter, where two links interfere if they are within the interference range of each-other (which is more than the communication range) and use the same channel for communication. However, the proposed protocol can be extended for any model of interference, as long as the interference can be characterized at the mesh STAs.

6.3 Selective Greedy Forwarding (SelG): Protocol Design

The proposed protocol has two stages. In the first stage, which is executed periodically, a set of PNCs are pre-determined using the proactive path selection mechanism. In the second stage, during actual data transmission, a candidate is selected from the set of PNCs, based on the impact of the current network conditions. It can be noted that there can be multiple flows from different sources to the same destination. In the proposed scheme, the forwarder set is constructed individually at every sources, for each destination, and is not flow specific.

For the ease of presentation, this section assumes that the traffic in the network are to and from the mesh gates. Therefore every mesh STAs in the network finds out the mesh path towards the mesh gates. However, the proposed scheme can be extended for finding out the mesh path between any two mesh STAs, as discussed in subsequent sections.

6.3.1 Stage 1: Construction of the Set of Potential Forwarders

The proactive method of the HWMP protocol is used to find out the set of PNCs of a mesh STA from its one-hop neighborhood. As discussed earlier, the proactive tree rooted at the mesh gates are constructed through periodic PPREQ message broadcast. For the

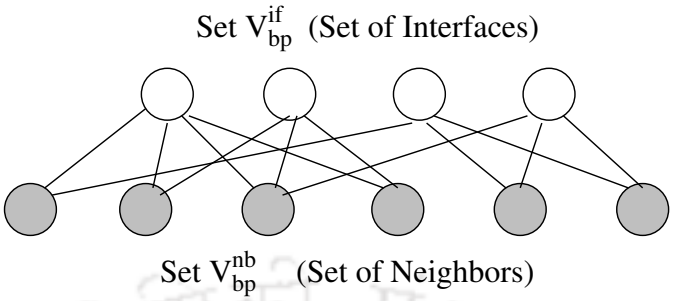

Figure 6.1: Bipartite graph model for finding minimum set of interfaces required to broadcast PPREQ messages

conventional HWMP protocol, PPREQ messages are broadcast through every interfaces of each mesh STA. However, it increases control overhead in the network. This chapter proposes to limit the broadcast of the PPREQ messages through a set of interfaces, such that every neighbor receives at least one copy of the PPREQ message. To find out the minimal set of interfaces that suffices the above purpose, every mesh STA should have sufficient knowledge of all peer neighbors through each interface. This can be accomplished by IEEE 802.11s *mesh peer management* (MPM) Protocol [25], where every mesh STA broadcast peering beacons through every interfaces periodically to keep aware of the local network connectivity. With this information, finding minimal set of interfaces for PPREQ broadcast can be modeled as a graph theoretic problem as follows.

Construction of the Minimal Set of Interfaces for PPREQ Broadcast

Let STA_i and STA_j be the two mesh STAs, each have Γ_i and Γ_j set of interfaces. Let $X_{ij} = \{(I_i^m, I_j^n) \mid I_i^m \in \Gamma_i,\ I_j^n \in \Gamma_j,\ I_i^m$ and I_j^n are tuned to the same channel$\}$. Then communication is possible between STA_i and STA_j through any $(I_i^m, I_j^n) \in X_{ij}$. Let, $\mathbb{N}_1^i$ denotes the set of one-hop neighbors for STA_i. A bipartite graph $\mathcal{G}_{bp}(\mathbb{V}_{bp}, \mathbb{E}_{bp})$ is constructed as follows, where $\mathbb{V}_{bp}$ is the set of vertices, and $\mathbb{E}_{bp}$ is the set of edges.

- Every interface $I_i^k \in \Gamma_i$ and every $STA_\ell \in \mathbb{N}_1^i$ is represented as a vertex in $\mathbb{V}_{bp}$.
- There exists an undirected edge from I_i^k to STA_ℓ if $(I_i^k, I_\ell^n) \in X_{il}$, i.e. STA_ℓ has at least one interface which is tuned to the same channel as of I_i^k.

Let the vertex set is divided into two subsets, $\mathbb{V}_{bp}^{if} \subset \mathbb{V}_{bp}$ and $\mathbb{V}_{bp}^{nb} \subset \mathbb{V}_{bp}$, where the set $\mathbb{V}_{bp}^{if}$ contains the vertices from Γ_i and the set $\mathbb{V}_{bp}^{nb}$ contains the vertices from $\mathbb{N}_1^i$. An example of this construction is shown in Figure 6.1. The term, *'Interface cover'* is defined as follows.

Algorithm 6.1 Find minimum set of interfaces to cover all neighbors

1: Sort the vertices in the set $\mathbb{V}_{bp}^{if}$ according to their degree
2: **while** Set $\mathbb{V}_{bp}^{nb}$ is non-empty **do**
3: Select the vertex $v \in \mathbb{V}_{bp}^{if}$ with the highest degree, and delete all the edges and the corresponding vertices in $\mathbb{V}_{bp}^{nb}$ that are incident to v.
4: Add the interface corresponding to the vertex v to the set of required interfaces, and delete v from $\mathbb{V}_{bp}^{if}$
5: **end while**

Definition 6.1. *The interface cover of STA_i, denoted as $\mathcal{H}_i$, is the subset of $\mathbb{V}_{bp}^{if}$, such that every vertex of the set $\mathbb{V}_{bp}^{nb}$ is incident to at-least one edge $(I_i^k, STA_\ell) \in \mathbb{E}_{bp}$ with the following constraints;*

(C-1) $I_i^k \in \mathcal{H}_i$, and

(C-2) $STA_\ell \in \mathbb{V}_{bp}^{nb}$

Let $\mathcal{M}_i \subseteq \Gamma_i$ denotes the minimum set of interfaces required for PPREQ broadcast at STA_i, ensuring that every $STA_\ell \in \mathbb{N}_1^i$ receives at least one copy of the message. Then then the following axiom holds true.

Axiom 6.1. $\mathcal{M}_i = \min_{\mathcal{H}_i} |\mathcal{H}_i|$, *where $|\mathcal{H}_i|$ denotes the cardinality of the set $\mathcal{H}_i$.*

Proof. The proof is trivial and can be directly derived from the definition of the interface cover. □

Based on the Axiom 6.1, a greedy strategy is presented in Algorithm 6.1 to solve this problem. Algorithm 6.1 repeatedly finds out the interfaces that can broadcast the PPREQ messages to the maximum number of neighbors (the corresponding vertex in $\mathbb{V}_{bp}^{if}$ with maximum degree), and includes that interface to the set of required interfaces. The computation is local and requires $O(|\Gamma_i|)$ rounds where $|\Gamma_i|$ denotes the cardinality of the set Γ_i, and thus linear in nature.

Set of Potential Forwarders

The set of PNCs are constructed using the proactive approach through the receipt of the PPREQ broadcast at different interfaces. On receiving a PPREQ message from STA_j at interface I_i^k, STA_i decides whether to include $\langle STA_j, I_i^k \rangle$ to the set of PNCs. It can be

noted that for multi-interface mesh network, the mesh path is decided by the next-hop mesh STA as well as the interface that should be used to communicate with that mesh STA. Therefore, the (MP,interface) pair is stored in the set of PNCs. Further it can be noted that because of the assumption of static channel assignment, the associated interface to communicate with a neighboring mesh STA remains valid for the entire duration of the network operations.

Let ξ denotes the maximum number of PNCs for a mesh STA. The value of ξ depends on the flexibility of the mesh path selection architecture, and the effect of ξ is discussed later in this chapter. If $\xi = 1$, the proposed scheme is reduced to the conventional proactive path selection mechanism. On receiving the PPREQ messages from its neighbors, a mesh STA stores the first ξ number of candidates, based on the path metric value, as the set of PNCs. An iterative process is used for this purpose. Let $\mathbb{F}_i$ denote the set of PNCs for STA_i. Every entry in $\mathbb{F}_i$ has three tuples $\langle STA_j, I_i^k, \mathfrak{P}_{ij}^k \rangle$, where $\mathfrak{P}_{ij}^k$ is the path metric value[1] between STA_i and STA_j, when the corresponding PPREQ message from STA_j is received through interface $I_i^k \in \Gamma_i$. Let $\mathfrak{C}_{i\ell}^k$ denote the airtime link metric between STA_i and STA_ℓ, using interface $I_i^k \in \Gamma_i$. On receiving a PPREQ message from STA_j through interface I_i^k, with path metric value $\mathfrak{P}_{ij}^k$, STA_i executes Algorithm 6.2.

According to the algorithm, when a mesh STA receives a PPREQ message, if the entry is already in the set of PNCs, then it updates the corresponding path metric value with the value received. If not, then it checks whether the sender of the PPREQ message can be elected as a candidate for the next-hop, by comparing the received path metric value with the existing values. If the path metric value for the PPREQ sender is less, then the entry with the highest path metric value is replaced with the metric value of the PPREQ sender. When there is a change in the set of PNCs, the mesh STA broadcast a new PPREQ message with the minimum updated path metric value, from the set of PNCs. Otherwise, the PPREQ messages is broadcast if another PPREQ message with the same sequence number is not broadcast earlier (to avoid the path loops).

[1]The difference between the link metric and the path metric should be noted. The link metric is the airtime link value between two mesh STAs (using a specific interface for communication). The path metric is the aggregate of the link metric values for all the links in the path. The aggregation depends on the properties of the link metric values. Airtime link metric is additive in nature, and therefore the path metric is the sum of the individual link metrics.

Algorithm 6.2 On receiving a PPREQ from STA_j through interface I_i^k of STA_i, with the path metric value $\mathfrak{P}_{ij}^k$

1: **if** $\langle STA_j, I_i^k \rangle \in \mathbb{F}_i$ **then**
2: Update $\mathfrak{P}_{ij}^k$ in $\mathbb{F}_i$
3: **else**
4: Find a candidate $\langle STA_\ell, I_i^q \rangle$ with maximum $\mathfrak{P}_{i\ell}^q$ from $\mathbb{F}_i$
5: **if** $\mathfrak{P}_{i\ell}^q > \mathfrak{P}_{ij}^k$ **then**
6: Replace the entry $\langle STA_\ell, I_i^q, \mathfrak{P}_{i\ell}^q \rangle$ with $\langle STA_j, I_i^k, \mathfrak{P}_{ij}^k \rangle$
7: Find the candidate $\langle STA_m, I_i^r \rangle$ with the minimum $(\mathfrak{P}_{im}^r + \mathfrak{C}_{im}^r)$ from $\mathbb{F}_i$.
8: Broadcast a PPREQ message with the metric value $(\mathfrak{P}_{im}^r + \mathfrak{C}_{im}^r)$ through the set of interfaces calculated using Algorithm 6.1.
9: **end if**
10: **end if**
11: **if** PPREQ with same sequence number is NOT broadcasted **then**
12: Find a candidate $\langle STA_m, I_i^r \rangle$ with the minimum $(\mathfrak{P}_{im}^r + \mathfrak{C}_{im}^r)$ from $\mathbb{F}_i$.
13: Broadcast a PPREQ message with the metric value $(\mathfrak{P}_{im}^r + \mathfrak{C}_{im}^r)$ through the set of interfaces calculated using Algorithm 6.1.
14: **end if**

Information Collection During Stage 1

It can be noted that the path metric values are stored along with the candidates in the set of PNC. Additionally, every STA_i maintains another table $\mathcal{L}_i$, where the rows correspond to the candidates in the PNC set of STA_i, and the columns correspond to the interfaces of STA_i. Every entry $\mathcal{L}_i[STA_j, I_i^k]$ stores the airtime link value for the link to the PNC STA_j through the interface I_i^k. Whenever a candidate is inserted or updated in the PNC set, the corresponding row in $\mathcal{L}$ is updated also. If STA_j is not reachable through I_i^k, then corresponding entry is ∞. Thus $\mathcal{L}$ stores the link metric information during the time when a mesh STA is selected as a PNC.

The path metric and the link metrics are used in the second stage to analyze the effect of the link metric deviation (the deviation of the link metric at the time of its use for the calculation of the set of potential next-hops, and the current value during communication) over the path metrics. This reflects the variability in the network and the channel conditions. This measure of the network and the channel variability is used to decide the most stable and optimal route using a local greedy selection, as described in

the next subsection.

6.3.2 Stage 2: The Greedy Selection of the Best Candidate

During the actual data transmission, a candidate mesh STA from the set of PNCs are selected as the next hop. This selection is based on the channel interference, airtime link value of the PNCs and the current channel characteristics. IEEE 802.11s uses dynamic TDMA based channel scheduling where time is divided into delivery traffic indication message (DTIM) intervals. At the current DTIM interval, data scheduling for the next DTIM interval is done through a reservation mechanism, called the *mesh coordinated channel access* (MCCA). During MCCA handshaking, every mesh STA broadcast MCCA advertisement messages, that contain the two hop interference information at the data sender and the data receiver. Thus interference characteristic of the next DTIM interval can be estimated from the current MCCA scheduling information. Whenever a new flow is introduced in the network, the greedy selection mechanism characterizes the interference based on the current data scheduling in the two hop neighborhood, and selects the best candidate from the set of PNCs.

Interference Characterization

As discussed earlier, this chapter considers the protocol model for interference [186, 187, 214]. Let R_c denotes the communication range of an interface. Then according to the protocol model, two interfaces interfere with each other, if they are in the same channel and are at-most $q \times R_c$ distance apart, where the value of q depends on the physical layer characterization. For general multi-interface multi-channel mesh network, $q \leq 2$ because of the capture effect and message-in-message communications [189, 215–217]. Protocol interference model is an approximation of the physical interference model. However, it is distributed in nature, and can be computed locally at every interface with local neighborhood information [187]. In [214], the authors have shown that with proper parameter settings (such as transmit power and capture threshold), protocol interference model can perform as good as the physical interference model. Further if $q \leq 2$, protocol interference model can be used correctly to capture interference information with two-hop broadcasting and network overhearing.

From MPM and MCCA protocols of the IEEE 802.11s mesh standard, every mesh STA is aware of all the interfaces in its two-hop neighborhood, that interfere with its own interfaces. Let $H(I_i^k)$ denotes the set of interfaces which interfere with interface I_i^k of

STA_i. Assume $Z(I_i^k)$ is an indicator variable such that,

$$Z(I_i^k) = \begin{cases} 1 & \text{If } I_i^k \text{ is currently being used} \\ & \text{for communication} \\ 0 & \text{Otherwise} \end{cases}$$

According to the protocol interference model, only one interface can transmit among the interfaces that interfere with each other. Consider an interface $I_i^k \in \Gamma_i$. Then either I_i^k can transmit or a set of interfaces from $H(I_i^k)$ can transmit, where no two interfaces interfere with each other.

Theorem 6.2. *For every interface $I_i^k \in \Gamma_i$ of STA_i, following condition must hold true for minimum interference data communication,*

$$Z(I_i^k) + \sum_{I_j^m \in H(I_i^k)} Z(I_j^m) \leq 1.11364\alpha \tag{6.1}$$

where α is the beam-width of the interface I_i^k, expressed in radians.

Proof. The proof extends the concept provided in Lemma 1, given in [53], for protocol interference model in multi-interface mesh network. According to the protocol interference model, two interfaces interfere with each other, if they are at-most $q \times R_c$ distance apart. Consider the following two cases,

Case I. Assume I_i^k transmits. In this case, none of the interfaces in $H(I_i^k)$ can transmit. Therefore,

$$Z(I_i^k) = 1$$
$$\sum_{I_j^m \in H(I_i^k)} Z(I_j^m) = 0$$

This satisfies the inequality given in (6.1).

Case II. Assume I_i^k does not transmit. In this case, two interfaces from $H(I_i^k)$ can transmit, provided that they are at-least $q \times R_c$ distance apart. Let us assume that there exists $\mathfrak{S}$ number of interfaces in $H(I_i^k)$, who are at least $q \times R_c$ distance apart. Considering the fact that all interfaces in $H(I_i^k)$ must be within the disk centered at I_i^k and with radius $q \times R_c$ (based of the protocol model consideration, interference range is at-most $q \times R_c$), the problem of finding $\mathfrak{S}$ can be reduced to the circle packing problem discussed in [218]. Let us consider

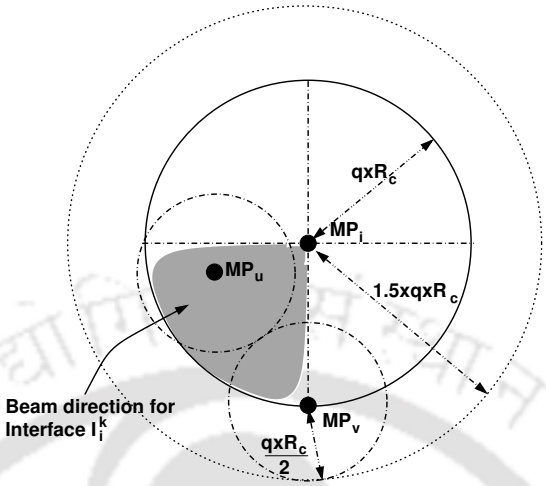

Figure 6.2: Interference characterization

Fig. 6.2. If STA_i does not use interface I_i^k, then the interfaces of STA_u and STA_v can transmit simultaneously if they are at-least $q \times R_c$ distance apart. Without considering the directionality of the interfaces, the problem of "finding maximum number of interfaces that can simultaneously transmit", is similar to the problem of "finding maximum number of non-overlapping circles of radius $(q \times R_c)/2$ that can be packed within a circle of radius $1.5 \times q \times R_c$". From [218], the value is 7. Therefore, for uniform distribution of the directional beams of the interfaces,

$$\mathfrak{S} \leq \left(\frac{\alpha}{2\pi} \times 7 \approx 1.11364\alpha\right)$$

where α is the beam-width of the interface I_i^k, expressed in radians. As a result,

$$Z(I_i^k) = 0$$
$$\sum_{I_j^m \in H(I_i^k)} Z(I_j^m) \leq 1.11364\alpha$$

This follows the theorem. □

The interference characteristics for multi-interface mesh networks, as derived in equation (6.1), gives a theoretical upper bound for selecting maximum number of interfaces for simultaneous interference-free communications. The bound is free of the q value, which indicates that interference range does not affect interface selection, until the set of interfering interfaces ($H(I_i^k)$) are identified properly. IEEE 802.11s *MCCA advertisement message* provides the support for populating the set of interfering interfaces in every DTIM

interval. In practice interference-free interface selection can not be guaranteed because of the approximation in the protocol interference model[2]. However, as shown in [214], with proper power adjustments, protocol interference model can capture interference with minimum error, and therefore, equation (6.1) can provide the bound for the minimum interference interface selection. Accordingly, equation (6.1) works as a constraint for the greedy selection to support the minimum interference mesh path selection. The next section provides the utility function for the greedy selection strategy.

Design of the Utility Function

The utility function is designed based on the effect of the current network dynamics (channel condition and interference) over the path metric information, to find out the set of PNCs. Let $\overline{\mathfrak{C}_{ij}^k}$ denote the link metric value between STA_i and STA_j through interface $I_i^k \in \Gamma_i$, when STA_j was selected as a PNC. Similarly assume that $\overline{\mathfrak{P}_{ij}^k}$ denotes the path metric during the PNC computation. The utility function for the greedy selection of STA_j, denoted as $\mathcal{U}(STA_j, I_i^k)$ is expressed as follows;

$$\mathcal{U}(STA_j, I_i^k) = \begin{cases} \left(1 + \sqrt{\frac{\left(\overline{\mathfrak{C}_{ij}^k}\right)^2 - \left(\mathfrak{C}_{ij}^k\right)^2}{\left(\overline{\mathfrak{C}_{ij}^k}\right)^2}}\right) \times \overline{\mathfrak{P}_{ij}^k}; & \text{if } \overline{\mathfrak{C}_{ij}^k} < \mathfrak{C}_{ij}^k \\ \left(1 - \sqrt{\frac{\left(\overline{\mathfrak{C}_{ij}^k}\right)^2 - \left(\mathfrak{C}_{ij}^k\right)^2}{\left(\overline{\mathfrak{C}_{ij}^k}\right)^2}}\right) \times \overline{\mathfrak{P}_{ij}^k}; & \text{if } \overline{\mathfrak{C}_{ij}^k} > \mathfrak{C}_{ij}^k \\ \overline{\mathfrak{P}_{ij}^k}; & \text{if } \overline{\mathfrak{C}_{ij}^k} = \mathfrak{C}_{ij}^k \end{cases} \tag{6.2}$$

The utility function estimates the path metric value based on the statistical dispersion in the current link metric value. A negative dispersion in the link metric value indicates possible cost reduction in the path metric value. Similarly, a positive dispersion in the link metric indicates cost inflation in the path metric. It can be noted that based on the stored information, the values of $\overline{\mathfrak{C}_{ij}^k}$ and $\overline{\mathfrak{P}_{ij}^k}$ are obtained as follows;

$$\overline{\mathfrak{C}_{ij}^k} = \mathcal{L}_i[STA_j, I_i^k]$$
$$\overline{\mathfrak{P}_{ij}^k} = \mathbb{F}_i[STA_j, I_i^k]$$

[2]Protocol interference model can not handle cumulative interference [214]. Therefore, the set of interfaces that introduce interferences due to cumulative power effect, can not be identified properly through MCCA broadcast messages. As a result, small error is observed in the set of interfering interfaces.

The utility function along with the interference constraint is used for the greedy selection of $\langle STA_j, I_i^k \rangle$ as the next-hop forwarder, discussed next.

The Greedy Selection Strategy

The greedy selection is based on a constrained optimization problem, formulated as follows.

Problem 6.1.

$$\min_{\langle STA_j, I_i^k \rangle} \quad \mathcal{U}(STA_j, I_i^k)$$

$$s.t. \quad Z(I_i^k) + \sum_{e' \in H(I_i^k)} Z(e') \leq 1.11364\alpha$$

$$STA_j \in \mathbb{F}_i$$

$$I_i^k \in \Gamma_i$$

The constrained optimization given in Problem 6.1 returns the $\langle STA_j, I_i^k \rangle$ pair that provides minimum utility maintaining the interference constraint. The convergent time of the constrained optimization is analyzed using following theorem.

Theorem 6.3. *Problem 6.1 can be solved within $O(|\mathbb{F}_i| \times |\Gamma_i|)$ time complexity.*

Proof. Let $\mathcal{Y}_i = \langle STA_j, I_i^k \rangle$ represent the optimal solution of Problem 6.1 for STA_i. Instead of allowing $\mathcal{Y}_i$ to take specific (MP, interface) value, let us define $\mathcal{Y}_i$ to be a vector in $\{\mathscr{O}_1, \mathscr{O}_2, ..., \mathscr{O}_k\}$, where each $\mathscr{O}_j$ takes a possible solution, and is represented by an integer value from $[0...k]$. Let this integer is chosen as follows: consider an equilateral simplex Σ_k in $\mathbb{R}^{k-1}$ with vertices $b_1, b_2, ..., b_k$. Let $c_k = \frac{b_1 + b_2 + ... + b_k}{k}$ be the centroid of Σ_k, and let $\mathscr{O}_j = b_j - c_k$ for $1 \leq j \leq k$. Then problem 6.1 is represented as an integer semidefinite program with finite solution bound. From [219], the problem can be solved within $O(k)$ time complexity by exploring all the elements in the vector $\{\mathscr{O}_1, \mathscr{O}_2, ..., \mathscr{O}_k\}$. In the present scenario, $k = |\mathbb{F}_i| \times |\Gamma_i|$. This follows the theorem. □

Nevertheless in practice, the numeric value of the bound $O(|\mathbb{F}_i| \times |\Gamma_i|)$ is very less (maximum within the order of two digits). So the running time for the problem is significantly low. The above selection procedure returns the next-hop candidate from the set of PNCs, and corresponding interface to be used, considering the link metric and its dispersion, as well as the interference constraint.

6.3.3 Extension of the SelG Protocol for Path Selection Between Two Mesh STAs

The SelG protocol is discussed till now from the context of the mesh path selection from a mesh STA to the mesh gates. According to the proactive HWMP protocol, the mesh gates periodically broadcast PPREQ messages. On hearing the PPREQ messages, every mesh STA populates the set of PNCs. However the protocol can be also extended for finding out the mesh path between two mesh STAs. For this purpose, every mesh STA maintains a *SelG table*, denoted as $\mathscr{T}_{SelG}$. For STA_i, $\mathscr{T}_{SelG_i}$ has two columns, where the first column contains the destination STA_j, and the second column stores the set of PNCs, when the destination is STA_j, denotes as $\mathbb{F}_i^j$. Before the first time communication between STA_i and STA_j, the source STA_i broadcast a PREQ message[3], according to the reactive HWMP protocol, using the selected interfaces, as discussed in Algorithm 6.1. Once the PREQ from STA_i is reached at STA_j, the PREP message propagates back to STA_i, using a similar procedure described in Algorithm, 6.1. On hearing the PREQ and PREP messages, every intermediate mesh STAs insert an entry corresponding to STA_i (if PREQ is received) or STA_j (if PREP is received) in its $\mathscr{T}_{SelG}$, based on Algorithm 6.2 as discussed earlier.

Assume a mesh STA receives a PREQ message where the destination is STA_j. Further assume that it already has an entry for STA_j in its $\mathscr{T}_{SelG}$. Then the mesh STA immediately replies back with a gratuitous PREP message. However, to avoid the stale entries in $\mathscr{T}_{SelG}$, every entry is associated with a lifetime interval, on expiry of which the entry is deleted. The duration of the lifetime interval is set by the service provider, based on the network deployment characteristics. For example, the lifetime interval would be less for an indoor mesh network compared to an outdoor mesh network, because the channel variability is more in an indoor environment compared to an outdoor environment.

Once the set of PNCs are computed, and an entry is made in $\mathscr{T}_{SelG}$, for all subsequent communications, the greedy selection mechanism is used to find out the next-hop candidate, until the lifetime of the entry expires. Once the lifetime expires, the set of PNCs are recomputed by broadcasting the PREQ messages. However, a higher lifetime value can be supported for the SelG, compared to the lifetime of the forwarding tables built using the proactive protocols.

[3]It can be noted that for communication between two mesh STAs, PREQ messages are used instead of PPREQ, according to the standard HWMP protocol.

6.3.4 The Size of the Set of Potential Forwarders

The performance of the SelG protocol relies on the size of the initial set of PNCs. If the size is too small, then the behavior of the SelG protocol becomes similar to the proactive protocols. On the other hand, large number of entries in the set of PNCs may trap the protocol to the local best solutions (the local optimum based on the greedy selection), which is not the globally best solution, with minimum path metric value and interference constraints. Therefore, the size of the set of PNCs need to be chosen carefully for the best performance of the protocol.

In the proposed protocol, the size of the set of PNC is limited based on the dispersion in the path metric values received from the individual neighbors. Assume STA_i has the set of PNCs $\mathbb{F}_i$. Let STA_i receives a PPREQ (or a PREQ in case of on-demand path selection between two mesh STAs) from STA_j through the interface $I_i^k \in \Gamma_i$. Then $\langle STA_j, I_i^k \rangle$ in included in $\mathbb{F}_i$, if and only if following condition is satisfied,

$$\sqrt{\frac{\left(\mathfrak{P}_{ij}^k\right)^2 - \left(\widehat{\mathfrak{P}_{ij}^k}\right)^2}{\left(\widehat{\mathfrak{P}_{ij}^k}\right)^2}} \leq \delta \tag{6.4}$$

where,

$$\widehat{\mathfrak{P}_{ij}^k} = \min\{\mathfrak{P}_{i\ell}^r | \langle STA_\ell, I_i^r \rangle \in \mathbb{F}_i\}$$

and δ is a constant, called the *'forwarder percentage'*. The value of δ depends on the path loss components, and can be decided by the service provider based on the deployment scenarios. The effect of δ is analyzed in this chapter through simulation and experimental results.

6.3.5 Routing Efficiency of SelG

To ensure stable mesh paths, a path selection protocol should support following characteristics,

1. isotonic path selection, and
2. loop-free forwarding.

The concept of isotonicity is introduced in [220] and [221]. Assume two mesh paths $\mathscr{P}_1$ and $\mathscr{P}_2$ and two links $\mathscr{L}_1$ and $\mathscr{L}_2$. The isotonicity of a path selection (or routing) metric is defined as follows.

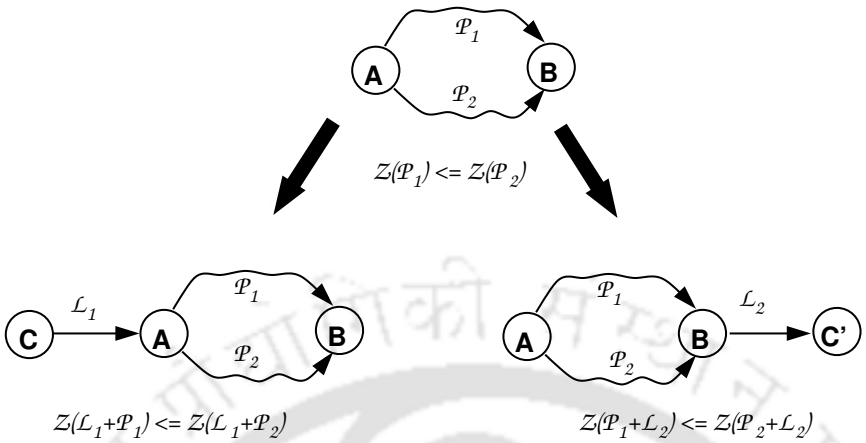

Figure 6.3: Explanation of Isotonicity

Definition 6.2. *A path selection (or routing) decision metric $\mathcal{Z}(.)$ is called isotonic if $\mathcal{Z}(\mathscr{P}_1) \leq \mathcal{Z}(\mathscr{P}_2)$ implies both $\mathcal{Z}(\mathscr{L}_1 \oplus \mathscr{P}_1) \leq \mathcal{Z}(\mathscr{L}_1 \oplus \mathscr{P}_2)$ and $\mathcal{Z}(\mathscr{P}_1 \oplus \mathscr{L}_2) \leq \mathcal{Z}(\mathscr{P}_2 \oplus \mathscr{L}_2)$, where the operator $\oplus$ denotes addition of a link to a path.*

The concept of isotonicity is explained using a figure, as shown in Fig. 6.3. Assume there exists two paths between the nodes A and B, $\mathscr{P}_1$ and $\mathscr{P}_2$ respectively. Further assume that the path metric value for $\mathscr{P}_1$ is less than the path metric value for $\mathscr{P}_2$. Let us add a link $\mathscr{L}_1$ from node C to node A. If isotonicity is satisfied, the path metric value from C to B through the path $\mathscr{P}_1$ should be less that the path metric value through the path $\mathscr{P}_2$. Similarly, if the link is added to node B, the isotonicity of the path metric is to be satisfied also.

Theorem 6.4. *The utility function, given in equation (6.2), for the decision making in the SelG protocol, supports isotonicity.*

Proof. The airtime link metric value is additive in nature, and therefore it supports isotonicity. According to Algorithm 6.2, before broadcasting a PPREQ message, a mesh STA, STA_i, updates the path metric value as follows,

$$\mathfrak{P}_{ij}^{k\,*} = \min\{\mathfrak{P}_{ij}^{k} + \mathfrak{C}_{ij}^{k} | \langle STA_j, I_i^k \rangle \in \mathbb{F}_i\} \tag{6.5}$$

where $\mathfrak{P}_{ij}^{k\,*}$ is the updated path metric value. Considering two sets $\mathbb{A} \subseteq \mathbb{R}$ and $\mathbb{B} \subseteq \mathbb{R}$, where $\mathbb{R}$ is the set of real numbers. if $\min\{x|x \in \mathbb{A}\} \leq \min\{y|y \in \mathbb{B}\}$, then for any $\omega \in \mathbb{R}$, following inequality always holds true.

$$\min\{x|x \in \mathbb{A}\} + \omega \leq \min\{y|y \in \mathbb{B}\} + \omega$$

Based upon this inequality, it can be easily seen that ${\mathfrak{P}_{ij}^k}^*$ is isotonic. During greedy selection, let us assume the link dispersion factor be ρ. Considering ${\mathfrak{P}_{ij}^k}^* \leq {\mathfrak{P}_{uv}^w}^*$ for two candidate forwarders $\langle STA_j, I_j^k \rangle$ and $\langle STA_v, I_u^w \rangle$, following inequalities always hold true.

$$(1+\rho) \times {\mathfrak{P}_{ij}^k}^* \leq (1+\rho) \times {\mathfrak{P}_{uv}^w}^* \tag{6.6}$$

$$(1-\rho) \times {\mathfrak{P}_{ij}^k}^* \leq (1-\rho) \times {\mathfrak{P}_{uv}^w}^* \tag{6.7}$$

Therefore the utility function, as given in equation (6.2), also follows the isotonicity property. □

The isotonicity property guarantees stable mesh paths in the network [220, 221], that is the mesh paths do not fall into the ping-pong effect, when the network and the channel condition is stable, and the best path at a moment can be selected unconditionally. The path is changed only when the network and the channel conditions are dispersed sufficiently to provide a better path. It can be noted that the interference constraint does not judge the quality of a path. It just gives a binary decision on whether to use a candidate or not, from the set of PNCs, such that the minimum interference mesh path selection is possible. The candidate that gives the minimal utility value, according to the equation (6.2), is allowed to transmit only when the interference constraint is satisfied.

As discussed earlier, another important property to judge a mesh path selection protocol is to check whether loop-free property is satisfied. Following theorem shows that the proposed SelG protocol is loop-free.

Theorem 6.5. *The greedy selection does not introduce a forwarding loop.*

Proof. The method of contradiction is used to proof the theorem. For the notational shorthand, let us use only the next-hop mesh STA as the candidate from the set of PNCs, and imply that the corresponding interface is used. Let $\mathfrak{P}_i$ and $\mathfrak{C}_i$ denote the path metric and the link metric for the next hop STA_i respectively, with the implication of corresponding interfaces.

Let us assume that the greedy selection introduces a forwarding loop at STA_i. Assume the forwarding loop be $\{STA_i, STA_j, ..., STA_k, STA_i\}$. Because of the additive and non-zero properties of the airtime metric value,

$$\begin{aligned} \min\{\mathfrak{P}_i + \mathfrak{C}_i\} < \min\{\mathfrak{P}_j + \mathfrak{C}_j\} < ... \\ < \min\{\mathfrak{P}_k + \mathfrak{C}_k\} < \min\{\mathfrak{P}_i + \mathfrak{C}_i\} \end{aligned} \tag{6.8}$$

$\forall i;\ \min\{\mathfrak{P}_i + \mathfrak{C}_i\} \in \mathbb{R}^+$, where $\mathbb{R}^+$ is the set of positive real numbers. Therefore, the inequality given in equation (6.8) is never possible. This contradicts with our assumption.

Hence, the greedy selection never introduces a forwarding loop. □

6.4 Simulation Results

The proposed scheme is implemented and simulated using Qualnet Network simulator version 5.0.1 [71]. Qualnet supports IEEE 802.11s complaint HWMP protocol for the MAC layer path selection in a mesh network. The proposed SelG protocol is implemented as an extension of the HWMP protocol.

6.4.1 Scenario Settings

The network consists of 100 mesh STAs distributed uniformly in the arena such that every mesh STA has on average (mean) 5 neighbors and maximum 8 neighbors. Every mesh STA is equipped with 4 interfaces. The proposed SelG protocol is implemented at the IEEE 802.11s MAC layer, that operates with 54 Mbps physical layer data rate and 3 non-overlapping channels. Channel assignment is done statically using the centralized algorithm proposed in [170]. Out of the 100 mesh STAs, 5 mesh STAs have been selected as mesh gates. This 5 mesh gates are also placed uniformly in the arena. To capture the channel variability, the log-distance path loss model is used, with path loss parameters $\gamma = 3.0$ and $\sigma = 7$, that represents the path loss in an indoor environment [222].

6.4.2 Mesh STA to Mesh Gate Communication

This section analyzes the performance of the proposed SelG protocol when all the communications are towards or from mesh gates. The traffic generation model of Qualnet is used to generate flows from the mesh STAs. Every different traffic source inside a mesh STA can be considered as client nodes associated with the mesh STA. The simulation is executed for 200 seconds. For every scenario settings, 10 different simulations have been executed with different seed values, and the average is taken to plot the graphs. However the outcomes from every settings are also shown in the graphs to indicate the variation in the results, called the confidence intervals. The traffic start time is chosen exponentially between 1 sec and 100 sec, using log-normal distribution, and the traffic duration is selected using Pareto truncated distribution (capture random but self-similar nature of the traffic) with shortest duration as 50 sec, longest duration as 180 sec, scale parameter 3 and tail index as 1.5. Packet generation rate is chosen using a log-normal distribution with mean 64 kbps. This traffic distribution captures the real-time nature of a mesh network.

The performance of the proposed SelG protocol is quantified using following metrics,

1. *the average goodput* of all the flows, that denotes average non-duplicate data bits received per second,

2. *the average end-to-end delay* of all the flows,

3. *the average jitter* for the flows, and

4. *the Jain's fairness index* [197], defined as $(\sum x_i)^2/(n\times\sum x_i^2)$, where x_i is the goodput of flow i, and n is the total number of flows.

Effect of the Number of Flows per mesh STA

For these set of experiments, the number of flows generated per mesh STA is increased to evaluate the performance metrics. The performance of the proposed SelG protocol is measured for two different δ values, 0.05 and 0.1. $\delta = 0.1$ indicates that the set of PNCs can support more number of entries, from which the greedy selection chooses the best one as the next-hop relay. The performance of the SelG protocol is also compared with the conventional HWMP protocol. Increasing the number of flows per mesh STA also increases the network congestion and packet losses due to channel contention. The proposed SelG protocol handles contention and congestion using the interference constraint, and the utility function for the greedy selection deals with the channel variabilities.

Figure 6.4 to Figure 6.7 show the effect of the number of flows per mesh STA, over the network performance measured in terms of the average goodput, average end-to-end delay, average jitter and the fairness index. The proposed SelG performs better compared to the conventional HWMP for average goodput, as shown in Figure 6.4, because the next hop is selected based on the current channel and interference conditions, which makes the mesh path selection decision more efficient. As the network load (in terms of number of flows per mesh STA) increases, the variation in channel contention and network congestion also increases with time (the traffic rate for every flow varies with time, because of the exponential start time and the Pareto truncated duration, as used for the simulation purpose). The conventional HWMP can not cop up with this variabilities in the channel and the network conditions, and the path selected at the beginning of the communication continues for the entire lifetime of the flow. On the contrary, the proposed SelG protocol adapt to the variabilities in the network and the channel conditions, and select the relay (the next-hop forwarder) that provides best performance at the current condition. The

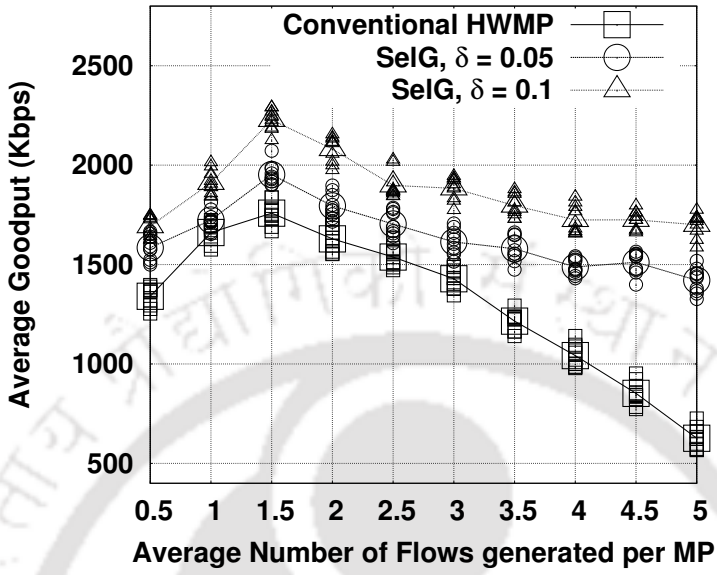

Figure 6.4: Number of flows vs goodput

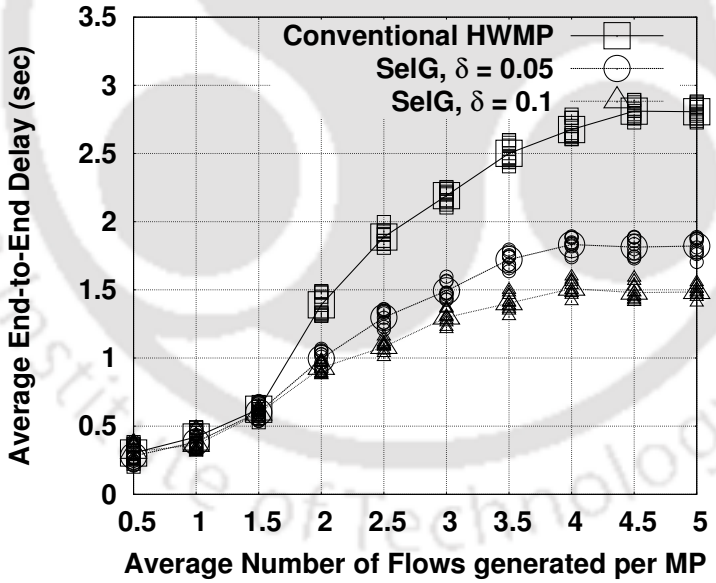

Figure 6.5: Number of flows vs end-to-end delay

selection of minimum interference path also reduces the end-to-end delay, as shown in Figure 6.5.

Figure 6.6 shows that the SelG protocol reduces the average jitter. Jitter is introduced in the network, if different packets of a flow experience different delays. In the conventional

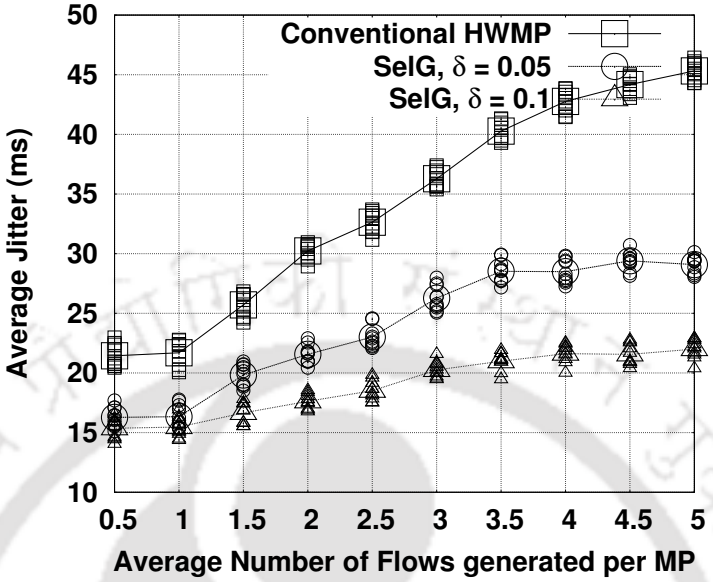

Figure 6.6: Number of flows vs average jitter

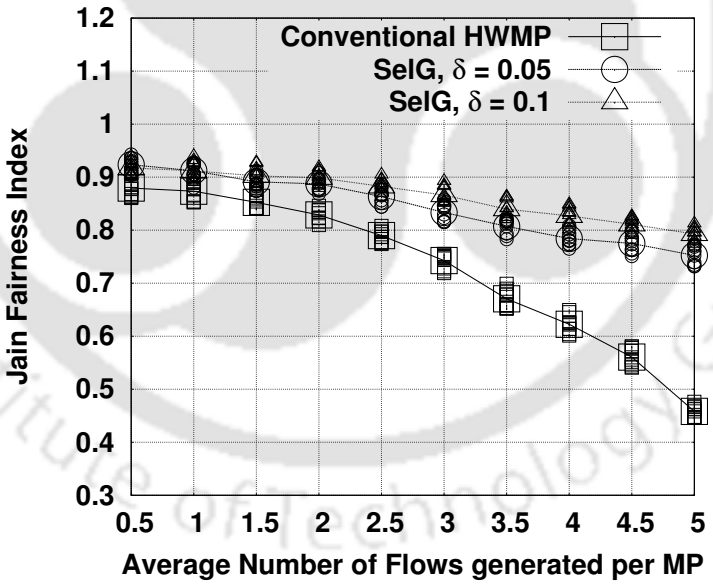

Figure 6.7: Number of flows vs fairness index

HWMP protocol, all the packets for a flow follow the same path. Therefore, the variability in the path conditions, in terms of the channel loss, contention and the network interference, affects the end-to-end delay of the packets. As a result, jitter is introduced in the flows. The SelG protocol updates the next-hop relay, if it can find out a better relay

based on the channel and the network conditions. Therefore, the effect of the channel and the network variabilities affect less on the end-to-end flow performance. Further, less jitter reflects more path stability, in which SelG outperforms the HWMP protocol.

The proposed SelG protocol also defeats the HWMP protocol in terms of fairness index, as shown in Figure 6.7. The fairness is more in case of the proposed SelG protocol, as the dynamic channel and the network conditions have less impact on the mesh paths. The flows adopt the changes in the network and the channel conditions, and selects the best path at the current moment. The differences in the fairness value is significant when number of flows generated per mesh STA is high, which reflects high interference in the network. The interference constraint used in the greedy selection of the next-hop relay bounds the packet losses due to the interference, and improves the overall network performance.

It can be noted that for all the four parameters shown above, the performance of SelG increases if δ value increases. As mentioned, increasing δ value allows more number of candidates to include in the set of PNCs. Therefore, the path diversity for multi-interface mesh network can be better explored based on the channel and the network dynamics, which reflects in the performance improvement for $\delta = 0.1$, compared to $\delta = 0.05$. However, the performance improvement with respect to the δ value is not monotonic, that means higher δ value does not always gives better performance, as analyzed in the next subsection.

Effect of the Forwarder Percentage

Increasing the value of *forwarder percentage*, in terms of δ value, implies that more number of mesh STAs are selected as the PNCs in the first phase of the proposed protocol. Figure 6.8 and Figure 6.9 show that increasing the number of PNCs improves the network performance initially for the average goodput and the end-to-end delay upto a limit. However, the performance improvement is not monotonic. Figure 6.8 shows that the average goodput reaches in a steady state after $\delta \geq 0.15$. After that, increasing the δ value does not reflect performance improvement in terms of average goodput. For average, end-to-end delay, the performance becomes steady after $\delta \geq 0.2$, as shown in Figure 6.9.

The interesting result is observed for the jitter and the fairness index values, as shown in Figure 6.10 and Figure 6.11. Increasing the δ value decreases the jitter value initially. However, after a limit, the jitter start increasing. The reason behind this is as follows. Considering a large number of mesh STAs in the set of PNCs decreases the path stability, by giving possibility to select the next-hop based on the local greedy selection. Therefore

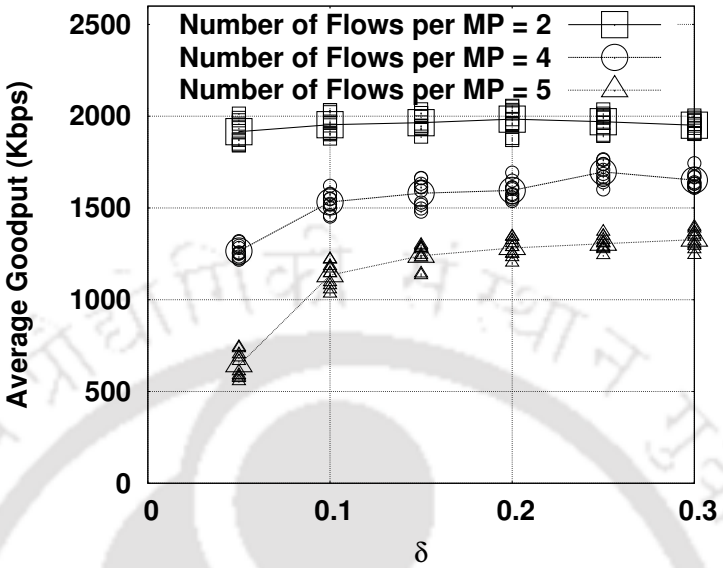

Figure 6.8: δ vs average goodput

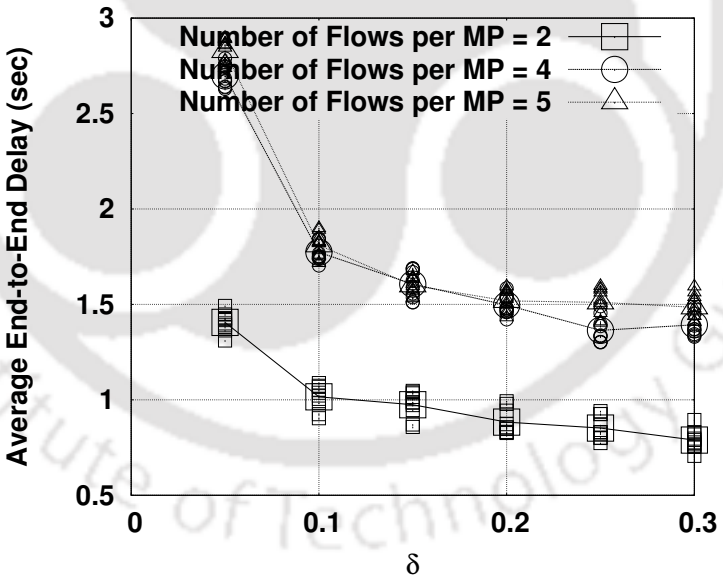

Figure 6.9: δ vs end-to-end delay

the system may trap into the local optima, where the local best information does not necessarily guarantee the global best path. Some packets choose the locally best next hop, which may not be the part of the globally best path, thus increasing the delay for those packets significantly, and incorporating additional jitter. Similar scenario occurs for the

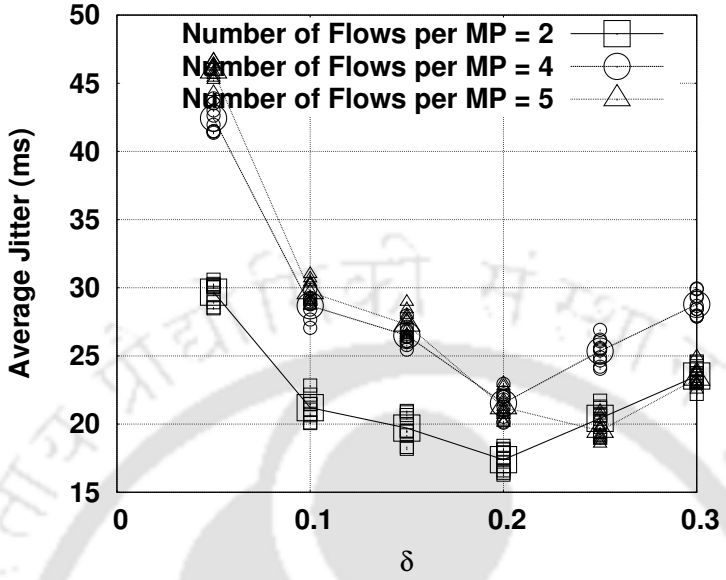

Figure 6.10: δ vs average jitter

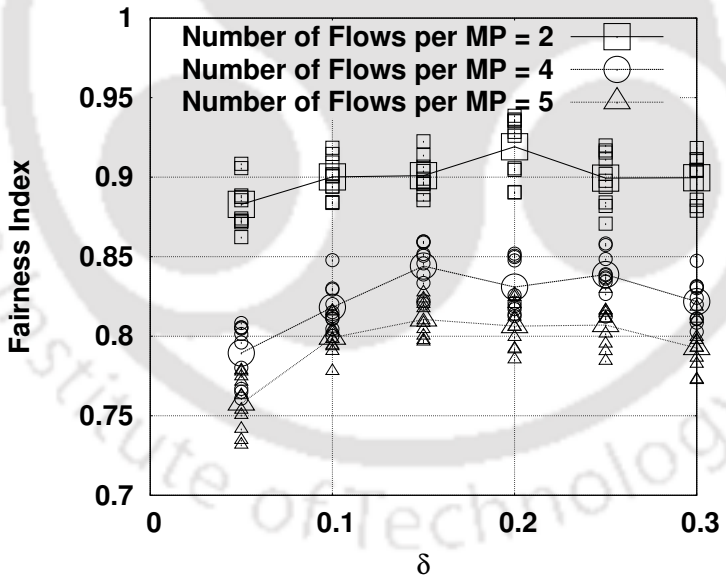

Figure 6.11: δ vs fairness index

fairness index. Unfairness gets introduced among the flows because of trapping in the local optima. Therefore the δ value should be limited in a such a way, so that the path diversity does not get over-explored, which may lead to network instability. As the δ value bounds the statistical dispersion of the link metric values, the optimal value of δ need to be

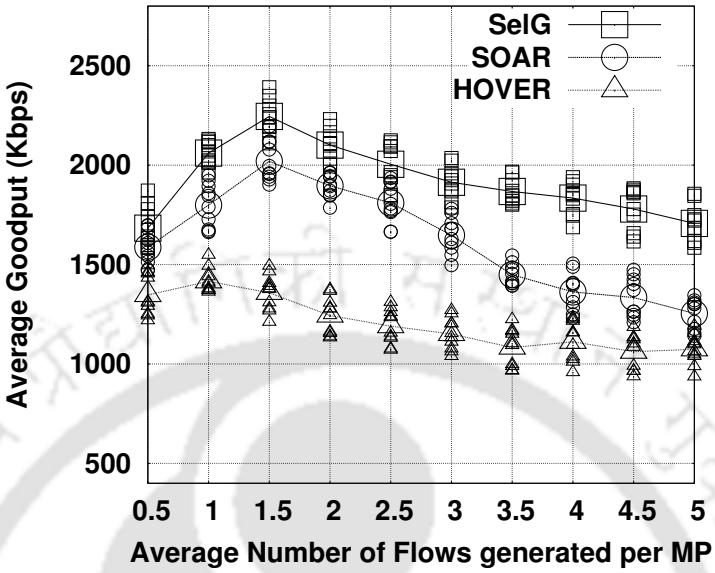

Figure 6.12: Comparison of the average goodput

selected based on the variance in the path loss components. From extensive simulations, it has been observed that, in most of the cases, the δ value equals to the variance in the path loss components gives the near-optimal outcomes.

Comparison with Other Protocols

The proposed SelG protocol is compared with the *SOAR* [162] and *HOVER* [146] protocols proposed in the literature for efficient path selection in a mesh network. The SOAR protocol provides an opportunistic path selection (or routing) scheme over the mesh protocols. On the other hand, the HOVER protocol uses a hybrid approach for deciding the mesh path in a mesh network. The SOAR and the HOVER protocols are implemented in Qualnet as an extension to the existing mesh path selection (or routing) architectures. Similar traffic settings, as discussed earlier, are used to compare the performance of SelG with SOAR and HOVER. For SelG, the δ value is taken as 0.1.

Figure 6.12 compares the average goodput of the SelG with that of the SOAR and HOVER. The goodput for the HOVER protocol is minimum, as the control overhead in terms of RREQ and RREP packets, are high compared to the SOAR and SelG protocols. SOAR uses an opportunistic approach to reduce the path selection control overhead. However, the selection procedure of the PNC uses an iterative approach, by pruning a node from the PNC, based on the link metric value. This iterative pruning mechanism

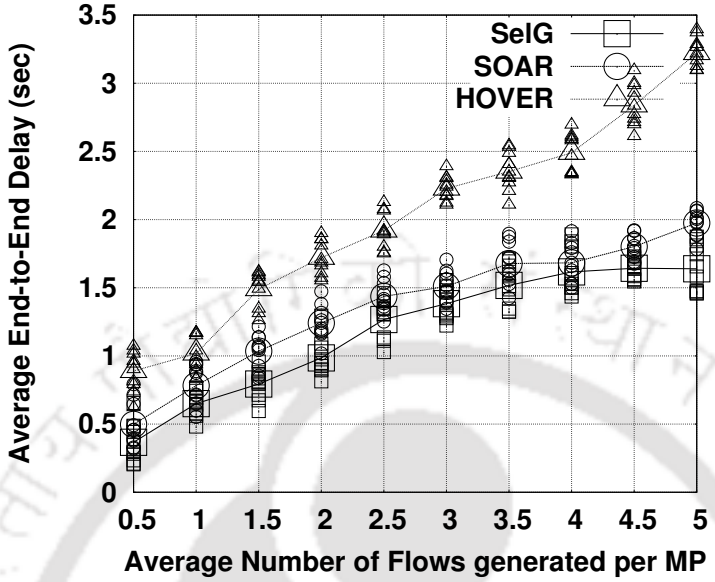

Figure 6.13: Comparison of the average end-to-end delay

affects the network stability, that reduces the average goodput of the flows. Further, the node that rebroadcast a packet first, may not belong to the optimal path. The possibility of this event is high for SOAR, as it does not consider the effect of the local changes over the global path metric value. The proposed SelG protocol uses the greedy selection by considering the statistical effect of the changes in the link metric value, over the path metric value, that increases the path stability while exploring the path diversity. Further no coordination among the forwarding nodes is required in the case of the proposed SelG protocol, which improves the network performance in terms of the average goodput of the flows.

The comparison among the SelG, SOAR and HOVER protocols are shown in Figure 6.13 in terms of average end-to-end delay. The average end-to-end delay is maximum for HOVER, as every time a flow is introduced in the network, HOVER uses the on-demand distance vector protocol to find out the mesh paths. Though intermediate mesh STAs can immediately return a path, if they have one in their forwarding table, the lifetime of the entries in the forwarding tables for HOVER is low that triggers rebroadcast of the RREQ packets. The opportunistic forwarding in the SOAR protocol reduces the end-to-end delay. However, SOAR can not provide minimum delay for all the flows because of the frequent trapping in the local solution due to un-managed coordination among the forwarders. The SelG protocol provides minimum end-to-end delay among these three

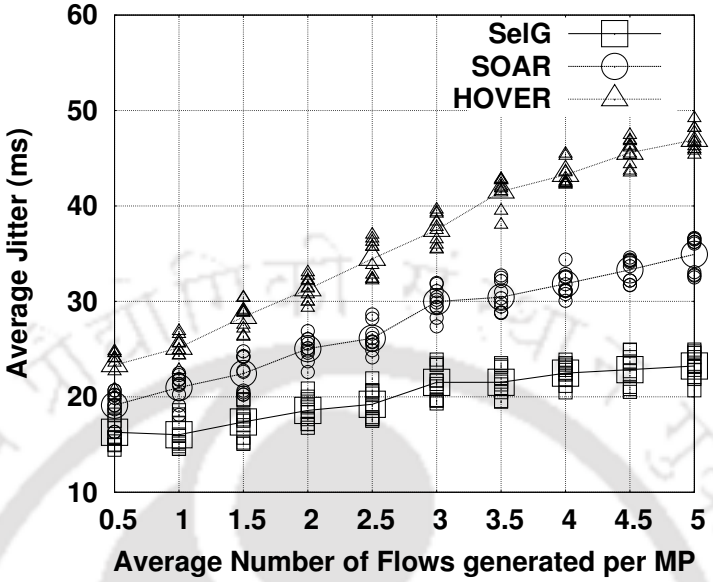

Figure 6.14: Comparison of the average jitter

protocols, due to two main reasons. First, the utility function estimates the effect of the local changes over the global path metrics, during the greedy selection, and second, the minimum interference mesh path selection reduces the extra delay that might be introduced due to channel contention. HOVER and SOAR do not consider minimum interference paths, and therefore, per-hop contention and channel access delay affects the overall end-to-end delay for the flows.

Figure 6.14 compares the thee protocols in terms of average packet jitter. HOVER and SOAR do not consider the interference effect over the path selection. Therefore, in the dynamic network scenarios, different packets experience different amount of per-hop contention and channel access delay, which reflects in their average packet jitter value. The SelG protocol results in the minimum packet jitter among these three protocols, by incorporating both the channel and the network variabilities in the mesh path decision. The fairness index for the three protocols has been shown in Figure 6.15. The proposed SelG protocol provides maximum route stability, by considering the local effect on the global path selection criteria, which reflects in the fairness index. In case of the HOVER protocol, network congestion may occur when every flow selects the shortest path based on the path selection metric. Similarly, the forwarder set in SOAR is constructed based on the shortest path routing, which also may result in network congestion when number of flows is high. It can be noted that SOAR does not explicitly consider the congestion or

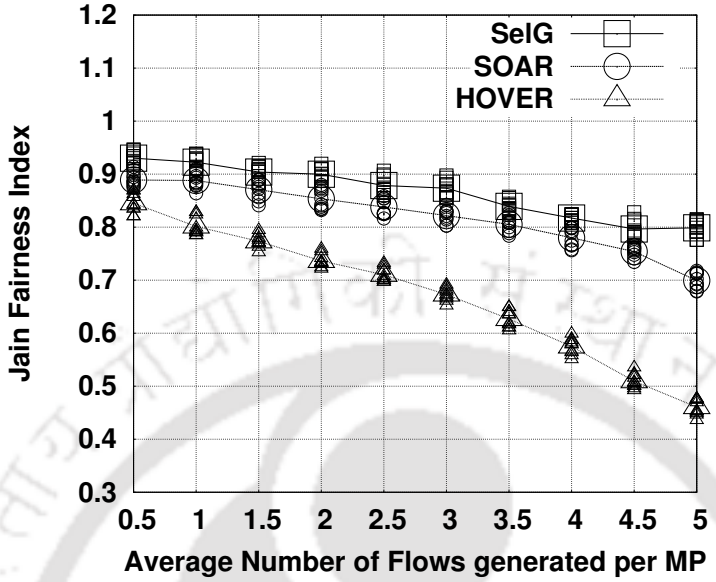

Figure 6.15: Comparison of the fairness index

interference effects, even during the packet broadcast. Further, receiving the packet earlier does not guarantee that the packet is received through the minimum interference path. The proposed SelG protocol aims to satisfy the minimum interference constraint along with minimizing the utility. As a result, the shortest paths are selected only when the interference constraint is satisfied. If the interference constraint is not satisfied, the flows are temporarily redirected to one of the next best available paths, until the interference constraint gets satisfied. This way, the congestion is avoided. Network congestion results in severe unfairness, as the goodput for the flows in congestion degrades severely. Therefore, SelG provides better fairness compared to SOAR and HOVER, as reflected in Figure 6.15.

6.4.3 Communication Between Two Mesh STAs

For these sets of experiments, the network scenario is kept similar to the one as described for mesh STA to mesh gates communication. Number of flows has been varied for every scenario to measure the performance metrics. The traffic sources and the destinations are selected uniformly among the mesh STAs. Every scenario is executed for 10 different times with different sets of sources and destinations, and the average is taken to plot the graphs. The performance of the proposed SelG protocol is compared with the reactive HWMP and SOAR protocols. The lifetime of the entries in the forwarding table is taken as 3 min for the reactive HWMP protocol, and 6 min for the SelG protocol. The δ value

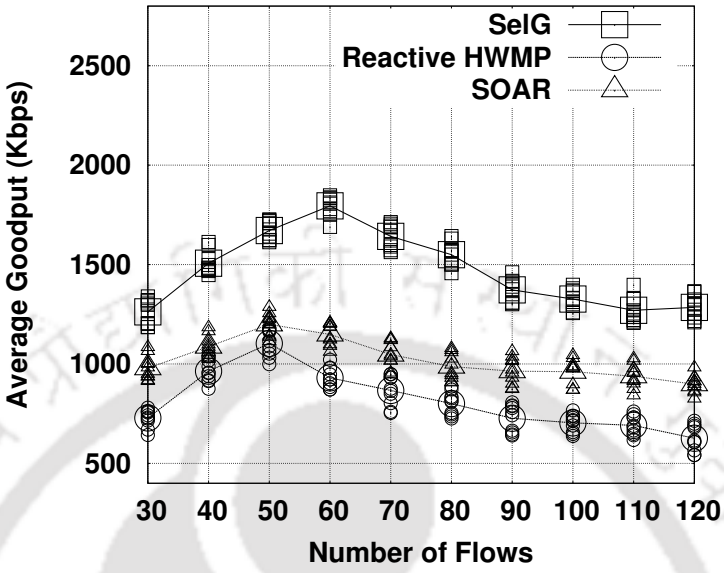

Figure 6.16: Comparison of the average goodput

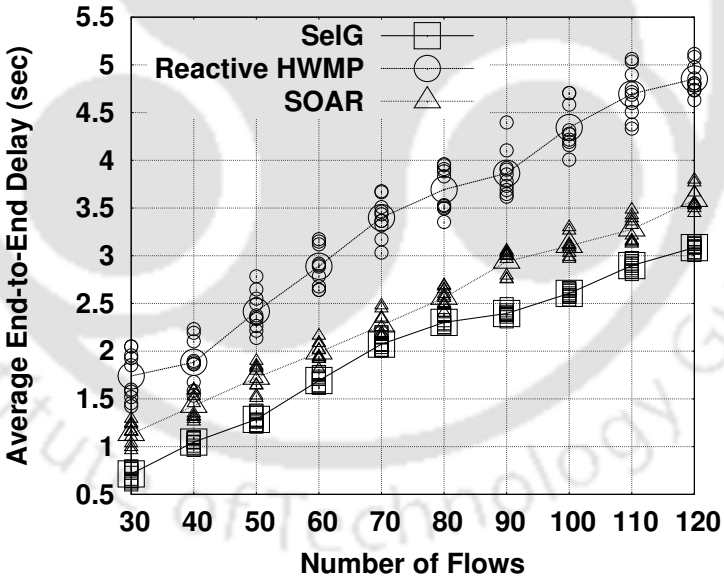

Figure 6.17: Comparison of the average end-to-end delay

for the SelG protocol is assumed to be 0.1.

Figure 6.16 compares the three protocols with respect to average goodput for the flows. The figure reveals that the average goodput for the SelG is highest among the three. The reactive HWMP needs to find out the mesh path every-time a flow is

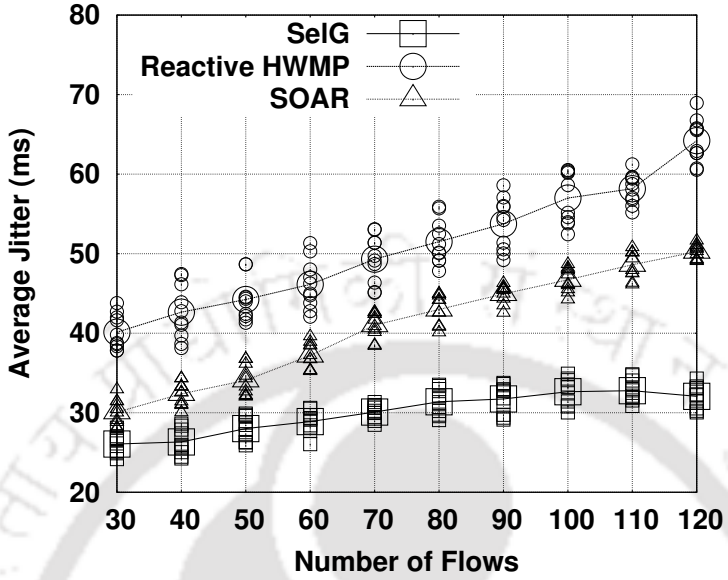

Figure 6.18: Comparison of the average jitter

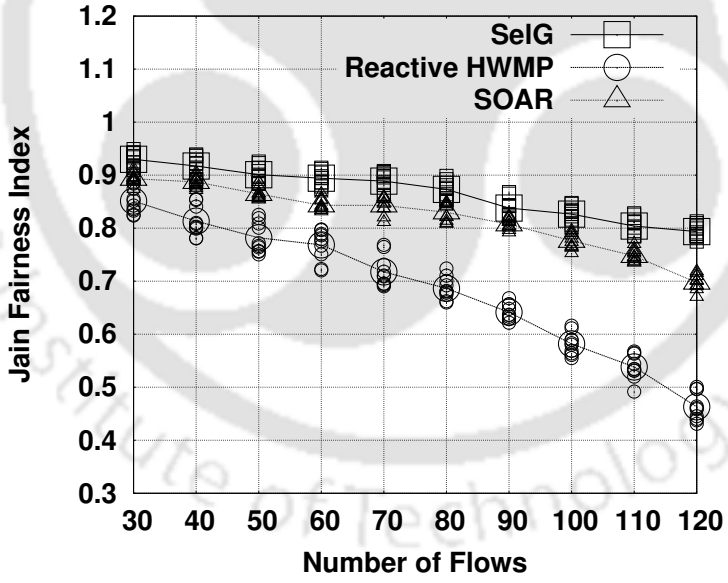

Figure 6.19: Comparison of the fairness index

introduces, henceforth decreasing the average goodput. Further, the channel contention and the interference also affects the performance of the reactive HWMP and SOAR protocols. Frequent path updates are not required for SelG as it uses statistical dispersion measurement for estimating the effect of local changes on the global path values. The

isotonicity of the utility function makes SelG stable under small network and channel fluctuations, as a result of which, the average end-to-end delay and jitter for SelG is minimum, as shown in Figure 6.17 and Figure 6.18. Figure 6.19 compares the fairness among the three protocols. As the figure reveals, SelG results in better fairness compared to SOAR and reactive HWMP. It can be observed from the figures, that SelG improves the end-to-end performance significantly, when network load (in terms of number of flows) is high enough. The uniform distribution of the flows in the network, as realized by the interference constraint of the SelG, reduces interference and channel contention in the network, which improves overall performance by reducing the contention and congestion losses. Further, the path selection control overhead is low for the SelG protocol, compared to other two protocols.

6.5 Summary

This chapter proposes a two phase mesh path selection protocol over the conventional HWMP to overcome the shortcomings of both the proactive and the reactive approaches in multi-interface mesh network. Due to the fluctuation in wireless channel characteristics and the interference conditions, proactive HWMP does not fit well for multi-interface network. Reactive mode of HWMP floods the network with lots of control packets. In the proposed protocol, a set of PNCs are selected from the one-hop neighborhood using a proactive approach, and then a greedy selection is used during the actual data communication, to select the optimal next-hop candidate from the set of PNCs, based on the current channel conditions and interference constraints. The results from the simulation experiments show that the proposed scheme works better than HWMP and other related protocols.

Upto this chapter, the performances of the proposed schemes have been analyzed through the simulation results. Next chapter gives a detailed analysis of the performance of the improved mesh protocols, compared to the IEEE 802.11s standard, using the results obtained from a practical mesh testbed.

Chapter 7

Evaluation of WMN through a Practical Indoor Mesh Testbed

For all the protocol amendments proposed till the last chapter, the results from the simulation experiments are used to evaluate the performance enhancements of the protocols in a WMN built over the IEEE 802.11s technology. The simulation allows to evaluate the performance in a broader range of scenarios, whereas the results from a practical testbed experiment provide outcomes from a more realistic settings. This chapter analyzes the performance of the proposed protocols over a practical indoor mesh testbed, deployed in the research labs of the Department of Computer Science and Engineering, Indian Institute of Technology, Guwahati. All the proposed protocols, except the rate adaptation mechanism, have been implemented in mesh protocol stack. Because of the driver restriction, as will be discussed in subsequent sections, the rate adaptation protocol could not be implemented over the testbed. In view of the complete implementation of the proposed set of improvements over the basic IEEE 802.11s technology, a separate chapter is dedicated to analyze the results from the testbed, rather than merging it with previous chapters. The testbed details and the results obtained from the experiments are reported in subsequent sections.

7.1 Implementation Basics

The testbed is built with 11 mesh routers with open source Linux kernel support (kernel version 2.6.14). However, the driver support is proprietary, and therefore direct access to the firmware level modifications (the physical layer and some part of the data link

layer, including logical link layer and partial MAC protocols) are not possible. For this reason, the testbed is used to analyze the performance of the proposed channel access and mesh path selection protocols only. The multi-rate support is not implemented in the routers, as it requires direct interaction with the chipset driver, which is beyond the scope of support. The proposed channel access and the mesh path selection protocols are implemented as an extension to the kernel network module, in the form of *'Loadable Kernel Module'* (LKM) [223]. A LKM is an object file that contains code to extend the running kernel or the base kernel. LKMs are typically used to add support for new hardware and file-systems, or for adding system calls. When the functionality provided by an LKM is no longer required, it can be unloaded in order to free memory and other resources. In the implementation of the proposed protocols over the mesh routers, the required functionalities are executed within the LKM, and the results are feedback to the driver to tune the necessary driver parameters. For example, the LKM for the channel access executes the proposed optimization, as described in Chapter 3 and Chapter 4, and feeds back the required MAC parameters (such as MAF limit for the MCCA channel access) to the hardware driver. Similarly the LKM corresponding to the proposed SelG protocol finds out the next-hop forwarder and sets the next-hop variable accordingly in the IP layer of the kernel protocol stack. It can be noted that, though the driver is proprietary and the source can not be modified, it gives access to some of the access parameters, like the MAF limit, which can be assigned to a specific value from the kernel level. The next section gives the details of the chipset and configuration properties for the routers.

For the ease of presentation, individual contributions in this thesis build the protocols from the scratch over the basic IEEE 802.11s standard. Chapter 3 proposes an improved scheduling and mesh path selection protocol for directional multi-interface scheduling, whereas Chapter 4 designs a service differentiation and call admission control mechanisms over the IEEE 802.11s set of protocols for supporting service differentiation in the mesh network. As a consequence, Chapter 6 proposes a new mesh path selection paradigm, called the SelG. SelG uses a two phase mesh path selection scheme, however, the ALM is used as the path selection metric for illustration purpose. In the combined implementation of the proposed set of protocols over the mesh testbed, SelG uses S-ALM, as proposed in Chapter 3, instead of the ALM. Further, the information obtained from SelG (through PREQ or PPREQ messages) is used to implement the call admission control mechanism, as proposed in Chapter 4. This way the individual concepts proposed in different chapters are merged to analyze the performance improvement of the proposed set of protocols over the standard IEEE 802.11s protocol stack.

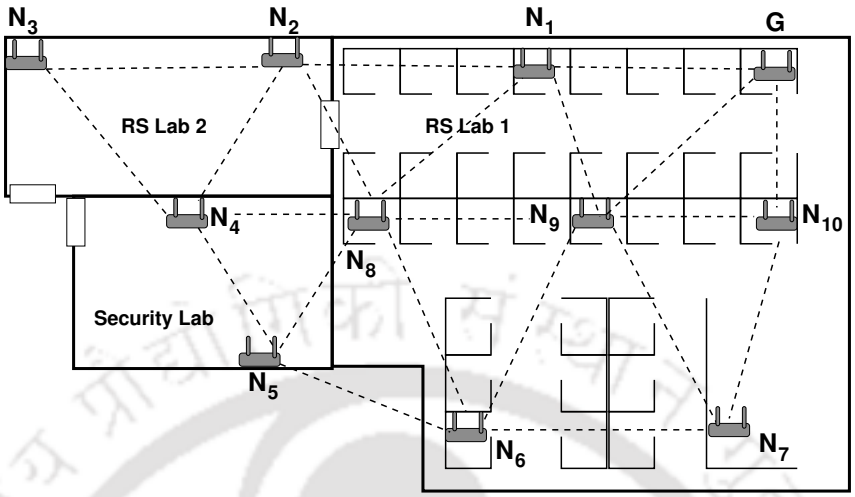

Figure 7.1: IEEE 802.11 Indoor Mesh Testbed and Connectivity Layout

7.2 Router Properties and Configuration

Each node (mesh routers) in the testbed is a Skiva Easyconnect RT001 N300 WiFi router with RaLink RT-3352 chipset [70]. The Ralink RT-3352 router on chip combines 802.11b/g/n draft compliant 2T2R MAC along with BBP/PA/RF MIMO, a high performance 400MHz MIPS24KEc CPU core, a Gigabit Ethernet MAC, 5-ports integrated 10/100 Ethernet Swtich/PHY, 64MB of SDRAM and 32MB of Flash. This chip can support up to 54 Mbps data rate using IEEE 802.11b/g physical layer technology, and up to 300 Mbps data rate using IEEE 802.11n technology. It can be noted that the backbone mesh testbed implementation used in this work supports IEEE 802.11b/g technology with 54 Mbps data rate. Every router is equipped with two dual stream MIMO interfaces. Therefore, four simultaneous transmission beams can operate, provided they do not interfere with each other. The routers use a static channel assignment, where the operating frequency band for every interface is predetermined and pre-configured. The mesh routers works as the mesh STA for the backbone network, and therefore, the terms router and mesh STA are used interchangeably in this chapter.

The proposed scheme is implemented and evaluated using a 11-node IEEE 802.11 indoor mesh testbed deployed over the IIT Guwahati Computer Science department research labs, as shown in Fig. 7.1. The connectivity among the nodes is shown using dotted lines. The node G works as the mesh gate.

Two types of traffic flows are randomly distributed in the network - flows from the mesh routers to the mesh gate, and intercommunication among the mesh routers. Both

TCP and UDP flows are introduced in the network. TCP and UDP flows are generated based on the File Transfer Protocol (FTP) and the Trivial File Transfer Protocol (TFTP), respectively. Every TFTP client generates data at an average rate of $1Mbps$. The performance data of the routers are collected for 6 hrs, and the average performance is shown in the graphs.

7.3 Evaluation of the Scheduling, Mesh Path Selection and QoS

As discussed, the distributed optimization problem proposed in Chapter 3 (for single class traffic) and Chapter 4 (for multi-class traffic) has been implemented in the LKM as an extension to the standard IEEE 802.11s set of protocols. The LKM solves the optimization, and finds out the optimum MAF limit such that the required traffic demand can be satisfied. In the testbed driver implementation, the MAF limit is exported as a system level parameter that can be set from the kernel. This feature of the hardware driver is explored to implement the LKM, where the LKM finds out the optimal MAF limit, and sets it to the hardware driver by triggering a interrupt procedure, at the beginning of every DTIM interval. On average, approximately 30 clients are randomly distributed in the testbed area, that connects to the mesh STAs for the Internet access. There are on average 5 different application flows from every client, with both TFTP and FTP as the application traffics. Approximately 20% of the total flows use TFTP traffic, and rest other flows use FTP traffic[1].

In the graphs, 'Direc Sched + ALM' denotes the proposed directional scheduling along mesh path selection with ALM as the link metric, and 'Direc Sched + S-ALM' denotes the proposed directional scheduling along mesh path selection with S-ALM as the link metric (Chapter 3). Further, 'Direc Sched + S-ALM + QoS' denotes the service differentiation and call admission control over the scheduling and mesh path selection mechanism, as proposed in Chapter 4.

7.3.1 Single Class Traffic: Performance Improvement

To analyze the performance improvement of single class traffics in a directional mesh environment, based on the proposed scheduling and mesh path selection mechanism, three

[1]Now-a-days, most of the Internet traffics are TCP traffics. Similar scenario is used in the testbed traffic setup.

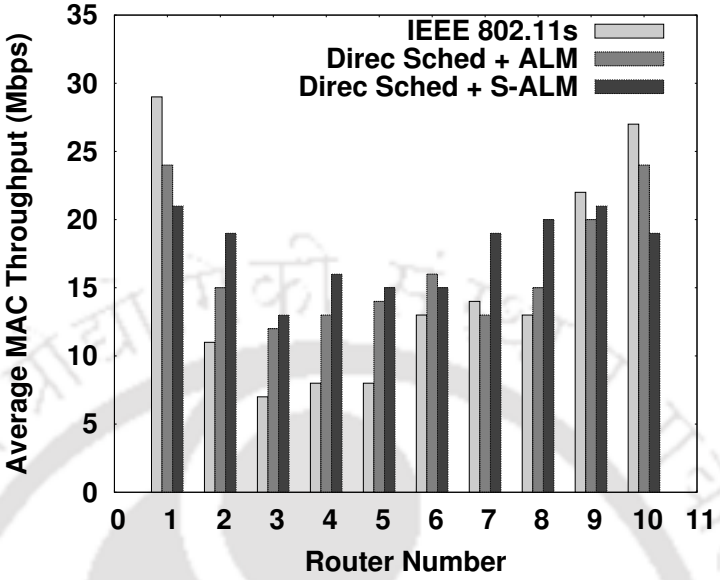

Figure 7.2: Average MAC Throughput per Router

performance metrics are measured from the packet trace data obtained from the testbed - average per router MAC throughput, average per flow throughput and the fairness index. Average per router MAC throughput is calculated as the average amount of data sent successfully per second. It can be noted that only successful data transmission is considered for the throughput calculation. Though the actual transmission rate may be much higher, the data may be dropped from the next hop relay due to the buffer overflow from the interface, which is a common problem in the multi-hop mesh path selection, as discussed in Chapter 2. Average per flow throughput is calculated as the average throughput of all the MAC layer flows in the network. For the calculation of the per-flow throughput, only MAC layer protocol overhead is considered. Application layer throughput may be less than the MAC layer throughput, based on the upper layer protocol overheads. Fairness index is measured in terms of the Jain Fairness Index [197].

Figure 7.2 shows the average MAC throughput for the 10 routers deployed in the testbed. Two different variants of the proposed joint scheduling and mesh path selection are implemented, one with the HWMP protocol operated along the ALM metric, and another with the HWMP protocol operated along the S-ALM protocol. As discussed in Chapter 3, S-ALM considers the effect of the interface scheduling while selecting the best forwarding path. The proposed joint scheduling and mesh path selection protocol is compared with the standard IEEE 802.11s set of protocols (MCCA with HWMP). The

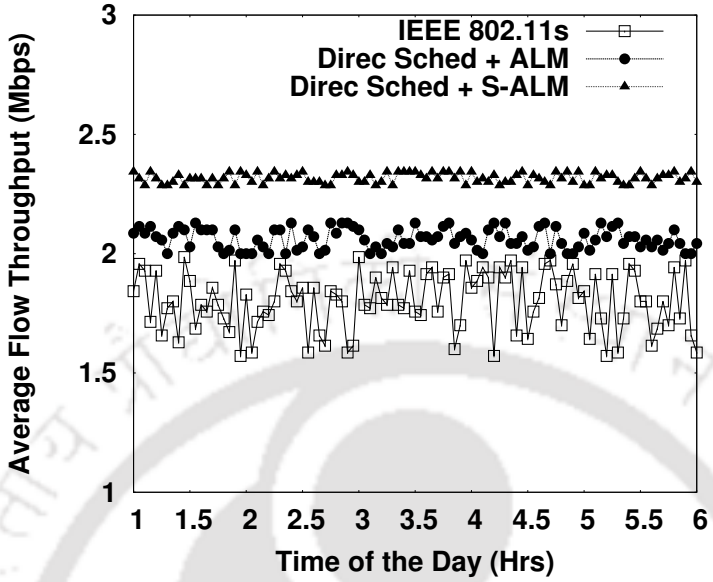

Figure 7.3: Average per Flow Throughput

figure reveals that the variation in the MAC throughput among the routers is very high in case of the standard IEEE 802.11s protocol. According to the figure, while router N_1 attends 28 Mbps, router N_3 attends only 6 Mbps. As discussed, all the routers in the testbed operate at 54 Mbps data rate. Router N_3 is at the farthest hop away from the mesh gate, while router N_1 is only in single hop away. That is why most of the packets from router N_3 are dropped due to buffer overflow, because of the uneven flow distribution and scheduling in the IEEE 802.11s set of protocols. The proposed scheduling mechanism improves the average performance of the routers in terms of MAC layer throughput. Though the throughput for router N_1 degrades a bit, the throughput for router N_3 improves significantly. The scheduling and mesh path selection mechanism along with the S-ALM further reduces the variance in the MAC throughput of the routers by distributing the flows evenly in the network, based on selecting the forwarding paths depending on the scheduling information.

The reduction in the deviation in MAC throughput improves the end-to-end flow performance, as can be seen from Figure 7.3. The figure reveals that the average per flow throughput improves significantly for the proposed scheduling and mesh path selection mechanism, compared to the standard IEEE 802.11s protocols. Figure 7.4 shows the improvement in fairness among the flows, in terms of the Jain fairness index. The proposed scheduling mechanism distribute the total bandwidth evenly among the contending routers

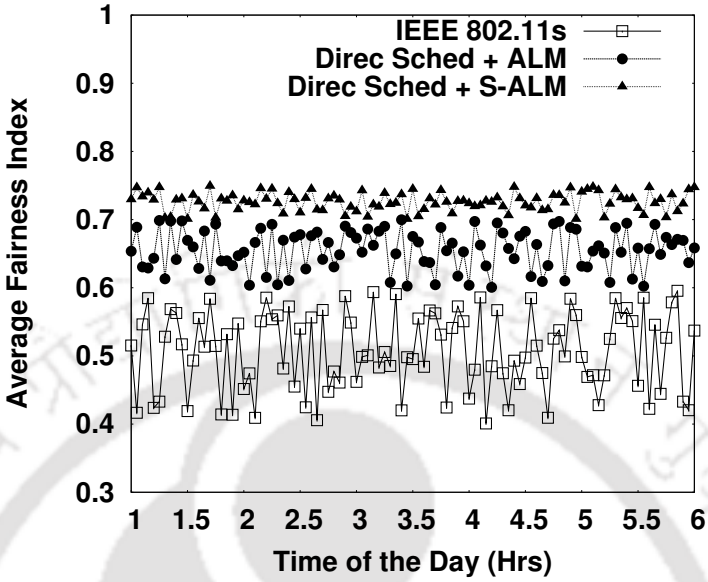

Figure 7.4: Fairness Index

based on their traffic load, which in turn improves the end-to-end flow semantics in the network. The S-ALM metric further improves the fairness by selecting the best forwarding path for a new flow admitted in the network. Further, because of the variation in the network interference (interference among the sub-flows of a flow, as well as the interference among different flows), there are frequent drops in the fairness index, as shown in Figure 7.4. Whenever a new flow gets admitted, or an existing flow terminates, the fairness index gets dropped in case of the standard protocols. The proposed scheduling and mesh path selection along with the S-ALM metric reduce the sudden drops in the fairness index by considering the current scheduling information during the path selection procedure.

7.3.2 Multi Class Traffic: Inter-class Service Differentiation and Intra-class Fairness

To analyze the performance of the service differentiation and call admission control mechanism over the scheduling and mesh path selection mechanism proposed in Chapter 3, the QoS support has been compared with the scheme of Chapter 3 with respect to two parameters - average proportional fairness index, and average Jain fairness index. Average proportional fairness index is computed using the similar procedure discussed in Chapter 4. Average Jain fairness index is computed as follows. Let there are q number of traffic classes

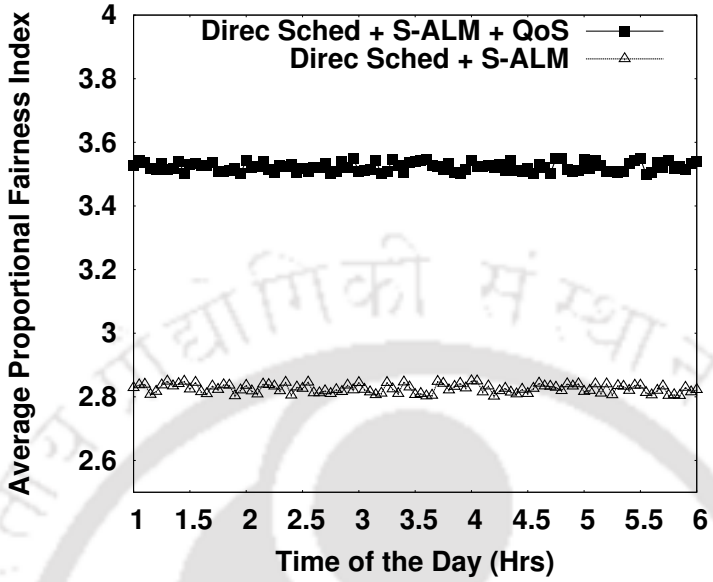

Figure 7.5: Average Proportional Fairness Index: Inter-class Service Differentiation

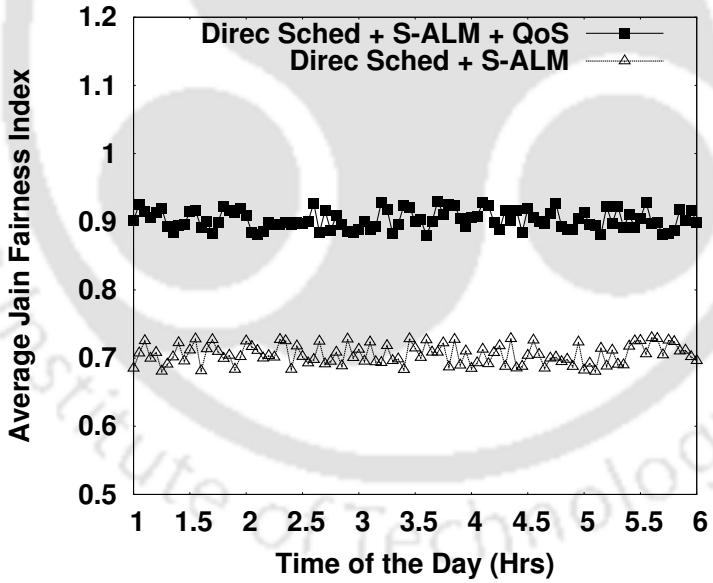

Figure 7.6: Average Jain Fairness Index: Intra-class Fairness

$TC_1, TC_2, ..., TC_q$. Then,

$$\text{Average Jain Fairness Index} = \frac{\sum_{\forall TC_i} JF_i}{q} \tag{7.1}$$

where JF_i is the Jain Fairness index for the traffic class TC_i.

The standard four class traffic are distributed in the network. Voice over IP (VoIP) is used as the voice traffic, video streaming is used for the video traffic, FTP is used as the background traffic and TFTP is classified as best effort service. 10% of the total traffics is the voice traffic, 20% is the video traffic, 20% is the background traffic, and rest 50% is the best effort traffic.

Figure 7.5 shows the average proportional fairness index for the flows in the network, and Figure 7.6 depicts average Jain fairness index in the network. Proportional fairness index reflects the inter-class service differentiation, while the average Jain fairness index shows the intra-class fairness. Both the figures reveal that the proposed service differentiation and call admission control schemes improve the inter-class service differentiation as well as intra-class fairness in the network.

7.4 Evaluation of the SelG Protocol: Mesh Path Selection Performance

The proposed SelG protocol is implemented as a LKM in the mesh path selection module of the routers' kernel. This LKM is loaded whenever a router needs to decide the forwarding paths. The proactive and the reactive HWMP protocols are also implemented separately in the kernel. The performance of the SelG is compared with the proactive and the reactive HWMP protocols. As earlier, the routers are configured to operate in $54Mbps$ data rate, along with the scheduling and peer-selection protocols. For the SelG protocol, the δ value is taken as 0.1, and the lifetime of the entries in the forwarding tables are set to 6 min. For HWMP, the lifetime of the entries in the forwarding table are fixed at 3 min.

The performance of the proposed SelG protocol is compared with the proactive and the reactive HWMP protocol, using the results obtained from the testbed. When the routers are configured to operate in the proactive mesh path selection mode, all the flows, even the flows between two routers, are re-routed through the mesh gates. However, when the routers are configured in the reactive mode, the reactive HWMP protocol is used to find out the paths between the routers to the mesh gates, as well as between two routers. In a third setting, the HWMP is configured in the hybrid mode, where the proactive mode is used only for the routers to the gateway, and the reactive mode is used to find out the forwarding paths between two routers. Therefore, in a nutshell, the proposed SelG scheme is compared with three different HWMP configurations - the proactive mode, the reactive mode and the hybrid mode.

Figure 7.7 compares the proposed SelG protocol with the HWMP protocol with

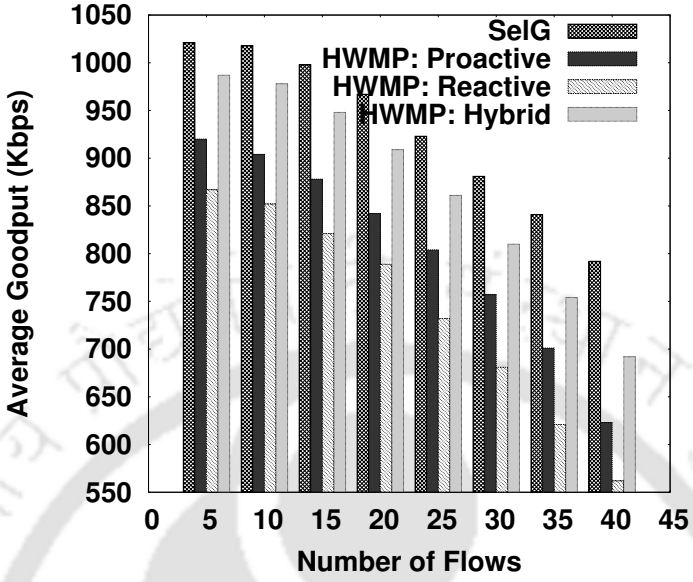

Figure 7.7: Average Goodput

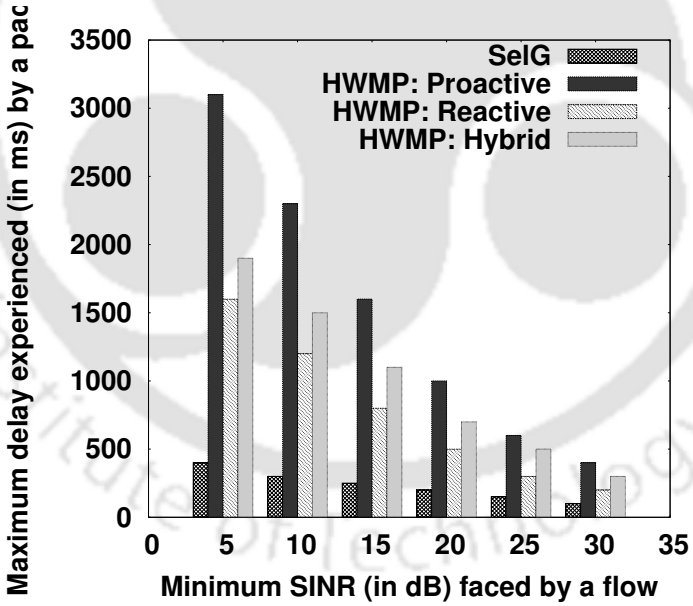

Figure 7.8: Average Packet Drop

respect to average goodput for the flows. As mentioned the description of the scenario setup, half of the flows are from routers to the gateway, and rest halves are between two routers. For proactive HWMP protocol, the goodput of the flows between two routers affects as they need to forward the packets via the gateways. Though reactive HWMP

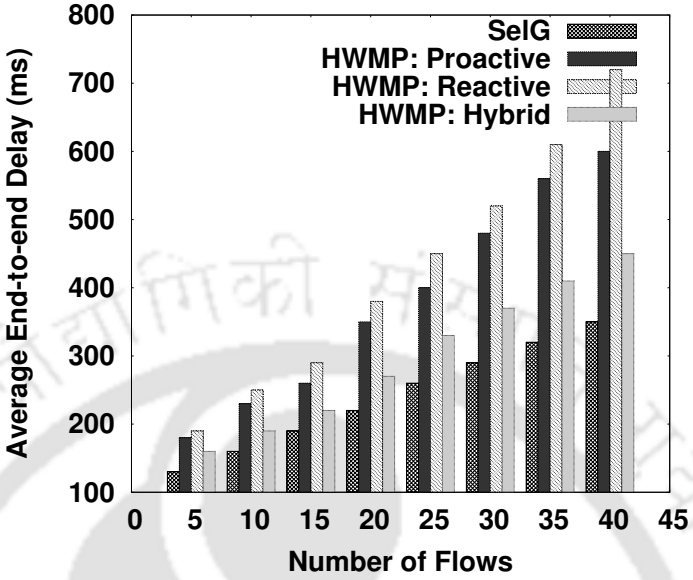

Figure 7.9: Average End-to-end Delay

improves the goodput for these flows, the overall goodput drops because of the excessive control overheads. It has been observed from the experiments, that for some settings the control overhead even goes beyond 20% of the total traffic. The channel variability is more in the indoor environment, which affects the mesh path selection decisions in HWMP. The average variance in the channel quality is measured in terms of signal-to-interference and noise ratio (SINR), and it has been observed, that average SINR variance in our indoor testbed environment is about 40% of the mean SINR value. Further in some cases, the SINR drops to a very low value due to sudden noise from external factors, like signal interference from high voltage electrical devices. It has been observed that, the packets experiences high delay in these cases, for the proactive HWMP protocol. Even the reactive HWMP can not handle these cases, because they rely on the path metric value calculated during the path-establishment phase. From the logs of the individual routers, the maximum delay experienced by a packet of a flow, and the minimum SINR value observed by that flow are calculated[2], and a graph is plotted, as shown in Figure 7.8. The figure reveals, when the channel quality is low, the maximum delay experienced by a

[2]The minimum SINR value observed by a flow, indicates the minimum SINR value at the routers that may act as a forwarder for that flow. Therefore, for HWMP protocol, the minimum SINR value is observed at one of the routers in the forwarding path. However, for the SelG protocol, the router with the minimum SINR may be one of the candidates from the set of potential forwarders, and not necessarily be the routers in the actual forwarding path.

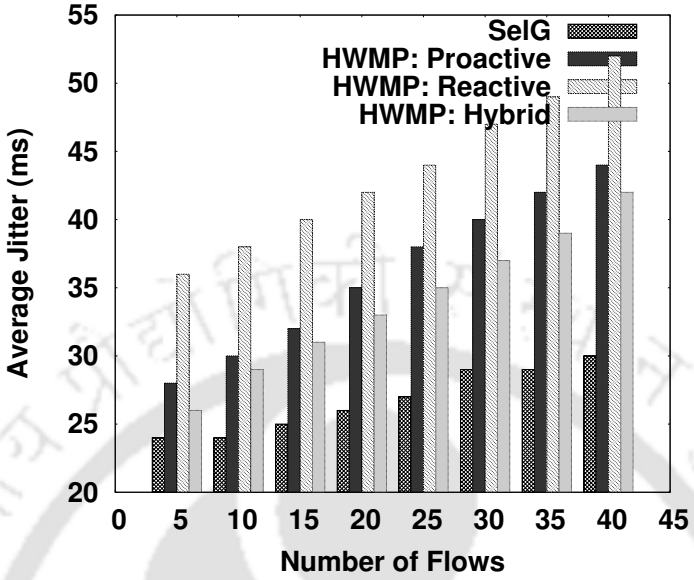

Figure 7.10: Average Jitter

packet is very high in case of the proactive HWMP protocol. Though the reactive HWMP can alleviate a bit, however, the delay is still considerably high. The hybrid mode of HWMP gives an in-between result. This figure indicate that the HWMP protocol can not adapt the link fluctuations. On the contrary, the proposed SelG protocol provides following advantages over the traditional HWMP protocol,

(i) The SelG protocol adapts to the channel fluctuation. Figure 7.8 reveals that for the SelG protocol, even at the low SINR value, the increment in the maximum delay experienced by a packet is low. If one of the candidate from the set of potential forwarders experience sudden SINR drops, SelG may redirect the packet through another router which provides better link value. It may be noted that a low SINR value results in a low link metric value, because of the poor link quality.

(ii) The control overhead for SelG protocol is lower than the HWMP protocol. The lifetime of the entries in SelG forwarding table is more than the lifetime of the entries in the HWMP forwarding table.

Figure 7.9 compares SelG and HWMP with respect to average end-to-end delay. Because of the reasons analyzed till now, SelG provides lower end-to-end delay than the HWMP protocol. The jitter value is also less for the SelG protocol, as shown in Figure 7.10. Because of the route stability and minimum interference interface selection, the proposed

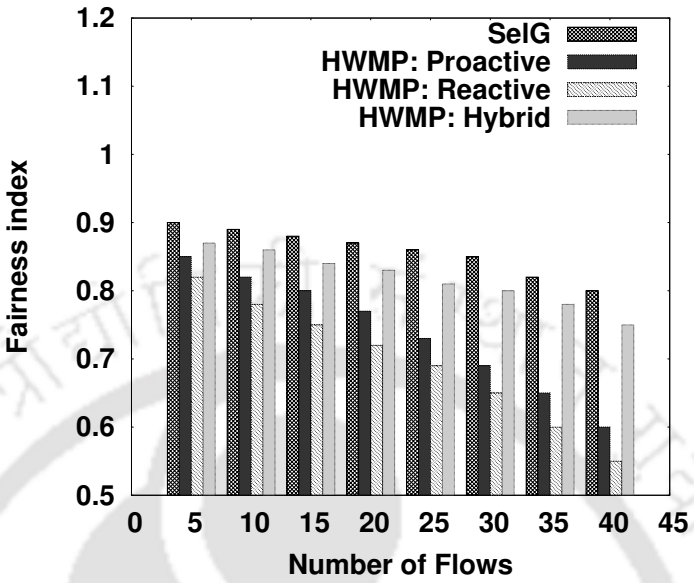

Figure 7.11: Fairness Index

SelG protocol provides better fairness among the flows, compared to the HWMP protocol, as reflected in Figure 7.11. The graph shows that proactive HWMP provides more fairness compared to the reactive HWMP. The reason is that all the flows are forwarded through the mesh gates, and therefore, the maximum goodput for all the flows is bounded to the network capacity of the mesh gates. Reactive HWMP distributes flows unevenly in network, and may result in network congestion, as discussed earlier, which is reflected in fairness calculation. The adaptive next-hop selection based on interference constraint, as used in the proposed SelG protocol, improves the network performance significantly.

7.5 Summary

This chapter analyzes the performance of the proposed scheduling, mesh path selection and service differentiation protocols from the results obtained from an indoor testbed. Though the rate adaptation protocol could not be implemented in the testbed due to the proprietary driver restrictions, rest three protocols are implemented, and the overall performance improvement is analyzed. The results show that the directional scheduling and mesh path selection protocol with S-ALM improves the network capacity significantly. At the same time, the QoS provisioning mechanism provides better service differentiation and fairness in terms of inter-class service differentiation and intra-class fairness. The

SelG protocol results in an efficient mesh path selection protocol in a mesh network by handling the network dynamics effectively. The testbed results clearly show the overall performance improvement of a mesh network in a real scenario, by using the proposed set of protocols, compared to the standard IEEE 802.11s set of protocols.

Chapter 8

Conclusion and Future Directions

This thesis proposes a set of amendments for effective use of the IEEE 802.11s standard to provide broadband connectivity through wireless mesh backbone. For this purpose, directional communication is considered over the IEEE 802.11s standard to support effective spatial reuse, by allowing simultaneous transmissions and receptions, while minimizing the network interference. In this direction, the major contributions of this thesis is summarized as follows.

To improve the network capacity through the spacial reuse, a joint scheduling and mesh path selection mechanism is proposed in the first contribution (Chapter 3) of this thesis, for proper allocation of network resources in a mesh network, where directional antenna system is used for communication. A centralized optimization problem is formulated for this purpose, and the convexity of the centralized optimization is explored to design a distributed per STA solution. The optimization problem finds out the required channel share for every interface to support equal-time access opportunity for every flows considering the network interference, and accordingly tune the MAF limit in MCCA access mechanism to achieve this share. Further the ALM for HWMP is tuned to incorporate the effect of the channel scheduling over the mesh path selection, and a new path selection metric, S-ALM is proposed.

QoS provisioning in a mesh network is another important design aspect which is explored in Chapter 4. For QoS provisioning in a mesh network, $(\alpha, \wp)$ proportional fairness criteria is incorporated to support inter-class service differentiation and intra-class fairness simultaneously. The centralized optimization problem in this scenario is shown to be log-convex, and this property is used to design a distributed per STA solution based on sub-gradient optimization method. A call admission control mechanism is designed over

the mesh path selection protocol to support better service assurance in a network with moderate to high traffic load.

The next work in this direction (Chapter 5) augments the basic IEEE 802.11s set of protocols for multi-rate support in mesh networks. Based on the channel encoding, low data rates can sustain for long transmission ranges, whereas high data rates can support short transmission ranges. Long transmission ranges reduce number of hops to be traversed to reach the destination, however increase congestion in the network. A multi-rate WMN is theoretically modeled as a G/G/1 queuing network, and the diffusion approximation method is used to find out a closed form solution of the end-to-end forwarding delay, and maximum achievable throughput. The theoretical analysis shows that there is a trade-off among data rate, number of hops and interference, in a multi-rate multi-interface mesh network. This rate-hop-interference trade-off is explored to design augmentations over IEEE 802.11s topology management (MPM), channel access (MCCA) and mesh path selection (HWMP) protocols to support multi-rate adaptation.

The traditional mesh path selection mechanism in a mesh network uses one of the four approaches - proactive, reactive, hybrid or opportunistic. The work proposed in Chapter 6 discusses about a new mesh path selection protocol for mesh network, called 'Selective Greedy' (SelG) mesh path selection, which is different from the traditional approaches. The SelG protocol works in two phases. In the first phase, a set of potential forwarders are selected using proactive approaches. In the second phase, one of the MPs from the potential forwarders are selected as the next-hop relay, using greedy approach. This greedy approach considers the effect of link information variation over the path information, and selects the mesh STA that provides maximum utility (minimum path variation).

The performance of all the four contributions presented in this thesis are evaluated through simulation results, and the performance metrics are compared with other related protocols proposed in the literature. Finally, this thesis presents the performance results of the combined set of proposed protocol augmentations, except the multi-rate adaptation, through the results obtained from a indoor mesh testbed, which is reported in Chapter 7. The multi-rate adaptation is not implemented in the testbed due to the restriction in proprietary drivers. The testbed results show the overall performance improvement of the proposed set of protocol augmentations in a real time environment, compared to the IEEE 802.11s standard protocols.

The performance of an IEEE 802.11s mesh network can be further enhanced with the amendment of more advanced features, which can be kept as the future directions in this research area. Some of these amendments are discussed briefly, as follows.

IEEE 802.11s supports mesh path selection protocol at the MAC layer for efficient path selection based on channel access information. However, transport layer protocols, like TCP, work independently. In a multi-hop mesh environment, end-to-end path characteristics depend on the link characteristics, and link characteristics are available from the lower layer access and mesh path selection protocols. Therefore, efficient TCP designing for mesh network may consider lower layer information available at the end devices for assigning suitable values to the TCP parameters. Conversely, the end-to-end information available at TCP can also be used by the lower layers for scheduling and mesh path selection purposes. As an example, in a dynamic mesh network, TCP may trigger unnecessary congestion control avoidance actions based on the RTT estimation, depending on the scheduling and mesh path selection mechanisms. The RTT estimation at the TCP end devices (mesh clients, in general) may use the information from the mesh path selection protocol to measure RTT variations. This way, a cross layer design may be incorporated to improve TCP end-to-end utilizations.

Recent developments in physical layer modulation technology can support upto 600 Mbps data rates using IEEE 802.11n dual streaming method. IEEE 802.11n can operate in two different bands, and simultaneous usage of two different bands in a single interface is possible through the MIMO dual streaming approaches. This introduces additional challenges during the design of the scheduling and mesh path selection protocols, as the interference estimation should consider both the bands simultaneously. Further, MIMO rate adaptation is different from the traditional rate adaptation schemes, as a trade-off exists between the data rate and number of data streams to be used. As shown in [224], depending on the external interference, some data rates operates better in single streaming compared to the double streaming. Therefore, the rate adaptation technique proposed in this thesis is not directly applicable for IEEE 802.11n dual streaming. The rate-adaptation technique should also consider the rate-interference-streaming trade-off along with the rate-hop-interference trade-off.

The recent developments in *'Software Defined Radio'* (SDR) have opened several new research directions in *Green Computing* and *Green Networking*. As an example, this thesis considers equal transmission power for all the interfaces, where every interface transmits at the maximum transmission power supported by the selected data rate. Reduction in transmission power may introduce higher channel error rate, but can also reduce interference in the network. Reduction in transmission power is possible if both the communicating entities are at close proximity. Therefore, the MPs in a SDR environment should be able to select the transmission power in an adaptive way that can reduce the

network interference, while providing maximum end-to-end performance gains. Further, efficient power control schemes can be designed based on the scheduling and mesh path selection informations. At the same time, the scheduling and mesh path selection protocols should select the ⟨interface, next hop⟩ pairs, that results in minimum power consumption. This way, the joint power control, scheduling and mesh path selection mechanism can further improve the performance of IEEE 802.11s protocols in a mesh backbone network.

References

[1] I. F. Akyildiz, X. Wang, and W. Wang, "Wireless mesh networks: a survey," *Comput. Netw.*, vol. 47, no. 4, pp. 445–487, Mar. 2005.

[2] Y. Amir, C. Danilov, R. Musuăloiu-Elefteri, and N. Rivera, "The SMesh wireless mesh network," *ACM Trans. Comput. Syst.*, vol. 28, no. 3, pp. 6:1–6:49, Sep. 2008.

[3] G. R. Hiertz, S. Max, E. Weiß, L. Berlemann, D. Denteneer, and S. Mangold, "Mesh technology enabling ubiquitous wireless networks: invited paper," in *Proceedings of the 2nd annual international workshop on Wireless internet*, 2006.

[4] X. Wang and A. O. Lim, "IEEE 802.11s wireless mesh networks: Framework and challenges," *Ad Hoc Networks*, vol. 6, no. 6, pp. 970–984, Aug. 2008.

[5] I. F. Akyildiz and X. Wang, "A survey on wireless mesh networks," *Comm. Mag.*, vol. 43, no. 9, pp. S23–S30, Sep. 2005.

[6] S. Max, E. Weiss, and G. R. Hiertz, "Benefits and limitations of spatial reuse in wireless mesh networks," in *Proceedings of the 10th ACM Symposium on Modeling, analysis, and simulation of wireless and mobile systems*, 2007, pp. 244–251.

[7] R. Bruno, M. Conti, and E. Gregori, "Mesh networks: commodity multihop ad hoc networks," *IEEE Comm. Mag.*, vol. 43, no. 3, pp. 123–131, Mar. 2005.

[8] S. Das, K. Papagiannaki, S. Banerjee, and Y. C. Tay, "SWARM: the power of structure in community wireless mesh networks," *IEEE/ACM Transactions on Networking*, vol. 19, no. 3, pp. 760–773, Jun. 2011.

[9] S. Bury and N. J. Race, "Towards resilient community wireless mesh networks," in *Proceedings of the 2nd international conference on Autonomous Infrastructure, Management and Security: Resilient Networks and Services*, 2008, pp. 195–199.

[10] W. Allen, A. Martin, and A. Rangarajan, "Designing and deploying a rural ad-hoc community mesh network testbed," in *Proceedings of the IEEE Conference on Local Computer Networks 30th Anniversary*, 2005, pp. 740–743.

[11] J. Ishmael, S. Bury, D. Pezaros, and N. Race, "Deploying rural community wireless mesh networks," *IEEE Internet Computing*, vol. 12, no. 4, pp. 22–29, Jul. 2008.

[12] N. Saxena, M. Denko, and D. Banerji, "A hierarchical architecture for detecting selfish behaviour in community wireless mesh networks," *Computer Communication*, vol. 34, no. 4, pp. 548–555, Apr. 2011.

[13] V. Gabale, R. Mehta, J. Patani, K. Ramakrishnan, and B. Raman, "Deployments made easy: essentials of managing a (rural) wireless mesh network," in *Proceedings of the 3rd ACM Symposium on Computing for Development*, 2013, pp. 10:1–10:10.

[14] G. Bernardi, P. Buneman, and M. K. Marina, "Tegola tiered mesh network testbed in rural scotland," in *Proceedings of the ACM workshop on Wireless networks and systems for developing regions*, 2008, pp. 9–16.

[15] S. Garg and G. Kanade, "Topology construction for rural wireless mesh networks - a geometric approach," in *Proceedings of the 2011 international conference on Computational science and its applications - Volume Part III*, 2011, pp. 107–120.

[16] K. Chebrolu and B. Raman, "FRACTEL: a fresh perspective on (rural) mesh networks," in *Proceedings of the workshop on Networked systems for developing regions*, 2007, pp. 8:1–8:6.

[17] G. Ding, J. Vicente, S. Rungta, D. Krishnaswamy, W. Chan, and K. Miao, "Overlays on wireless mesh networks: implementation and cross-layer searching," in *Proceedings of the 9th IFIP/IEEE international conference on Management of Multimedia and Mobile Networks and Services*, 2006, pp. 171–182.

[18] D. Wu, D. Gupta, and P. Mohapatra, "Qurinet: A wide-area wireless mesh testbed for research and experimental evaluations," *Ad Hoc Networks*, vol. 9, no. 7, pp. 1221–1237, Sep. 2011.

[19] Y. Takahashi, Y. Owada, H. Okada, and K. Mase, "A wireless mesh network testbed in rural mountain areas," in *Proceedings of the second ACM international workshop on Wireless network testbeds, experimental evaluation and characterization*, 2007, pp. 91–92.

[20] "Durban Wireless Community." [Online]. Available: http://newsite.dwc.za.net

[21] "AirJaldi." [Online]. Available: http://drupal.airjaldi.com/

[22] "BrisMesh." [Online]. Available: http://brismesh.proboards.com/

[23] "The Mesh, Darwin." [Online]. Available: http://the-mesh.org/

[24] "RHBMesh, North Yorkshire." [Online]. Available: http://rhbmesh.net/

[25] "IEEE standard for information technology–telecommunications and information exchange between systems local and metropolitan area networks–specific requirements part 11: Wireless LAN medium access control (MAC) and physical layer (PHY) specifications," *IEEE Std 802.11-2012 (Revision of IEEE Std 802.11-2007)*, pp. 1–2793, March 2012.

[26] "WNBU Aironet 1500 Lightweight Mesh AP." [Online]. Available: http://www.cisco.com/web/PT/assets/docs/wireless_mesh.pdf

[27] D. Wu, "Deployment and performance enhancement of wireless mesh networks," Ph.D. dissertation, Davis, CA, USA, 2010.

[28] T. Vanhatupa, M. Hännikäinen, and T. D. Hämäläinen, "Performance model for IEEE 802.11s wireless mesh network deployment design," *Journal of Parallel and Distributed Computing*, vol. 68, no. 3, pp. 291–305, Mar. 2008.

[29] R. B. Dilmaghani and R. R. Rao, "Hybrid wireless mesh network deployment: a communication testbed for disaster scenarios," in *Proceedings of the 1st international workshop on Wireless network testbeds, experimental evaluation & characterization*, 2006.

[30] X. Xu, S. Tang, X. Mao, and X.-Y. Li, "Distributed gateway placement for cost minimization in wireless mesh networks," in *Proceedings of the IEEE 30th International Conference on Distributed Computing Systems*, 2010, pp. 507–515.

[31] F. Zeng and Z. Chen, "Load balancing placement of gateways in wireless mesh networks with qos constraints," in *Proceedings of the 9th International Conference for Young Computer Scientists*, 2008, pp. 445–450.

[32] S. Ding, "A survey on integrating MANETs with the Internet: Challenges and designs," *Computer Communication*, vol. 31, no. 14, pp. 3537–3551, Sep. 2008.

[33] J. Jun and M. L. Sichitiu, "The nominal capacity of wireless mesh networks," *Wireless Commun.*, vol. 10, no. 5, pp. 8–14, Oct. 2003.

[34] C. Molle and M.-E. Voge, "A quantitative analysis of the capacity of wireless mesh networks," *Comm. Letters.*, vol. 14, no. 5, pp. 438–440, May 2010.

[35] J. Ben-Othman, Ben-Othman, L. Mokdad, Mokdad, and M. O. Cheikh, Cheikh, "On improving the performance of IEEE 802.11s based wireless mesh networks using directional antenna," in *Proceedings of the IEEE 35th Conference on Local Computer Networks*, 2010, pp. 785–790.

[36] X. Liu, H. Okada, and K. Mase, "Performance of wireless mesh networks with three sector antenna," in *Proceedings of the Sixth International Conference on Mobile Ad-hoc and Sensor Networks*, 2010, pp. 146–153.

[37] E. Ulukan and O. Gürbüz, "Angular MAC: a framework for directional antennas in wireless mesh networks," *Wireless Networks*, vol. 14, no. 2, pp. 259–275, Mar. 2008.

[38] A. P. Subramanian, H. Lundgren, and T. Salonidis, "Experimental characterization of sectorized antennas in dense 802.11 wireless mesh networks," in *Proceedings of the tenth ACM international symposium on Mobile ad hoc networking and computing*, 2009, pp. 259–268.

[39] R. Braden, D. Clark, and S. Shenker, "Integrated services in the Internet architecture: an overview," RFC, United States, 1994.

[40] S. Blake, D. Black, M. Carlson, E. Davies, Z. Wang, and W. Weiss, "An architecture for differentiated service," RFC, United States, 1998.

[41] P. E. Engelstad and O. N. Osterbo, "Delay and throughput analysis of IEEE 802.11e EDCA with starvation prediction," in *Proceedings of the IEEE Conference on Local Computer Networks 30th Anniversary*, 2005.

[42] N. Ramos, D. Panigrahi, and S. Dey, "Dynamic adaptation policies to improve quality of service of real-time multimedia applications in IEEE 802.11e WLAN networks," *Wireless Networks*, vol. 13, no. 4, pp. 511–535, Aug. 2007.

[43] S. Lv, X. Wang, and X. Zhou, "On the rate adaptation for IEEE 802.11 wireless networks," *Comput. Netw.*, vol. 54, no. 17, pp. 3173–3186, Dec. 2010.

[44] K. Yang, J.-f. Ma, and Z.-h. Miao, "Hybrid routing protocol for wireless mesh network," in *Proceedings of the International Conference on Computational Intelligence and Security - Volume 01*, 2009, pp. 547–551.

[45] S. Khan, A. A. Pirzada, and M. Portmann, "Performance comparison of reactive routing protocols for hybrid wireless mesh networks," in *Proceedings of the 2nd International Conference on Wireless Broadband and Ultra Wideband Communications*, 2007, pp. 78–83.

[46] R. G. Garroppo, S. Giordano, and L. Tavanti, "A joint experimental and simulation study of the IEEE 802.11s HWMP protocol and airtime link metric," *International Journal on Communication Systems*, vol. 25, no. 2, pp. 92–110, Feb. 2012.

[47] Y. Song, C. Zhang, and Y. Fang, "Routing optimization in wireless mesh networks under uncertain traffic demands," in *Proceedings of the 5th International ICST Conference on Heterogeneous Networking for Quality, Reliability, Security and Robustness*, 2008, pp. 3:1–3:7.

[48] A. Capone, G. Carello, I. Filippini, S. Gualandi, and F. Malucelli, "Routing, scheduling and channel assignment in wireless mesh networks: Optimization models and algorithms," *Ad Hoc Networks*, vol. 8, no. 6, pp. 545–563, Aug. 2010.

[49] W. Fu, "Analytical model for capacity and delay optimization in wireless mesh networks," Ph.D. dissertation, Cincinnati, OH, USA, 2010.

[50] F. Bokhari and G. Zaruba, "AMIRA: interference-aware routing using ant colony optimization in wireless mesh networks," in *Proceedings of the IEEE conference on Wireless Communications & Networking Conference*, 2009, pp. 2577–2582.

[51] D. Li, B. Wang, and X. Jia, "Topology control for throughput optimization in wireless mesh networks," in *Proceedings of the 4th International Conference on Mobile Ad-hoc and Sensor Networks*, 2008, pp. 161–168.

[52] G. Boudour, C. Teyssié, and Z. Mammeri, "Scheduling-based reservation mac protocol for bandwidth and delay optimization in wireless mesh networks," in *Proceedings of the IEEE International Conference on Wireless & Mobile Computing, Networking & Communication*, 2008, pp. 272–277.

[53] M. Alicherry, R. Bhatia, and L. E. Li, "Joint channel assignment and routing for throughput optimization in multi-radio wireless mesh networks," in *Proceedings of*

the 11th annual international conference on Mobile computing and networking, 2005, pp. 58–72.

[54] Y. Li, L. Zhou, Y. Yang, and H.-C. Chao, "Optimization architecture for joint multi-path routing and scheduling in wireless mesh networks," *Math. Comput. Model.*, vol. 53, no. 3-4, pp. 458–470, Feb. 2011.

[55] Y. Li, Y. Xiong, L. Zhou, and R. Zhu, "Adaptive optimization-based routing in wireless mesh networks," *Wirel. Pers. Commun.*, vol. 56, no. 3, pp. 403–415, Feb. 2011.

[56] R. Susitaival, "Load balancing by joint optimization of routing and scheduling in wireless mesh networks," in *Proceedings of the 20th international teletraffic conference on Managing traffic performance in converged networks*, 2007, pp. 483–494.

[57] Y. Song, C. Zhang, and Y. Fang, "Harnessing traffic uncertainties in wireless mesh networks–a stochastic optimization approach," *Mobile Networks and Applications*, vol. 14, no. 2, pp. 124–133, Apr. 2009.

[58] R. F. Malik and T. A. Rahman, *Routing Optimization Scheme in Wireless Mesh Network: The Implementation of New Particle Swarm Optimization in OLSR*. Germany: LAP Lambert Academic Publishing, 2012.

[59] T. H. Szymanski, "Throughput and QoS optimization in nonuniform multichannel wireless mesh networks," in *Proceedings of the 4th ACM symposium on QoS and security for wireless and mobile networks*, 2008, pp. 9–19.

[60] P. S. Mogre, "Cross-layer bandwidth management and optimization in TDMA based wireless mesh networks using network coding," *SIGMultimedia Rec.*, vol. 2, no. 3, pp. 7–9, Sep. 2010.

[61] J. Yuan, Z. Li, W. Yu, and B. Li, "A cross-layer optimization framework for multihop multicast in wireless mesh networks," *IEEE Journal on Selected Areas in Communication*, vol. 24, no. 11, pp. 2092–2103, Nov. 2006.

[62] E. Pourfakhar and A. M. Rahmani, "Optimization of multicast routing based on a reliable effective framework in wireless mesh networks," in *Proceedings of the 10th Pacific Rim Conference on Multimedia: Advances in Multimedia Information Processing*, 2009, pp. 416–427.

[63] J. Tang, G. Xue, and W. Zhang, "Cross-layer optimization for end-to-end rate allocation in multi-radio wireless mesh networks," *Wireless Networks*, vol. 15, no. 1, pp. 53–64, Jan. 2009.

[64] M. Alicherry, R. Bhatia, and L. E. Li, "Joint channel assignment and routing for throughput optimization in multiradio wireless mesh networks," *IEEE Journal on Selected Areas in Communication*, vol. 24, no. 11, pp. 1960–1971, Nov. 2006.

[65] C. Caillouet, S. Pérennes, and H. Rivano, "Framework for optimizing the capacity of wireless mesh networks," *Computer Communication*, vol. 34, no. 13, pp. 1645–1659, Aug. 2011.

[66] Y. Jin, W. Wang, Y. Jiang, and M. Yang, "On a joint temporal-spatial multi-channel assignment and routing scheme in resource-constrained wireless mesh networks," *Ad Hoc Networks*, vol. 10, no. 3, pp. 401–420, May 2012.

[67] R. Saket, "Intractability results for problems in computational learning and approximation," Ph.D. dissertation, Atlanta, GA, USA, 2009.

[68] N. Ruangchaijatupon and Y. Ji, "Proportional fairness with minimum rate guarantee scheduling in a multiuser ofdma wireless network," in *Proceedings of the International Conference on Wireless Communications and Mobile Computing: Connecting the World Wirelessly*, 2009, pp. 1102–1106.

[69] S. H. Y. Wong, H. Yang, S. Lu, and V. Bharghavan, "Robust rate adaptation for 802.11 wireless networks," in *Proceedings of the 12th annual international conference on Mobile computing and networking*, 2006, pp. 146–157.

[70] RaLink RT3352 series IEEE 802.11n routers-on-chip. [Online]. Available: http://www.mediatek.com/_en/01_products/04_pro.php?sn=1006

[71] "Qualnet 5.0.1 network simulator." [Online]. Available: http://www.scalable-networks.com/products/qualnet/

[72] J. Garcia-Luna-Aceves, C. L. Fullmer, E. Madruga, D. Beyer, and T. Frivold, "Wireless internet gateways (WINGS)," in *Proceedings of 1997 Military Communications Conference*, vol. 3, 1997, pp. 1271–1276.

[73] B. Schrick and M. J. Riezenman, "Wireless broadband in a box," *IEEE Spectrum*, vol. 39, no. 6, pp. 38–43, 2002.

[74] S. Max, E. Weiss, G. R. Hiertz, and B. Walke, "Capacity bounds of deployment concepts for wireless mesh networks," *Perform. Eval.*, vol. 66, no. 3-5, pp. 272–286, Mar. 2009.

[75] M. Mansoori and M. Mahdavi, "Asymptotic throughput capacity analysis of multi-channel, multi-interface wireless mesh networks," *Wirel. Pers. Commun.*, vol. 68, no. 1, pp. 213–245, Jan. 2013.

[76] A. Behzad and I. Rubin, "On the performance of graph-based scheduling algorithms for packet radio networks," in *in Proceedings of the IEEE Global Telecommunications Conference*, vol. 6, 2003, pp. 3432–3436.

[77] P. Djukic and S. Valaee, "Delay aware link scheduling for multi-hop TDMA wireless networks," *IEEE/ACM Transactions on Networking*, vol. 17, no. 3, pp. 870–883, Jun. 2009.

[78] G. Brar, D. M. Blough, and P. Santi, "Computationally efficient scheduling with the physical interference model for throughput improvement in wireless mesh networks," in *Proceedings of the 12th annual international conference on Mobile computing and networking*, 2006, pp. 2–13.

[79] P. Djukic and S. Valaee, "Distributed link scheduling for TDMA mesh networks," in *Proceedings of the IEEE International Conference on Communications*, 2007, pp. 3823–3828.

[80] K. Papadaki and V. Friderikos, "Approximate dynamic programming for link scheduling in wireless mesh networks," *Comput. Oper. Res.*, vol. 35, no. 12, pp. 3848–3859, Dec. 2008.

[81] H. Yu, P. Mohapatra, and X. Liu, "Channel assignment and link scheduling in multi-radio multi-channel wireless mesh networks," *Mobile Networks and Applications*, vol. 13, no. 1-2, pp. 169–185, Apr. 2008.

[82] N. Kumar, M. Kumar, and R. B. Patel, "Capacity and interference aware link scheduling with channel assignment in wireless mesh networks," *J. Netw. Comput. Appl.*, vol. 34, no. 1, pp. 30–38, Jan. 2011.

[83] P. Cappanera, L. Lenzini, A. Lori, G. Stea, and G. Vaglini, "Optimal link scheduling for real-time traffic in wireless mesh networks in both per-flow and per-path

frameworks," in *Proceedings of the IEEE International Symposium on A World of Wireless, Mobile and Multimedia Networks*, 2010, pp. 1–9.

[84] H. Yu, P. Mohapatra, and X. Liu, "Dynamic channel assignment and link scheduling in multi-radio multi-channel wireless mesh networks," in *Proceedings of the Fourth Annual International Conference on Mobile and Ubiquitous Systems: Networking & Services*, 2007, pp. 1–8.

[85] Y.-C. Lin, S.-W. Hsiao, L.-P. Tung, Y. S. Sun, and M. C. Chen, "A distributed channel access scheduling scheme with clean-air spatial reuse for wireless mesh networks," in *Proceedings of the 7th international IFIP-TC6 networking conference on AdHoc and sensor networks, wireless networks, next generation internet*, 2008, pp. 856–864.

[86] A. A. Kanagasabapathy, A. A. Franklin, and C. S. R. Murthy, "A load aware channel assignment and link scheduling algorithm for multi-channel multi-radio wireless mesh networks," in *Proceedings of the 15th international conference on High performance computing*, 2008, pp. 183–195.

[87] J.-Y. Yoo, C. Sengul, R. Merz, and J. Kim, "Experimental analysis of backpressure scheduling in IEEE 802.11 wireless mesh networks," in *Proceedings of the IEEE International Conference on Communications*, 2011, pp. 1–5.

[88] ——, "Backpressure scheduling in IEEE 802.11 wireless mesh networks: Gap between theory and practice," *Comput. Netw.*, vol. 56, no. 12, pp. 2934–2948, Aug. 2012.

[89] R. R. Choudhury, X. Yang, R. Ramanathan, and N. H. Vaidya, "Using directional antennas for medium access control in ad hoc networks," in *Proceedings of the 8th annual international conference on Mobile computing and networking*, 2002, pp. 59–70.

[90] Z. Zhao and J. Mou, "A new link scheduling algorithm for multi-radio interfaces wireless mesh networks," in *Proceedings of the IEEE International Conference on Computer Science and Automation Engineering*, Jun. 2011, pp. 728–732.

[91] P. Dutta, V. Mhatre, D. Panigrahi, and R. Rastogi, "Joint routing and scheduling in multi-hop wireless networks with directional antennas," in *Proceedings of the IEEE International Conference on Computer Communication*, Mar. 2010, pp. 1–5.

[92] M. Yazdanpanah, C. Assi, and Y. Shayan, "Cross-layer optimization for wireless mesh networks with smart antennas," *Journal of Computer Communications*, 2011.

[93] H. Su and X. Zhang, "Joint link scheduling and routing for directional-antenna based 60 GHz wireless mesh networks," in *Proceedings of the 28th IEEE conference on Global telecommunications*, 2009, pp. 6192–6197.

[94] S. K. Hazra and W. K. G. Seah, "Measurement-based link scheduling for maritime mesh networks with directional antennas," *International Journal on Network Management*, vol. 21, no. 2, pp. 83–105, Mar. 2011.

[95] B. Raman and K. Chebrolu, "Design and evaluation of a new MAC protocol for long-distance 802.11 mesh networks," in *Proceedings of the 11th annual international conference on Mobile computing and networking*, 2005, pp. 156–169.

[96] O. Vendik and D. Kozlov, "Phased antenna array with a sidelobe cancellation for suppression of jamming," *IEEE Antennas and Wireless Propagation Letters*, vol. 11, pp. 648–650, 2012.

[97] C. Chang, C. Chang, and Y. Lu, "Maximizing throughput by exploiting spatial reuse opportunities with smart antenna systems," in *Proceedings of IEEE International Conference on Communications*, 2010.

[98] T. Bonald, L. Massoulié, A. Proutière, and J. Virtamo, "A queueing analysis of max-min fairness, proportional fairness and balanced fairness," *Queueing Syst. Theory Appl.*, vol. 53, no. 1-2, pp. 65–84, Jun. 2006.

[99] Z. Rosberg, J. Matthews, and M. Zukerman, "A network rate management protocol with TCP congestion control and fairness for all," *Comput. Netw.*, vol. 54, no. 9, pp. 1358–1374, Jun. 2010.

[100] X. Wang and K. Kar, "Cross-layer rate optimization for proportional fairness in multihop wireless networks with random access," *IEEE Journal on Selected Areas in communications*, vol. 24, no. 8, pp. 1548–1559, Aug. 2006.

[101] H. Zhou, P. Fan, and J. Li, "Cooperative proportional fairness scheduling for wireless transmissions," in *Proceedings of the International Conference on Wireless Communications and Mobile Computing: Connecting the World Wirelessly*, 2009, pp. 12–16.

[102] J.-Y. Yoo and J. W. Kim, "Centralized flow coordination for proportional fairness in enterprise wireless mesh networks," *SIGMOBILE Mob. Computer Communication Rev.*, vol. 14, no. 3, pp. 52–54, Dec. 2010.

[103] J. F. Lee, W. Liao, and M. C. Chen, "Proportional fairness for QoS enhancement in IEEE 802.11e WLANs," in *Proceedings of the IEEE Conference on Local Computer Networks 30th Anniversary*, 2005, pp. 503–504.

[104] S. Singh, U. Madhow, and E. Belding, "Beyond proportional fairness: A resource biasing framework for shaping throughput profiles in multihop wireless networks," in *Proceedings of the 27th IEEE Conference on Computer Communications*, Apr. 2008, pp. 2396–2404.

[105] K. Jamshaid and P. A. Ward, "Gateway-assisted max-min rate allocation for wireless mesh networks," in *Proceedings of the 12th ACM international conference on Modeling, analysis and simulation of wireless and mobile systems*, 2009, pp. 38–45.

[106] L. Zhang, W. Luo, S. Chen, and Y. Jian, "End-to-end max-min fairness in multihop wireless networks: Theory and protocol," *Journal of Parallel and Distributed Computing*, vol. 72, no. 3, pp. 462–474, Mar. 2012.

[107] D. J. Leith, Q. Cao, and V. G. Subramanian, "Max-min fairness in 802.11 mesh networks," *IEEE/ACM Transactions on Networking*, vol. 20, no. 3, pp. 756–769, Jun. 2012.

[108] E.-C. Park, D.-Y. Kim, C.-H. Choi, and J. So, "Improving quality of service and assuring fairness in WLAN access networks," *IEEE Transactions on Mobile Computing*, vol. 6, no. 4, pp. 337–350, Apr. 2007.

[109] J. Mo and J. Walrand, "Fair end-to-end window-based congestion control," *IEEE/ACM Transactions on Networking*, vol. 8, no. 5, pp. 556–567, Oct. 2000.

[110] S. Singh, U. Madhow, and E. M. Belding, "Shaping throughput profiles in multihop wireless networks: A resource-biasing approach," *IEEE Transactions on Mobile Computing*, vol. 11, no. 3, Mar. 2012.

[111] J. C. Bicket, "Bit-rate selection in wireless networks," Ph.D. dissertation, Massachusetts Institute of Technology, 2005.

[112] J. He, W. Guan, L. Bai, and K. Chen, "Theoretic analysis of IEEE 802.11 rate adaptation algorithm samplerate," *IEEE Communications Letters*, vol. 15, no. 5, pp. 524–526, 2011.

[113] X. Chen, P. Gangwal, and D. Qiao, "RAM: Rate adaptation in mobile environments," *IEEE Transactions on Mobile Computing*, vol. 11, no. 3, pp. 464–477, 2012.

[114] G. Holland, N. Vaidya, and P. Bahl, "A rate-adaptive MAC protocol for multi-hop wireless networks," in *Proceedings of the 7th annual international conference on Mobile computing and networking*, 2001, pp. 236–251.

[115] T. Guo and R. Carrasco, "CRBAR: Cooperative relay-based auto rate MAC for multirate wireless networks," *IEEE Transactions on Wireless Communications*, vol. 8, no. 12, pp. 5938–5947, 2009.

[116] S. Kim, L. Verma, S. Choi, and D. Qiao, "Collision-aware rate adaptation in multi-rate WLANs: Design and implementation," *Computer Networks*, vol. 54, no. 17, pp. 3011–3030, 2010.

[117] L. Zhang, Y.-J. Cheng, and X. Zhou, "Rate avalanche: Effects on the performance of multi-rate 802.11 wireless networks," *Simulation Modelling Practice and Theory*, vol. 17, no. 3, pp. 487–503, 2009.

[118] P. A. K. Acharya, A. Sharma, E. M. Belding, K. C. Almeroth, and K. Papagiannaki, "Rate adaptation in congested wireless networks through real-time measurements," *IEEE Transactions on Mobile Computing*, vol. 9, no. 11, pp. 1535–1550, Nov. 2010.

[119] M. Laddomada, F. Mesiti, M. Mondin, and F. Daneshgaran, "On the throughput performance of multirate IEEE 802.11 networks with variable-loaded stations: analysis, modeling, and a novel proportional fairness criterion," *IEEE Transactions on Wireless Communications*, vol. 9, no. 5, pp. 1594–1607, 2010.

[120] C. Heegard, "Range versus rate in IEEE 802.11g wireless local area networks," in *September meeting IEEE*, vol. 802, 2001.

[121] R. Seide, "Capacity, coverage, and deployment considerations for IEEE 802.11g, white paper," *Cisco Syst., San Jose, CA*, 2003.

[122] S.-T. Sheu, Y. Tsai, and J. Chen, "MR^2RP: the multi-rate and multi-range routing protocol for IEEE 802.11 ad hoc wireless networks," *Wireless Networks*, vol. 9, no. 2, pp. 165–177, Mar. 2003.

[123] Y. Seok, J. Park, and Y. Choi, "Multi-rate aware routing protocol for mobile ad hoc networks," in *Proceedings of the 57th IEEE Semiannual Vehicular Technology Conference*, vol. 3, 2003, pp. 1749–1752.

[124] Z. Li, A. Das, A. K. Gupta, and S. Nandi, "Full auto rate MAC protocol for wireless ad hoc networks," *IEE proceedings-communications*, vol. 152, no. 3, pp. 311–319, 2005.

[125] T. Liu and W. Liao, "Capacity-aware routing in multi-channel multi-rate wireless mesh networks," in *Proceedings of the IEEE International Conference on Communications*, vol. 5, 2006, pp. 1971–1976.

[126] T.-S. Kim, G. Jakllari, S. V. Krishnamurthy, and M. Faloutsos, "An integrated routing and rate adaptation framework for multi-rate multi-hop wireless networks," *Wireless Networks*, pp. 1–19, 2012.

[127] B. Sadeghi, V. Kanodia, A. Sabharwal, and E. Knightly, "OAR: an opportunistic auto-rate media access protocol for ad hoc networks," *Wireless Networks*, vol. 11, no. 1-2, pp. 39–53, Jan. 2005.

[128] J. Luo, C. Rosenberg, and A. Girard, "Engineering wireless mesh networks: joint scheduling, routing, power control, and rate adaptation," *IEEE/ACM Transactions on Networking,*, vol. 18, no. 5, pp. 1387–1400, 2010.

[129] S.-C. Wang and A. Helmy, "BEWARE: background traffic-aware rate adaptation for IEEE 802.11," *IEEE/ACM Transactions on Networking*, vol. 19, no. 4, Aug. 2011.

[130] P. A. K. Acharya, A. Sharma, E. M. Belding, K. C. Almeroth, and K. Papagiannaki, "Congestion-aware rate adaptation in wireless networks: A measurement-driven approach," in *Proceedings of 5th Annual IEEE Communications Society Conference on Sensor, Mesh and Ad Hoc Communications and Networks*, 2008, pp. 1–9.

[131] M. Vutukuru, H. Balakrishnan, and K. Jamieson, "Cross-layer wireless bit rate adaptation," *SIGCOMM Computer Communication Rev.*, vol. 39, no. 4, pp. 3–14, Aug. 2009.

[132] T.-Y. Lin and J. C. Hou, "Interplay of spatial reuse and SINR-determined data rates in CSMA/CA-based, multi-hop, multi-rate wireless networks," in *Proceedings of 26th IEEE International Conference on Computer Communications*, 2007, pp. 803–811.

[133] A. A. Kulkarni, S. Menezes, and R. Prakash, "FREEZE: Rate adaptation in wireless LANs using channel contention estimates," in *Proceedings of Third International Conference on Communication Systems and Networks*, 2011, pp. 1–6.

[134] P. R. Jelenković, P. Momčilović, and M. S. Squillante, "Scalability of wireless networks," *IEEE/ACM Transactions on Networking*, vol. 15, no. 2, pp. 295–308, Apr. 2007.

[135] D. Passos and C. V. N. Albuquerque, "A joint approach to routing metric and rate adaptation in wireless mesh networks," *IEEE/ACM Transactions on Networking*, vol. 20, no. 4, pp. 999–1009, Aug. 2012.

[136] M. S. Thompson, A. B. MacKenzie, and L. A. DaSilva, "A method of proactive MANET routing protocol evaluation applied to the OLSR protocol," in *Proceedings of the 6th ACM international workshop on Wireless network testbeds, experimental evaluation and characterization*, 2011, pp. 27–34.

[137] I. Gawedzki and K. Al Agha, "How to avoid packet droppers with proactive routing protocols for ad hoc networks," *International Journal on Network Management*, vol. 18, no. 2, pp. 195–208, Mar. 2008.

[138] T. Mukherjee, S. K. S. Gupta, and G. Varsamopoulos, "Analytical model for optimizing periodic route maintenance in proactive routing for manets," in *Proceedings of the 10th ACM Symposium on Modeling, analysis, and simulation of wireless and mobile systems*, 2007, pp. 201–208.

[139] R. Hou, K.-S. Lui, H.-S. Chiu, K. L. Yeung, and F. Baker, "Routing in multi-hop wireless mesh networks with bandwidth guarantees," in *Proceedings of the tenth ACM international symposium on Mobile ad hoc networking and computing*, 2009, pp. 353–354.

[140] A. O. Lim, Y. Kado, B. Zhang, and X. Wang, "A study of root driven routing protocol for wireless LAN mesh networks," in *Proceedings of the 3rd international conference on Wireless internet*, 2007, pp. 3:1–3:10.

[141] C. Sengul, A. C. Viana, and A. Ziviani, "A survey of adaptive services to cope with dynamics in wireless self-organizing networks," *ACM Computing Survey*, vol. 44, no. 4, pp. 23:1–23:35, Sep. 2012.

[142] M. Abolhasan and J. Lipman, "Self-selection route discovery strategies for reactive routing in ad hoc networks," in *Proceedings of the first international conference on Integrated internet ad hoc and sensor networks*, 2006.

[143] N. Zhou, H. Wu, and A. A. Abouzeid, "Reactive routing overhead in networks with unreliable nodes," in *Proceedings of the 9th annual international conference on Mobile computing and networking*, 2003, pp. 147–160.

[144] P. Samar, M. R. Pearlman, and Z. J. Haas, "Independent zone routing: an adaptive hybrid routing framework for ad hoc wireless networks," *IEEE/ACM Transactions Networking*, vol. 12, no. 4, pp. 595–608, Aug. 2004.

[145] V. Ramasubramanian, Z. J. Haas, and E. G. Sirer, "SHARP: a hybrid adaptive routing protocol for mobile ad hoc networks," in *Proceedings of the 4th ACM international symposium on Mobile ad hoc networking & computing*, 2003, pp. 303–314.

[146] S. Mir, A. A. Pirzada, and M. Portmann, "HOVER: hybrid on-demand distance vector routing for wireless mesh networks," in *Proceedings of the thirty-first Australasian conference on Computer science*, 2008, pp. 63–71.

[147] A. Boukerche and Z. Zhang, "A hybrid-routing based intra-domain mobility management scheme for wireless mesh networks," in *Proceedings of the 11th international symposium on Modeling, analysis and simulation of wireless and mobile systems*, 2008, pp. 268–275.

[148] S. Roy and J. J. Garcia-Luna-Aceves, "Node-centric hybrid routing for ad hoc networks," in *Proceedings of the International Workshop on Mobility and Wireless Access*, 2002.

[149] R. Draves, J. Padhye, and B. Zill, "Routing in multi-radio, multi-hop wireless mesh networks," in *Proceedings of the 10th ACM Annual International Conference on Mobile Computing and Networking*, 2004, pp. 114–128.

[150] C. E. Koksal and H. Balakrishnan, "Quality-aware routing metrics for time-varying wireless mesh networks," *IEEE Journal on Selected Areas in Communications*, vol. 24, no. 11, pp. 1984–1994, 2006.

[151] S. Waharte, R. Boutaba, Y. Iraqi, and B. Ishibashi, "Routing protocols in wireless mesh networks: challenges and design considerations," *Multimedia Tools and Applications*, vol. 29, no. 3, pp. 285–303, 2006.

[152] A. Khatkar and Y. Singh, "Performance evaluation of hybrid routing protocols in mobile ad hoc networks," in *in Proceedings of Second International Conference on Advanced Computing & Communication Technologies*, 2012, pp. 542–545.

[153] M. E. M. Campista, P. M. Esposito, I. M. Moraes, L. Costa, O. Duarte, D. G. Passos, C. V. N. de Albuquerque, D. C. M. Saade, and M. G. Rubinstein, "Routing metrics and protocols for wireless mesh networks," *IEEE Network*, vol. 22, no. 1, pp. 6–12, 2008.

[154] V. Mhatre, H. Lundgren, F. Baccelli, and C. Diot, "Joint MAC-aware routing and load balancing in mesh networks," in *Proceedings of the ACM International Conference on Emerging Networking Experiments and Technologies*, 2007, pp. 19:1–19:12.

[155] P. Wang and S. Bohacek, "An overview of tractable computation of optimal scheduling and routing in mesh networks," *SIGMETRICS Performance Evaluation Review*, vol. 35, no. 2, pp. 18–20, Sep. 2007.

[156] R. Bruno, M. Conti, and A. Pinizzotto, "Capacity-aware routing in heterogeneous mesh networks: an analytical approach," in *Proceedings of the 12th ACM international conference on Modeling, analysis and simulation of wireless and mobile systems*, 2009, pp. 73–81.

[157] A. Dhananjay, H. Zhang, J. Li, and L. Subramanian, "Practical, distributed channel assignment and routing in dual-radio mesh networks," *SIGCOMM Computer Communication Rev.*, vol. 39, no. 4, pp. 99–110, Aug. 2009.

[158] J. Tang, G. Xue, and W. Zhang, "Interference-aware topology control and QoS routing in multi-channel wireless mesh networks," in *Proceedings of the 6th ACM international symposium on Mobile ad hoc networking and computing*, 2005, pp. 68–77.

[159] F. Kandah, W. Zhang, C. Wang, and J. Li, "Diverse path routing with interference and reusability consideration in wireless mesh networks," *Mobile Networks and Applications*, vol. 17, no. 1, pp. 100–109, Feb. 2012.

[160] D. Passos and C. V. N. Albuquerque, "A joint approach to routing metrics and rate adaptation in wireless mesh networks," *IEEE/ACM Transactions on Networking*, vol. 20, no. 4, pp. 999–1009, Aug. 2012.

[161] N. Ghazisaidi, C. M. Assi, and M. Maier, "Intelligent wireless mesh path selection algorithm using fuzzy decision making," *Wireless Networks*, vol. 18, no. 2, pp. 129–146, Feb. 2012.

[162] E. Rozner, J. Seshadri, Y. Mehta, and L. Qiu, "SOAR: Simple opportunistic adaptive routing protocol for wireless mesh networks," *IEEE Transactions on Mobile Computing*, vol. 8, no. 12, pp. 1622–1635, 2009.

[163] M. Afanasyev and A. C. Snoeren, "The importance of being overheard: throughput gains in wireless mesh networks," in *Proceedings of the 9th ACM SIGCOMM conference on Internet measurement conference*, 2009, pp. 384–396.

[164] L. Paquereau and B. E. Helvik, "Opportunistic ant-based path management for wireless mesh networks," in *Proceedings of the 7th international conference on Swarm intelligence*, 2010, pp. 480–487.

[165] U. Sadiq, M. Kumar, and M. Wright, "CRISP: collusion-resistant incentive-compatible routing and forwarding in opportunistic networks," in *Proceedings of the 15th ACM international conference on Modeling, analysis and simulation of wireless and mobile systems*, 2012, pp. 69–78.

[166] A. Bezzina, M. Ayari, R. Langar, and F. Kamoun, "An interference-aware routing metric for multi-radio multi-channel wireless mesh networks," in *Proceedings of the 2012 IEEE 8th International Conference on Wireless and Mobile Computing, Networking and Communications*, 2012, pp. 284–291.

[167] B. Qi, F. Shen, and S. Raza, "iBATD: A new routing metric for multi-radio wireless mesh networks," in *Proceedings of the 9th International Conference on Information Technology*, 2012.

[168] C. Perkins, E. Belding-Royer, and S. Das, "RFC 3561-ad hoc on-demand distance vector (AODV) routing," *Internet RFCs*, pp. 1–38, 2003.

[169] R. G. Garroppo, S. Giordano, and L. Tavanti, "Implementation frameworks for IEEE 802.11s systems," *Computer Communication*, vol. 33, no. 3, pp. 336–349, Feb. 2010.

[170] C. T. de Oliveira, F. Theoleyre, and A. Duda, "Channel assignment strategies for optimal network capacity of IEEE 802.11s," in *Proceedings of the 9th ACM symposium on Performance evaluation of wireless ad hoc, sensor, and ubiquitous networks*, 2012, pp. 53–60.

[171] D. Fu, B. Staehle, R. Pries, and D. Staehle, "On the potential of IEEE 802.11s intra-mesh congestion control," in *Proceedings of the 13th ACM international conference on Modeling, analysis, and simulation of wireless and mobile systems*, 2010, pp. 299–306.

[172] B.-G. Choi, M. Kim, M. Y. Chung, and J. Y. Lee, "Adaptive hybrid medium access control scheme for traffic concentration problem in the mesh portal of IEEE 802.11s-based wireless mesh networks," in *Proceedings of the 5th International Conference on Ubiquitous Information Management and Communication*, pp. 63:1–63:8.

[173] A. Krasilov, A. Lyakhov, and A. Safonov, "Interference, even with MCCA channel access method in IEEE 802.11s mesh networks," in *Proceedings of the 2011 IEEE Eighth International Conference on Mobile Ad-Hoc and Sensor Systems*, 2011, pp. 752–757.

[174] M. I. Rafique, M. Porsch, and T. Bauschert, "Simple modifications in HWMP for wireless mesh networks with smart antennas," in *Proceedings of the 17th international conference on Energy-aware communications*, 2011, pp. 21–30.

[175] E. Khorov, A. Lyakhov, and A. Safonov, "Flexibility of routing framework architecture in IEEE 802.11s mesh networks," in *Proceedings of the 2011 IEEE Eighth International Conference on Mobile Ad-Hoc and Sensor Systems*, 2011, pp. 777–782.

[176] M. Bahr, "Proposed routing for IEEE 802.11s WLAN mesh networks," in *Proceedings of the 2nd International Wireless Internet Conference*, 2006.

[177] M. Pinheiro, S. Sampaio, F. Vasques, and P. Souto, "A DHT-based approach for path selection and message forwarding in IEEE 802.11s industrial wireless mesh networks," in *Proceedings of the 14th IEEE International Conference on Emerging Technologies and Factory Automation*, 2009, pp. 1021–1030.

[178] L. Yang and S.-H. Chung, "HWMP+: An improved traffic load sheme for wireless mesh networks," in *Proceedings of the 14th IEEE International Conference on High Performance Computing and Communications*, 2012, pp. 722–727.

[179] M. Abid and S. Biaz, "Airtime pingpong effect characterization in IEEE 802.11s wireless mesh networks," *Computing*, pp. 1–25, 2013.

[180] W. J. Jung, S. H. Min, B. G. Kim, H. S. Choi, J. Y. Lee, and B. C. Kim, "R-HWMP: Reservation-based HWMP supporting end-to-end qos in wireless mesh networks," in *Proceedings of the International Conference on Information Networking*, Jan 2013, pp. 385–390.

[181] J. C. Liberti and T. S. Rappaport, *Smart Antennas for Wireless Communications: IS-95 and Third Generation CDMA Applications*. Upper Saddle River, NJ, USA: Prentice Hall PTR, 1999.

[182] V. A. Siris and M. Delakis, "Interference-aware channel assignment in a metropolitan multi-radio wireless mesh network with directional antennas," *Computer Communication*, vol. 34, no. 12, pp. 1518–1528, Aug. 2011.

[183] W. Sun, T. Fu, F. Xia, Z. Qin, and R. Cong, "A dynamic channel assignment strategy based on cross-layer design for wireless mesh networks," *International Journal on Communication System*, vol. 25, no. 9, pp. 1122–1138, Sep. 2012.

[184] A. P. Subramanian, H. Gupta, S. R. Das, and J. Cao, "Minimum interference channel assignment in multiradio wireless mesh networks," *IEEE Transactions on Mobile Computing*, vol. 7, no. 12, pp. 1459–1473, Dec. 2008.

[185] L. Narayanan and Y. Tang, "Worst-case analysis of a dynamic channel assignment strategy," *Discrete Appl. Math.*, vol. 140, no. 1-3, pp. 115–141, May 2004.

[186] P. Gupta and P. Kumar, "The capacity of wireless networks," *IEEE Transactions on Information Theory*, vol. 46, no. 2, pp. 388–404, 2000.

[187] Y. Shi, Y. T. Hou, J. Liu, and S. Kompella, "How to correctly use the protocol interference model for multi-hop wireless networks," in *Proceedings of the tenth ACM international symposium on Mobile ad hoc networking and computing*, 2009, pp. 239–248.

[188] S. Leng, W. Ser, and C. C. Ko, "Adaptive beamformer derived from a constrained null steering design," *Signal Process.*, vol. 90, no. 5, pp. 1530–1541, May 2010.

[189] J. Lee, W. Kim, S.-J. Lee, D. Jo, J. Ryu, T. Kwon, and Y. Choi, "An experimental study on the capture effect in 802.11a networks," in *Proceedings of the second ACM*

international workshop on Wireless network testbeds, experimental evaluation and characterization, 2007, pp. 19–26.

[190] H. Zhao, E. Garcia-Palacios, S. Wang, J. Wei, and D. Ma, "Evaluating the impact of network density, hidden nodes and capture effect for throughput guarantee in multi-hop wireless networks," *Ad Hoc Networks*, vol. 11, no. 1, pp. 54–69, Jan. 2013.

[191] X. Che, X. Liu, X. Ju, and H. Zhang, "Adaptive instantiation of the protocol interference model in mission-critical wireless networks," in *Proceedings of the 7th Annual IEEE Communications Society Conference on Sensor Mesh and Ad Hoc Communications and Networks*, Jun. 2010.

[192] V. Kapnadak, M. Senel, and E. J. Coyle, "Distributed iterative quantization for interference characterization in wireless networks," *Digit. Signal Process.*, vol. 22, no. 1, pp. 96–105, Jan. 2012.

[193] A. Ghiasian, H. Saidi, and B. Omoomi, "Application of line graph for link scheduling in wireless networks under M-hop interference model," in *Proceedings of the Third International Conference on Advances in Mesh Networks*, pp. 69–74.

[194] E. Karamad, R. Adve, and J. Chow, "Power control and interference management in dense wireless networks," *CoRR*, 2012.

[195] H. K. Khalil, "Nonlinear systems," *Prentice-Hall,Upper Saddle River,NJ*, 1996.

[196] A. Nedic and A. Ozdaglar, "On the rate of convergence of distributed subgradient methods for multi-agent optimization," in *Proceedings of 46th IEEE Conference on Decision and Control*, Dec. 2007, pp. 4711–4716.

[197] R. Jain, D. M. Chiu, and W. Hawe, "A quantitative measure of fairness and discrimination for resource allocation in shared computer systems," Digital Equipment Corporation, DEC-TR-301, Tech. Rep., Sep. 1984.

[198] Z. Hu and P. Verma, "Gateway placement in backbone wireless mesh networks using directional antennas," in *Proceedings of the 2011 Ninth Annual Communication Networks and Services Research Conference*, 2011, pp. 175–180.

[199] M. B. Pursley and T. C. R. IV, "Properties and performance of the IEEE 802.11b complementary-code-key signal sets," *IEEE Transactions on Communications*, vol. 57, no. 2, pp. 440–449, 2009.

[200] X. G. Meng, S. H. Y. Wong, Y. Yuan, and S. Lu, "Characterizing flows in large wireless data networks," in *Proceedings of the 10th annual international conference on Mobile computing and networking*, 2004, pp. 174–186.

[201] S. Prasanthi, S.-H. Chung, and W.-S. Kim, "An enhanced TCP scheme for distinguishing non-congestion losses from packet reordering over wireless mesh networks," in *Proceedings of the 2011 IEEE International Conference on High Performance Computing and Communications*, 2011, pp. 440–447.

[202] A. L. Ruscelli, G. Cecchetti, A. Alifano, and G. Lipari, "Enhancement of QoS support of HCCA schedulers using EDCA function in IEEE 802.11e networks," *Ad Hoc Networks*, vol. 10, no. 2, pp. 147–161, Mar. 2012.

[203] L. Lenzini, E. Mingozzi, and C. Vallati, "A distributed delay-balancing slot allocation algorithm for 802.11s mesh coordinated channel access under dynamic traffic conditions," in *Proceedings of IEEE 7th International Conference on Mobile Adhoc and Sensor Systems*, 2010, pp. 432–441.

[204] M. S. Bazaraa, H. D. Sherali, and C. M. Shetty, *Nonlinear Programming: Theory and Algorithms*. New York:Wiley, 1993.

[205] D. Yuan, S. Xu, and H. Zhao, "Distributed primal-dual subgradient method for multiagent optimization via consensus algorithms," *IEEE Transactions on Systems Man and Cybernatics*, vol. 41, no. 6, pp. 1715–1724, Dec. 2011.

[206] A. Nedic and A. Ozdaglar, "Distributed subgradient methods for multi-agent optimization," *IEEE Transactions on Automatic Control*, vol. 54, no. 1, pp. 48–61, Jan. 2009.

[207] B. He, B. Xie, and D. P. Agrawal, "Optimizing deployment of Internet gateway in wireless mesh networks," *Computer Communication*, vol. 31, no. 7, pp. 1259–1275, May 2008.

[208] Cisco Aironet 1500 Series Wireless Mesh AP Version 5.0 Design Guide. [Online]. Available: http://www.cisco.com/en/US/docs/wireless/technology/mesh/design/guide/MeshAP.html

[209] G. Bolch, S. Greiner, H. d. Meer, and K. S. Trivedi, *Queueing Networks and Markov Chains*. Wiley-Interscience, Chapter 5, pp. 423-430, 2005.

[210] C. Joo and N. B. Shroff, "Performance of random access scheduling schemes in multi-hop wireless networks," *IEEE/ACM Transactions on Networking*, vol. 17, no. 5, pp. 1481–1493, 2009.

[211] "Multiband Atheros Driver for WiFi (MadWiFi) user documention: RSSI in MadWiFi." [Online]. Available: http://madwifi-project.org/wiki/UserDocs/RSSI

[212] P. Assouad, "Plongements lipschitziens dans $\mathbb{R}^n$," *Bulletin de la Société Mathématique de France*, vol. 111, pp. 429–448, 1983.

[213] N. Bisnik and A. Abouzeid, "Delay and throughput in random access wireless mesh networks," in *Proceedings of the IEEE International Conference on Communications*, Jun. 2006, pp. 403–408.

[214] A. Iyer, C. Rosenberg, and A. Karnik, "What is the right model for wireless channel interference?" *IEEE Transactions on Wireless Communications*, vol. 8, no. 5, pp. 2662–2671, 2009.

[215] M. Kodialam and T. Nandagopal, "Characterizing the capacity region in multi-radio multi-channel wireless mesh networks," in *Proceedings of the 11th ACM Annual International Conference on Mobile Computing and Networking*, 2005, pp. 73–87.

[216] C. Ware, J. Chicharo, and T. Wysocki, "Simulation of capture behaviour in IEEE 802.11 radio modems," in *Proceedings of the IEEE VTS 54th Vehicular Technology Conference*, vol. 3, 2001, pp. 1393–1397.

[217] J. Lee, J. Ryu, S.-J. Lee, and T. T. Kwon, "Improved modeling of IEEE 802.11 a PHY through fine-grained measurements," *Computer Networks*, vol. 54, no. 4, pp. 641–657, 2010.

[218] S. Kravitz, "Packing cylinders into cylindrical containers," *Mathematics Magazine*, vol. 40, no. 2, pp. 65–71, Mar. 1967.

[219] C. H. Papadimitriou, "On the complexity of integer programming," *Journal of ACM*, vol. 28, no. 4, pp. 765–768, Oct. 1981.

[220] J. a. L. Sobrinho, "Algebra and algorithms for QoS path computation and hop-by-hop routing in the Internet," *IEEE/ACM Transactions on Networking*, vol. 10, no. 4, pp. 541–550, Aug. 2002.

[221] ——, "Network routing with path vector protocols: theory and applications," in *Proceedings of the 2003 conference on Applications, technologies, architectures, and protocols for computer communications*, 2003, pp. 49–60.

[222] J.-E. Berg, R. Bownds, and F. Lotse, "Path loss and fading models for microcells at 900 mhz," in *Proceedings of the IEEE 42nd Vehicular Technology Conference*, 1992, pp. 666–671.

[223] B. Henderson, "Linux loadable kernel module HOWTO," *The Linux Docu*, 2001.

[224] I. Pefkianakis, Y. Hu, S. H. Wong, H. Yang, and S. Lu, "MIMO rate adaptation in 802.11n wireless networks," in *Proceedings of the Sixteenth Annual International Conference on Mobile Computing and Networking*, 2010, pp. 257–268.

Publications Related to Thesis

Published/Accepted:

Journals

1. **Sandip Chakraborty**, Pravati Swain, Sukumar Nandi, "Proportional Fairness in MAC Layer Channel Access of IEEE 802.11s EDCA based Wireless Mesh Networks", Ad Hoc Networks, Elsevier, Volume 11, Issue 1, January 2013, Pages 570-584

2. **Sandip Chakraborty**, Sukumar Nandi, "IEEE 802.11s Mesh Backbone for Vehicular Communication: Fairness and Throughput", IEEE Transactions on Vehicular Technology, Volume 62, Issue 5, June 2013, Pages 2193-2203

3. **Sandip Chakraborty**, Sukumar Nandi, "Selective Greedy Routing: Exploring the Path Diversity in Backbone Mesh Networks", ACM/Springer Journal of Wireless Networks (In Press)

4. **Sandip Chakraborty**, Sidharth Sharma, Sukumar Nandi, "MAC Layer Channel Access and Forwarding in a Directional Multi-Interface Mesh Network", IEEE Transactions on Mobile Computing (Minor Revision)

Conference Proceedings

1. **Sandip Chakraborty**, Sidharth Sharma, Sukumar Nandi, "Performance Optimization in Single Channel Directional Multi-Interface IEEE 802.11s EDCA using Beam Prioritization", in the proc. of the IEEE International Conference on Communications (IEEE ICC 2012), June 10-15, 2012, Ottawa, Canada

2. **Sandip Chakraborty**, Sukumar Nandi, "A HiperLAN/2 based MAC Protocol for Efficient Vehicle-to-Infrastructure Communication using Directional Wireless Mesh Backbone", in the proc. of the 11th IEEE International Conference on Ubiquitous

Computing and Communications (IEEE IUCC 2012), 25-27 June 2012, Liverpool, UK

3. **Sandip Chakraborty**, Sukumar Nandi, "Achieving Fairness for Multi-Class Traffic in Directional Multi-Interface IEEE 802.11s MCCA", in the proc. of the 18th IEEE International Conference on Networks (IEEE ICON 2012), 12-14 December 2012, Singapore

4. **Sandip Chakraborty**, Suchetana Chakraborty, Sukumar Nandi, "Beyond Conventional Routing Protocols: Opportunistic Path Selection for IEEE 802.11s Mesh Networks", in the proc. of the 24th IEEE International Symposium on Personal, Indoor and Mobile Radio Communications (IEEE PIMRC 2013), 08-11 September 2013, London, UK

5. **Sandip Chakraborty**, Sukumar Nandi, "Surpassing Flow Fairness in Mesh Network: How to Ensure Equity among End Users?", in proc. of the IEEE International Conference on Advanced Networks and Telecommunications Systems (IEEE ANTS 2013), 15-18 December 2013, Chennai, India (**Best Paper Award**)

6. **Sandip Chakraborty**, Subhrendu Chattopadhyay, Suchetana Chakraborty, Sukumar Nandi, "Defending Concealedness in IEEE 802.11n", in proc. of the Sixth International Conference on Communication Systems and Networks (COMSNETS 2014), 07-09 January, 2014, Bangalore, India

7. **Sandip Chakraborty**, Sukumar Nandi, "Evaluating the Effect of Path Diversity over QoS and QoE in a High Speed Indoor Mesh Backbone" in proc. of the Sixth International Conference on Communication Systems and Networks (COMSNETS 2014), 07-09 January, 2014, Bangalore, India

Communicated:

Journals

1. **Sandip Chakraborty**, Sukumar Nandi, "IEEE 802.11s MCCA: Distributed Service Level Flow Control and Fairness", IEEE Transactions on Mobile Computing

2. **Sandip Chakraborty**, Sukumar Nandi, "Rate Adaptation in IEEE 802.11s Mesh Networks: Path Length vs Network Contention", Ad Hoc Networks, Elsevier

Brief Biography of the Author

Sandip Chakraborty was born in Kolkata, West Bengal, India on 22nd January, 1987. After completing his schooling in Kolkata, he has completed the B.Eng. degree from the *Department of Information Technology, Jadavpur University*, Kolkata, India in the year 2009. He has received *University Gold Medal* for securing first position in the B.Eng (Information Technology) and the *Arun Kumar Bandyopadhyay Memorial Bronze Medal*, awarded by Jadavpur University, for securing the second highest aggregate of marks among all the courses of B.Eng examination. He has also received *TATA Consultancy Services Best Student Project Award* for his Bachelor's project. He completed his M.Tech. degree from the *Department of Computer Science and Engineering, Indian Institute of Technology Guwahati*, India in 2011, where he has continued working toward the PhD degree under the supervision of Prof. Sukumar Nandi. He has been awarded *'Best Graduate Student Award'* by TATA Consultancy Services, India for his academic performance in M. Tech programme. He has received *TCS Research Fellowship* from TATA Consultancy Services, India for pursuing his PhD programme. Based on his research outcome, he has been awarded *National Internet Exchange of India* (NIXI) Fellowship for the year 2013-2014. His research interests include wireless ad hoc and mesh networks, wireless sensor networks, distributed algorithms, performance modeling of communication Systems, etc. He has also worked in other fields, such as fault-tolerance computing, network security, mobile middleware etc., in cooperation with other research groups at IIT Guwahati.

Other Publications of the Author

Book Chapters

1. Suchetana Chakraborty, **Sandip Chakraborty**, Sukumar Nandi, Sushanta Karmakar, "Sensory Data Gathering for Road-Traffic Monitoring: Energy Efficiency, Reliability and Fault-tolerance" in Springer Series: Modelling and OptimiSation in Science and Technology, Title: Modelling and Processing for Next Generation Big Data Technologies and Applications

Journals

1. Suchetana Chakraborty, **Sandip Chakraborty**, Sukumar Nandi, Sushanta Karmakar, "Reliability in delay sensitive sensor networks with arbitrary node failures: Deployment and topology management", International Journal of Wireless Information Networks, Springer (Accepted)

2. Suchetana Chakraborty, **Sandip Chakraborty**, Sukumar Nandi, Sushanta Karmakar, "ADCROSS: Adaptive Data Collection from Road Surveilling Sensors", IEEE Transactions on Intelligent Transportation Systems (In Press)

3. Abhijit Sarma, **Sandip Chakraborty**, Sukumar Nandi, Anchal Choubey, "Context Aware Inter-BSS Handoff in IEEE 802.11 Networks: Efficient Resource Utilization and Performance Improvement", Wireless Personal Communications, Springer (In Press)

4. Aditya Yadav, Maushumi Barooah, **Sandip Chakraborty**, Sukumar Nandi, "Vertical Handover over Intermediate Switching Framework: Assuring Service Quality for Mobile Users", Wireless Personal Communications, Springer (In Press)

5. Subhrangsu Mandal, **Sandip Chakraborty**, Sushanta Karmakar, "Distributed Deterministic 1-2 Skip List for Peer-to-Peer System", Springer Journal of Peer-to-Peer Networking and Applications (In Press)

6. Suchetana Chakraborty, **Sandip Chakraborty**, Sushanta Karmakar, Sukumar Nandi, "Dynamic Tree Switching for Distributed Message-Passing Applications", Journal of Network and System Management, Springer (In Press)

7. Ramesh Singh, **Sandip Chakraborty**, Sushanta Karmakar, "Concurrent Deterministic 1-2 Skip List in Distributed Message Passing Systems", International Journal of Parallel, Emergent and Distributed Systems, Taylors and Francis (In Press)

8. Aditya Yadav, Maushumi Barooah, **Sandip Chakraborty**, Sukumar Nandi, Sanjay Ahuja, "Evaluation of the End-to-End TCP Performance for Vertical Handover using Intermediate Switching Network", International Journal of Communication Networks and Distributed System, Inderscience, Volume 12, Issue 3, April 2014, Pages 327-351

9. Suchetana Chakraborty, **Sandip Chakraborty**, Sukumar Nandi, Sushanta Karmakar, "Convergecast Tree Management from Arbitrary Node Failure in Sensor Network", Ad Hoc Networks, Elsevier, Volume 11, Issue 6, August 2013, Pages 1796-1819

10. Maushumi Barooah, **Sandip Chakraborty**, Sukumar nandi and Dhananjay U. Kotwal, "An Architectural Framework for Seamless Handoff between IEEE 802.11 and UMTS Network" Springer/ACM Journal of Wireless Networks, Volume 19, Issue 4, March 2013, Pages 411-429

11. Ishita Bhakta, **Sandip Chakraborty**, Barsha Mitra, Debarshi Kumar Sanyal, Samiran Chattopadhyay and Matangini Chattopadhyay "A DiffServ Architecture for QoS Aware Routing for Delay Sensitive and Best Effort Services in IEEE 802.16 Mesh Networks", Volume 2011 (2011), Article ID 951310, Journal of Computer Networks and Communications, Hindwai Publishing Corporation

Conference Proceedings

1. **Sandip Chakraborty**, Suchetana Chakraborty, Sushanta Karmakar and Hridoy Dutta, "Hierarchical Topology Adaptation for Distributed Convergecast Applications", in proc. of the 29th ACM Symposium On Applied Computing, Dependable

and Adaptive Distributed Systems Track (ACM SAC - DADS), Gyeongju, Korea, March 24 - 28, 2014

2. Suchetana Chakraborty, **Sandip Chakraborty**, Sukumar Nandi, Sushanta Karmakar, "RelBAS:Reliable Data Gathering from Border Area Sensors", in the proc. of the 18th IEEE Computer Society International Symposium on Computers and Communications (IEEE ISCC 2013), Split, Croatia, July 7-10, 2013

3. Suchetana Chakraborty, **Sandip Chakraborty**, Sukumar Nandi, Sushanta Karmakar, "Exploring Gradient in Sensor Deployment Pattern for Data Gathering with Sleep based Energy Saving", in the proc. of the IEEE 9th International Wireless Communication and Mobile Computing Conference (IEEE IWCMC 2013), Sardinia, Italy, July 1-5, 2013

4. Suchetana Chakraborty, **Sandip Chakraborty**, Sukumar Nandi, Sushanta Karmakar, "Energy-efficient Data Gathering for Road-side Sensor Networks ensuring Reliability and Fault-tolerance", in the proc. of the 27th IEEE International Conference on Advanced Information Networking and Applications (IEEE AINA-2013), Barcelona, Spain, March 25-28, 2013

5. Vikas Kumar, **Sandip Chakraborty**, Ferdous A Barbhuiya, Sukumar Nandi, "Detection of Stealth Man-In-The-Middle Attack in Wireless LAN", in the proc. of the 2nd IEEE International Conference on Parallel, Distributed and Grid Computing (PDGC 2012), 06-08 December 2012, India

6. Subhrangsu Mandal, **Sandip Chakraborty**, Sushanta Karmakar, "Deterministic 1-2 Skip List in Distributed System", in the proc. of the 2nd IEEE International Conference on Parallel, Distributed and Grid Computing (PDGC 2012), 06-08 December 2012, India **(Second Best Paper Award)**

7. Suchetana Chakraborty, **Sandip Chakraborty**, Sukumar Nandi and Sushanta Karmakar, "A Novel Crash-Tolerant Data Gathering in Wireless Sensor Networks" 13th IEEE/IFIP Network Operations and Management Symposium (IEEE NOMS 2012), April 16-20, 2012

8. Pravati Swain, **Sandip Chakraborty**, Sukumar Nandi and Purandar Bhaduri,"Performance Analysis of IEEE 802.11 IBSS Power Save Mode using Discrete-Time Markov chain", in the proc. of the 27th ACM Symposium On Applied Computing (ACM SAC 2012), Italy, March 2012

9. **Sandip Chakraborty** and Sukumar Nandi, "MAC Layer Fairness in IEEE 802.11 DCF Based Wireless Mesh Network", in the proc. of the International Conference on Computing, Networking and Communications (IEEE ICNC 2012), February 2012, Maui, Hawaii, USA

10. Maushumi Barooah, Sanjay Ahuja, **Sandip Chakraborty**, Sukumar Nandi "TCP Performance for WLAN-GPRS Handover in an Intermediate Switching Network based Framework", 5th IEEE International Conference on Advanced Networks and Telecommunication Systems (IEEE ANTS 2011), Bangalore, India, December 18-21, 2011

11. Prithu Banerjee, Mahasweta Mitra, Ferdous A. Barbhuiya, **Sandip Chakraborty** and Sukumar Nandi, "An Efficient Decentralized Rekeying Scheme to Secure Hierarchical Geographic Multicast Routing in Wireless Sensor Networks", in the proc. of the Seventh International Conference on Information Systems Security (ICISS 2011),(Springer LNCS Volume 7093/2011, 294-308)

12. **Sandip Chakraborty** and Sukumar Nandi, "Achieving MAC Layer Fairness in Wireless Mesh Backbone based Vehicular Network", in the proc. of the 2nd International Conference on Computer and Communication Technology (ICCCT 2011) September 15-17, 2011

13. Suchetana Chakraborty, **Sandip Chakraborty**, Sukumar Nandi and Sushanta Karmakar, "A Reliable and Total Order Tree Based Broadcast in Wireless Sensor Network", in the proc. of the 2nd International Conference on Computer and Communication Technology (ICCCT 2011) September 15-17, 2011

14. Suchetana Chakraborty, **Sandip Chakraborty**, Sukumar Nandi and Sushanta Karmakar, "A Tree-Based Local Repairing Approach for Increasing Lifetime of Query Driven WSN", in the proc. of the 2011 International Symposium on Pervasive Systems, Algorithms and Networks (IEEE I-SPAN 2011) August 24-26, 2011

15. Pravati Swain, **Sandip Chakraborty**, Sukumar Nandi and Purandar Bhaduri, "Throughput Analysis of the IEEE 802.11 Power Save Mode in Single Hop Ad hoc Networks", in the proc. of the 2011 International Conference on Wireless Networks (ICWN'11), July 18-21, 2011, USA

16. Ishita Bhakta, **Sandip Chakraborty**, Barsha Mitra, Debarshi Kumar Sanyal, Samiran Chattopdhyay and Matangini Chattopadhyay, "Designing an Efficient

Delay Sensitive Routing Metric for IEEE 802.16 Mesh Networks", in the proc. of the International Conference on Wireless and Optical Communications (ICWOC 2011), 2011

17. **Sandip Chakraborty**, Soumyadip Majumder, Ferdous A. Barbhuiya and Sukumar Nandi, "A Scalable Rekeying Scheme for Secure Multicast in IEEE 802.16 Network", in the proc. of First International Conference on Computer Science and Information Technology (COSIT 2011), Bangalore, India, January 2011.

18. **Sandip Chakraborty**, Soumyadip Majumder and Diganta Goswami, "A Model for Load Balancing in Distributed System using epsilon-Congestion Game", in the proc. of The Second International Workshop on Distributed System (IWDS 2010), Kanpur, India, November 2010.

19. Debarshi Kumar Sanyal, **Sandip Chakraborty**, Matangini Chattopadhyay and Samiran Chattopadhyay, "Congestion Game in Wireless Channels with Multipacket Reception Capability", in the proc. of International Conference of Advances in Information and Communication Technologies (ICT 2010), Kerala, India, September 2010. (Springer CCIS, 2010, Volume 101, Part 1, 201-205)

20. **Sandip Chakraborty**, Debarshi Kumar Sanyal, Abhirup Ghosh, Abhijnan Chakraborty, Samiran Chattopadhyay and Matangini Chattopadhyay, "Tuning Hold-off Exponents for Performance Optimization in IEEE 802.16 Mesh Distributed Coordinated Scheduler", in the proc. of 2nd International Conference on Computer and Automation Engineering (ICCAE 2010), Singapore, February 2010

Miscellaneous

1. Diganta Goswami, Samit Bhattacharya, Ferdous Ahmed Barbhuiya, **Sandip Chakraborty**, "Information and Communication Technology For Education, Healthcare and Rural Development", Narosa Publishing House, ISBN: 978-81-8487-205-7 (Proceedings of Twenty sixth Nantional Convention of Computer Engineers, Organized by Institute of Engineers, India)

2. **Sandip Chakraborty**, Soumyadip Majumder, Diganta Goswami, "Approximate Congestion Games for Load Balancing in Distributed Environment", The Computing Research Repository (CoRR), vol abs/1305.3354, 2013

Department of Computer Science and Engineering

Indian Institute of Technology Guwahati

Guwahati 781039, India